2008-05-01

Analysis of MIMO Communications Systems Based on Experimentally Observed Channels

Pat Chambers
Technological University Dublin, pchambers@tudublin.ie

Analysis of MIMO Communications Systems Based on Experimentally Observed Channels

By

Pat Chambers B.Sc.

A Thesis Submitted for the Degree of
Doctor of Philosophy
in the Dublin Institute of Technology

School of Electronic and Communications Engineering
Faculty of Engineering
Dublin Institute of Technology

May 2008

Supervisor: Dr. Conor Downing

Abstract

This thesis presents an analysis of multiple-input/multiple-output (MIMO) where the objective is to provide a unified solution to the problems of (i) crosstalk coupling in transmission line channels (ii) multi-path fading in the time variant high frequency wireless channel. In the case of transmission line channels, a comparative analysis is presented of the performance of MIMO communications systems based on balanced CAT 5 twisted-pair transmission lines, balanced twisted-pair telephone transmission lines scheme as well as unbalanced flat-pair transmission line. The unbalanced flat-pair transmission lines are viewed as a model for digital subscriber lines (DSLs) which may be deemed out-of-range for high speed internet connections because of the circumstances of poor balanced, high insertion losses and high degrees of crosstalk. This comparative analysis is then extended to examine effect of imperfect knowledge of the transmission line channels on MIMO communications system performance. In the case of wireless channels, an analysis is presented which investigates the effect of both the Rayleigh and Ricean channels on MIMO communications system performance. Again the analysis of the wireless channels is extended to examine the effect of imperfect knowledge of the channel on MIMO communications systems performance. All of the analyses in this work are based on experimentally observed channels.

In the case of the transmission line channels, it is concluded that MIMO communications systems do offer the possibility of high speed internet connectivity on transmission lines that, hereto, would have been considered out-of-range for such services. Considering the cat 5 transmission line channels, it is concluded that the MIMO communications system provide enhancement at frequencies above 50 MHz

and therefore the possibly of extending length and coverage above the standard 100 metres is proposed. On the other hand, the improved performance of the twisted-pair telephone transmission lines is consistent over the range from 300 kHz to 100 MHz when the MIMO system is applied. For all the transmission line channels that are examined, the extent of imperfect knowledge of the channel that can be allowed while maintaining a reasonable MIMO communications system performance is indicated. In the case of the wireless channels, it is concluded that MIMO communications system performance is better in the case of Rayleigh channel than in the case of Ricean channel provided that the degree of correlation of the multi-path channel impulse response components is equivalent. Also, as the number of transmitters and receivers increases, the effect of a given degree of imperfect knowledge of the wireless channel becomes more detrimental on MIMO communication system performance. This work thus indicates the extent of imperfect knowledge of the wireless channel that can be allowed while maintaining a reasonable MIMO communications system performance. The trade-off between increased capacity gain and decreased accuracy of knowledge of the channel as the dimension N_T was increased is highlighted.

I certify that this thesis which I now submit for the award of PhD is entirely my own work and has not been taken from the work of others save and to the extent that such work has been cited and acknowledged within the text of my work.

This thesis was prepared according to the regulations for postgraduate study by research of the Dublin Institute of Technology and has not been submitted in whole or in part for an award in any other Institute or University.

The work reported on in this thesis conforms to the principles and requirements on the Institute's guidelines for ethics in research.

The Institute has permission to keep, to lend or to copy this thesis in whole or in part, on condition that any such use of the material of the thesis be duly acknowledged.

Signature_____Date_____

Candidate

Acknowledgements

First of all I would like to thank my principal supervisor Dr. Conor Downing for his encouragement, guidance and friendship throughout this work. I am also indebted to Prof. Frank Boland of Trinity College Dublin for his contribution to this work.

This work was completed with the aid of a Dublin Institute of Technology Postgraduate Scholarship.

I would like to thank Dr. Gerry Farrell for his support of this work and indeed for his kind contributions of additional travel expenses throughout its progression. I would also like to thank Dr. Max Ammann and Matthias John for their help and encouragement and not least for their contribution of specially designed ultrawide band antennas to this work. I would like to thank Dr. Brendan O'Sullivan for his contribution to this work. I also thank the technicians: Andy Dillon, Tom Fallon and Ronan Murphy for their technical support throughout this work.

In no particular order, I also acknowledge the encouragement and support that I have received from various friends of mine: Dave Whelan, Ronán Byrne, Alan Touhy, John-Paul O'Keefe, Dave Martin, Ken Buckmaster, Yvonne Blake and Des Hayes.

I would also like to thank some my fellow postgrads with whom I graduated at primary degree level: Dave Flemming, Dr. Ray McCue, Sharon McDermott, Dr. Luke O'Neill and Ger Duff. I would also like to thank some of my fellow postgrads who are in the school of electronics and communications with me: Sergio Curto and Guiseppe Ruvio. I wish them all the best of luck in completing their respective PhD theses. I also wish to thank Niall Coakley not least for organising some part-time teaching hours during the course of the work. I would especially like to thank Tony Grennan for helpful discussions and also wish him the best of luck in completing his PhD thesis.

Most importantly thanks to my wonderful family, my parents George and Trudy, my brother Ciarán and his wife Helen, my Aunt Margaret, Lindy and all my cousins. I dedicate this thesis to my brother Robert Chambers.

“You see, telegraph is a kind of a very, very long cat. You pull his tail in New York and his head is meowing in Los Angeles. Do you understand this? And radio operates exactly the same way: you send signals here, they receive them there. The only difference is that there is no cat.”

Albert Einstein.

Table of Contents

Table of Figures

Table of Tables

Glossary of Symbols Used

$\lvert\cdot\rvert$	The absolute value of a scalar element or the absolute values of the scalar elements of an entire vector/matrix.
$\lVert\cdot\rVert$	Vector or matrix norm.
~	Is statistically distributed as.
$(\cdot)_i$	The i^{th} scalar element of a vector.
$(\cdot)_{i,i}$	The i^{th} diagonal scalar element of a matrix.
$(\cdot)_{i,j}$	The intersection of the i^{th} element of the row of a matrix and the j^{th} element of the column of a matrix.
$(\cdot)_j$	The j^{th} row of a matrix.
$(\cdot)^H$	The Hermitian transpose of a matrix.
$(\cdot)^T$	The conjugate transpose of a vector or complex scalar element.
a	Transmit symbol vector.
AWGN	Added white Guassian noise.
b	Receive symbol vector.
B	Bandwidth.
CSI	Channel State Information.
C	Shannon capacity of a SISO communications system in bits/sec/Hz.
$C_{\mathbf{D}}$	Shannon capacity of a MIMO communications system in bits/sec/Hz.

$C_{\mathbf{D+E}}$	Shannon capacity of a MIMO communications system, in bits/sec/Hz, where there is imperfect channel knowledge at the receiver.
$C_{\substack{\mathbf{D+E} \\ Lower}}$	Lower bound on the Shannon capacity of a MIMO communications system, in bits/sec/Hz, where there is imperfect channel knowledge at the receiver.
$\in \mathrm{C}$	A complex number.
$\in \mathrm{C}^{N}$	A complex $N \times 1$ vector.
$\in \mathrm{C}^{N \times N}$	A complex $N \times N$ matrix.
CN	Complex normal distribution.
σ_i	The i^{th} singular value.
$\mathbf{D}$	Diagonal matrix of singular values.
DSP	Digital signal processing.
dB	Decibel
dBm	Decibel normalised to 1 milliwatt.
$diag\{.\}$	A diagonal matrix formed from the diagonal elements of another matrix.
FEXT	Far end crosstalk.
$\mathbf{E}$	A matrix whose diagonal terms refer to perturbations in the singular values of the matrix, $\mathbf{H}$, and whose off diagonal terms refer to the degree in the loss in orthogonality of these singular values.
$E\{.\}$	Expectation ensemble average operator.
$\exp\{.\}$	Exponential function.

$\mathbf{h}$	Vector of channel impulse response.
$\mathbf{H}$	Channel matrix/Matrix of CSI.
$\overset{3}{\mathbf{H}}$	Three dimensional channel matrix.
$\mathbf{I}$	Identity matrix.
(i.i.d)	Independently and identically distributed.
λ	Wavelength of electromagnetic radiation (without subscript).
λ_i	The i^{th} eigenvalue (with subscript).
MIMO	Multiple-input/multiple-output.
MISO	Multiple-input/single-output.
$\mathbf{n}$	vector of uncorrelated AWGN components.
$\boldsymbol{\eta}$	vector of uncorrelated AWGN components.
NEXT	Near end crosstalk.
N_T	Number of transmitters.
N_R	Number of receivers.
φ	Noise power or noise variance.
π	Pi.
P	Receive signal power.
Q.E.D	Quod erat demonstrandum (which was to be demonstrated).
$\mathbf{QR}$	The Gram-Schmit orthogonalisation process, the $\mathbf{QR}$ decomposition. $\mathbf{Q}$ is an orthogonal/unitary matrix, i.e. $\mathbf{QQ}^H = \mathbf{I}$ and $\mathbf{R}$ is a right triangular matrix.

$\mathbf{S}$	Space-time block code matrix.
SIMO	Single-input/multiple-output.
SISO	Single-input/single-output.
SNR	Signal power to noise power ratio.
SVD	Singular value decomposition.
$\mathbf{U}$	A matrix whose columns contain the eigenvectors of the matrix, $\mathbf{H}\mathbf{H}^H$.
$\mathbf{V}$	A matrix whose columns contain the eigenvectors of the matrix, $\mathbf{H}^H\mathbf{H}$.
$\text{var}\{\cdot\}$	Variance of the scalar elements of a statistically distributed matrix/vector. Also, the variance of statistically distributed single scalar element.
W	Watts.
χ_k^2	Chi-squared distributed random variable with k degrees of freedom.
$\mathbf{x}$	Transmit vector.
$\mathbf{y}$	Receive vector.

Chapter 1: Introduction

1.1 Introduction

In communications systems which employ high frequency wireless links, a major problem is that of multi-path propagation. Given any realistic urban, sub-urban or indoor environment when high bandwidth wireless applications are being used, multi-path signal propagation will occur as the transmitted electromagnetic radiation is reflected from objects as it travels to the receiver. The net result is a phenomenon known as, 'multi-path fading' where there occur significant losses in received power at certain frequencies within the bandwidth of which the wireless application would be operating. Moreover, the frequencies at which these losses in receive power occur seem to change randomly in time as a result of the fact that any realistic environment is dynamic in nature. In turn, communications channels which occur as result of high frequency wireless applications may be described as being significantly time variant. Historically, a possible solution to this problem is to employ what are known as 'diversity techniques'. Broadly speaking, these techniques seek to mitigate the nefarious effects of multi-path propagation by taking the signal output of two or more antennas at the receiver and, by virtue of the fact that on average the signal received at any given antenna will not experience the same multi-path fading statistics, reconstruct the signal in a manner where the average receive power is greater.

In contrast, since transmission line communication channels, which are considered to be time invariant, operate in close proximity to one another, their bandwidth of operation is limited due to the electromagnetic coupling, known as 'crosstalk', which occurs as a result of this close physical proximity. As well as this, transmission lines also offer much higher ratios of receive signal power, P, to noise power, φ, than high bandwidth wireless communications systems. However, it can be seen from Shannon's well known capacity equation for the added white Gaussian noise channel, i.e. $C = B\log_2(1 + P/\varphi)$, that the potential data capacity, C in bits/sec, increases only logarithmically with the ratio, P/φ, but increases linearly with bandwidth, B. Thus the benefit of increased bandwidth of operation in respect of transmission line communications systems becomes clear and consequently there is a benefit in terms of increased mitigation of the effect of crosstalk on these communications systems.

1.2 Motivation and Approach to Analyses

In this work, an analysis of multiple-input/multiple-output (MIMO) communications systems is presented. The objective is to provide a unified solution to the problems of (i) multi-path fading in the time variant high frequency wireless channel and (ii) crosstalk coupling in transmission line channels. A diagram of a MIMO communications system is presented in fig. 1.1

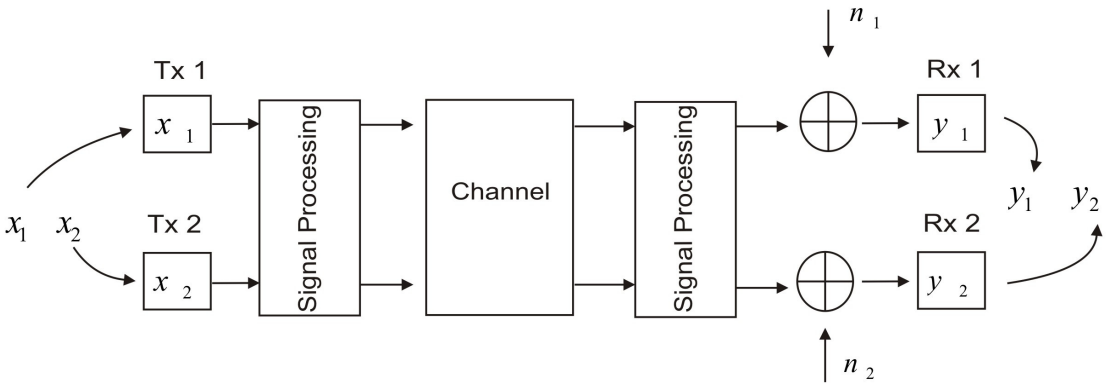

Figure 1.1: A MIMO Communications System.

Clearly, x_1 and x_2 are two transmit symbols whose relationship with the two receive symbols y_1 and y_2 is based on the effect of the channel, the signal processing stages at both the transmit and receive ends as well as the additive noise components: n_1 and n_2. For the sake of simplicity only two parallel data streams are considered. The signal processing at either end is based on knowledge of the channel.

In relation to both transmission line channels and wireless channels, this thesis makes direct reference to experimentally observed channels. In the case of the transmission lines, the transmission line channels from the following cabling schemes are considered: a balanced five twisted-pair telephone line cabling scheme, a balanced Cat 5 four twisted-pair cabling scheme and an unbalanced flat-pair cabling scheme.

It is argued that the physical measurements on the balanced transmission lines are indicative of the typical standard of transmission lines that would be seen to exist between a customer premises and a subscriber exchange or indicative of the typical standard of transmission lines that would be seen to exist in a small local area network (LAN). The unbalanced flat-pair transmission lines are not obviously typical of any component of a transmission line communications system architecture. However, it

should be appreciated that the physical measurements of the unbalanced transmission lines are at least indicative of transmission line channels where internet users in customer premises would normally be deemed out of range for high speed internet connections either due to the fact that the transmission lines are imperfectly balanced or that the distance between the customer premises and the subscriber exchange is so great that crosstalk levels and insertions losses are too high for high speed internet connections. It can be summarised at this point that the overall objective of all of the analyses presented in this work, pertaining to transmission lines, is to compare these balanced and unbalanced transmission line channels with regard to both SISO and MIMO communications systems.

In the case of the wireless channels, channel impulse response measurements and transfer functions are derived from measurements made with ultra wideband (UWB) monopole antennas which have a nominal centre frequency of 5.2 GHz. The approach taken here is to make virtual array measurements where measurements indicative of antenna arrays are made by shifting a single transmit antenna and a single receive antenna through a series of spatial permutations. The aforementioned centre frequency can facilitate physical measurements which are indicative of a single carrier frequency centred at 5.2 GHz. Another feature of the approach taken here is the fact that the measurements are made in a specially constructed highly reflective enclosure which means that a typical channel impulse response will contain components which are commensurate with the idea of multi-path electromagnetic propagation between a transmit antenna and a receive antenna. By removing the line-of-sight channel impulse response component in software, this allows for a comparison of MIMO

communications systems operating on Rayleigh channels with to that operating on Ricean channels on the condition that the degree of correlation of the multi-path channel impulse components remains the same.

1.3 Structure of Thesis

Chapter 2 presents a comprehensive literature review concerning some of the main challenges in designing transmission line and antenna wireless links. The continuous channel capacity equation was introduced as a metric for performance and contrasted against discrete channel capacity. The idea of what is meant by SISO or a MIMO communications system are defined in the separate contexts of transmission line channels and wireless channels. The study of Kyritsi et al. [93] concerning the effect of imperfect knowledge of the channel on the performance of MIMO communications systems will be introduced in chapter 2 since much of the analysis presented in the latter half of this thesis extend the conclusions of this study. Chapter 2 also seeks to introduce an appropriate and consistent mathematical notation which will be used throughout this thesis.

Chapter 3 discusses the methodology which was used in order to obtain physical measurements of balanced transmission line channels, unbalanced transmission line channels and wireless channels. Channel matrices were derived from these measurements. Vectors containing the time domain impulse response of these channels were also derived. In the case of the transmission line channels, a novel aspect of these physical measurements is that direct connection and far-end crosstalk (FEXT) measurements were made in the frequency range from 300 kHz to 100 MHz on unbalanced flat-pair transmission lines which has not been reported before. In the case of the wireless channels, the virtual array methodology of Ingram et al.[82] [83]

was paralleled in order to make physical measurements in a specially built reflective enclosure relevant to a communications system using a transmitter array and a receiver array. Apart from the specially built reflective enclosure, a novel aspect of the overall approach for these wireless channel measurements in this chapter is the fact that Rayleigh channels were observed experimentally by removing in software the line-of-sight channel impulse response component. From this, channel matrices as well as vectors containing a channel impulse response were then derived. This allowed for an experimental comparison of Rayleigh channels with Ricean channels under the condition that the degree of correlation of the multi-path channel impulse components remains the same.

In chapter 4, the channel matrices which were derived from the physical measurements in chapter 3 were related directly to capacity calculations of both MIMO and SISO communications systems. A comparative analysis of MIMO communications systems, which were based on the various transmission line channels mentioned previously, was presented. Specifically, the capacity calculations pertain to a low transmit power spectral density (PSD) of -80 dBm/Hz which would occur when digital subscriber lines (DSLs) operate in known radio bands as well as a high power spectral density of -60 dBm/Hz which would occur when DSLs are not operating in known radio bands. It was seen that the capacity gain for MIMO systems over SISO systems was minimal when the transmit PSD was -80 dBm/Hz. However, given a transmit PSD of -60 dBm/Hz, improvements in capacity gain were indicated. Specifically the MIMO capacity gain was reasonably consistent with respect to frequency for the case of the balanced telephone transmission lines, however the MIMO capacity gain for the balanced cat 5 transmission line was seen mainly at frequencies above 50 MHz. In the case of the unbalanced flat-pair transmission lines,

the capacity gain was seen mainly at frequencies below approximately 15 MHz thus supporting the enhancement of 2–3 MHz asymmetric digital subscriber line standards on poor quality transmission lines. In the case of MIMO communications systems based on wireless channels, the means of experimentally observing Rayleigh and Ricean channels was incorporated into the capacity analysis of this chapter. Comparative results in respect of this were presented which support the idea that Rayleigh channels provide superior performance. A feature of this analysis of the fading statistics, in relation to MIMO communications systems, is that the experimental observation of Rayleigh channels and Ricean channels was made where the degree of correlation of the multi-path channel impulse response components was equivalent in either case.

The objective of chapter 5 is to support the novel ideas presented in chapter 4 by using simulations which incorporated appropriate physical measurements from chapter 3. It was seen that results analyses of this chapter offered insight into channel matrix conditioning which ultimately supports the analysis of chapter 4.

Chapter 6 begins by introducing the reasons as to why the assumption of perfect knowledge of the channel may not be observed practically. Given the time variant nature of the wireless channel, it is proposed that in the case of the wireless channels, it is likely that the transfer functions will change at a rate incommensurate with the assumption of the quasi-static channel. In contrast it is proposed that in the case of the transmission line channels which are considered to be time-invariant, there may be imperfect knowledge of the channel due to incorrect assessment of the channel transfer functions. A random matrix that is characterised by the variance of its random complex normal independent and identically distributed scalar elements was

introduced in order to quantify the effect of imperfect knowledge of the channel. In the case of both the balanced twisted-pair telephone lines and the balanced twisted-pair cat 5 transmission lines, a fairly consistent drop in capacity with respect to frequency for a fixed number of transit and receive elements, N_T, and fixed variance, $\text{var}\{\Delta\mathbf{H}\}$ was observed. However, the relative drop in capacity increased as N_T was increased for a given fixed variance, $\text{var}\{\Delta\mathbf{H}\}$. Thus a given extent of imperfect knowledge of the channel as characterised by the variance, $\text{var}\{\Delta\mathbf{H}\}$, becomes more detrimental to performance as the dimension, N_T, increases. The unbalanced flat-pair transmission line channels showed good capacity gains at relatively low frequencies, even with varying degrees of imperfect knowledge of the channel. Thus the idea is further reinforced that current 2-3 MHz ADSLs standards could therefore be deployed in the circumstances of poor balance, high insertion losses and high degrees of crosstalk using MIMO techniques. A similar analysis was performed on the capacity of MIMO communications systems based on wireless channels. It was concluded that as the amount of antennas used in the transmitter and receiver array was increased, the performance of the MIMO communications systems became more sensitive to the effect of a given variance of the random matrix. These particular results in the context of the MIMO communications system based on wireless channels paralleled the work of Kyritsi [93] and others [103] [138] [137] [14] [20] [113] [64] [143]. However since, in this work, the extent of the imperfect knowledge of the channel is quantified by the variance of the complex normally distributed scalar elements of a matrix, the results themselves will be seen to be novel while providing an important foundation for the analysis of chapter 7.

The focus of chapter 7 is to extend the analysis of chapter 6 by seeking to address the stochastic nature of the calculations therein by applying a lower bound on the capacity of MIMO communications systems when there is imperfect knowledge of the channel. In doing this, chapter 7 provides some insight into the required accuracy of the knowledge of the channel in order to provide a viable MIMO communications system. Furthermore, the analysis of chapter 7 makes reference to a quantity known as the leakage level. The purpose of incorporating the leakage level into the analysis is to introduce a degree of generality into the discussion with regard to quantifying the extent of the imperfect knowledge of the channel. Specifically, the use of the leakage level as a metric for imperfect knowledge of the channel means that the matrix, $\Delta\mathbf{H}$, may be defined in an alternative manner, e.g. a different statistical distribution, with reproducibility of the results contained within this chapter. Also, for any given dimension, N_T, the drop in capacity remains consistent when the extent of the imperfect knowledge of the channel is quantified by the leakage level. Further to this, the novelty of the approach to the analysis of this chapter 7 can best be summarised by the fact that the derivation of lower bound on the capacity is entirely novel. Combining this lower bound with concept of the leakage level further extends the novelty of the results that are given. The results in this chapter propose appropriate leakage levels for each of the various channels that are considered in this work.

In summary, the original material in this thesis is as follows:

1. Measurements of far end crosstalk signal paths and transmission line signal paths on unbalanced flat-pair transmission lines over a frequency range from 300 kHz to 100 MHz.

2. Incorporation of the virtual array methodology of Ingram et al. [82] [83] into a wireless channel measurement campaign conducted in a specially built reflective enclosure. Additionally, the use of software to develop these virtual array measurements in order to make them indicative of wireless channels whose fading statistics were both Rayleigh distributed and Ricean distributed and additionally where the degree of correlation of the multi-path channel impulse response components was equivalent in either case.
3. Capacity analysis of MIMO communications systems based on balanced cat 5 twisted-pair transmission lines, balanced telephone transmission line channels and unbalanced flat-pair transmission line channels.
4. Ccapacity analysis of MIMO communications systems based on experimental observation of both Rayleigh and Ricean channels where the degree of correlation of the multi-path channel impulse response components was equivalent in either case.
5. Development of SIMULINK simulations to compare multi-carrier modulation signals in the context of MIMO communications systems based on balanced cat 5 twisted-pair transmission lines, balanced telephone transmission line channels and unbalanced flat-pair transmission line channels.
6. Development of SIMULINK simulations to compare multi-carrier modulation signals in the context of MIMO communications systems based on wireless channels whose fading statistics were Rayleigh distributed with those whose fading statistics were Ricean distributed where the degree of correlation of the multi-path channel impulse response components was equivalent in either case.

7. Capacity analysis of MIMO communications systems based on balanced cat 5 twisted-pair transmission lines, balanced telephone transmission line channels and unbalanced flat-pair transmission line channel where the extent of imperfect knowledge of the channel is quantified by the variance of the complex normally distributed scalar elements of a matrix.
8. Capacity analysis of MIMO communications systems wireless channels where the extent of imperfect knowledge of the channel is quantified by the variance of the complex normally distributed scalar elements of a matrix.
9. Derivation of a novel lower bound on the capacity of MIMO communications systems where there is imperfect knowledge of the channel.
10. Leakage level analysis of MIMO communications systems based on balanced cat 5 twisted-pair transmission lines, balanced telephone transmission line channels and unbalanced flat-pair transmission line channels using the lower bound on the capacity of MIMO communications systems.
11. Leakage level analysis of MIMO communications systems based on wireless channels using the lower bound on the capacity of MIMO communications systems.

Chapter 2: Review of SISO and MIMO Communications Systems

2.1 Introduction

The purpose of this chapter is to discuss the concepts of single-input/single-output (SISO) and multiple-input/multiple-output (MIMO) communications systems while also making reference to appropriate mathematical notation which will be used throughout the thesis. Starting with Shannon's model for a digital communications system, some of the main problems in designing SISO communications systems, in the case of both transmission line channels and wireless channels, are highlighted. In either case, the MIMO communications system is then introduced in a manner that indicates how it may be useful in solving some of the problems that have been highlighted in relation to SISO communications systems.

2.2 Digital Communications Systems

In this section, a brief overview of digital communications systems is provided. In 1948, Shannon outlined what a digital communications system is, while also giving an equation, known as the Shannon capacity equation [122]. Although this equation assumes a boundless degree of complexity within the design of the digital communications system itself, it may be used to assess the performance of various types of digital communications system. Shannon's paper itself is quite lengthy but a review of some of the key points in this paper which are relevant to this work are presented in this section together with the notation that will be used throughout the course of this work.

2.2.1 Description of a Digital Communications System

In his paper, Shannon [122] defined a communications system as a series of stages. These are shown in fig. 2.1

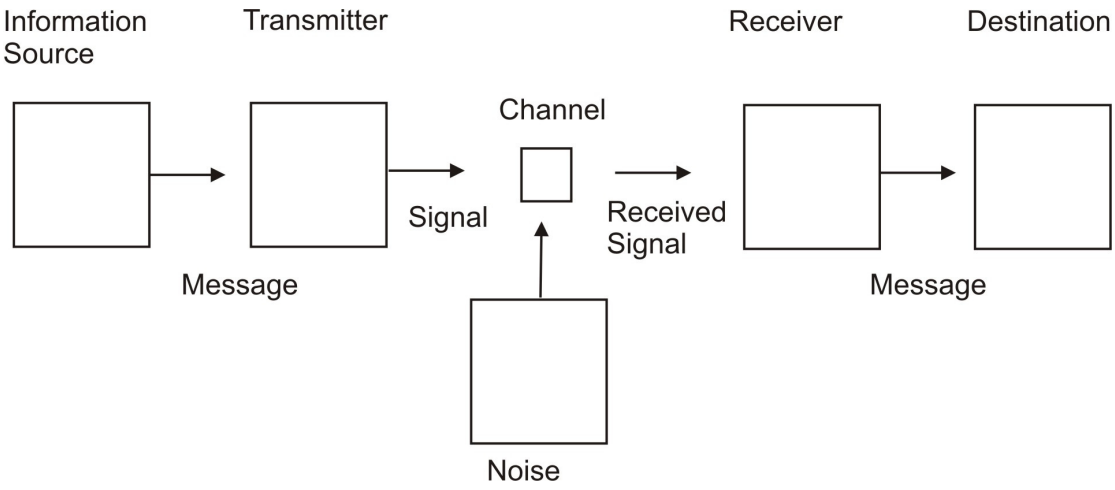

Figure 2.1: A digital communications system as outlined by Shannon.

This scheme provides a model for a digital communications system. It contains an information source, a transmitter, a channel, a receiver and destination. The information source describes a signal to be sent down the channel. It can be simply an audio signal for radio transmission, i.e. a digital audio broadcast (DAB) system, which would be a single function of time. It could also be a more complex signal, such as a Digital Video Broadcast (DVB) where there are moving images and as such the signal is a function of time and other variables such as the red, green and blue intensity levels on the screen. The transmitter then operates on the information source to make these signals suitable for transmission on the channel. This may entail various tasks such as coding and modulation.

The channel is the physical medium which exists between the transmitter and the receiver. It is used to carry the transmitted data to the receiver but it has two very important characteristics, its bandwidth and the amount of additive noise that appears on it. When a signal is transmitted onto the channel, the bandwidth of the signal provides a measure of the extent of significant spectral content of the signal [157]. Bandwidth is trivial to define when the signal is strictly band-limited, for example in the case of the frequency domain representation of a sinc pulse which exhibits a sharp 'brickwall' frequency response. However for signals that are not strictly band-limited, there is no universally accepted definition of bandwidth and a review of different definitions for bandwidth in this case may be found in [157].

Fig. 2.1 also depicts an additive noise component. Noise refers to unwanted signals that can disturb the processing of the signal at the receiver of the communications system. The receiver attempts to reconstruct the original transmit signal of the information source by performing various signal processing operations. Finally, the stage known as, 'the destination', describes how the information is made available to the person who is viewing it, e.g. certain audio-visual devices or a computer, as well the persons themselves.

2.2.2 Information and Entropy

Noise, information and the concept of 'entropy' are linked. Entropy is derived from thermodynamics and may be thought of as a measure of the degree of randomness of a system. In 1877, Boltzmann defined entropy, S, as [116] [102]:

$$S = -k_B \sum \left[p_i \log_e p_i \right] \tag{2.1}$$

p_i is the probability that a particle, "i", will be in a given microstate. k_b is Boltzmann's constant which is 1.3806504×10^{-23} Joules/Kelvin. The expression $p_i \log_e p_i$ is summed over all particles in the system to give its entropy, S, which itself has units of Joules/Kelvin. The Claussius statement of the second law of thermodynamics states that heat flow, ΔQ, always takes place in the direction of going from a higher temperature body to a lower temperature body until an equilibrium temperature, T, occurs and never the other way around if there is no work done by the surroundings. The second law of thermodynamics when no work is done by the surroundings can be expressed as:

$$\Delta S \geq \frac{\Delta Q}{T} \tag{2.2}$$

The increase in the entropy of states, ΔS, occurs in the cooler body due to the warmer body when this equilibrium temperature, T, is reached. There is never a flow of heat, $-\Delta Q$, from the cooler body to the warmer body, thus there is never a decrease in the entropy of states, $-\Delta S$, in the warmer body due to the cooler body provided no work is done by the surroundings. In summary, heat flow, ΔQ, and the change in entropy, ΔS, proceed in one direction only.

In 1861, Maxwell challenged the second law of thermodynamics with his infamous "Maxwell's demon". Maxwell proposed that the flow of heat between two chambers be controlled by some entity who would have charge of a frictionless door [107]. When molecules from the cooler chamber were on a collision course with the door, the entity or Maxwell's demon would open the door for just enough time to let them in to the warmer chamber. The warmer chamber would then fill up at the expense of

the cooler chamber. This means that there is effectively a flow of heat from the cooler chamber to the warmer one. The second law of thermodynamics remained valid but the idea brought about by Maxwell's thought experiment persisted until 1929 when Szilard [43] pointed out that the demon would have to know a lot about the molecules in either chamber in order to perform. This led to a connection between information and entropy and it is from this discussion that information theory originates. This connection was then clarified by Shannon [122] who showed that information, like quantities such as mass and voltage, may be considered as measurable. In doing this Shannon stated that entropy, in the context of digital or telegraphic communications systems, was a measure of the uncertainty and hence information.

In order to define entropy as a measure of information in the context of digital communication systems, it is first necessary to define a collection of N transmit symbols or source symbols, X :

$$X = \{x_0 \quad x_1 \quad x_2 \quad \ldots \quad \ldots \quad x_{N-1}\} \tag{2.3}$$

Each symbol has a probability of occurrence, p_i , such that:

$$\sum_{i=0}^{N-1} p_i = 1 \tag{2.4}$$

An expression for the entropy of the source, X , written as $H_{Ent}(X)$, may now be written because a given probability of occurrence, p_i, has been assigned to each symbol, x_i.

$$H_{Ent}(X) = E\{ I(b_i) \} = \sum_{i=0}^{N-1} p_i \log_2\left[\frac{1}{p_i}\right] \tag{2.5}$$

$I(b_i)$ is the information gained after observing the event b_i, which has been written as the logarithmic function: $\log_2\left[\frac{1}{p_i}\right]$ in equation (2.5). Since, $E\{\cdot\}$, is the ensemble average operator, the entropy of the source X, $H_{Ent}(X)$, is a measure of the average information content of the source. In the context of digital communications systems, the entropy or average information content, H_{Ent}, defined in equation (2.5) has units of bits. Shannon was able to extend this idea of entropy to the idea of communication system capacity or channel capacity.

2.2.3 Mutual Information and Channel Capacity

A model for the discrete-time memoryless channel perturbed by additive white Gausssian noise (AWGN) samples, n_i, is depicted in fig. 2.2.

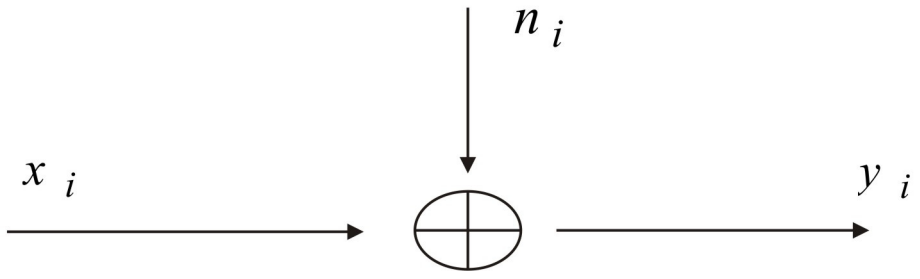

Figure 2.2: The discrete-time memoryless AWGN channel.

x_i is a continuous random variable which is obtained by sampling a random process whose statistical characterisation does not vary with time, i.e. a stationary process.

This random process is band-limited to a bandwidth of B Hz. The samples, x_i, are transmitted onto the channel over a time T secs. If the number of samples, $N_{samples}$, transmitted over a time, T, be defined as[1]:

$$N_{samples} = 2BT \tag{2.6}$$

And the relationship between the relationship between the transmit samples, x_i, and the receive samples, y_i, be defined as:

$$y_i = x_i + n_i \qquad i = 1,2,...,N_{samples} \tag{2.7}$$

Then the average transmit power, P, in respect of this process is:

$$P = E\left\{ \left| x_i \right|^2 \right\} \tag{2.8}$$

The AWGN noise that perturbs the channel is band-limited to a bandwidth, B, and has a two sided power spectral density of $\frac{N_0}{2}$. n_i is a sample of this AWGN which has mean of zero and a variance, φ, given by:

$$\varphi = BN_0 \tag{2.9}$$

Consider now that the samples: x_i ,and , y_i, are selected from respective alphabets: X and Y, which denote all of the possible channel inputs and channel outputs. The entropy $H_{ent}(X)$ represents the uncertainty of the channel input before observing any

[1] $2B$ is the Nyquist sampling rate for the stationary process from which the samples, x_i, are derived.

channel output. It is also possible to denote a quantity known as a conditional entropy, $H_{ent}(X \mid Y)$, which represents the uncertainty of the channel input having observed the channel output. In respect of these entropies, the mutual information of the channel, $I(X;Y)$ is defined as:

$$I(X;Y) = H_{ent}(X) - H_{ent}(X \mid Y) \tag{2.10}$$

$I(X;Y)$ may thus be thought of as the uncertainty of the channel input that is resolved by observing the channel output. In contrast, if two continuous Gaussian random variables, $\bar{X}$ and $\bar{Y}$, are considered where $f_{\bar{X}}(x)$[2] is the probability density function of $\bar{X}$ then:

$$H_{ent}\left(\bar{X}\right) = \int_{-\infty}^{\infty} f_{\bar{X}}(x) \log_2\left[\frac{1}{f_{\bar{X}}(x)}\right] dx \tag{2.11}$$

Since, $\bar{X}$, is a continuous function, the notation $H_{ent}\left(\bar{X}\right)$ is referred to as a differential entropy in contrast to the entropy $H_{Ent}(X)$ introduced in equation (2.5) which is an absolute entropy. The quantity $H_{ent}\left(\bar{Y}\right)$ can be defined in a similar manner. Gaussian random variables have two very important properties [157]:

---

[2] To clarify, here' x ' is the dummy variable where the cumulative distribution function, $F_{\bar{X}}(x)$, can be written as $F_{\bar{X}}(x) = P\left(\bar{X} \le x\right)$ and hence the corresponding probability density function, $f_{\bar{X}}(x)$, is thus written as: $f_{\bar{X}}(x) = \frac{d}{dx} F_{\bar{X}}(x)$.

Property (i): For a finite variance, φ, the Gaussian random variable has the largest differential entropy attainable by any random variable.

Property (ii): The entropy of a Gaussian random variable $\bar{X}$ is uniquely determined by the variance of $\bar{X}$ and is independent of the mean of $\bar{X}$.

The channel capacity, C, is the maximum mutual information between the transmit and receive channel inputs, therefore:

$$C = \max\{I(X;Y)\} \tag{2.12}$$

The notation, $\max\{\cdot\}$, refers to the maximum over all possible probability density functions. Keeping this mind, consider the following expressions for the mutual information of the channel in fig. 2.2, starting with:

$$I(x_i; y_i) = H_{ent}(x_i) - H_{ent}(x_i \mid y_i) \tag{2.13}$$

Mutual information $\{I(x_i; y_i)\}$has the property of being symmetric [157], therefore:

$$I(x_i; y_i) = H_{ent}(y_i) - H_{ent}(y_i \mid x_i) \tag{2.14}$$

The entropy of the AWGN onto the channel, $H_{ent}(n_i)$, can be written [157]:

$$H_{ent}(n_i) = H_{ent}(y_i \mid x_i) \tag{2.15}$$

Thus:

$$I(x_i; y_i) = H_{ent}(y_i) - H_{ent}(n_i) \tag{2.16}$$

If it is assumed that y_i and n_i are independent continuous Gaussian random variables then it can be shown that differential entropy of the variable, y_i, i.e. $H_{ent}(y_i)$ reduces to [157]:

$$H_{ent}(y_i) = \frac{1}{2}\log_2[2\pi e(P+\varphi)] \tag{2.17}$$

Where the variance of y_i is $P+\varphi$. Similarly, it can also be shown that $H_{ent}(n_i)$ reduces to [157]:

$$H_{ent}(n_i) = \frac{1}{2}\log_2[2\pi e(\varphi)] \tag{2.18}$$

Where, φ, was previously defined as the noise variance. Again since it has been assumed that y_i and n_i are independent continuous Gaussian random variables, equation (2.12) now reduces to Shannon's famous result:

$$C = \frac{1}{2}\log_2\left[1+\frac{P}{\varphi}\right] \tag{2.19}$$

In this case, the channel capacity, C, is expressed in bits/transmission. The channel is used a number of times equivalent to $N_{samples}$ for the transmission of a number of samples equivalent to $N_{samples}$ over a time, T seconds. Therefore, the capacity per unit time is:

$$C = \left[\frac{N_{Sample}}{T}\right]\frac{1}{2}\log_2\left[1+\frac{P}{\varphi}\right] \tag{2.20}$$

By definition in equation (2.6), $N_{samples} = 2BT$, thus the capacity per unit time is written more conveniently as:

$$C = B\log_2\left[1+\frac{P}{\varphi}\right] \tag{2.21}$$

In the case of equations (2.20) and (2.21), the units of C in this case are bits/second. To clarify, C is the information capacity of a continuous channel of bandwidth B Hertz which is perturbed by two sided AWGN noise of power spectral density, $\frac{N_0}{2}$, and average transmit power, P. It is derived on the basis that the variables: x_i, y_i and n_i are statistically independent continuous random Gaussian variables. Equation (2.21) sets an upper limit on the rate of information that can be transmitted in order to obtain an arbitrarily low probability of error at the receiver.

2.2.4 The Ideal System

Distinguishing between a signal energy and signal power, the average transmit power, P, defined in equation (2.8), may also be defined in terms of the transmitted energy per bit, E_b, and the transmit bit rate in bits/sec, R_b, as:

$$P = E_b R_b \tag{2.22}$$

Further to this, consider the specific case of the 'ideal communications system' [157], which has a transmit bit rate equivalent to the capacity, C, and thus the average transmit power, P, may be written as:

$$P = E_b C \tag{2.23}$$

Since $\varphi = BN_0$, the ideal system can be defined by the expression:

$$\frac{C}{B} = \log_2\left[1 + \frac{E_b}{N_0}\frac{C}{B}\right] \tag{2.24}$$

Thus:

$$2^{\frac{C}{B}} = 1 + \frac{E_b}{N_0}\frac{C}{B} \tag{2.25}$$

$$\frac{2^{\frac{C}{B}} - 1}{\left[\frac{C}{B}\right]} = \frac{E_b}{N_0} \tag{2.26}$$

The ratio, $\frac{C}{B}$, may be referred to as the bandwidth efficiency of the ideal system with

ratio, $\frac{E_b}{N_0}$, denoting the ratio of signal energy-per-bit to noise power spectral density. A plot of these ratios is shown in fig. 2.3 and together they define a capacity boundary on a bandwidth efficiency diagram[3]. Also shown in fig. 2.3 is the Shannon limit. The Shannon limit is the ratio of $\frac{E_b}{N_0}$ which can ensure reliable transmission over an infinite bandwidth, numerically it can be expressed as:

$$\begin{aligned}\lim_{B\to\infty}\left(\frac{E_b}{N_0}\right) &= \log_e 2 \\ &= 0.693 \\ &= -1.6\ \text{dB}\end{aligned} \tag{2.27}$$

[3] A bandwidth efficiency diagram highlights the potential trade-offs between the quantities: $\frac{E_b}{N_0}$ and $\frac{R_b}{B}$ for various communication systems. Clearly for the specific case of the capacity boundary which, by definition, arises from the analysis of the ideal system, the quantity $\frac{R_b}{B}$ is equivalent to $\frac{C}{B}$.

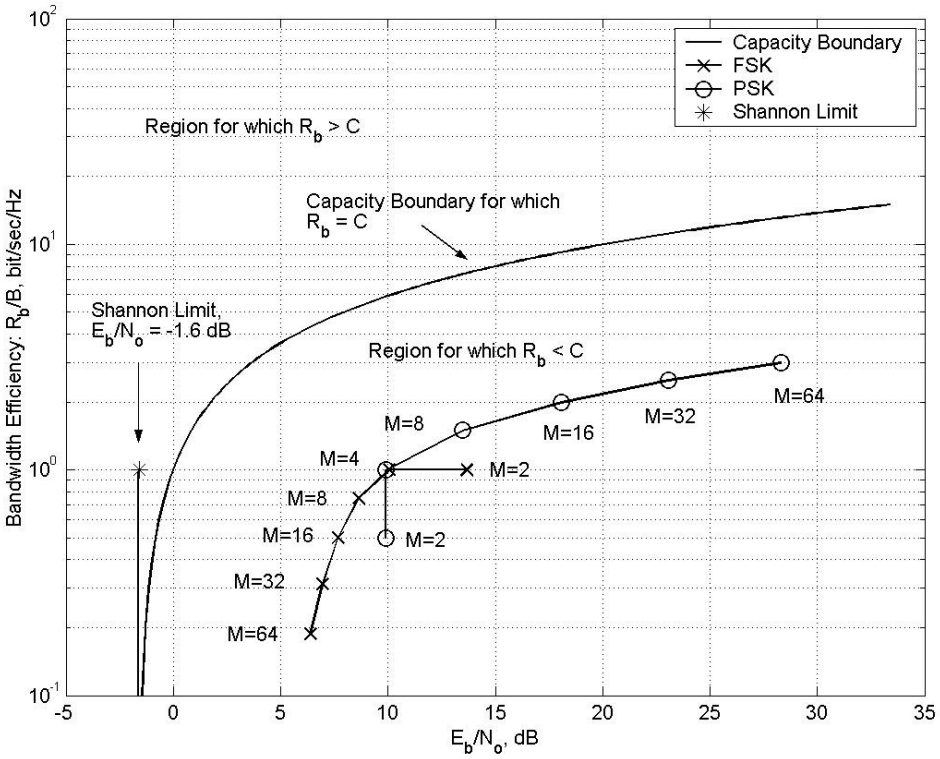

Figure 2.3: Bandwidth efficiency diagram showing the capacity boundary, Shannon limit and operating points for FSK and PSK modulation schemes of various constellation sizes [157].

By definition, the ratio $\frac{R_b}{B}$ approaches zero as the Shannon boundary asymptotically approaches the vertical line which crosses the axis labelled $\frac{E_b}{N_0}$ at a value of -1.6 dB. However, the capacity, C, for an infinite bandwidth system can be expressed analytically as [157]:

$$\lim_{B \to \infty}(C) = \frac{P}{N_0}\log_2 e \tag{2.28}$$

Also shown in fig. 2.3 are the combinations of $\frac{E_b}{N_0}$ and $\frac{R_b}{B}$ which ensure a probability of bit error of $P_e = 10^{-5}$. These are known as known as operating points [157]. Two cases are considered, the case of an unencoded modulation scheme known as frequency shift keying (FSK) and the case of an unencoded modulation scheme known as phase shift keying (PSK).[4] In either case, operating points are plotted for various constellation or M-ary sizes in fig 2.3. FSK clearly operates in a low power and high bandwidth regime since, as constellation size increases, the operating point shifts closer to the Shannon limit. On the contrary, PSK operates in a high power and low bandwidth regime since as the as the constellation size increases, the operating point shifts in the opposite direction because higher ratios of $\frac{E_b}{N_0}$ are required to maintain $P_e = 10^{-5}$.

Finally in this section, it is important to clarify that operating points which occur north or west of the capacity boundary, i.e. in the region labelled $R_b > C$ in fig 2.3, can never achieve an arbitrarily low probability of error, P_e. To ensure an arbitrarily small value for P_e, the operating point for a given communication system must fall south or east of the capacity boundary, i.e. in the region labelled $R_b < C$ in fig 2.3 . This fact is a consequence of Shannon's third theorem which indicates that there is a maximum to the rate at which any communication system can operate reliably when the system is constrained in power [157].

[4] Equations for these operating points may be found in the appendix, A1.

2.2.5 The Discrete Channel

At the end of section (2.2.3), it was stipulated that equation (2.21) was derived on the basis of two properties, (i) and (ii), which imply ultimately that the variables: x_i, y_i and n_i are continuous random Guassian variables. Hence equation (2.21) refers to the capacity of the continuous channel. In this section, the capacities of some discrete channels are computed and compared with the continuous case. In these discrete channels, the transmit and receive symbol alphabets are finite and are chosen over a uniform distribution.

Taking the approach of Ungerboeck [159] in the context of two dimensional modulation schemes, the signal to noise ratio (SNR) is defined as:

$$SNR = \frac{P}{2\varphi} \tag{2.29}$$

Where P is constrained such that:

$$P = E\left\{ \left| x_i \right|^2 \right\} = 1 \tag{2.30}$$

Consistent with Ungerboeck's [159] approach, the capacity, C, of the continuous channel is calculated from:

$$C = \log_2\left[1 + SNR\right] \tag{2.31}$$

In this case C has units of bits per modulation interval (bits/T). For the case of the various two dimensional digital modulation schemes, Ungerboeck [159] gives the following expression for discrete channel capacity, C_M :

$$C_M = \log_2(M) - \frac{1}{M} \times \sum_{k=0}^{M-1} E\left\{ \log_2 \sum_{i=0}^{M-1} \exp\left[- \frac{\left| x_i + n_i - x_k \right|^2 - \left| n_i \right|^2}{2\varphi} \right] \right\} \qquad (2.32)$$

x_i, is a sample from the transmit sequence which is derived from a given two dimensional modulation scheme. n_i is a noise sample whose variance is 2φ subject to the constraint of the normalisation in equation (2.30). In fig. 2.4, the capacity, C, is plotted over a range of SNRs along with calculations of C_M in the case of the following modulation schemes:

- 4-PSK[5]
- 8-PSK
- 16-quadrature amplitude modulation (QAM)
- 64-QAM

Also, plots of the points which indicate bit error rates $P_e = 10^{-5}$ are shown for each of these modulation schemes when they are unencoded.

[5] 4-PSK refers to phase shift keying whose constellation size or M-ary size is M = 4, etc

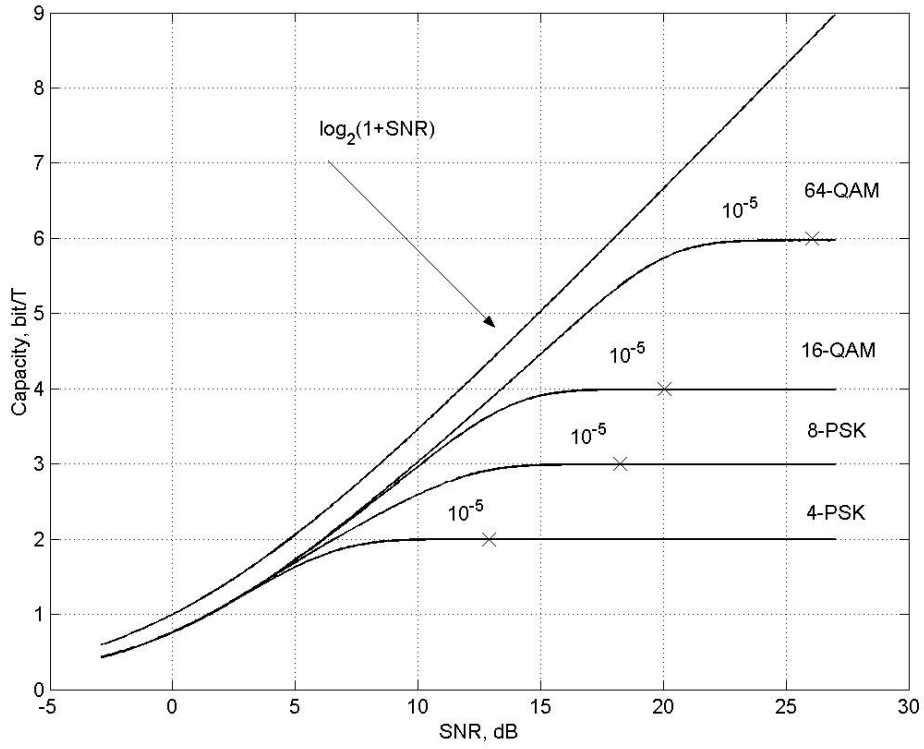

Figure 2.4: Comparison of the capacity, C, of the continuous channel with some discrete capacities, C_M, for various two-dimensional modulation schemes including bit error rates: $P_e = 10^{-5}$ with respect to SNR [159][6].

Looking at fig. 2.4. the following conclusions may be drawn:

(i) The capacity for the continuous channel increases monotonically over the range of SNR whereas the capacities of the discrete channels appear to saturate. This due to the fact that M-ary constellation schemes cannot transmit at rate beyond that set by $\log_2 M$. Furthermore, the saturation is not sharp, it occurs gradually with respect to SNR.

[6] Not shown in fig. 2.4 is the fact that the discrete channel capacity for certain modulation schemes will not be as good as others for a given SNR and constellation/M-ary size. In [159], it is possible to compare 16-PSK with 16-QAM

(ii) In the high SNR region, for a given value of SNR the capacity of the M-ary constellation schemes are less than that of the continuous channel. As stated in [166], this discrepancy is due to the fact that a uniform rather than Gaussian distribution is chosen over the signal set.

(iii) Since the values of $P_e = 10^{-5}$ occur at SNRs that are higher than the theoretical error-free transmission, clearly coding effort can lower these SNRs.

(i) indicates even if an appropriate modulation scheme and coding were chosen for a given SNR, there is a loss in SNR with respect to capacity just before saturation. The problem highlighted in (ii) can partially be solved by a technique known as N-sphere shaping. This technique involves the projection of the uniform probability distribution, which occurs in the discrete channel case, to an N-dimensional sphere. The result is a non-uniform probability distribution which approaches the Gaussian distribution as N approaches infinity. This technique is discussed in the context of phase amplitude modulation (PAM) in [166] where the discrepancy between the discrete and continuous channel capacity is 1.53 dB in the high SNR region. The improvement in capacity with respect to SNR is known as the shaping gain and the authors of [166] plot the shaping gain with respect to dimension, N, as well as discussing the relative merits of various shaping techniques. They also indicate that shaping gains of 1 dB are possible under certain conditions. Finally, in relation to (ii), at low SNRs, i.e. at 0 dB or below, the discrepancy between the continuous channel capacity and the discrete channel capacity becomes negligible when binary alphabets are used [166].

This section highlights the discrepancy between the continuous channel capacity as a figure for merit against that of the more realistic discrete channel capacity. The reader is thus cautioned to the significance of the continuous capacity as metric for communication system performance both in the context of this thesis as well as much of the literature on MIMO communications systems which uses it [150] [106] [37] [35] [95] [108] [10] [46] [51] [50] [140] [16] [17] [40] [36] [39]. It is argued that in the context of this work, the analyses presented are comparative in nature and thus the choice of the continuous channel capacity as a figure of merit is reasonable.

2.3 SISO Communications Systems Based on Transmission Line Channels

In the context of transmission lines, a single-input/single-output (SISO) communications system will used throughout this thesis to designate the scenario depicted in fig 2.1. There is clearly one transmitter, one channel and one receiver. In theory any neighbouring transmission lines are thought of as SISO communications systems which function independently. In reality however, these communications systems do not function independently and as a result, it is possible to identify two distinct types of signal path:

(i) A signal path from a given transmitter along the physically conducting transmission line to a corresponding receiver.

(ii) A signal path from a given transmitter which couples onto another transmission line, due to far end crosstalk (FEXT), and as a result is detected at another receiver which is not the same as the corresponding receiver mentioned in (i).

Although crosstalk may be divided into two categories: near end crosstalk (NEXT) and far end crosstalk (FEXT), the analysis in this work neglects the effect of NEXT since it can be cancelled effectively using echo cancellation techniques [171]. In the analyses that follow in later chapters, figures for noise power will be chosen which reflect the assumption of echo canceller implantation. Considering now these signal paths, define a transmit vector $\mathbf{x}$ as:

$$\mathbf{x} = \begin{bmatrix} x_1 \\ x_2 \\ \vdots \\ x_{N_T} \end{bmatrix} \tag{2.33}$$

From the notation, it can be seen that there are N_T transmitters. Similarly defining the a corresponding receive vector, $\mathbf{y}$:

$$\mathbf{y} = \begin{bmatrix} y_1 \\ y_2 \\ \vdots \\ y_{N_T} \end{bmatrix} \tag{2.34}$$

There are clearly an equivalent number, N_T, of transmitters as receivers. As a result of the two distinct signal paths identified in (i) and (ii), the relationship between a receive vector, $\mathbf{y}$, and a transmit vector, $\mathbf{x}$, may be written using Teletar's linear model [152]:

$$\mathbf{y} = \mathbf{H}\mathbf{x} + \mathbf{n} \tag{2.35}$$

$\mathbf{H}$ is referred throughout this work as the 'channel matrix' and is defined as:

$$\mathbf{H} = \begin{bmatrix} h_{1,1} & h_{1,2} & \cdots & h_{1,N_T} \\ h_{2,1} & h_{2,2} & \cdots & \vdots \\ \vdots & \vdots & \ddots & \vdots \\ h_{N_T,1} & h_{N_T,2} & \cdots & h_{N_T,N_T} \end{bmatrix} \tag{2.36}$$

The diagonal terms of $\mathbf{H}$ are complex transfer functions which correspond to the signal paths described in (i) and the off-diagonal terms are complex transfer functions which correspond to the signal paths described in (ii). The vector, $\mathbf{n}$, contains uncorrelated AWGN components and is defined:

$$\mathbf{n} = \begin{bmatrix} n_1 \\ n_2 \\ \vdots \\ n_{N_T} \end{bmatrix} \tag{2.37}$$

This mathematical relationship is depicted in the context of two neighbouring transmission lines fig. 2.5 in the context where there is no noise[7].

[7] The vector of AWGN has been omitted from fig.2.5 for the sake of clarity.

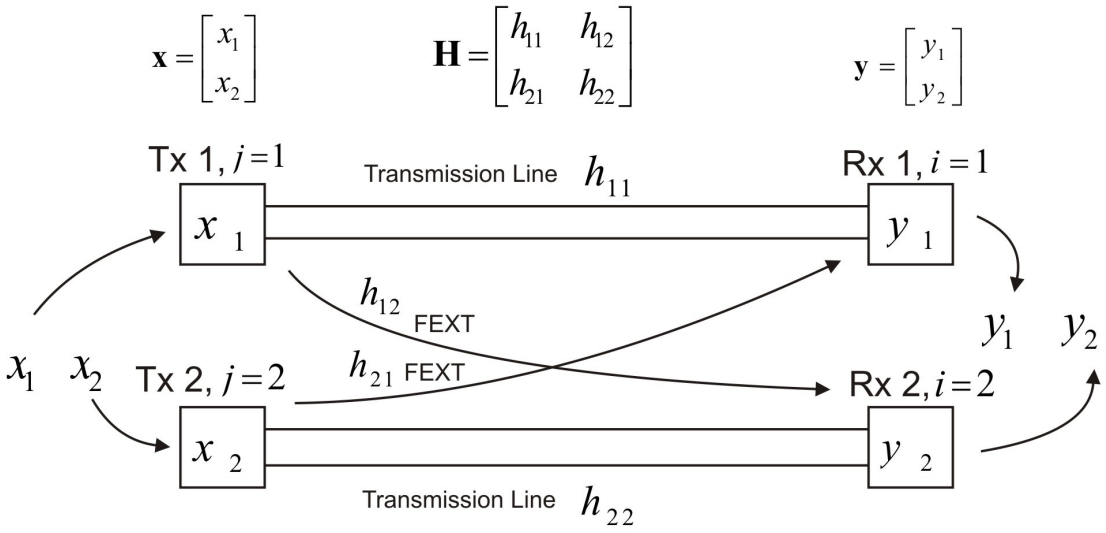

Figure 2.5: A SISO communications system based on transmission line channels. Equations written above the various operations clarify how Teletar's linear model in equation (2.7) may be applied in this situation. The dimension $N_T = 2$.

Fig. 2.5 is quite similar to the model for transmission lines as presented by Fang and Cioffi [49]. An expression for the capacity of the SISO communications system depicted in fig. 2.3 comes from work by Helenius et al [75] with similar expressions appearing in [163] [164]. The use of notation in this paper by Helenius [75] *et al.* is somewhat inconsistent, but it will now be set out clearly in a fashion relevant to fig. (2.2). Firstly consider the following notation which will used throughout this thesis:

- Denote the scalar elements[8] of a matrix using subscript notation: $(\cdot)_{i,j}$.
- Denote the diagonal elements of a matrix using the sub-script notation: $(\cdot)_{i,i}$[9].

[8] A convention adopted by Stewart [125] is used throughout this thesis where the elements of vectors or matrices are referred to as scalar elements regardless of whether they are real or complex valued.

- Denote a vector formed from the j^{th} column of a matrix using the notation: $\underset{j}{(\cdot)}$.
- Denote the i^{th} element of a vector using the notation: $(\cdot)_i$ and if the vector is derived from the j^{th} column of a matrix then: $\underset{j}{(\cdot)}_i$.
- Denote the absolute value of a complex quantity using the notation, $|\cdot|$.

The capacity of the SISO communications system based on transmission line channels can be written in terms of the power, P, of the transmit signal as well as the AWGN power as detected at i^{th} receiver, φ_i, as [75] :

$$C = \sum_{i=1}^{N_T} \log_2 \left[1 + \frac{P\left|\mathbf{H}_{i,i}\right|^2}{\varphi_i + P\left[\sum_{j=i}\left\{\left|\underset{j}{\mathbf{H}}\right|^2\right\} - \left|\mathbf{H}_{i,i}\right|^2\right]} \right] \tag{2.38}$$

It is a common convention in literature to normalise the capacity, C, with respect to bandwidth and this has been done in equation (2.38). In light of what was outlined in section 2.2.5, C actually refers to the bandwidth efficiency of the ideal system but will hereafter be simply referred to a capacity in line with convention. The units of C are bits/sec/Hz. Inspection of fig. 2.5, in conjunction with equation (2.38) reveals that in a mathematical sense it is possible to make reference to a j^{th} transmitter, an i^{th} receiver and an i^{th} transmission line. P is the transmit power in watts and thus the product, $P\left|\mathbf{H}_{i,i}\right|^2$, is the receive power in watts at the i^{th} receiver as a result of a signal

[9] Since in this case $i = j$

path similar to the one described in (i). φ_i is in units watts. The term, $\sum_{j=i}\left\{\left|\mathbf{H}_j\right|^2\right\}$, refers to the sum over the particular j^{th} column vector which would intersect the relevant i^{th} row of the matrix, $\mathbf{H}$. Thus the term, $\sum_{j=i}\left\{\left|\mathbf{H}_j\right|^2\right\}-\left|\mathbf{H}_{i,i}\right|^2$, is a measure the FEXT signal paths described in (ii). Since this term appears in the denominator of equation (2.38) it has the same effect on the capacity as the AWGN power term, φ_i.

Models for FEXT [75] [118] [49] [15] and, indeed, measurements of FEXT [22] [23] show that it is frequency dependent. This means that the term, $\sum_{j=i}\left\{\left|\mathbf{H}_j\right|^2\right\}-\left|\mathbf{H}_{i,i}\right|^2$, in equation (2.8) increases with increasing frequency. Due to insertion losses, the term, $\mathbf{H}_{i,i}$, decreases with increasing frequency. In summary, SISO communications systems based on transmission line channels are characterised by a decrease in performance with increasing frequency. The capacity in equation (2.38) will thus be higher at lower frequencies where the effects of FEXT and insertion losses are less. Equation (2.38) outlines the challenges faced in transmitting signals over SISO communications systems based on transmission line channels and will be used in this thesis in calculations of the capacity of such SISO communications systems.

2.4 MIMO Communications Systems Based on Transmission Line Channels

The discussion in section 2.3 highlighted the effect of FEXT on the performance of SISO communications systems based on transmission channels. The MIMO communications systems is discussed in detail in chapter 4, however, the objective of

this section is to provide the reader with some brief introductory comments as to how MIMO communications systems based on transmission line channels can mitigate the effect of FEXT on performance.

In the context of MIMO communications systems based on transmission line channels, Mutjabi [108] states that:

"To develop an intuition for the capacity that can be achieved in a linear MIMO channel, consider the singular value decomposition of the channel matrix, $\mathbf{H}$."

The singular value decomposition will be discussed in more detail in chapter 4 but when a singular value decomposition is performed on the channel matrix $\mathbf{H}$, it is transformed into a diagonal matrix, $\mathbf{D}$. $\mathbf{D}$ has the same dimensions, $N_T \times N_T$, as $\mathbf{H}$ but contains zero in its off-diagonal terms. As a result of this transformation, throughout this thesis, the capacity of MIMO communications systems will be written as $C_{\mathbf{D}}$:

$$C_{\mathbf{D}} = \sum_{i=1}^{N_T} \log_2 \left[1 + \frac{P\left|\mathbf{D}_{i,i}\right|^2}{\varphi} \right] \tag{2.39}$$

The units of $C_{\mathbf{D}}$ are bits/sec/Hz. Again the reader is reminded and cautioned to the use of the continuous channel capacity as a performance metric and the fact that $C_{\mathbf{D}}$ may be thought of as bandwidth efficiency. Taking into account the mathematical notation described and comparing equation (2.39) with equation (2.38), it can be concluded that the matrix, $\mathbf{D}$, now shows how the receive power, P, is distributed to each of the i^{th} receivers. It is implicit within equation (2.39) that since the matrix, $\mathbf{D}$,

in contrast with the matrix, $\mathbf{H}$, contains no off-diagonal terms, there is a relative performance improvement over the SISO communications system based on transmission line channels.

MIMO communications system based transmission line channels which use the singular value decomposition[10] to achieve the capacity given in equation (2.39) require knowledge of the channel matrix, $\mathbf{H}$, in order to provide appropriate signal processing at the transmit and receive end. Reasons as to why imperfect knowledge of the channel may arise in the context of transmission line channels are discussed in the works of Bostoen et. al [18] as well as Galli and S., Waring, D.L [57], and others [15] [141]. A study by Kyritsi [93] discusses the effect of imperfect knowledge of the channel on the Shannon capacity of MIMO communications systems, however Kyritsi's study concerned itself specifically with imperfect knowledge of wireless channels.

2.5 SISO Communications Systems Based on Wireless Channels

In the case of SISO communications systems based on wireless channels, it should be understood that throughout this work, there is only one transmitter and one receiver. In contrast to SISO communications systems based on transmission line channels which were discussed in section 2.3, this communications system is assumed to be entirely independent. Objects within the vicinity of the wireless channel that exists between the transmitter and receiver cause the transmitted electromagnetic radiation

[10] As well as using the singular value decomposition as a means of creating a MIMO communications system based on transmission line channels, it is also possible to use the QR decomposition. The details of this approach can be found in [62].

to be reflected before it arrives at the receiver. This gives rise to a phenomenon known as multi-path fading and given a dynamic environment this will manifest itself as a random fluctuation in receive power. This random fluctuation may be characterised by a random variable, h, which is defined arbitrarily as:

$$h \sim C(0,1) \tag{2.40}$$

The symbol, "~" should be read as, "is distributed as". The notation C is used to denote some arbitrary random complex distribution. For the sake of generality in discussion, this particular distribution is non-specific. Typical distributions that occur in wireless channels are Rayleigh and Rician distributions. In this notation, the position of the digit, '0', in parenthesis refers to the mean, i.e. zero mean, and position of the digit, '1', in the parenthesis indicates a variance of one. The capacity of SISO communications systems based on wireless channels is [59] [61]:

$$C = \log_2\left[1 + \frac{P|h|^2}{\varphi}\right] \tag{2.41}$$

In equation (2.41), the units of the capacity, C, are in bits/sec/Hz. P is the transmit signal power in watts while φ is the AWGN power as detected at the receiver The quantity, C, is the capacity of a SISO communications system based on wireless channels at an arbitrary instant of observation since h is a random quantity. For analyses of this type, the channel is assumed to be 'quasi-static' [59] [61] [152] [150]. This means that a finite amount of information, usually referred to as a, 'burst', is able to be transmitted over the channel before its transfer function changes.

The capacity defined in equation (2.41) is changes randomly with each instance h. As a result of this, two common types of capacity calculation are used to assess the performance of SISO communications system based on wireless channels. In work by Gesbert [59], these two capacities are referred to as (i) the outage capacity, C_{Out}, and (ii) the average capacity, C_{Av}, both of which measured in bits/sec/Hz. An expression for the capacity, C_{Out}, is [59]:

$$C_{Out} = \mathrm{Prob}\{C\} \geq 99.9\% \tag{2.42}$$

Here the notation, '$\mathrm{Prob}\{C\} \geq 99.9\%$', should read as, 'that capacity, C, that can be guaranteed 99.9 % of the time', or indeed simply, 'that capacity, C, that can be guaranteed with a high level of certainty'. The quantity, C_{Av}, is defined as the capacity that arises when the average is taken over all possible occurrences of C as it is defined in equation (2.41). In practice, C_{Av}, is usually this average calculated over an arbitrarily large amount of trials. If both methods for calculating, C_{Av}, should be equal then it is referred to as the, 'ergodic' capacity in bits/sec/Hz. For the purposes of this work, C_{Av} and the 'ergodic capacity' will be thought of as interchangeable terms. When the ratio, $\frac{P}{\varphi}$, is 10 dB, results presented by Gesbert [59] show that C_{Out}, for a SISO communications system based on wireless channels which is centred on a nominal carrier frequency, is approximately 0 bits/sec/Hz. The same results also show that C_{Av}, in the same case, is 3 bits/sec/Hz.

Although, no specific remarks have been made with regard to transmit and receive element complexity, it can be concluded at this point that performance of SISO

communications systems based on wireless channels are possible but that they may, at times, exhibit a degree of unreliability. It is stressed that by highlighting multi-path fading in respect of the time variant nature of the wireless channel, the objective in this section was to outline the challenges in designing SISO communications systems based on wireless channels. It is not, however, the objective of this work in this thesis to address the time variant nature of the wireless channel in the context of SISO communications systems and as such no results will ever be offered in this respect. As a result of this, in any future calculations presented in this work of the Shannon capacity of SISO communications systems based on wireless channels, the variable h will be set to unity.

2.6 MIMO communications Systems Based on Wireless Channels

In contrast to MIMO communications systems based on transmission line channels, the literature on MIMO communications systems based on wireless channels is markedly more extensive and encompasses a greater amount of techniques for implementation. In order to reflect this in the context of a literature review, this section is divided three sub-sections. Firstly, section 2.6.1 introduces antenna diversity. Although the content of section 2.6.1 is not to be considered as a discussion MIMO communications systems per se, it does however introduce many relevant concepts. The MIMO communications system will be introduced from the point of view of a discussion of space-time codes which will be provided in section 2.6.2. It will be seen that the discussion in section 2.6.2 is pertinent to MIMO communications systems since multiple transmit and multiple receive elements can be utilised by

space-time codes. In section 2.6.3, Foschini's layered architecture or 'BLAST' (Bell Labs' Layered Space-Time) is first discussed and then from this the relevance of the singular value decomposition to MIMO communications systems based on wireless channels is introduced. This will then be seen to unify the approach taken in this thesis in relation to the discussion of MIMO communications systems based on wireless channels and the MIMO communications systems based on transmission line channels.

2.6.1 Antenna Diversity

The concept of antenna diversity refers to the idea of using multiple elements at either end of a communications link to mitigate the effect of multi-path propagation and the time variant nature of the wireless channel. In a practical sense, many different types of antenna diversity exist which are classed by the method in which the signals at the receive end are combined. A comprehensive discussion of these practical aspects of antenna diversity can be found in the text by Durgin [47]. The focus of the discussion in this section is on a capacity analysis of antenna diversity with some accompanying comments of communications system complexity.

The idea is now considered where antenna diversity can be achieved when there are multiple antennas at the transmitter and one antenna at the receiver. This can be referred to as a multiple-input/single-output (MISO) wireless link. It is also possible to consider the idea that antenna diversity can be achieved in a situation where there is one antenna at the transmitter and multiple antennas at the receiver, this can be referred to as a single-input/multiple-output (SIMO) wireless link. In this section, the number of receive elements will be denoted by N_R and the number transmit elements

will be denoted N_T. Furthermore in this section, unless otherwise stated, N_T will be set $N_T = 1$. This means that the SIMO wireless link will be discussed for the most part in this section. For a given amount of receive antennas N_R, as indicated, there will be N_R individual transfer functions for each of the wireless channels which exist between the transmit element and the N_R various receive elements. Taking the specific case where an identical antenna pattern and polarization are used, such a communications system is said to be exploiting 'spatial divserity' [49]. In relation to this, a vector of transfer functions, i.e. $\mathbf{h}$, may now be defined.

$$\mathbf{h} = \begin{bmatrix} h_1 \\ h_2 \\ \vdots \\ h_j \end{bmatrix} \tag{2.43}$$

Again for the sake of generality, define the elements of $\mathbf{h}$ as: $\mathbf{h} \sim C(0,1)$. The relevant expression for the capacity, in bits/sec/Hz, is:

$$C = \log_2\left[1 + \frac{P}{\varphi}\mathbf{h}^T\mathbf{h}\right] \tag{2.44}$$

The notation, $(\cdot)^T$, denotes the conjugate transpose of a vector. Gesbert [59] states that the impact of such a communications scheme on the capacity is to increase both the outage capacity, C_{Out}, and the average C_{Av} over the single transmit and receive element scheme making the link more reliable. In a mathematical sense the ratio, $\frac{P}{\varphi}\mathbf{h}^T\mathbf{h}$, will be seen to increase with increasing amount of receive elements. However, this improvement in performance is quite gradual with respect to increasing

the number receiver elements because the quantity, $\mathbf{h}^T\mathbf{h}$, is increasing inside the $\log_2$ function. Gesbert [59] also warns that the, "spatial diversity benefits quickly level off", by making direct reference to two situations. The first situation is where there are eight receive elements with the second situation being where there are nineteen receive elements. Gesbert [59] shows that this increase in receive elements from eight to nineteen has little effect on both of the capacities C_{Out}, and C_{Av}.

Durgin [47] and Vucetic et al [135] highlight that, in theory, the increase in Shannon capacity is equivalent for the situation where N_R is set $N_R = 1$ and the dimension N_T is increased. Indeed, Wennstrom [139] argues that when an antenna diversity technique known as beamforming is used in the case of multiple transmit elements, then such an antenna set-up can, in a practical sense, be optimal in terms of approaching Shannon capacity for a given ratio, $\frac{P}{\varphi}$. The concept of beamforming is described in work by Haynes [73]. In short, beamforming, for the case of multiple transmit elements, would use weights derived from knowledge of the communications channels between each transmit element and the receive element. In [139], Wennstrom's observation is independent of any practical consideration of communication system complexity. It is generally more convenient, in terms of communications system complexity, to obtain knowledge of the wireless channel at the receive end than the transmit end [59] [61]. Indeed, Gesbert [59] argues that multiple antennas at the transmit end, given the case where there is no knowledge of the channel at the transmit end, has the net effect of only increasing the outage capacity, C_{Out}, and not the average capacity, C_{Av}. This would appear to indicate that there is only an increase in the reliability of the communications link but not an

increase in its average capacity. In contrast to this, for multiple receive elements both quantities C_{Out} and C_{Av} are seen to increase due to more easily obtainable knowledge of the wireless channel.

This section has thus argued that, from a capacity perspective, it is logical to restrict the amount of transmit antennas to $N_T = 1$, while allowing for there to be multiple receive elements, i.e. a SIMO wireless link. This does not mean, however, that antenna communications systems with multiple transmit antennas are never considered as will be seen in section 2.6.2.

2.6.2 Space-Time Codes

In relation to space-time codes, there two main types of coding paradigm for these MIMO communications systems [61]. These two categories are known as space-time trellis codes (STTCs) and space-time block codes (STBCs). For a given ratio of transmit signal power, P to noise power ratio, φ, i.e. $\frac{P}{\varphi}$, STTCs appear as an attractive means of transmitting data in this context since they offer superior bit error rates (BERs). This means that STTCs offer superior 'coding gain' by comparison to STBCs. However, the complexity overhead of STTCs is such that the degree of attention that they are receiving in literature is gradually being superseded by the relatively lower complexity STBCs [59]. The greater emphasis on the appropriate design of STBCs that occurs in literature will be reflected here by discussing only STBSs and not STTCs. A comparative study of STTcs and STBCs may be found in work by Sandhu et al. [119].

Considering the case where is one transmit antenna and two receive antennas, Alamouti [2] was the first to consider the idea of a space-time block code (STBC) where, in a spatial sense, the data are transmitted in blocks of symbols rather than one symbol at a time. Firstly, two symbols: s_0 and s_1, where $s_0, s_1 \in \mathrm{C}$, are launched onto the communications channel over an arbitrary length time interval. Secondly, over the next similar time interval, another pair of symbols are launched which bear a specific mathematical relationship with respect to the first pair, these are: $-s_1^T$ and s_0^T. Denoting the conjugate transpose of a complex number as, $(\cdot)^T$, it is now possible to consider a matrix, $\mathbf{S}$:

$$\mathbf{S} = \begin{bmatrix} s_0 & -s_1^T \\ s_1 & s_0^T \end{bmatrix} \tag{2.45}$$

The rows of $\mathbf{S}$ denote antennas while the columns denote time-slots. Fig. 2.6 depicts Alamouti's STBC communications system.

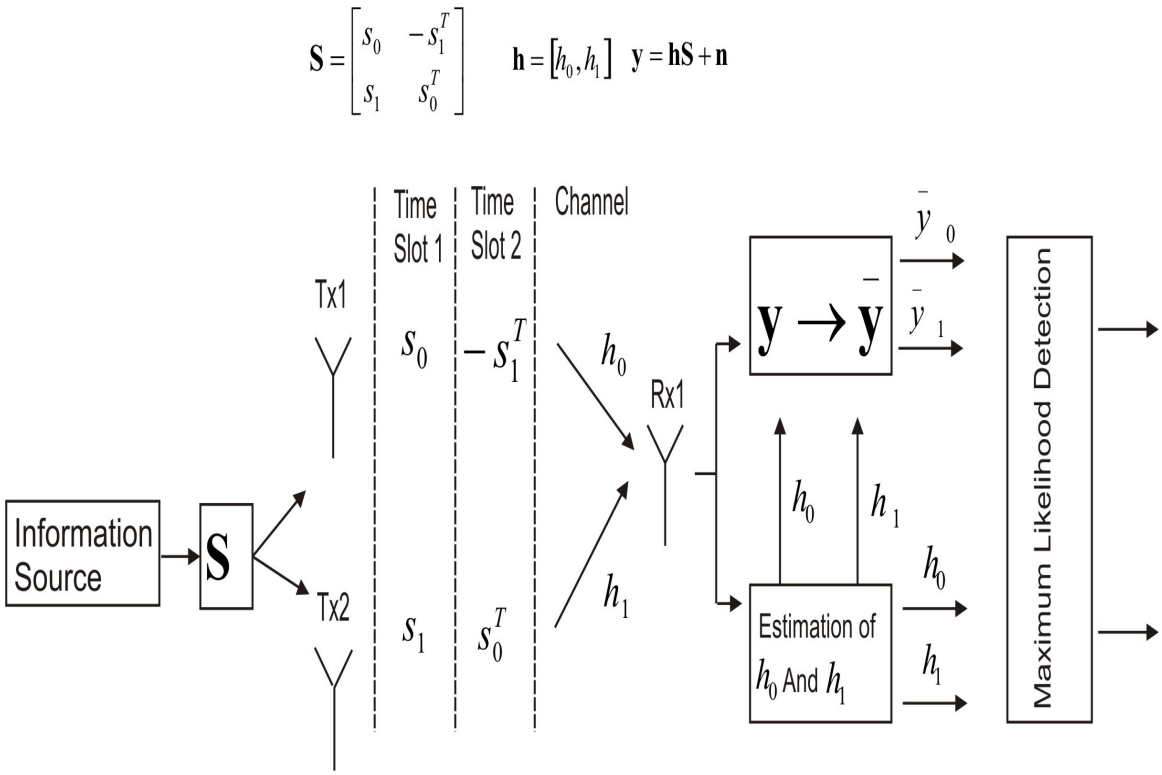

Figure 2.6: Alamouti's Space-Time Block Code Communications System.

The receiver detects and then collects data over two timeframes. If the vector of channel transfer functions is written as $\mathbf{h} = [h_0, h_1]$, then the appropriate receive vector, $\mathbf{y}$, is written as:

$$\mathbf{y} = \mathbf{hS} + \mathbf{n} \tag{2.46}$$

The vector, $\mathbf{n}$, is a vector of uncorrelated AWGN components. The matrix $\mathbf{S}$ may be thought of as a means of coding the two symbols, s_0 and s_1, across space and time and indeed may be thought of as an, 'array in time'. The mapping: $\mathbf{y} \rightarrow \bar{\mathbf{y}}$ depicted on the right hand side (RHS) of fig. 2.6 is now described in a series of mathematical steps. Although, $\mathbf{h}$ has been defined in this context as a vector, if the vector $\mathbf{y}^T$ is now considered then equation (2.46) may be rewritten as [61] [109]:

$$\mathbf{y}^T = \bar{\mathbf{H}}\mathbf{s} + \mathbf{n} \tag{2.47}$$

The vector, $\mathbf{s}$, contains the scalars which occur in time slot one and is defined as:

$$\mathbf{s} = \begin{bmatrix} s_0 \\ s_1 \end{bmatrix} \tag{2.48}$$

This leaves the matrix, $\bar{\mathbf{H}}$, to be defined as:

$$\bar{\mathbf{H}} = \begin{bmatrix} h_0 & h_1 \\ h_1^T & -h_0^T \end{bmatrix} \tag{2.49}$$

This matrix $\bar{\mathbf{H}}$ is orthogonal by design when subject to appropriate normalisation as can be seen in the expression which follows:

$$\bar{\mathbf{H}}\bar{\mathbf{H}}^H = \bar{\mathbf{H}}^H\bar{\mathbf{H}} = \left[|h_0|^2 + |h_1|^2\right]\mathbf{I}_2 \tag{2.50}$$

The matrix, $\mathbf{I}_2$, refers to the 2×2 identity matrix and the notation, $(\cdot)^H$, refers to the Hermitian transpose or conjugate transpose of a matrix. In order to decode the symbols at the receiver, the assumption made is that the channel transfer functions contained in $\mathbf{h} = [h_0, h_1]$ remain constant over the time period which is constituted by the two time slots, i.e. time slot 1 and time slot 2. Setting the factor, α, $\alpha = |h_0|^2 + |h_1|^2$, then another receive vector, $\bar{\mathbf{y}}$ may be defined as:

$$\bar{\mathbf{y}} = \bar{\mathbf{H}}^H\mathbf{y}^T = \alpha\mathbf{s} + \bar{\mathbf{n}} \tag{2.51}$$

Where the vector $\bar{\mathbf{n}}$ is defined as:

$$\bar{\mathbf{n}} = \bar{\mathbf{H}}^{H} \mathbf{n}. \tag{2.52}$$

The vector, $\bar{\mathbf{y}}$, is then passed to the maximum likelihood decoder whose task it is to retrieve the original transmit vector $\mathbf{s}$ from $\bar{\mathbf{y}}$. In summary therefore, this communications system may be thought of as retrieving two complex symbols based on the appropriate transmission of four complex symbols as contained in the matrix, $\mathbf{S}$. An appropriate expression for maximum likelihood detection in this context is given as:

$$\mathbf{s} = arg\ min \left\| \bar{\mathbf{y}} - \alpha \mathbf{s} \right\|^2 \qquad \mathbf{s} \in \mathbf{T} \tag{2.53}$$

The notation, $\|(\cdot)-(\cdot)\|^2$, refers to the squared Euclidean distance between two vectors. The matrix, $\mathbf{T}$, is defined here as a matrix that contains all possible combinations of the scalars contained in $\mathbf{s}$. The notation, $arg\ min$, thus means that the vector $\mathbf{s}$ is selected iteratively from the matrix $\mathbf{T}$ on the basis that the Euclidean distance squared between the vectors $\alpha\mathbf{s}$ and $\bar{\mathbf{y}}$ is minimised. Gesbert [61] gives an expression for the SNR of this communications system:

$$SNR = \frac{P}{\varphi}\alpha \tag{2.54}$$

As stated by Durgin [47], this Alamouti STBC communications system is equivalent to a communications system consisting of one transmitter and two receivers.

However, in reality, transmit diversity has now been achieved without the need for knowledge of the channels at the transmitter. It is also possible to implement a similar communications system using the same STBC for the case where there are two receivers [47].

The Almouti STBC is a transmission rate one code, which means that there is a one-to-one correspondence between the number of input symbols to the number of output symbols into the space time coder. Alamouti's scheme is unique when a modulation scheme using complex valued constellations is used in this particular regard. Specifically, the dimension of the transmit vector $\mathbf{s}$ is equivalent to the dimensions of a square matrix $\bar{\mathbf{H}}$. This one-to-one correspondence means that there is no coding delay or that there is a code rate of unity. Should $\bar{\mathbf{H}}$ be rectangular in respect of $\mathbf{s}$, this one-to-one correspondence does not hold and there is said to be a coding delay. In equation (2.51) the matrix, $\bar{\mathbf{H}}$, which arises from the space-time code $\mathbf{S}$, is square. However for situations where $N_T > 2$ with $\mathbf{s} \in \mathrm{C}$[11], in a mathematical sense, the matrices $\mathbf{S}$ and $\bar{\mathbf{H}}$ can never be square in dimension giving rise to a coding delay. If the mathematical condition $\mathbf{s} \in \mathrm{C}$ is changed to $\mathbf{s} \in R$, then for the cases where $N_T = 2,4,8$[12] it is possible to attain a full transmission rate [135][130][128]. This means that a one-to-one correspondence between the number of input symbols to the number of output symbols into the space time coder can be achieved. The reason for this is that square orthogonal code designs do exist in the case of real numbers but not

[11] $\in \mathrm{C}$ denotes the set of complex numbers. $\in R$ denotes the set of real valued numbers.

[12] As noted in [130], for the case where $N_T = 4$, this particular STBC is based on Hamilton's famous quaternion number.

for complex numbers. In a practical sense, this may mean sacrificing the amount of information in the modulation scheme for the low complexity in the STBC scheme. This could mean switching from a quadrature amplitude modulation (QAM) scheme which would require $\mathbf{s} \in \mathrm{C}$, to a pulse amplitude modulation scheme which only requires $\mathbf{s} \in R$. However, Tarokh *et al* [128] have shown that complex modulation constellations can achieve, at the very maximum, a $\frac{3}{4}$ transmission rate by appropriate design of the code matrix for cases where $N_T = 3,4$ only. They further showed that for all cases where $N_T > 4$, the maximum transmission rate is $\frac{1}{2}$. Also, in an attempt to remedy this barrier offered here by mathematics, Tirkkonen et al. have introduced, 'quasi-orthogonal' STBCs [131]. In this case, the transmission rate of one is maintained for the case where $N_T > 2$ with $\mathbf{s} \in \mathrm{C}$, but there is a loss in the BER performance, due to a loss in orthogonality or the 'quasi-orthogonality' offered by the code matrix. This loss in BER is a trade off for the superior transmission rate.

Using space-time block codes it is therefore possible to minimise the effect of multi-path fading by using an orthogonal code design to exploit antenna diversity provided by N_T, transmit elements. Space-time block codes therefore form the basis for a type of MIMO communications system. Although they do not offer the same degree of coding gain by comparison to STTC coding techniques, their comparably lower complexity is attractive from a design complexity point of view. One particular drawback of STBCs that has not been addressed here so far is the detrimental effect of imperfect knowledge of the channel on their performance. A possible solution to this is to use diffrential STBC (DSTBC) coding designs which do not require channel

knowledge at either the receiver or the transmitter. Work, by Tarokh [135] and others [129] [79] [77] [76], has addressed the design of DSTBCs. The basic premise on which they operate is that the data is encoded with respect to the interval between the symbols as opposed to encoding the data with respect to the actual value of the symbols themselves. However, successful operation of these differential STBCs is contingent on the quasi-static assumption holding for each burst of data. The drop in coding gain for the DSTBC designs is 3 dB with respect to the conventional STBCs discussed previously.

Finally, the invention of turbo coding technique in 1993 jointly by Berrou, Glavieux and Thitimajshima [147], is noted as a type of coding technique that can achieve near Shannon capacity results. Recent research at most notably the University of York has seen the proposal of a new type of space-time coding called, 'differential turbo space-time block coding' based on turbo coding over a rapidly changing channel where the quasi-static assumption no longer holds. The interested reader is referred to [123] [146] [145].

2.6.3 MIMO Communications Systems Based on Wireless Channels

In order to introduce an appropriate expression for the capacity of MIMO communications systems based on wireless channels, it is necessary to start with a brief mathematical description of what has been described as one of the first MIMO prototypes [47], i.e. Foschini's layered architecture. This system is sometimes referred to as 'BLAST' (Bell Labs' Layered Space-Time) architecture.

A more detailed description of this architecture can be found in [55] but Foschini's layered architecture is now described concisely as follows. Defining the channel matrix, $\mathbf{H}$, as:

$$\mathbf{H} \sim CR(0,1) \tag{2.55}$$

Specifically an uncorrelated Rayleigh fading channel with equal average power on all elements is considered and thus the notation, CR, denotes the complex Rayleigh distribution. This specific channel fading scenario has been described by Durgin [47] as the ideal MIMO channel and allows for the derivation of specific capacity equations which will be given at a later stage. To simplify the analysis here, the noiseless case of Teletar's linear model is given as:

$$\mathbf{y} = \mathbf{H}\mathbf{x} \tag{2.56}$$

Since[13]:

$$\mathbf{H}\mathbf{H}^{-1} = \mathbf{I}, \tag{2.57}$$

Then:

$$\mathbf{y} = \mathbf{H}\mathbf{H}^{-1}\mathbf{x} = \mathbf{I}\mathbf{x} \tag{2.58}$$

Thus in theory, each channel could then be separated by a simple linear combination of $\mathbf{H}^{-1}$ on the receive vector $\mathbf{y}$ and thus the transmit vector $\mathbf{x}$ could be retrieved at the receiver. The problem with such a straightforward architecture, however, is the

[13] The notation, $(\cdot)^{-1}$, refers to matrix inverse throughout.

presence of low powered channels between the transmit elements and the receive elements [47]. As result, some of data streams between the transmit elements and the receive elements which arise due to appropriate partitioning of the data into $\mathbf{x}$ can be irretrievable.

Foschini's layered architecture offers a solution to this problem by cycling the data before partitioning it in $\mathbf{x}$. The result of this is that each data stream or, indeed simply, each element of the transmit vector $\mathbf{x}$ will experience on average the same channel. In terms of the scalar elements of the vector, $\mathbf{x}$, the correspondence between these scalar elements and a given transmit element shifts with respect to an allotted time slot. This idea is highlighted in fig. 2.7 for a communications system where $N_T = 4$. In this case, a 'layer' corresponds to four time slots, with layer 1 equal to time slots one through to four, layer two is then equal to time slots two through to five, etc

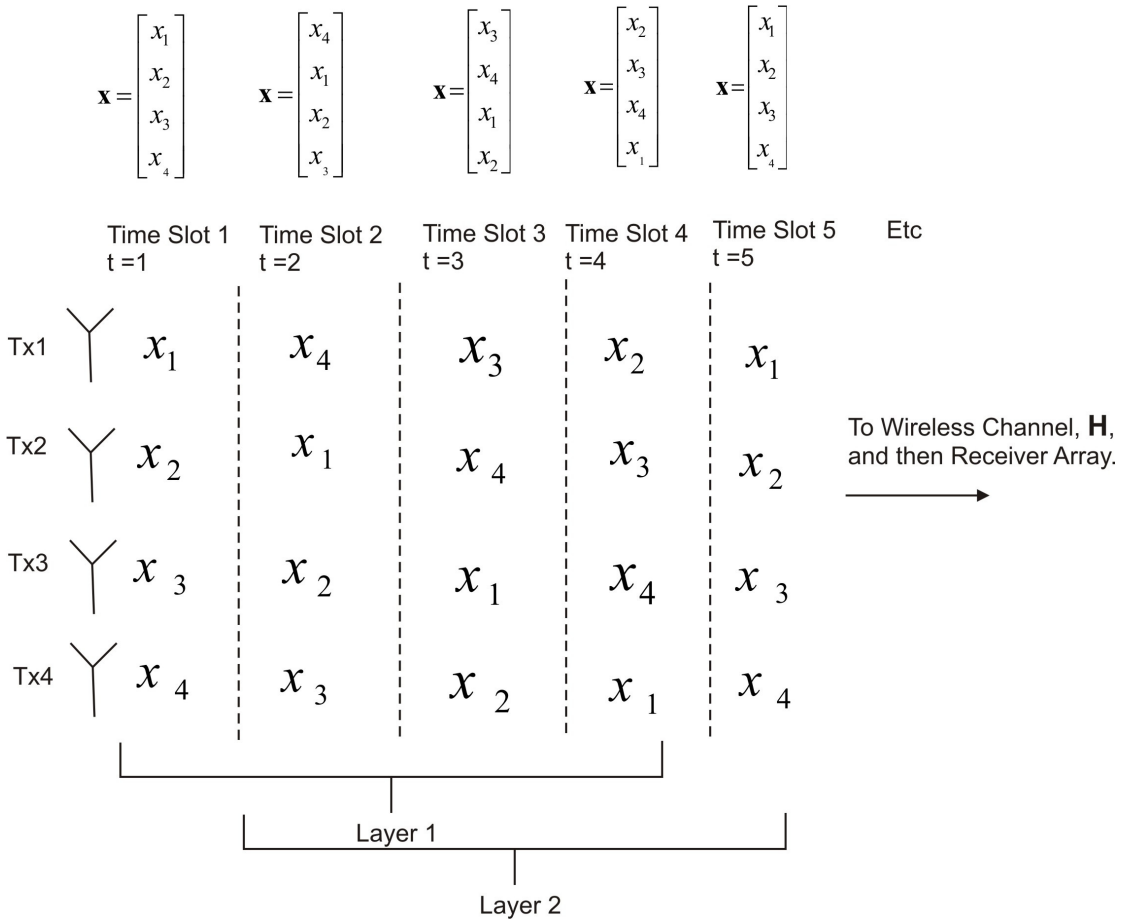

Figure 2.7: Transmission Scheme for Foschini's layered architecture for $N_T = 4$. Time slot 6 would come next and it reverts back to the sequence in time slot 2 and the cycle continues. Each layer corresponds to four time slots.

For this communications system, it is necessary to elaborate on the noiseless case of Teletar's linear model in equation (2.56). Although the matrix, $\mathbf{H}$, may change from time slot to time slot, it is assumed to remain constant with respect to a given layer. In the context of a time period corresponding to one layer:

$$\mathbf{y}(t) = \mathbf{H}\mathbf{x}(t) \tag{2.59}$$

The transmit vector, $\mathbf{x}(t)$, will be a function of the time slot number, t. Each scalar element with the vector $\mathbf{x}$ will correspond to a component of the transmit data stream. A similar conclusion can be inferred for the receiver vector, $\mathbf{y}(t)$. At the receiver, the first data stream, $\bar{x}_1$ which corresponds to the transmitted scalar element x_1, is retrieved from layer one. In theory, of course $\bar{x}_1 \approx x_1$, but the notation, " $\bar{}$ ", serves to distinguish the fact that $\bar{x}_1$ is retrieved from appropriate the stream of received data, corresponding to the vector $\mathbf{y}$, thus:

$$\bar{x}_1(t) = \mathbf{H}^{-1}_{j\,1}\,\mathbf{H}_{i\,1}\,\mathbf{x}(t) \qquad \forall i, j = 1,2,...,N_T$$

$$= \begin{bmatrix}1 & 0 & 0 & 0\end{bmatrix}\mathbf{x}(t) \tag{2.60}$$

$\mathbf{H}_{i\,1}$ refers to the first column of $\mathbf{H}$ since equation (2.60) has been qualified by the notation $\forall i, j = 1,2,...,N_T$. By virtue of the same qualifying notation, $\mathbf{H}^{-1}_{j\,1}$ refers to first row of the matrix $\mathbf{H}^{-1}$. Layer two can now be used to retrieve the data stream which corresponds to $\bar{x}_2(t)$:

$$\bar{x}_2(t) = \mathbf{H}^{-1}_{j\,2}\,\mathbf{H}_{i\,2}\,\mathbf{x}(t) \qquad \forall i, j = 2,3,...,N_T$$

$$= \begin{bmatrix}0 & 1 & 0 & 0\end{bmatrix}\mathbf{x}(t) \tag{2.61}$$

The process outlined in equation (2.60) is similar to the process in equation (2.61) with the key difference that the qualifying notation has been changed to

$\forall i, j = 2,3,...,N_T$. This now means that $\mathbf{H}^{-1}{}_{2}{}_{j}$ refers to the second row of $\mathbf{H}^{-1}$ but where the mathematical effect of the first column of $\mathbf{H}^{-1}$ has been removed, similarly $\mathbf{H}_{2}{}_{i}$ is the second column of $\mathbf{H}$ but where the mathematical effect of the first row has been removed. This process is referred to as 'interference suppression' which has been applied at this stage. It can be applied because the data stream referred to as $\bar{x}_1(t)$ is known and is removed from the receive signal vector $\mathbf{y}(t)$. In a mathematical sense, the removal of $\bar{x}_1(t)$ corresponds to an increase in the degrees of freedom which define $\bar{x}_2(t)$. From a practical point of view it is also possible to say that there has been increase in the diversity order. A similar conclusion can be inferred for the calculation of the data stream $\bar{x}_3(t)$ in layer three but where there would be a further increase in the diversity order due to the fact that the effect of the removal of data streams $\bar{x}_1(t)$ and $\bar{x}_2(t)$.

Clearly in order to retrieve all the data streams, a computation of the matrix, $\mathbf{H}^{-1}$, is necessary. This can be achieved using the singular value decomposition or the QR composition and a comparison of either method may be found in [142]. The capacity, in bits/sec/Hz, of the channel which corresponds to the data stream, $\bar{x}_1(t)$, i.e. $C(\bar{x}_1(t))$, is written as [150] [55] [47]:

$$C(\bar{x}_1(t)) = \log_2\left[1+\frac{P}{\varphi}\chi_2^2\right] \tag{2.62}$$

Owing to the way in which the channel matrix, $\mathbf{H}$, was defined in equation (2.55), the variable, χ^2, is chi-squared random variable. The qualifying subscript notation, $(\cdot)_2$, which indicates that it has two degrees of freedom.

Similarly, in the case of $C(\bar{x}_2(t))$, the corresponding chi-squared random variable, χ^2, will have four degrees of freedom, thus:

$$C(\bar{x}_2(t)) = \log_2\left[1+\frac{P}{\varphi}\chi_4^2\right] \tag{2.63}$$

The total capacity, C, in bits/sec/Hz, for a MIMO communications system defined by the dimension, N_T, of this type is given as [55]:

$$C = \sum_{k=1}^{N_T}\log_2\left[1+\frac{P}{\varphi}\chi_{2k}^2\right] \tag{2.64}$$

Equation (2.64) holds on the basis that the channel matrix, $\mathbf{H}$, was defined in terms of a complex Rayleigh distribution. Durgin [47] summarises Foschini's layered space-time architecture in the context where $N_T = 4$ as follows:

"…the receiver buffers the incoming streams of data and extracts streams in steps, each step lasting the duration of one single time slot. At every step, the receiver detects a layer of data, consisting of a single stream spanning a block of four time slots….This continues for other layers until time slot 5, when the receiver returned to detect the layer corresponding to stream 1."

Ariyavisitakul [7] [8] then showed that equation (2.64) was in actual fact a tight mathematical lower bound on a more optimal expression for the capacity. Ariyavisitakul provides a rigorous mathematical proof of this fact in the appendix to [8]. This more optimal expression for the capacity is written as [8]:

$$C_{\mathbf{D}} = \sum_{k=1}^{N_T} \log_2 \left[1 + \frac{P}{\varphi} \lambda_k \left\{ \mathbf{H}\mathbf{H}^H \right\} \right] \tag{2.65}$$

The notation, $C_{\mathbf{D}}$, is used here by anaology with case of the MIMO communications system based on the transmission line channels. $\lambda_k \{\cdot\}$ denotes the k^{th} eigenvalue of a matrix. In equation (2.65), $\lambda_k \left\{ \mathbf{H}\mathbf{H}^H \right\}$ refers to the k^{th} eigenvalue of the matrix $\mathbf{H}\mathbf{H}^H$. In relation to capacity gain offered by MIMO wireless systems, Gesbert [61] states that:

"the first results hinting at the capacity gains of MIMO (wireless communications systems) were published by Winters [140]."

Foschini and Gans [150] refer to equation (2.65) in a more general sense as the 'convenient formula for generalised capacity' in the context of wireless MIMO communications systems. Also, as indicated by Nguyen et al. [110] and Anderson [5], the most elegant means of achieving the capacity in equation (2.65) is to use the singular value decomposition. In common with many of the expressions for capacity thus far presented, the reader is reminded that equation (2.65) is in respect of continuous channels.

MIMO communications systems based on wireless channels require knowledge of the channel transfer functions given by the channel matrix, $\mathbf{H}$. In the case of the wireless channels, this is likely to occur because the channel changes at a rate quicker than the rate at which bursts of information are transmitted. The effect of this has been outlined in the studies by Médard [103], Weber et al [138] [137], Kyritsi et al. [93], Berriche et al. [14], Cano-Gutierrez et al. [20], and others [113] [64] [143] [153]. Indeed, Kyritsi et al. [93] concluded that as the amount of antennas used in the transmitter and receiver array was increased, the performance of the MIMO communications systems became more sensitive to a given extent of imperfect knowledge of the channel. Since the extent of imperfect knowledge of the channel is effectively defined as random quantity, studies by McKay and Collings [153], Goldsmith and Yoo [64] and Médard [103] have considered the derivation of a lower bound on the Shannon capacity of MIMO communications systems based on wireless channels.

2.7 Summary

In this chapter, the equation for the capacity of a communications system was introduced. The distinction was made between a continuous channel and a channel which uses discrete modulation schemes and thus the reader has been cautioned on the way in which the capacity metric is being applied throughout this thesis. The concepts of single-input/single-output (SISO) communications systems and multiple-input/multiple-output (MIMO) communications systems were introduced in the separate cases of transmission line channels and wireless channels. It is clarified that SISO in the context of transmission line channels refers to multiple neighbouring

transmission lines which couple each other in a nefarious manner due to FEXT. While MIMO, in this context, refers to the idea of using appropriate signal processing to mitigate the nefarious effect of FEXT coupling. In contrast, SISO in the context of wireless channels refers to idea of using a single transmit and single receive antenna for communication. While MIMO in this context refers to the use of using an array transmit antennas and an array of receive antennas. In either case, the approach taken was to introduce how limitations in SISO communications systems may be overcome by MIMO communications systems. The problem associated with channel knowledge in MIMO communications systems has also been highlighted.

Chapter 3: Experimental Observation of Channels

3.1 Introduction

Experimental observation of communications channels requires making physical measurements. The objective of this chapter is to outline the methodologies for making physical measurements on transmission line channels and wireless channels. Channel matrices containing transfer functions and vectors containing channel impulse responses will then be derived. The channel matrices are required to support the analysis of chapters 4, 6 and 7, whereas vectors containing appropriate channel impulse responses are required for the simulation model which will be introduced in chapters 5. The physical measurements of transmission line channels parallels the methodology of that described by Bostoen et al [18]. A novel aspect of this is the fact that direct connection and far-end crosstalk (FEXT) measurements are made in the frequency range from 300 kHz to 100 MHz on unbalanced transmission lines which has not been reported before. In the case of the wireless channels, the virtual array methodology of Ingram et al.[82] [83] is paralleled in order to make physical measurements indicative of a communications system using a transmitter array and a receiver array. However a novel aspect of the overall approach outlined for these wireless measurements is the fact that a specially constructed enclosure was built which was seen to be rich in multi-path reflections. As a result of this, Rayleigh channels are observed experimentally by removing in software the line-of-sight channel impulse response component. For the sake of clarity, all matrices and vectors which have been defined in this chapter are listed at the end of the chapter in order to provide a summary.

3.2 Transmission Line Channels

Physical measurement of gain and phase variation of the transmission scattering parameter (S -parameter), S_{21}, with frequency is central to the determination of the elements of channel matrix. S_{21}, is a two-port measurement of the ratio of the receive voltage to transmit voltage over a swept frequency response. In this work, this swept frequency response is from 300 kHz to 100 MHz. Measurements of S_{21} are made under matched conditions. In the case of the transmission line channels, measurements are made in both the frequency and time domain. Considering firstly, the frequency domain, the reader is reminded of the channel matrix introduced in chapter 2:

$$\mathbf{H} = \begin{bmatrix} h_{1,1} & h_{1,2} & \cdots & h_{1,N_T} \\ h_{2,1} & h_{2,2} & \cdots & \vdots \\ \vdots & \vdots & \ddots & \vdots \\ h_{N_T,1} & h_{N_T,2} & \cdots & h_{N_T,N_T} \end{bmatrix} \tag{3.1}$$

There are two distinct signal paths which were illustrated in chapter 2 and as can be seen in fig. 3.1, the off-diagonal terms of equation (3.1) pertain to measurements of far end crosstalk signal paths while the diagonal terms pertain to measurements of the direct connection signal paths. In both cases, transfer functions are calculated from:

$$h_{i,j} = |S_{21}| \exp\{j \angle S_{21}\} \tag{3.2}$$

$|S_{21}|$ is the magnitude of S_{21} while $\angle S_{21}$ is the phase angle of S_{21}. The measurement set-up is depicted in fig. 3.2.

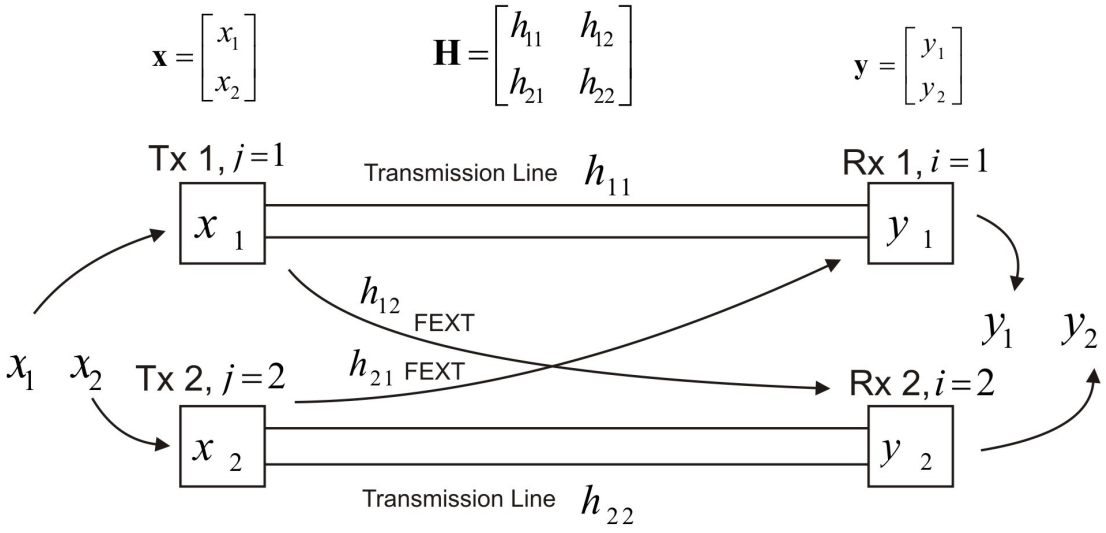

Figure 3.1: A multi-transmission line communications system defined by $N_T = 2$. The ground plane of the transmission lines has been omitted for the sake of generality. Equations are written above the various operations.

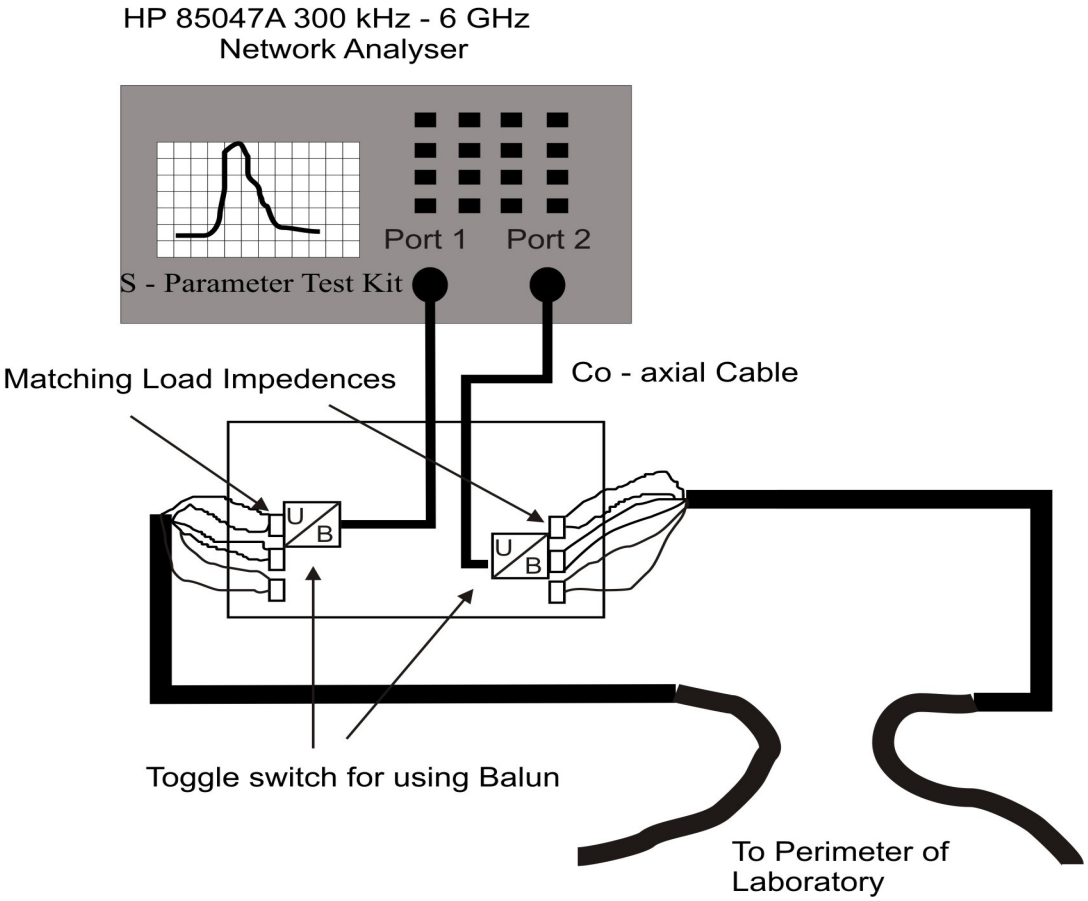

Figure 3.2: Experimental set-up for measurements of the S-parameters: S_{11} and S_{21}

Measurements were made using a HP 85047A microwave network analyser (MNA) capable of performing a swept frequency response over frequency range 300 kHz to 6 MHz. Fig. 3.2 shows that a balun may be switched in or out via a toggle switch to facilitate balanced or unbalanced transmission line operation. When the toggle switch is set to, 'B', the balun is activated. The balun is a device which facilitates an appropriate electrical interaction between the unbalanced currents in the co-axial cables and the balanced currents which are used in transmission over twisted-pair. The balun used was a 93 Ω BNC plug to RJ45 socket balun which was compatible with IBM 3270 system wiring [170]. Since the unbalanced transmission line would inherently not require a balanced current, the toggle switch, for the balun described, would be set to, 'U', for unbalanced transmission. Circuit diagrams which distinguish between balanced and unbalanced transmission are presented in fig 3.3 and 3.4. In either case, the reference plane of measurement may be extended just beyond the toggle switch for the balun, to the transmission line by means of a response calibration of the MNA. In the case of balanced transmission line measurements, this removed the effect of the balun on the measurements. It was done using the S-parameter test kit which is incorporated into the MNA. As a result of this response calibration, measurements were made exclusive of the effects of the co-axial leads. All transmission lines were removed from reels and were laid around the perimeter of the laboratory in order to make the measurements free from the effect of any cross coupling that would exist as the result of being on a reel. Three distinct types of transmission lines were measured and are described in table 3.1.

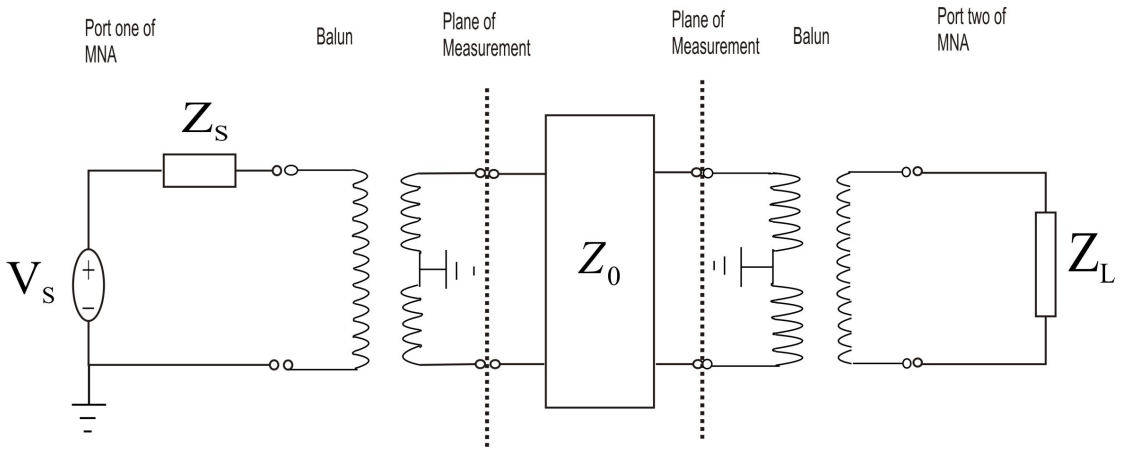

Figure 3.3: Circuit diagram depicting the balanced transmission line scheme. The transmission line has been depicted by the lumped component, Z_0. Matching is assumed thus: $Z_0 = Z_L = Z_S$.

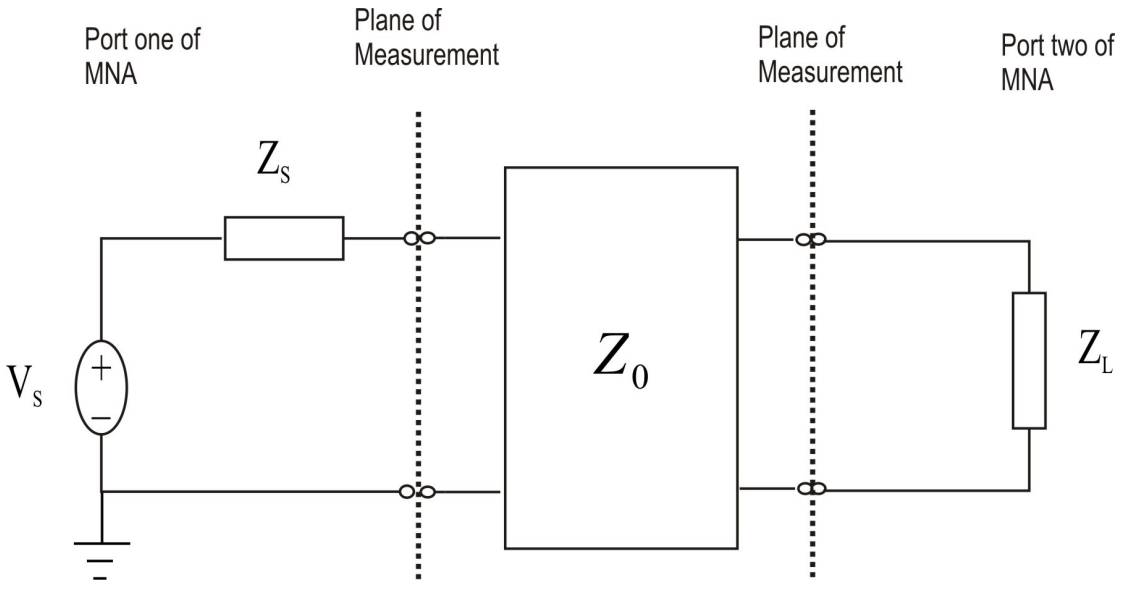

Figure 3.4: Circuit diagram depicting the unbalanced transmission line scheme. The transmission line has been depicted by the lumped component, Z_0. Matching is assumed thus: $Z_0 = Z_L = Z_S$.

Transmission Line Type	**Length**	**Twist-Rate**	**Thickness**
Cat 5 – Complies and exceeds ANSI/TIA/EIA[14] 568-A-5 and ISO/IEC 11801 drafts. Four Twisted-Pairs.	88 metres	Varied between one twist per cm and one twist per 3 cm length. Different rate on each pair.	0.5 mm: American wire guage (AWG) 24
Twisted-Pair Telephone cable. Five Twisted-Pairs	88 metres	1 twist per 8 cm. The same twist rate on all pairs	0.8 mm: AWG 20
Flat Pair: Burglar Alarm cable. Three Pairs	88 metres	Not Applicable	0.4 mm: AWG 26

Table 3.1: Specifications of experimentally observed transmission line channels.

In figs. 3.4 and 3.5, Z_L is the impedance into port two of the MNA and Z_S is the output impedance at port one of the MNA. Measurements were made under matched conditions and thus $Z_0 = Z_L = Z_S = 100\Omega$. In reality, any transmission line would be lossy over a frequency range of 300 kHz to 100 MHz and thus Z_0 is complex and varies with frequency. Indeed the four transmission line parameters R, L, G and C can readily be plotted for the case of Cat 5 transmission lines with respect to the frequency

[14] ANSI: American National Standards Institute, TIA: Telecommunications Industry Association, EIA: Electronics Industry Alliance, ISO: International Organisation for Standardisation, IEC: International Electro-technical Commission.

range of 300 kHz to 100 MHz using curve fitting methods [124] in figs 3.5 - 3.7.

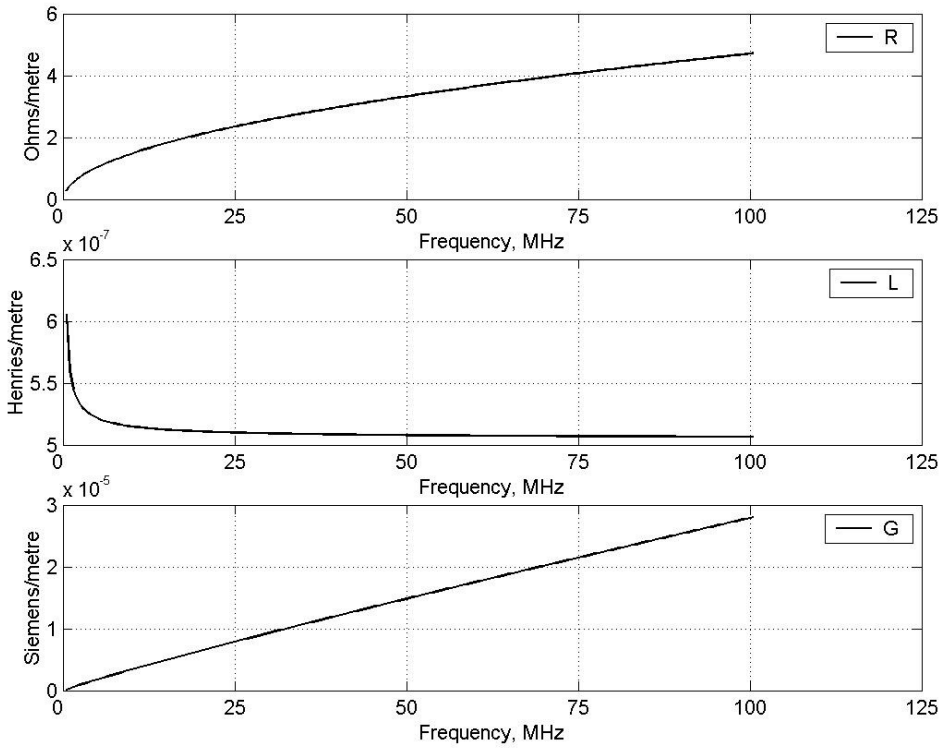

Figures 3.5-3.7: Three transmission line parameters: R, L, G over the frequency range from 300 kHz to 100 MHz plotted using curve fitting methods [124]. C remained at a value of 48.55×12 Farads per metre over the entire frequency range. Top: R in ohms per meter. Middle: L in Henries per metre. Bottom: G in Siemens per metre

Measurements of return loss, S_{11}, were made in order to quantify the goodness of matching over the frequency range of 300 kHz to 100 MHz . These return loss measurements are depicted in figs 3.8-3.10

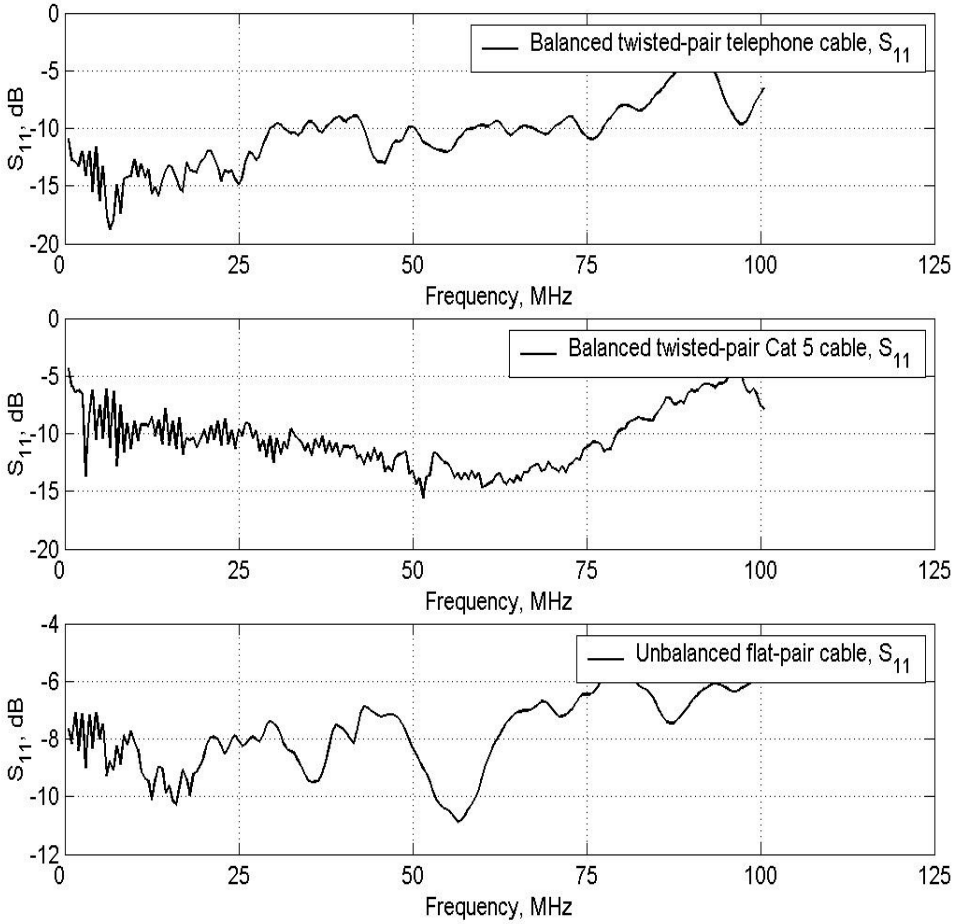

Figures 3.8-3.10: Measurements of S_{11}, the return loss, for telephone twisted-pair, cat 5 twisted-pair and unbalanced flat-pair respectively from top figure to bottom.

All transmission lines were terminated in 100Ω. Clearly, the return loss in the case of the telephone cable twisted-pair is low at low frequencies which is unsurprising given that it was designed to operate in the vocal frequency range. In contrast, the Cat 5 cable exhibits low return losses at high frequencies which is also unsurprising given that is designed to operate at comparatively higher frequencies than the telephone twisted-pair. The flat-pair exhibits higher figures for return loss figures over the frequency range than the other two transmission line schemes.

FEXT measurements were made by stimulating a given transmission line on port one and measuring on an alternate transmission line. All un-used pairs were terminated in $100\,\Omega$. Measurements were made firstly in the time domain in order to remove the effect of coupling between ports one and two by means of a process known as gating. This is particularly important in the context of FEXT measurements since these are quite sensitive in nature and thus any coupling between the two ports, however weak, could significantly alter the FEXT measurements. This coupling will be evident in the time domain as a received signal that is commensurate with the relatively short distance that it has travelled. A simple and approximate calculation of the expected time of arrival, $T_{arrival}$, of an electromagnetic pulse propagating down a transmission line with velocity factor, v_f, can be performed as:

$$T_{arrival} = \frac{L}{v_f c}$$
$$= \frac{88}{(0.6)(3\times10^8)}$$
$$= 489 \quad n\sec s$$

c is the speed of light in vacuum and v_f was chosen as 0.6. Windowing is required to alternate from frequency to the time domain signal representation. Windowing is a form of frequency domain filtering which is required to limit the effect of abrupt transitions which occur in the frequency domain at the start and stop sweep frequencies. It is a trade-off between side-lobe reduction and increased length of channel impulse response in the time-domain. It does not effect frequency domain measurements and is only apparent in the time domain. The 'normal' windowing option was chosen from a list: Minimum, Normal and Wide, since it provides a good trade-off between these effects [169]. The process of removing signals that are due to

coupling between the MNA ports, known as gating, can be facilitated by the MNA. Time domain measurements depicting both direct connection and FEXT signal paths are presented for three transmission line types are presented in figs 3.11 – 3.13.

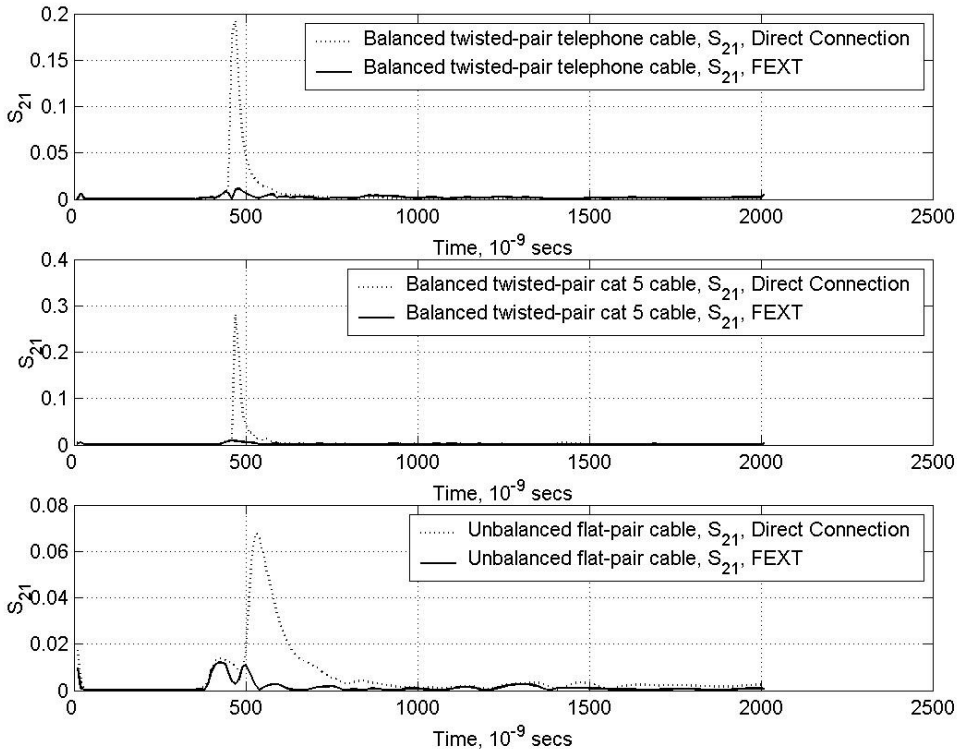

Figures 3.11-3.13: Measurements of S_{21} in the time domain, for telephone twisted-pair, cat 5 twisted-pair and unbalanced flat-pair respectively from top figure to bottom. Gating has been performed.

Clearly the time domain signals suffer less attenuation on cat 5 cabling than in the case of the telephone cable. The attenuation on the flat-pair is quite significant and it is because of this that it is deemed indicative of poor quality digital subscriber line (DSL). The propagation characteristics of the flat-pair appear unusual. This is thought to be due to a significant degree of both common mode and differential mode

propagation along the line. It may therefore be indicative of poorly balanced transmission lines. The corresponding frequency domain measurements are presented in fig. 3.14 – 3.16.

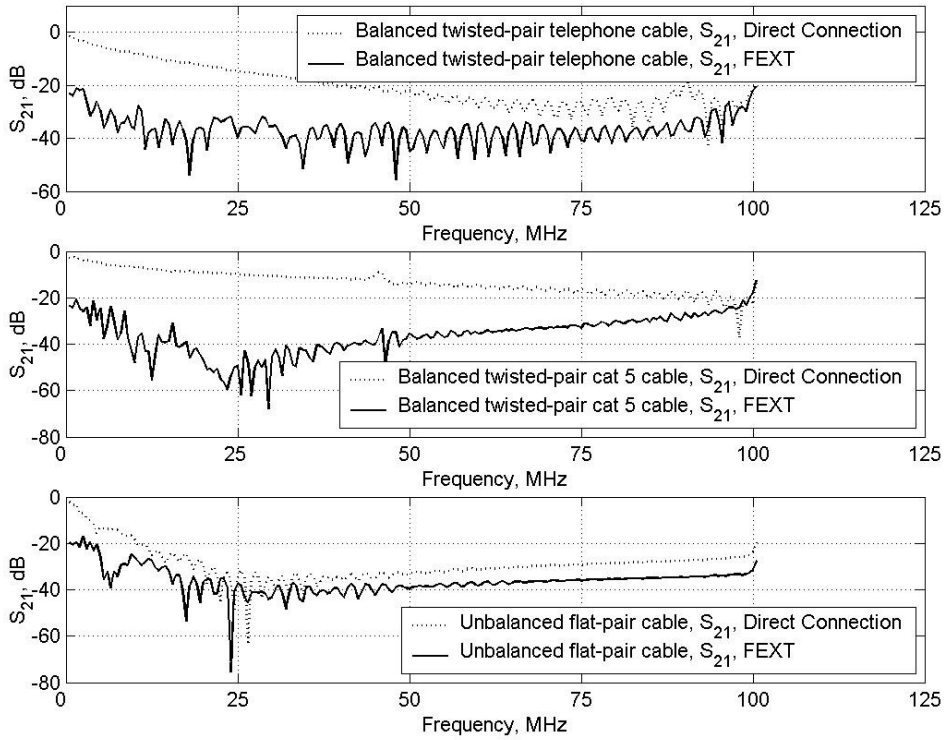

Figures 3.14-3.16: Measurements of S_{21} in the frequency domain, for telephone twisted-pair, cat 5 twisted-pair and unbalanced flat-pair respectively from top figure to bottom. The effect of MNA port coupling has been removed

The frequency domain measurements clearly indicate less attenuation and lower FEXT levels for the case of the cat 5 cable than for the other transmission lines. This concurs with the time domain measurements. Cat 5 cable complies with various standards as outlined in table 3.1. It is therefore argued that all other transmission line measurements may be benchmarked against Cat 5 as well as the analyses which follow.

3.3 Wireless Channels

By analogy with the previous section, the reader is reminded of the channel matrix:

$$\mathbf{H} = \begin{bmatrix} h_{1,1} & h_{1,2} & \cdots & h_{1,N_T} \\ h_{2,1} & h_{2,2} & \cdots & \vdots \\ \vdots & \vdots & \ddots & \vdots \\ h_{N_T,1} & h_{N_T,2} & \cdots & h_{N_T,N_T} \end{bmatrix} \tag{3.3}$$

However in the case of the wireless channels, the diagonal and off-diagonal terms of the channel matrix represent are pass-band transfer functions of multi-path wireless channels. The pass-band transfer function is defined as [120]:

$$h_{i,j} = \sum_{L=1}^{4} S_{21(L)} \exp\{j2\pi f \tau_{(L)}\} \exp\{j\angle S_{21(L)}\} \tag{3.4}$$

Considering a typical measurement of the multi-path wireless channel carried out in this work in fig 3.17, $S_{21(L)}$ is the amplitude response of the L^{th} multi-path component or 'tap' [120] or echo signature [67]. Similarly, the quantity, $\angle S_{21(L)}$, refers to the phase response of the L^{th} tap and $\tau_{(L)}$ refers to the time delay between the L^{th} tap and the tap which would be observed when there is through connection between port one and two of the MNA.

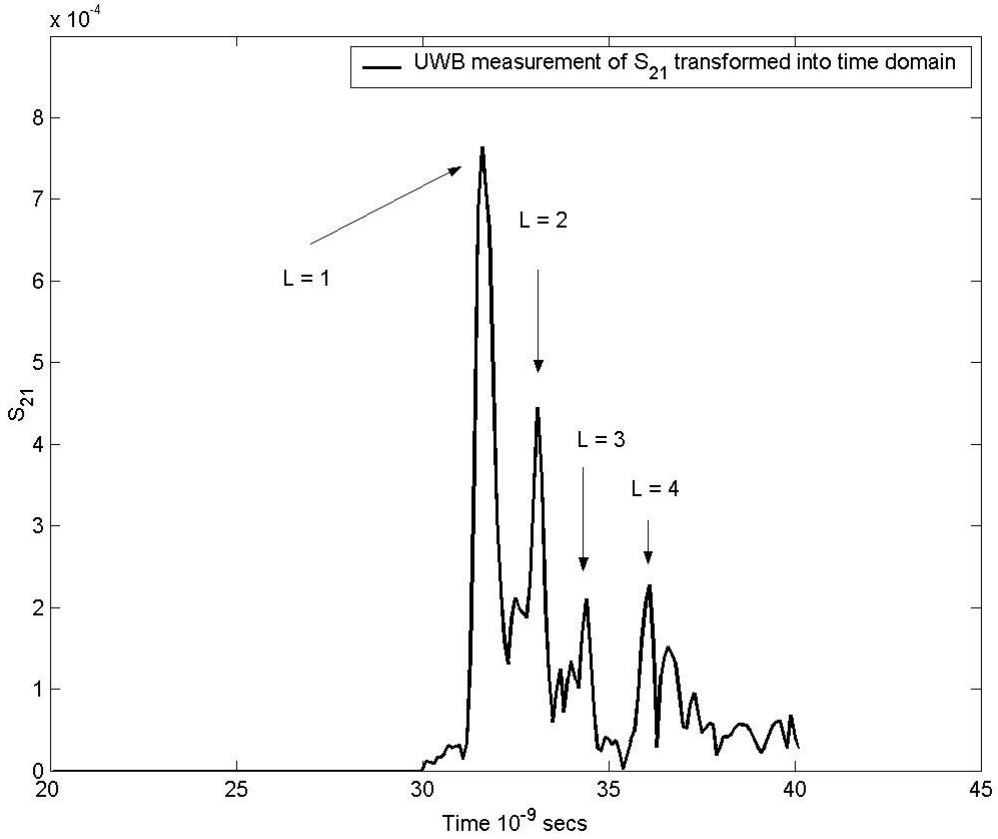

Figure 3.17: Multi-path channel impulse response

The quantity, f , in equation (3.4) refers to a carrier frequency. The choice of f is motivated by the fact that it is a popularly cited frequency encountered in literature [86] [97] [111] and is used in the IEEE 802.11a and HyperLAN standards [78]. Although various definitions for the ultra wide band (UWB) exist [117], it is discussed here in simple terms as the unlicensed frequency range from 3.1 GHz to 10.6 GHz where the isotropic transmit power spectral density is restricted to –41 dBm/MHz as assigned by the Federal Communications Commission (FCC) [127] [52]. The channel impulse response in fig 3.14 is formed from transformation of swept frequency response of S_{21} over the UWB frequency range. Considering the idea of the time-frequency uncertainty principle, the UWB is also deemed a sufficient bandwidth in order from which to form a channel impulse response in the time

domain which allows for experimental observation of multi-path reflections. A detailed mathematical description of the relationship between bandwidth and the corresponding duration of the time window, i.e. time-frequency uncertainty principle, can be found in [12].

A diagram of the experimental set-up for making wireless measurements is shown in fig. 3.18 along with a photo in fig. 3.19. The measurements were performed using an Anritsu 37369A Vector Network Analyser capable of performing a swept frequency response from 40 MHz to 40 GHz. This was clearly a different device to the one depicted in fig. 3.2 in the context of the transmission line channel measurements. A transmit and receive antenna, marked, 'Tx' and, 'Rx', respectively, are supported by retort stands. These antennas are printed strip monopole antennas which were designed by Ammann and John [3] and are impedance matched to their respective ports on the MNA. The S-parameter test kit, which is used in the calibration of the MNA, is used to extend the plane of measurement to the antennas themselves and thus the effect of the co-axial cables on any of the measurements has been removed. A series of microwave energy absorbing pads underneath appear under either retort stand in order to eliminate ground-plane reflection signal paths. A reflective enclosure is clearly marked in the bottom right hand side of the diagram. This enclosure was purposely constructed to give rise to a rich multi–path environment. Before making measurements of the multi-path channel, similar to the one in fig 3.17, measurements of the return loss from the Tx and Rx antennas, i.e. S_{11} and S_{22} respectively, were made over the UWB. These return loss measurements are given in fig. 3.19

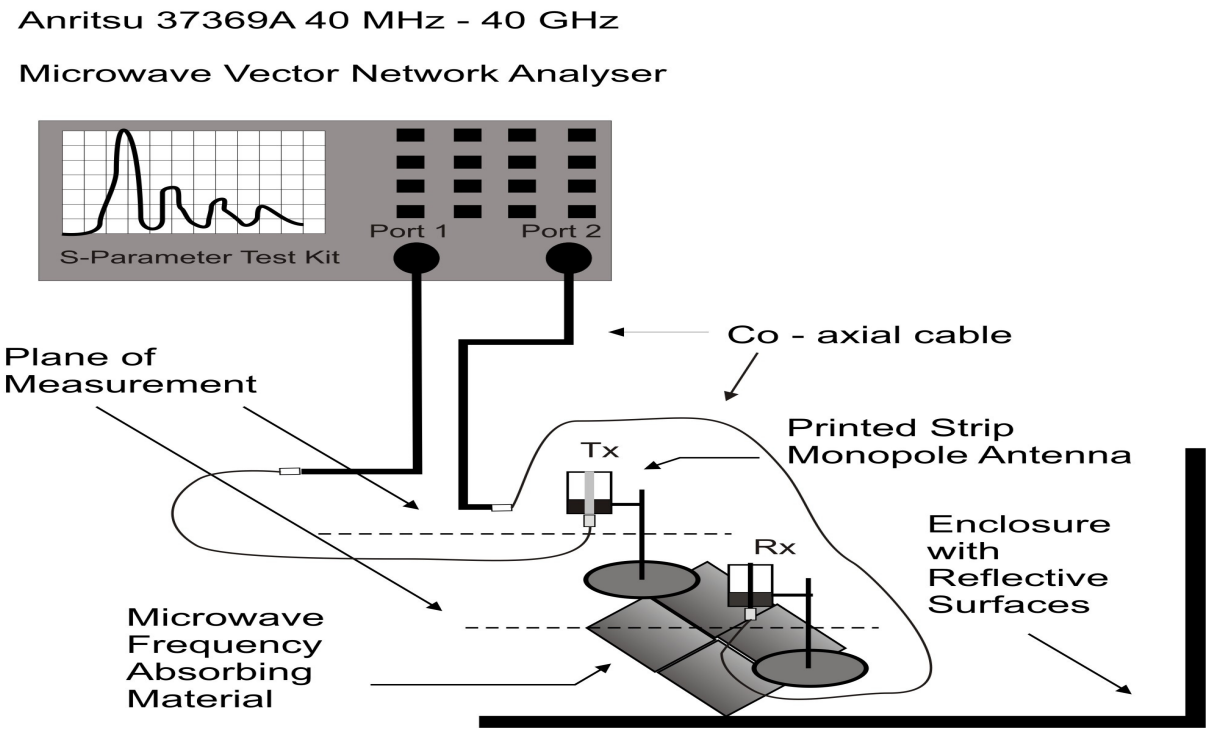

Figure 3.18: Experimental set-up for making measurements of S-parameters: S_{11}, S_{21}, and S_{22}.

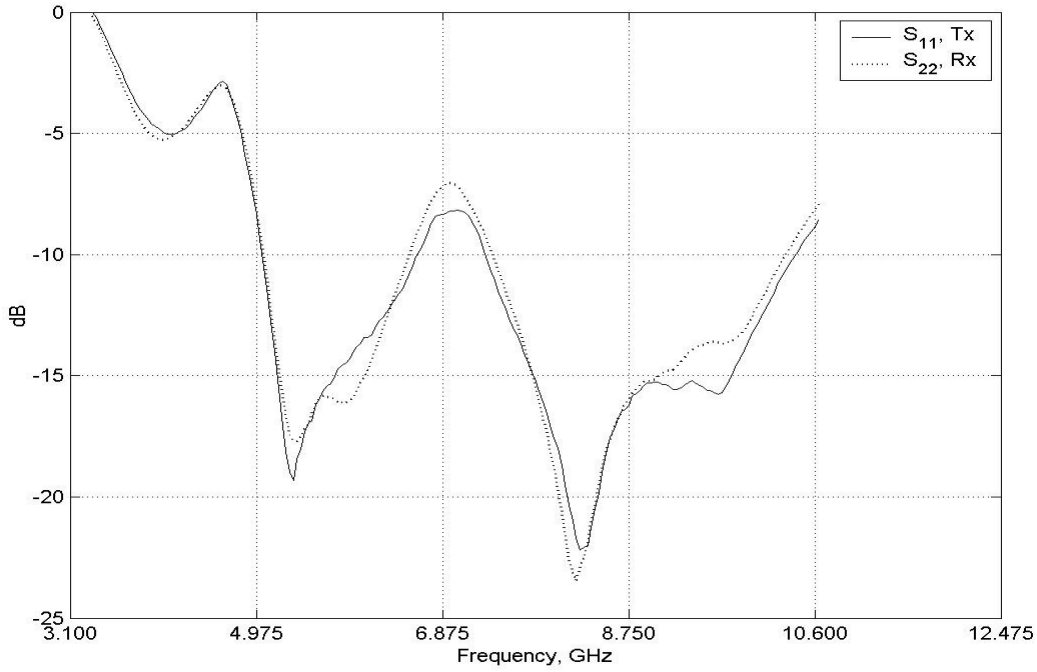

Figure 3.19: Measurements of return loss, S_{11} and S_{22}, over the UWB.

The return loss at the lower end of the UWB frequency range, i.e. at approximately 3.1 GHz, is high, but it is argued that the measurements using these antennas are indicative of a measurement in the UWB. Since the return loss is low at 5.2 GHz, the return loss measurements indicate that the carrier frequency of 5.2 GHz used in calculations of the passband transfer function is reasonable.

A diagram and photo of the multi–path environment which occurs as a result of the enclosure, depicted in fig 3.18, is given in fig. 3.20. Comparing fig. 3.17 and fig. 3.20, the first tap in fig. 3.17, i.e. where L = 1, should correspond to the signal path signal labelled as, 'line-of-sight (LOS)', in fig. 3.20. Similarly, the next two taps in fig. 3.17 should correspond to the two multi-path signals both labelled, 'first order/one reflection' in fig. 3.20. It may be inferred from fig. 3.20 that one of the first order multi-path signals traces a path which is substantially longer, in terms of distance, than the other. Thus, the two taps, labelled L = 2 and L = 3 in fig. 3.17, should correspond individually to the two first order multi-path-signal paths in respect to their times of arrival with respect to distance. Extending this argument, it may further be inferred that the multi-path signal component labelled, 'second order/two reflections', in fig. 3.20, should correspond to the final tap, labelled, 'L = 4', in fig. 3.17.

A time domain representation of a multi-path measurement has an equivalent frequency domain response, which consists of a series of frequency selective 'fades' or reductions in power. This idea has been stated explicitly by Bello [13] as well as Kaliath [85] and is integral in forming the idea of a wideband channel model.

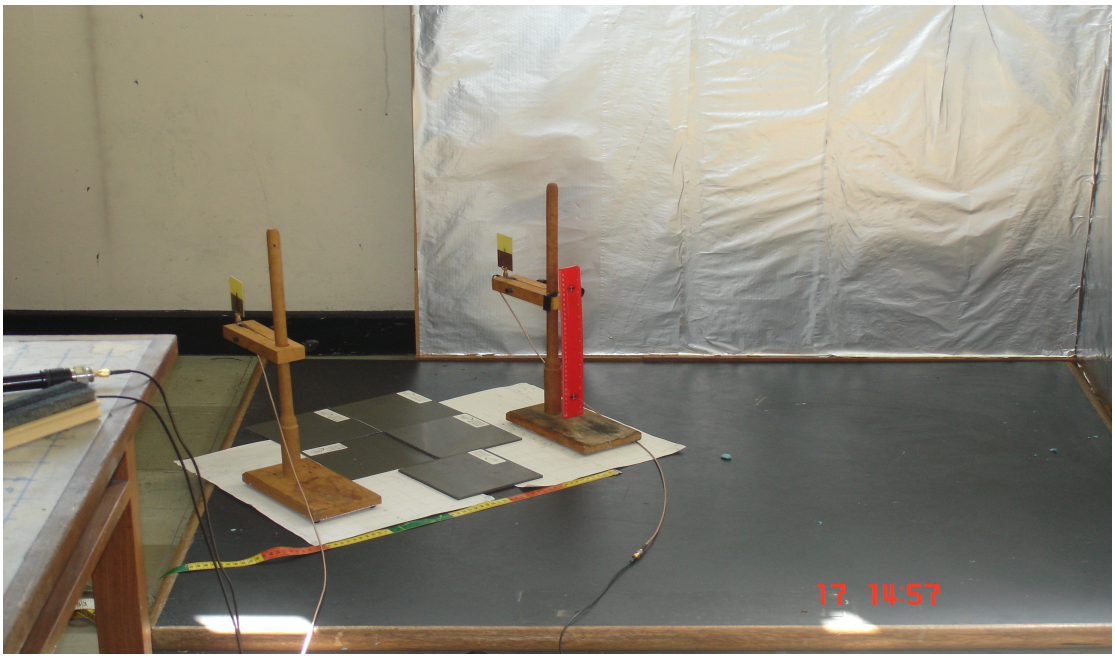

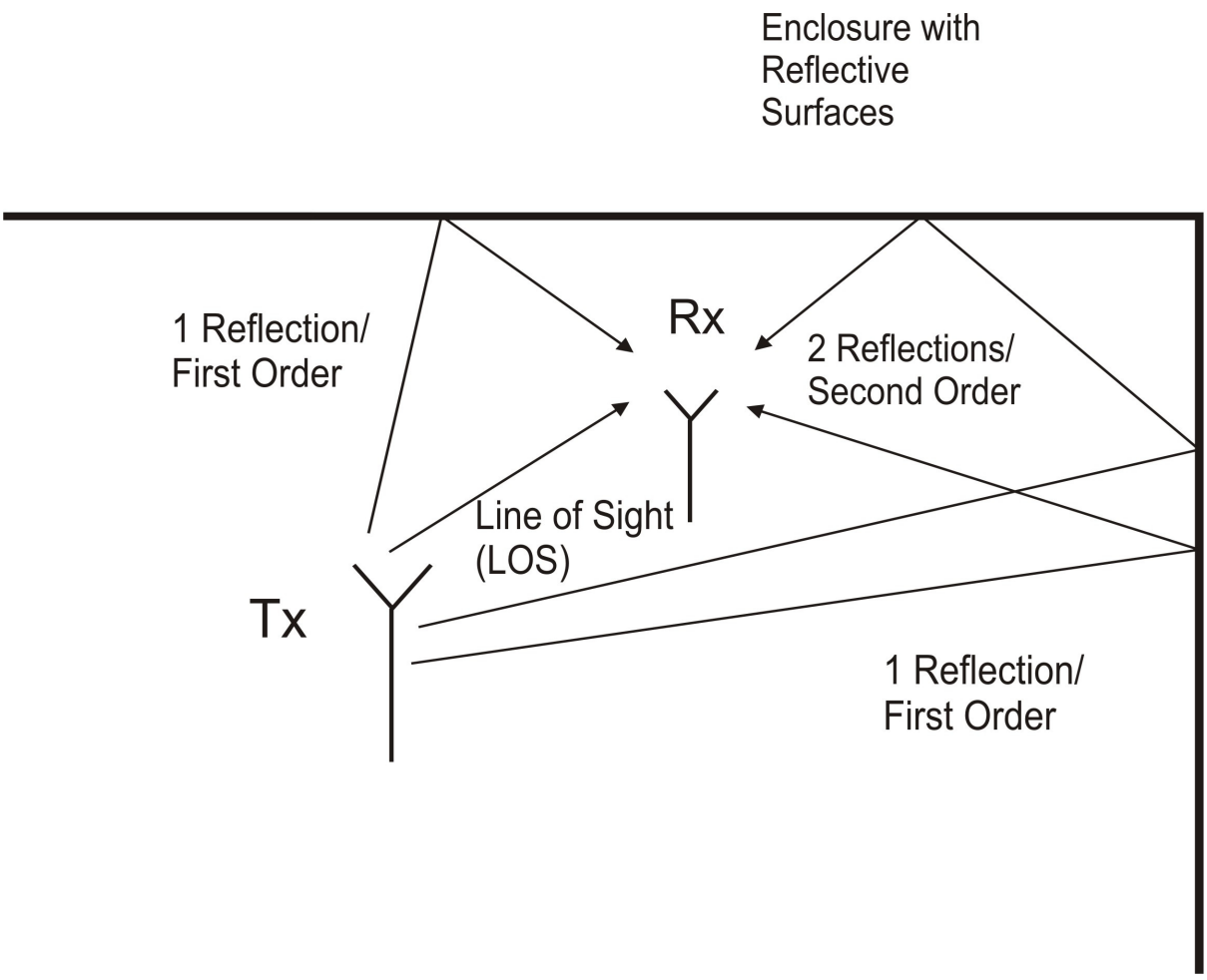

Figure 3.20: Diagram and photo of the multi–path environment which occurs as a result of the enclosure which has reflective surfaces.

In a communications system where the channel is time variant, these fades occur randomly with respect to frequency. As a result of this, the fading amplitude with respect to frequency is usually assessed as a statistical distribution. Two of the most common statistical distributions which are used to characterise multi-path wireless channels are known as the, 'Rayleigh' and 'Ricean' distributions. In this analysis the approach taken is that of Saunders [120] who states that,

"The Rayleigh distribution is an excellent approximation to measured amplitude fading statistics for channels in non line of sight situations".

In contrast, Saunders also states that,

"The Ricean distribution applies where one path (multi-path signal component) is much stronger than the other multi-path (components)".

The following transfer functions are now defined with respect to an appropriate qualifying sub-script notation which refers specifically to the channel impulse response component that has been removed.

$$h_{All} = \sum_{L} S_{21(L)} \exp\{j2\pi f \tau_{(L)}\} \exp\{j\angle S_{21(L)}\} \qquad \forall L = 1,2,3,4 \tag{3.5}$$

$$h_{LOS} = \sum_{L} S_{21(L)} \exp\{j2\pi f \tau_{(L)}\} \exp\{j\angle S_{21(L)}\} \qquad \forall L = 2,3,4 \tag{3.6}$$

$$h_{1^{st}\,order(1)} = \sum_{L} S_{21(L)} \exp\{j2\pi f \tau_{(L)}\} \exp\{j\angle S_{21(L)}\} \qquad \forall L = 1,3,4 \tag{3.7}$$

$$h_{1^{st}\,order(2)} = \sum_{L} S_{21(L)} \exp\{j2\pi f \tau_{(L)}\} \exp\{j\angle S_{21(L)}\} \qquad \forall L = 1,2,4 \tag{3.8}$$

$$h_{2^{nd}\,order} = \sum_{L} S_{21(L)} \exp\{j2\pi f \tau_{(L)}\} \exp\{j\angle S_{21(L)}\} \qquad \forall L = 1,2,3 \tag{3.9}$$

The subscript notation which appears in equations (3.5) to (3.9) refers to multi-path component which has been omitted from the calculation of the transfer function in each case. Equation (3.5) is merely a recasting of equation (3.4) for the sake of consistency in notation. Given the forgoing comments, h_{All}, is indicative of a Ricean channel and h_{LOS}, in equation (3.6) is a transfer function indicative of a 'Rayleigh channel', since the influence of line-of-sight multi-path component has been removed from the calculation of this transfer function.

Referring to fig. 3.15, not shown for the sake of clarity is a pair of grids with $\frac{\lambda}{2}$ increments, with respect to a frequency of 5.2 GHz, marked on them. The function of these grids is to facilitate measurements with respect to the 'virtual array' approach of for MIMO communications systems as outlined by Ingram et al [82][83][84]. The 'virtual array' approach to making physical measurements allows for the formation appropriate channel matrices. This approach allows for only one Tx and one Rx antenna to be used in order to make physical measurements which are indicative of an entire array of Tx and Rx antennas.

Taking the specific example where the dimension N_T, is set $N_T = 3$, the virtual array process is outlined in three steps in fig. 3.21. Reference is made to channel matrix subscript notation, $(\cdot)_{i,j}$, there are j transmitter positions and i receiver positions. In step one, the transmit antenna remains fixed in the position denoted $j = 1$ while three consecutive wireless channel measurements are made. For the first of these three measurements, the Rx antenna remains in the position denoted $i = 1$, but for the

second of these three measurements, it is then shifted to the position denoted $i = 2$. Similarly, for the third of these three measurements, the Rx antenna is shifted to the position denoted $i = 3$. In step two, this whole measurement process is then repeated but in this case the Tx antenna remains fixed in the position denoted $j = 2$, while the Rx antenna is then shifted as described previously for each of the respective three measurements required. Similarly, in step three, the Tx antenna remains fixed in the position denoted $j = 3$, while the Rx antenna is shifted as described in step one for each of the respective three measurements required.

The details of similar virtual array measurement campaigns can now be inferred for where the dimension, N_T is set $N_T = 2$, $N_T = 4$ or $N_T = 5$.

In respect of the shifts in position of $\frac{\lambda}{2}$, the approach adopted is in accordance with the views expressed in the following statement by Foschini and Gans [150] which appears to paraphrase a similar statement by Jakes [80]:

"The assumption of independent Rayleigh paths that we will also often make, is thought of as an idealized version of the result that for antenna elements placed on a rectangular lattice with half wavelength $\left(\frac{\lambda}{2}\right)$ spacing, the path losses tend to roughly decorrelate"

The chosen carrier frequency used in this analysis is 5.2 GHz, and thus the antenna spacing is set at 3 cm, i.e. $\frac{\lambda}{2}$.

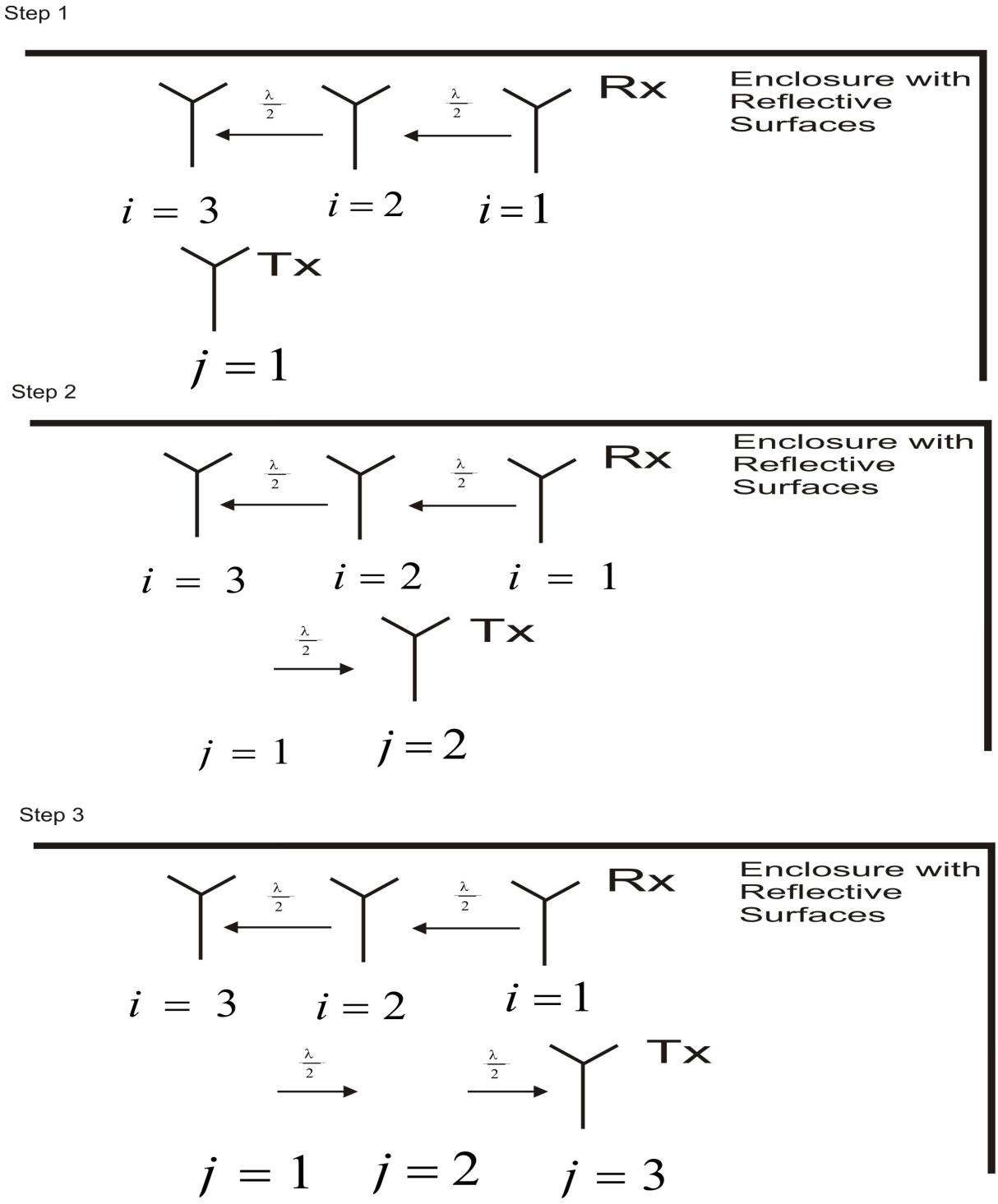

Figure 3.21: Virtual array approach to making measurements in three steps where the dimension, N_T, is set $N_T = 3$.

Having described virtual array approach, the appropriately subscripted channel transfer functions defined in equations (3.5) to (3.9) can be extended to appropriately subscripted channel matrices: $\mathbf{H}_{LOS}$, $\mathbf{H}_{All}$, $\mathbf{H}_{1^{st}Order(1)}$, $\mathbf{H}_{1^{st}Order(2)}$ and $\mathbf{H}_{2^{nd}Order}$. Furthermore, the scalar elements of the channel matrix, $\mathbf{H}_{LOS}$, are indicative of Rayleigh channels and similarly the scalar elements of $\mathbf{H}_{All}$ are indicative of Ricean channels. It is implicit that the dimension of these channel matrices can vary as N_T is set $N_T = 2$, $N_T = 3$, $N_T = 4$ or $N_T = 5$ as a result of the virtual array measurement campaign as outlined in fig. 3.18. As a result of this methodology, the experimental observation of the channel matrices: $\mathbf{H}_{All}$ and $\mathbf{H}_{LOS}$ have an equivalent degree of correlation in their multi-path channel impulse response components. This idea will be seen to be quite significant in relation to the analysis which will be based on these channel matrices.

It could be argued that Rayleigh channels per se may exhibit greater amounts of multi-path signals than what was indicated experimentally in fig 3.20. In order to support the fact that the channel matrix, $\mathbf{H}_{LOS}$, is indicative of a Rayleigh channel, the conditioning of this matrix is considered in terms of the eigenvalue properties of the matrix $\mathbf{H}_{LOS}\mathbf{H}_{LOS}^{H}$. The assumption that a Rayleigh distributed channel is observed in this experimental campaign when the line-of-sight channel impulse response is removed is now addressed. Consider firstly the Rayleigh fading channel, it has a Rayleigh distributed amplitude distribution, R, written as:

$$R = \sqrt{X^2 + Y^2} \tag{3.10}$$

Where X and Y are two uncorrelated normally distributed variables defined as:

$$X \sim N(0,1) \tag{3.11}$$

$$Y \sim N(0,1) \tag{3.12}$$

The phase response of the Rayleigh fading channel is uniformly distributed between 0 and 2π. Since both amplitude and phase information have now been defined for the Rayleigh channel, the notation $\sim CR$ is chosen to denote the Rayleigh channel in a mathematical sense. It is now possible to consider a matrix, $\mathbf{H}_{Ray}$, whose elements are complex random under the Rayleigh distribution:

$$\mathbf{H}_{Ray} \sim CR(0,1) \tag{3.13}$$

If $\mathbf{H}_{Ray}$ were of full rank and of dimension 5×5, it is then possible to consider the five eigenvalues, $\lambda_1,\lambda_2,...,\lambda_5$ of the matrix $\mathbf{H}_{Ray}\mathbf{H}_{Ray}^{H}$, or equivalently the squares of singular values of $\mathbf{H}_{Ray}$, in terms of the ratios:

$$\frac{\lambda_1}{\lambda_2},\frac{\lambda_1}{\lambda_3},\frac{\lambda_1}{\lambda_4},\frac{\lambda_1}{\lambda_5}$$

It will be seen in the forthcoming chapters that the maximum achievable capacity is attainable when all sub-channels have equal gains [92], this idea may then be written mathematically as:

$$\frac{\lambda_1}{\lambda_2},\frac{\lambda_1}{\lambda_3},\frac{\lambda_1}{\lambda_4},\frac{\lambda_1}{\lambda_5} = 0\text{dB} \tag{3.14}$$

These eigenvalues are denoted such that they are in descending magnitude from $\lambda_1,\lambda_2,...,\lambda_5$. In relation to this, this analysis will now consider the closeness of the

eigenvalue ratios to the condition in equation (3.14). The ratio $\frac{\lambda_1}{\lambda_5}$ can be referred to as the condition number of the matrix and so this exercise in fact considers matrix conditioning. In fig. 3.22, the closeness to the condition in equation (3.14) is considered for the case of the matrices: $\mathbf{H}_{Ray}$, $\mathbf{H}_{LOS}$ and $\mathbf{H}_{All}$. Since $\mathbf{H}_{Ray}$ is effectively a mathematically generated random matrix, the expected values of the ratios: $\frac{\lambda_1}{\lambda_2},\frac{\lambda_1}{\lambda_3},\frac{\lambda_1}{\lambda_4},\frac{\lambda_1}{\lambda_5}$, i.e. $E\left\{\frac{\lambda_1}{\lambda_2}\right\}$, $E\left\{\frac{\lambda_1}{\lambda_3}\right\}$, $E\left\{\frac{\lambda_1}{\lambda_4}\right\}$ and $E\left\{\frac{\lambda_1}{\lambda_5}\right\}$ are considered in this case. Each of the matrices: $\mathbf{H}_{Ray}$, $\mathbf{H}_{LOS}$ and $\mathbf{H}_{All}$ was normalised such that the sum of eigenvalues of the respective matrix $\mathbf{H}\mathbf{H}^H$ was unity in each case.

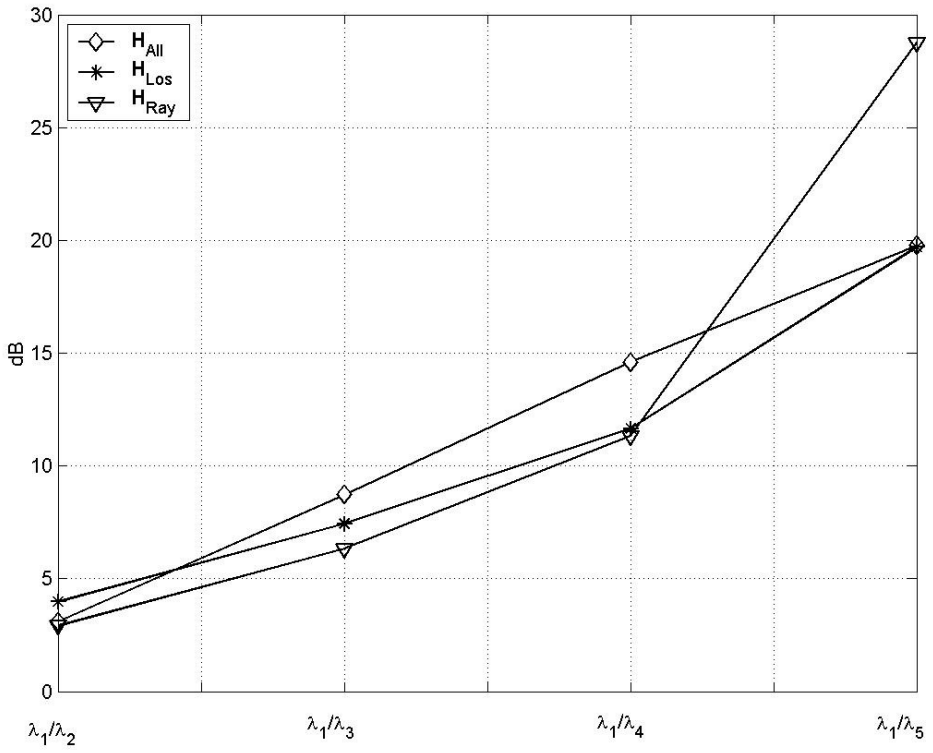

Figure 3.22: Eigenvalue distributions of $\mathbf{H}_{Ray}$, $\mathbf{H}_{LOS}$ and $\mathbf{H}_{All}$ in relation to the condition in equation (3.14).

Comparing the eigenvalue distribution in relation to $\mathbf{H}_{LOS}$ and $\mathbf{H}_{All}$, it can be seen that for the case $\mathbf{H}_{LOS}$ the ideal condition in equation (3.14) is more closely approximated than in the case of $\mathbf{H}_{All}$. In the case of $\mathbf{H}_{Ray}$, the first four eigenvalues approximate more closely the condition in equation (3.14) whereas the fifth eigenvalue is significantly skewed. Thus, it may be concluded that removal of the line-of-sight channel impulse response component significantly alters the eigenvalue distribution in a manner which more closely approximates the ideal condition in equation (3.14). The closeness of this to the case of the mathematically generated Rayleigh fading channel matrix, $\mathbf{H}_{Ray}$, has been indicated and it is argued that $\mathbf{H}_{LOS}$ is at least indicative of a Rayleigh channel.

Finally, time domain vectors are now defined using appropriate notation. Again, when this sub-script notation is applied to these time domain vectors, it does not reference elements within the vector but instead is purely descriptive of the measurement from which the vector is derived. The elements of two of these vectors, $\mathbf{h}_{All(1,1)}$, and $\mathbf{h}_{LOS(1,1)}$ are now plotted in fig. 3.23. The elements of $\mathbf{h}_{LOS(1,1)}$ are the same as the elements of $\mathbf{h}_{All(1,1)}$, except that software has been used to remove the tap which corresponds to the line-of-sight (LOS) channel impulse response component from this vector.

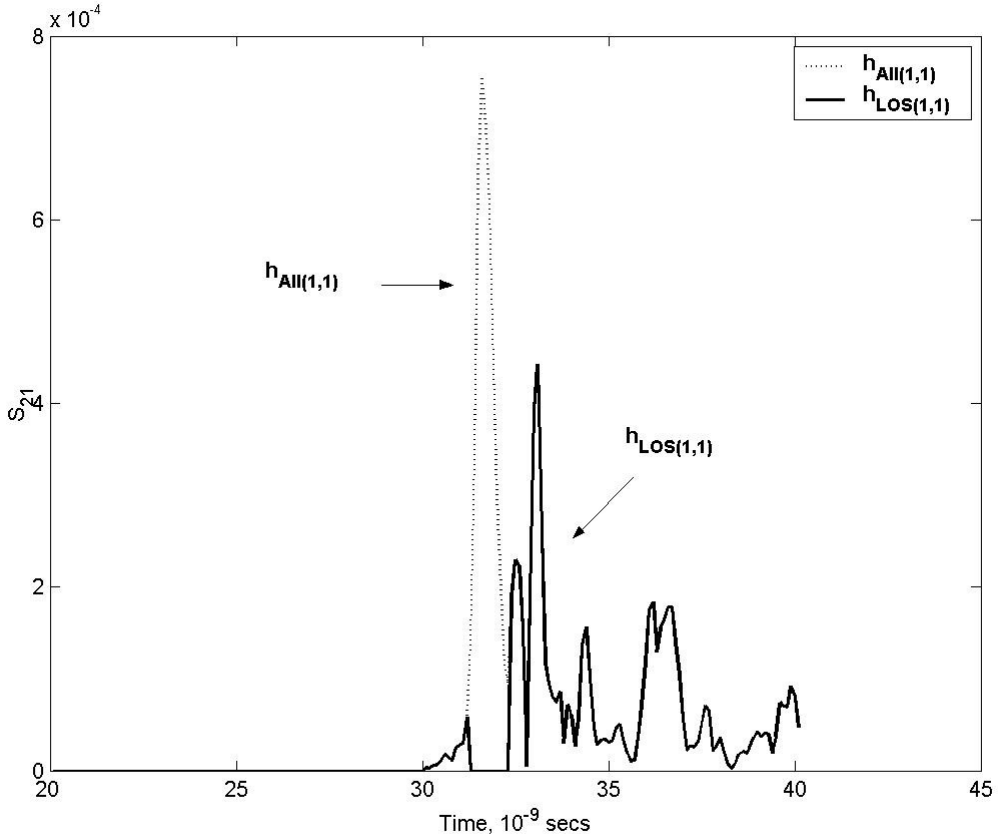

Figure 3.23: A plot of the two vectors, $\mathbf{h}_{All(1,1)}$, and $\mathbf{h}_{LOS(1,1)}$.

Taking the example where the dimension N_T is set $N_T = 3$, then a complete list of vectors pertaining to $\mathbf{h}_{All(i,j)}$ would be listed as follows:

$\mathbf{h}_{All(1,1)}$, $\mathbf{h}_{All(1,2)}$, $\mathbf{h}_{All(1,3)}$, $\mathbf{h}_{All(2,1)}$, $\mathbf{h}_{All(2,2)}$, $\mathbf{h}_{All(2,3)}$, $\mathbf{h}_{All(3,1)}$, $\mathbf{h}_{All(3,2)}$, $\mathbf{h}_{All(3,3)}$.

The appropriate list of vectors pertaining to $\mathbf{h}_{All(i,j)}$, in each case when the dimension, N_T, is set $N_T = 2$, $N_T = 4$, or $N_T = 5$, may be inferred by example. Again to clarify, the vector $\mathbf{h}_{LOS(1,1)}$ contains a channel impulse response indicative Rayleigh channel and similarly the scalar elements of $\mathbf{h}_{All(1,1)}$ are indicative of a Ricean channel.

Inspection of fig. 3.23 also reveals that if the Rayleigh channels are observed by simply removing the line-of-sight channel impulse response component using software then the channel impulse responses of the Ricean channel and the Rayleigh channel are equivalent except for this obvious exception. In a similar manner to the case of the channel matrices previously discussed, as a result of this methodology employed here the time vectors: $\mathbf{h}_{All(1,1)}$ and $\mathbf{h}_{LOS(1,1)}$ have an equivalent degree of correlation in their multi-path channel impulse response components. This idea will be seen to be quite significant in relation to the analysis and simulation which will be based on these vectors.

3.4 Summary

In this chapter, the methodology for making physical measurements on unbalanced transmission line channels, as well as balanced transmission line channels, using an HP 85047A MNA was outlined. This methodology paralleled that of Bostoen et al [18] but some novel aspects were highlighted. In the case of wireless channel measurements, an Anritsu 37369A MNA was used in a specially built enclosure in conjunction with the virtual array methodology of Ingram et al.[82][83][84]. This methodology was employed to make measurements indicative of an array of transmit antennas and receive antennas and again any novel aspects of this methodology were highlighted.

The measurements in this chapter were used to form a series of vectors and matrices which are now summarised:

In the case of the transmission line channels:

$\mathbf{H}_U(f)$: is channel matrix derived from transfer functions which were based measurements of S_{21} on an unbalanced three flat-pair transmission line cabling scheme. Off-diagonal terms represent FEXT signal paths, diagonal terms represent direct connection signal paths. It was evaluated over 201 points between 300 kHz and 100 MHz and its dimension is $N_T = 3$

$\mathbf{H}_B(f)$: is channel matrix derived from transfer functions which were based measurements of S_{21} on a balanced five twisted-pair transmission line telephone cabling scheme. Off-diagonal terms represent FEXT signal paths, diagonal terms represent direct connection signal paths. It was evaluated over 201 points between 300 kHz and 100 MHz and its dimension can be $N_T = 3$, $N_T = 4$ or $N_T = 5$.

$\mathbf{H}_C(f)$: is channel matrix derived from transfer functions which were based measurements of S_{21} on a balanced four twisted-pair transmission line cat 5 cabling scheme. Off-diagonal terms represent FEXT signal paths, diagonal terms represent direct connection signal paths. It was evaluated over 201 points between 300 kHz and 100 MHz and its dimension can be $N_T = 3$ or $N_T = 4$.

$\mathbf{h}_{U(i,j)}$: represents a family of $N_T \times N_T$ vectors, each of which contains 201 scalar elements which comprise a given channel impulse response measured on an unbalanced three flat-pair transmission line cabling scheme. For a given vector, when $i \neq j$, the channel impulse response of a signal path corresponding to FEXT is

indicated and when $i = j$ a direct connection signal path is indicated. The dimension N_T in this specific case is $N_T = 3$.

$\mathbf{h}_{B(i,j)}$: represents a family of $N_T \times N_T$ vectors, each of which contains 201 scalar elements which comprise a given channel impulse response measured on a balanced five twisted-pair transmission line telephone cabling scheme. For a given vector, when $i \neq j$, the channel impulse response of a signal path corresponding to FEXT is indicated and when $i = j$ a direct connection signal path is indicated. The dimension N_T in this specific case can be $N_T = 3$, $N_T = 4$ and $N_T = 5$

$\mathbf{h}_{C(i,j)}$: represents a family of $N_T \times N_T$ vectors, each of which contains 201 scalar elements which comprise a given channel impulse response measured on a balanced four twisted-pair transmission line cat 5 cabling scheme. For a given vector, when $i \neq j$, the channel impulse response of a signal path corresponding to FEXT is indicated and when $i = j$ a direct connection signal path is indicated. The dimension N_T in this specific case can be $N_T = 3$ or $N_T = 4$.

In the case of the wireless channels:

Channel matrices were defined, each of which contained transfer functions pertaining to various wireless channels that would be seen to exist between an array of transmit antennas and an array of receive antennas. With the obvious exception of $\mathbf{H}_{All}$, when computing the transfer functions for each channel matrix, a given channel impulse response was not factored in. The appropriate channel impulse response in each case

is denoted by the subscript that appears on each channel matrix. These channel matrices are as follows:

$\mathbf{H}_{All}$, $\mathbf{H}_{LOS}$, $\mathbf{H}_{1^{st}\,Order(1)}$, $\mathbf{H}_{1^{st}\,Order(2)}$ and $\mathbf{H}_{2^{nd}\,Order}$.

In each case, the dimension N_T can be $N_T = 2,3,4$ or 5.

The following vectors were also defined:

$\mathbf{h}_{All}$, $\mathbf{h}_{LOS}$, $\mathbf{h}_{1^{st}\,Order(1)}$, $\mathbf{h}_{1^{st}\,Order(2)}$ and $\mathbf{h}_{2^{nd}\,Order}$.

Each of these terms represents a family of $N_T \times N_T$ vectors, each of which contains 201 scalar elements which comprise a channel impulse response where the subscript notation denotes the channel impulse response component which was removed using software. Clearly, $\mathbf{h}_{All}$ contained all measured channel impulse response components and in each cased the dimension was $N_T = 5$.

Chapter 4: Capacity Analysis of MIMO Communications Systems

4.1 Introduction

In this chapter, the channel matrices which were derived from experimental observation of the channel in chapter 3 will be incorporated into comparative calculations of the capacities of MIMO and SISO communications systems. In the case of the transmission line channels, these comparative calculations propose the novel idea of using MIMO communications systems to allow, or indeed enhance, transmission lines which would have been previously deemed out-of-range in order that they can be used for high speed internet connections. In the case of the wireless channels, the idea that Rayleigh channels provide superior performance to Ricean channels is proposed on the basis of the conditions under which these channel were observed experimentally.

4.2 Capacity of MIMO Communications Systems

Teletar's linear model where the received vector $\mathbf{y}$ depends on the transmitted vector $\mathbf{x}$ is written mathematically as:

$$\mathbf{y} = \mathbf{H}\mathbf{x} + \mathbf{n} \tag{4.1}$$

In the case of transmission line channels, it was seen in chapter 2 that the off-diagonal terms of the matrix, $\mathbf{H}$, refer to the transfer functions of signal paths which arise due to far end crosstalk (FEXT). While the diagonal terms of the channel matrix, $\mathbf{H}$, refer to the transfer functions of the direct connections. In the case of wireless channels,

each of the scalar elements of the channel matrix, $\mathbf{H}$, is a transfer function of the wireless channel that exists between a given transmit antenna and a given receive antenna. $\mathbf{n}$ is a vector whose scalar elements are uncorrelated added white noise (AWGN) components. Throughout this analysis, the number of receive elements, N_T, will be set equal to the number of transmit elements, N_T. A depiction of Teletar's linear model is given in figure (4.1) where for the sake of clarity, the situation where $N_T = 2$ is illustrated.

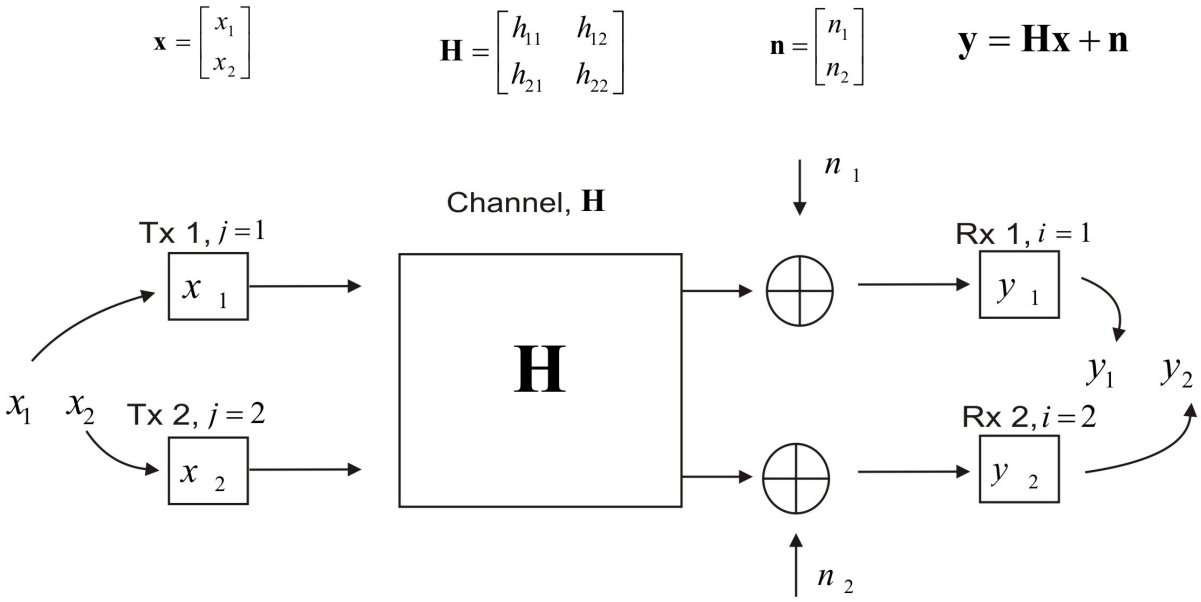

Figure 4.1: Teletar's linear model where the received vector $\mathbf{y}$ depends on the transmitted vector $\mathbf{x}$. Equations are written above the various operations. N_T is set $N_T = 2$.

The elements of the vector, $\mathbf{x}$, can be chosen from some complex valued alphabet of transmit symbols. The transfer functions contained in the channel matrix, $\mathbf{H}$, are also complex. The unified approach to the analysis of MIMO communications systems in the case of both transmission line channels and wireless channels which was

introduced in chapter 2 indicated the necessity of a singular value decomposition of the channel matrix, $\mathbf{H}$. The singular value decomposition of $\mathbf{H}$ may be written as:

$$\mathbf{H} = \mathbf{U}\mathbf{D}\mathbf{V}^H \tag{4.2}$$

The matrices: $\mathbf{H}, \mathbf{U}, \mathbf{D}$ and $\mathbf{V}$ have the following properties[105] [9] [126] [104] [48] [94] [134] [89] [136] [125]:

$$\mathbf{U}, \mathbf{H}, \mathbf{V} \in \mathrm{C}^{N_T \times N_T} \tag{4.3}$$

$$\underset{j}{\mathbf{U}}^T \underset{j}{\mathbf{U}} = \underset{j}{\mathbf{V}}^T \underset{j}{\mathbf{V}} = 1 \tag{4.4}$$

$$\begin{aligned} \mathbf{D} &= diag\{\sigma_1, \sigma_2, ..., \sigma_{N_T}\} \\ &= \begin{bmatrix} \sigma_1 & 0 & \cdots & 0 \\ 0 & \sigma_2 & \cdots & 0 \\ \vdots & \vdots & \ddots & \vdots \\ 0 & 0 & \cdots & \sigma_{N_T} \end{bmatrix} \end{aligned} \tag{4.5}$$

Equations (4.3) and (4.4) indicate that the matrices $\mathbf{U}$ and $\mathbf{V}$ are unitary matrices which means that, as stated in equation (4.4), the inner product of each of their constituent column vectors is unity or, equivalently, $\mathbf{U}^H\mathbf{U} = \mathbf{U}\mathbf{U}^H = \mathbf{V}^H\mathbf{V} = \mathbf{V}\mathbf{V}^H = \mathbf{I}_{N_T}$, where the notation, $\mathbf{I}_{N_T}$, denotes an identity matrix of appropriate dimension, N_T. Also, the columns of $\mathbf{U}$ and $\mathbf{V}$ contain the eigenvectors of the matrices $\mathbf{H}\mathbf{H}^H$ and $\mathbf{H}^H\mathbf{H}$ respectively. $\mathbf{D}$ is a diagonal matrix containing the non-negative square roots of the eigenvalues of $\mathbf{H}\mathbf{H}^H$ in numerical order with the highest appearing in the top-left most corner as σ_1 and lowest appearing bottom right most corner as σ_{N_T}. The eigenvalues of $\mathbf{H}\mathbf{H}^H$ will be denoted $\lambda_1, \lambda_2, ...\lambda_{N_T}$ with the non-negative square roots of these eigenvalues, which are

equivalent to the singular values of the matrix $\mathbf{H}$, being denoted $\sigma_1, \sigma_2, ...\sigma_{N_T}$. It should be noted in passing that owing to the Hermitian symmetry of the matrix, $\mathbf{HH}^H$, its eigenvalues are numerically equivalent to its singular values [105]. Returning to Teletar's linear model in equation (4.1), if the receive vector, $\mathbf{y}$, is appropriately weighted then the following substitution is made:

$$\bar{\mathbf{y}} = \mathbf{U}^H \mathbf{y} \tag{4.6}$$

Given the singular value decomposition of the matrix $\mathbf{H}$ in equation (4.2), Teletar's linear model may now be rewritten as:

$$\mathbf{y} = \mathbf{UDV}^H \mathbf{x} + \mathbf{n} \tag{4.7}$$

The substitution of equation (4.6) into Teletar's linear model into equation (4.7) gives:

$$\bar{\mathbf{y}} = \mathbf{DV}^H \mathbf{x} + \bar{\mathbf{n}} \tag{4.8}$$

The vector, $\bar{\mathbf{n}}$, is set $\bar{\mathbf{n}} = \mathbf{U}^H \mathbf{n}$ and refers to the way in which the vector of uncorrelated AWGN components, $\mathbf{n}$, has been transformed by appropriate weighting of the receive vector $\mathbf{y}$. Further to this, if the transmit vector, $\mathbf{x}$, is appropriately weighted then the following substitution is made:

$$\bar{\mathbf{x}} = \mathbf{Vx} \tag{4.9}$$

Then, incorporating the substitution in equation (4.9) into equation (4.8):

$$\bar{\mathbf{y}} = \mathbf{D}\bar{\mathbf{x}} + \bar{\mathbf{n}} \tag{4.10}$$

Equation (4.10) reveals that if the substitutions in equations (4.6) and (4.9) are made

then it is possible to transform the communications channel defined by $\mathbf{H}$ into a series of N_T orthogonal sub-channels defined by the matrix, $\mathbf{D}$. In saying this, the assumption has been made that the channel matrix, $\mathbf{H}$, is of rank, N_T. Thus, by definition, $\mathbf{H}$, has N_T linearly independent columns and rows and hence also has N_T non-zero singular values which would be contained along the main diagonal of the matrix, $\mathbf{D}$ [89]. Fig. (4.2) illustrates how the mathematical operations described transform the channel matrix, $\mathbf{H}$, from Teletar's linear model in figure (4.1) into a diagonal matrix, $\mathbf{D}$, thereby creating a MIMO communications system. In common with figure (4.1), N_T is set $N_T = 2$ for the sake of simplicity.

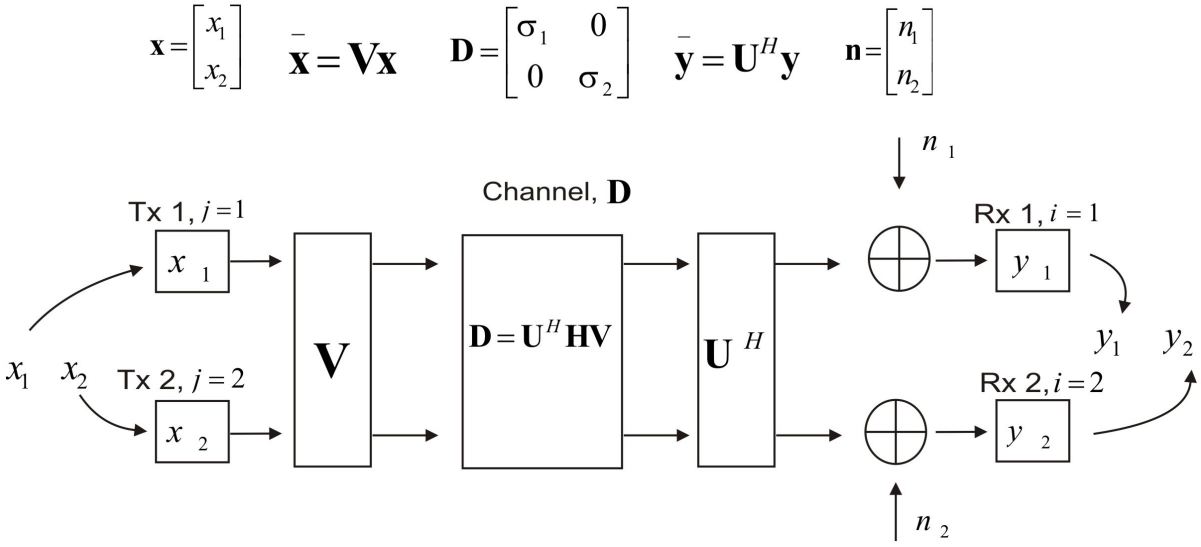

Figure 4.2: The MIMO communications system consisting of two transmit elements and two receivers elements. Equations are written above the various mathematical operations in the MIMO Communications system. N_T is set $N_T = 2$.

Foschini [150], Winters [140], Teletar [152] and many others [35] [95] [108] [10] have given the capacity a MIMO communications system. Since the MIMO communications system may be considered as a series of orthogonal sub-channels or 'eigenmodes', whose transfer functions are the singular values of the channel matrix, $\mathbf{H}$, the capacity, $C_{\mathbf{D}}$ in bits/sec/Hz, of a MIMO communications system now follows:

$$C_{\mathbf{D}} = \sum_{i=1}^{N_T} \log_2 \left[1 + \frac{P}{\varphi} \cdot [\sigma_i]^2 \right] \tag{4.11}$$

The use of the sub-script notation, $(\cdot)_{\mathbf{D}}$, distinguishes between the capacity of the MIMO communications systems and the capacity, C, of SISO communications systems. $C_{\mathbf{D}}$, has been referred to by Foschini [150] as, "the convenient formula for generalised capacity". It is more conventional in literature [150] [106] [37] [35] [95] [108] [10] [46] [51] [50] [140] [16] [17] [40] [36] [39] to write equation (4.11) as:

$$C_{\mathbf{D}} = \sum_{i=1}^{N_T} \log_2 \left[1 + \frac{P}{\varphi} \cdot \lambda_i \right] \tag{4.12}$$

It can be inferred from the discussion here that equations (4.11) and (4.12) are equivalent since the eigenvalues of the matrix $\mathbf{H}\mathbf{H}^H$ defined previously using the notation $\lambda_1, \lambda_2, ...\lambda_{N_T}$ are equivalent to the squares of the singular values of the matrix $\mathbf{H}$ defined previously using the notation: $\sigma_1, \sigma_2, ...\sigma_{N_T}$. Another equivalent of $C_{\mathbf{D}}$ incorporates the matrix notation outlined in this section, this is:

$$C_{\mathbf{D}} = \sum_{i=1}^{N_T} \log_2 \left[1 + \frac{P\left|\mathbf{D}_{i,i}\right|^2}{\varphi} \right] \tag{4.13}$$

Equations (4.11), (4.12) or (4.13) are equivalent forms. The reader is reminded that they refer to the capacity of the continuous channel as outlined in chapter 2. The units are in bits/sec/Hz, and thus may also be referred to as bandwidth efficiency but will be referred to as capacity throughout this thesis as is the convention in MIMO literature. Equation (4.13) is convenient since it makes direct reference to the matrix, $\mathbf{D}$, and will be the one used throughout this work.

4.3 Capacity Calculations and Channel Matrix Normalisation

It is clear from section 4.2 that a matrix, $\mathbf{V}$, is required at the transmitter and a matrix, $\mathbf{U}^H$, is required at the receiver. It should be stressed at this point that, in theory, knowledge of the communications channel at the transmitter could indeed be used to for the derive the matrix, $\mathbf{V}$. However, full knowledge of the communications channel at the transmitter can refer to the idea of waterfilling [59] [61]. Waterfilling, in the context of MIMO communications systems, requires a different form of the capacity equation to those presented in equations (4.11), (4.12) and (4.13). The interested reader is referred to [4] [5] [59] [61] [69] for an analysis and description of the concept of waterfilling in the context of MIMO communications systems since it is not the focus of this work.

It is assumed in this chapter that the receiver has perfect knowledge of the channel matrix, $\mathbf{H}$, and is furthermore able to pass the matrix, $\mathbf{V}$, back to the transmitter at a rate commensurate to the rate at which the channel might be changing. In the case of transmission line channels, typically the transfer functions which make up the scalar elements of the channel matrix, $\mathbf{H}$, are derived from one-port measurements. This methodology can lead to there being a discrepancy between the actual transfer

functions and those which are derived from these one-port measurements. As a result of this discrepancy, there is imperfect knowledge of the channel. A discussion of this discrepancy can be found in work by Galli and Waring [151], Bostoen et. al [18], Bingham [15], as well as Wong and Aboulnasr [141]. It is an objective of chapters 6 and 7 to address the effect on capacity of MIMO communications systems when this discrepancy occurs. In the case of the wireless channels, the channel is considered time-variant. A quasi-static channel is one which remains constant, or indeed may be attributed a given transfer function, over an arbitrary length of time. In common with the approach of Gesbert [59] [61], Foschini [150] and Teletar [152], in this work, a quasi-static channel is considered to be one where the channel remains constant long enough in order that it is possible for the receiver to be able to pass the matrix, $\mathbf{V}$, back to the transmitter. It is an objective of chapters 6 and 7 to address the effect on capacity of MIMO communications systems when the assumption of the quasi-static channel no longer holds.

Having stated the assumption on which the capcity calculations in this chapter hold, it is now necessary to outline the process of channel matrix normalization.

The process of normalising the channel matrix used in this work is similar in the case of both the transmission line channels and the wireless channels. Considering the channel matrix, $\mathbf{H}$, the appropriate Frobenious norm, $\|\mathbf{H}\|_F$, can be defined as:

$$\|\mathbf{H}\|_F = \sqrt{tr(\mathbf{H}\mathbf{H}^H)} = \sqrt{\sum_{i=1}^{N_T}\sum_{j=1}^{N_T}\left|\mathbf{H}_{i,j}\right|^2} \tag{4.14}$$

The normalised channel matrix, $\bar{\mathbf{H}}$, is now defined as:

$$\bar{\mathbf{H}} = \frac{\mathbf{H}}{\|\mathbf{H}\|_F} \tag{4.15}$$

Re-arranging equation (4.2):

$$\mathbf{D} = \mathbf{U}^H \mathbf{H} \mathbf{V} \tag{4.16}$$

It is now possible to write:

$$\frac{\mathbf{D}}{\|\mathbf{H}\|_F} = \mathbf{U}^H \left[\frac{\mathbf{H}}{\|\mathbf{H}\|_F} \right] \mathbf{V} \tag{4.17}$$

Normalising the channel matrix thus creates a normalised diagonal matrix, $\bar{\mathbf{D}}$, written as:

$$\bar{\mathbf{D}} = \frac{\mathbf{D}}{\|\mathbf{H}\|_F} \tag{4.18}$$

Furthermore since $\bar{\mathbf{D}}$ is diagonal and considering equation (4.14), it is now possible to write:

$$\bar{\mathbf{D}}\bar{\mathbf{D}} = \frac{\mathbf{D}}{\|\mathbf{H}\|_F} \frac{\mathbf{D}}{\|\mathbf{H}\|_F} = \frac{\mathbf{D}\mathbf{D}}{tr(\mathbf{D}\mathbf{D})} \tag{4.19}$$

Therefore:

$$tr\left(\bar{\mathbf{D}}\bar{\mathbf{D}} \right) = 1 \tag{4.20}$$

Substituting the normalised diagonal matrix into the expression for the MIMO capacity in equation (4.13) gives:

$$C_{\mathbf{D}} = \sum_{i=1}^{N_T} \log_2 \left[1 + \frac{P \left| \bar{\mathbf{D}}_{i,i} \right|^2}{\varphi} \right] \tag{4.21}$$

Thus the ratio, $\frac{P}{\varphi}$, may now be written as an equivalent expression inside a summation:

$$\begin{aligned} \frac{P}{\varphi} &= \sum_{i=1}^{N_T} \left[\frac{P}{\varphi} \bar{\mathbf{D}} \bar{\mathbf{D}}_{i,i} \right] \\ &= \sum_{i=1}^{N_T} \left[\frac{P}{\varphi} \left| \bar{\mathbf{D}}_{i,i} \right|^2 \right] \end{aligned} \tag{4.22}$$

It is shown that normalisation of the channel matrix ensures that the quantity, $\frac{P}{\varphi}$, is distributed entirely amongst the eigenmodes of the MIMO communications system.

4.4 Capacity calculations on Transmission Line Channels

In this section the capacity of MIMO and SISO communications systems based on transmission line channels are compared. A minor change to the normalisation of the channel matrix that was given in the previous section is now indicated:

$$\bar{\mathbf{H}}(f) = \frac{\mathbf{H}(f)}{\left\| \mathbf{H}(f=1) \right\|_F} \tag{4.23}$$

The matrix, $\mathbf{H}(f=1)$, is the channel matrix that has been defined at the first or lowest frequency of measurement. It is argued that this minor change in the normalisation

allows for the frequency dependence of capacity of the MIMO and SISO communications systems to be apparent in calculations. In respect of this, the frequency dependent capacity of the SISO communications system based on transmission line channels may now be calculated from:

$$C(f)=\sum_{i=1}^{N_T}\log_2\left[1+\frac{P\left|\bar{\mathbf{H}}(f)_{i,i}\right|^2}{\varphi+P\left[\sum_{j=i}\left\{\left|\bar{\mathbf{H}}(f)_{j}\right|^2\right\}-\left|\bar{\mathbf{H}}(f)_{i,i}\right|^2\right]}\right] \tag{4.24}$$

Similarly for MIMO:

$$C_{\mathbf{D}}(f)=\sum_{i=1}^{N_T}\log_2\left[1+\frac{P\left|\bar{\mathbf{D}}(f)_{i,i}\right|^2}{\varphi}\right] \tag{4.25}$$

The units of the continuous channel capacities in equations (4.24) and (4.25) are bits/sec/Hz. These capacities are now considered under following conditions:

(i) An added white Gaussian noise power spectral density, N_0, of -110 dBm/Hz is assumed. As indicated by Aslanis and Cioffi [171], this level exceeds that set by electronics alone but includes the noise floor set by an echo canceller.

(ii) A transmit bandwidth of 4.3125 kHz is assumed. This is the bandwidth set by the American National Standards Institute (ANSI) for a discrete multi-tone (DMT) tone in the asymmetric digital subscriber line (ADSL) T1.413 DMT standard [124] [172]. Each capacity is calculated at intervals of

approximately 496 kHz, i.e. at 201 intervals between 300 kHz to 100 MHz.

(iii) Two transmit power spectral densities are considered. The first one is -60 dBm/Hz which is the figure given in [124] for nominal transmit power density of high bit-rate digital subscriber line (VDSL) signals. The second one is -80 dBm/Hz, which is the transmit power spectral density given in [124] for VDSLs signal that occur in known radio frequency bands.

(iv) The balanced twisted-pair telephone cable, the balanced cat 5 twisted-pair and the unbalanced flat-pair are compared for a dimension, $N_T = 3$. The cat5 is also examined for a dimension, $N_T = 4$ and the twisted-pair is also examined for a dimension, $N_T = 5$.

(v) Cumulative plots of capacity with respect to bandwidth are also presented.

Starting with MIMO and SISO capacity calculations for twisted-pair telephone cable, cat 5 twisted-pair and flat pair for the dimension $N_T = 3$:

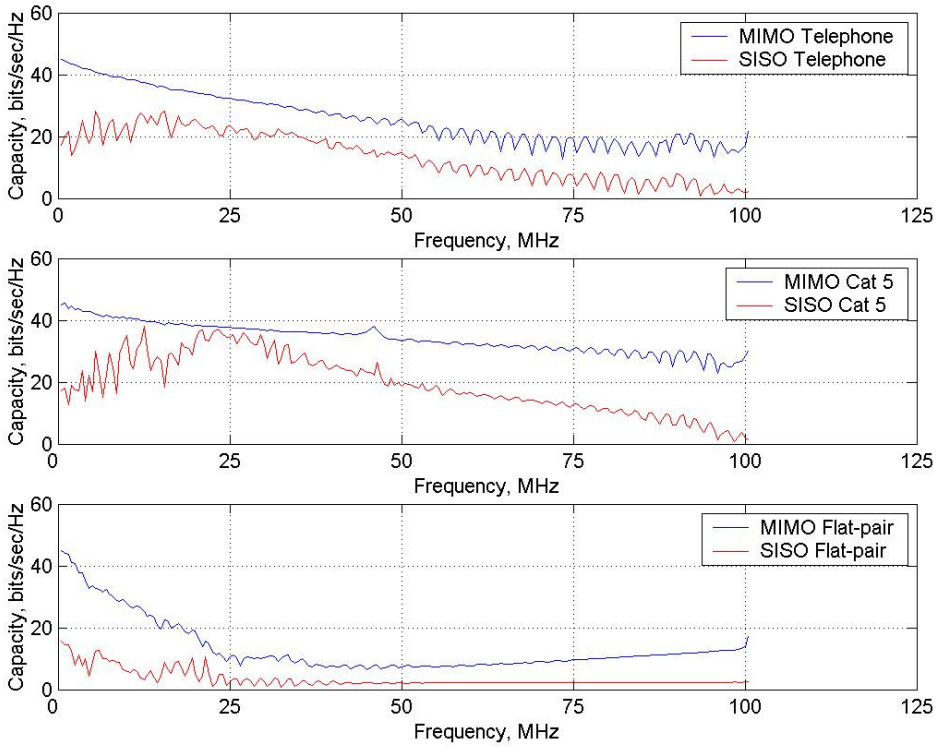

Figures 4.3-4.4: From top to bottom: MIMO and SISO capacity calculations for twisted-pair telephone cable (top, fig. 4.3), cat 5 twisted-pair (middle, fig. 4.4) and flat pair (bottom, fig. 4.5) for the dimension $N_T = 3$. The transmit power spectral density is $P_0 = -60$ dBm/Hz in all cases.

Looking at fig. 4.3, for the case of the MIMO communications system, the relative gain in capacity over the SISO communications system is quite consistent with respect to frequency for the twisted-pair telephone cable channels. In fig. 4.4, for the cat 5 twisted-pair, most of what is gained in terms of capacity for the MIMO communications systems over the SISO communications systems occurs at frequencies above 50 MHz. In fig. 4.5, there is a significant increase in capacity of MIMO over the SISO communications system up to approximately 20 MHz. Beyond 25 MHz, there appears to be a very minor increase in capacity for the MIMO communications system while the capacity of SISO communications system remains

more or less constant. This minor capacity increase is thought to be due to changes in the channel matrix conditioning as a result of increased presence of FEXT as frequency increases. However since the capacity increase is quite small in this region, this has not been considered in much detail. The cumulative capacities are now considered.

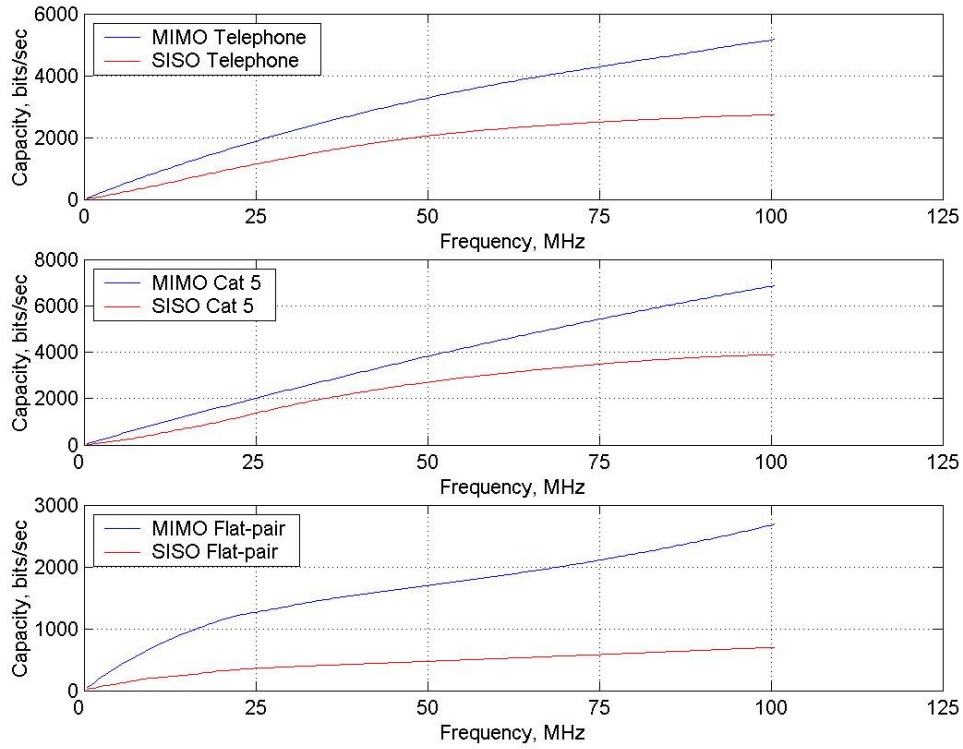

Figures 4.6-4.8: From top to bottom: MIMO and SISO cumulative capacity calculations for twisted-pair telephone cable (top, fig. 4.6), cat 5 twisted-pair (middle, fig. 4.7) and flat pair (bottom, fig. 4.8) for the dimension $N_T = 3$ and a transmit power spectral density is $P_0 = -60$ dBm/Hz.

Remembering that capacity is calculated at 496 kHz intervals, the curves in figs 4.6-4.8 are not entirely representative of the total capacity that is possible over any given frequency range. However, looking at fig. 4.7 it is indicated that cat 5 shows the

greatest overall capacity improvement in the context of the MIMO communications system over the other types of transmission line channels in figs 4.7 and 4.8. Again looking at fig. 4.7 in respect of the MIMO communications system, cat 5 exhibits the greatest consistent gain in capacity with frequency, in contrast to the case of the flat-pair in fig. 4.8 where most of what is gained in terms of capacity with respect to frequency has occurred before 25 MHz. Notwithstanding this, the analysis does confirm that the MIMO communications system may be used to enhance the flat-pair channels at frequencies below 25 MHz. As a result, this comparative analysis supports the novel idea of using MIMO communications systems to allow, or indeed enhance, transmission line channels that are poorly balanced or exhibit high degrees of insertion loss and FEXT. Given that present ADSL standards generally transmit over a bandwidth of only 2-3 MHz [124] [172], the idea is therefore offered here that MIMO communications systems may indeed serve to enhance internet connections which would have been previously deemed out-of-range in order that they can be used for high speed internet connections.

Increasing the dimension, N_T, from 3 to 4 for the case of the cat 5 twisted-pair channels, the capacities of the MIMO and SISO communications system are considered in figs 4.10 and 4.11. Fig. 4.11 is the cumulative capacity. In fig. 4.9, the appropriate plot depicting the same capacities for $N_T = 3$ has been reproduced for comparison. Looking at figs. 4.9 and 4.10 allows for the comparison of the capacity plots of the SISO communications system where $N_T = 3$ with that where $N_T = 4$. For $N_T = 4$ there are marginal increases in capacity in the frequency range up to 25 MHz. In the same regard, the capacity however drops quite quickly leaving equivalent figures for SISO capacities in figs. 4.9 and 4.10 at 50 MHz. Looking at fig 4.10 only,

and this time comparing the capacity of the MIMO and SISO communication systems where $N_T = 4$, there appears to be quite a significant improvement in the MIMO capacity over the SISO capacity particularly after 50 MHz. The lower cumulative capacity plot in fig. 4.11 indicates that there is a reasonably consistent increase in capacity for the case of the MIMO communications system over the entire frequency range. However, fig. 4.11 shows that most of what is gained in terms of capacity for the case of the SISO communications system occurs before 50 MHz

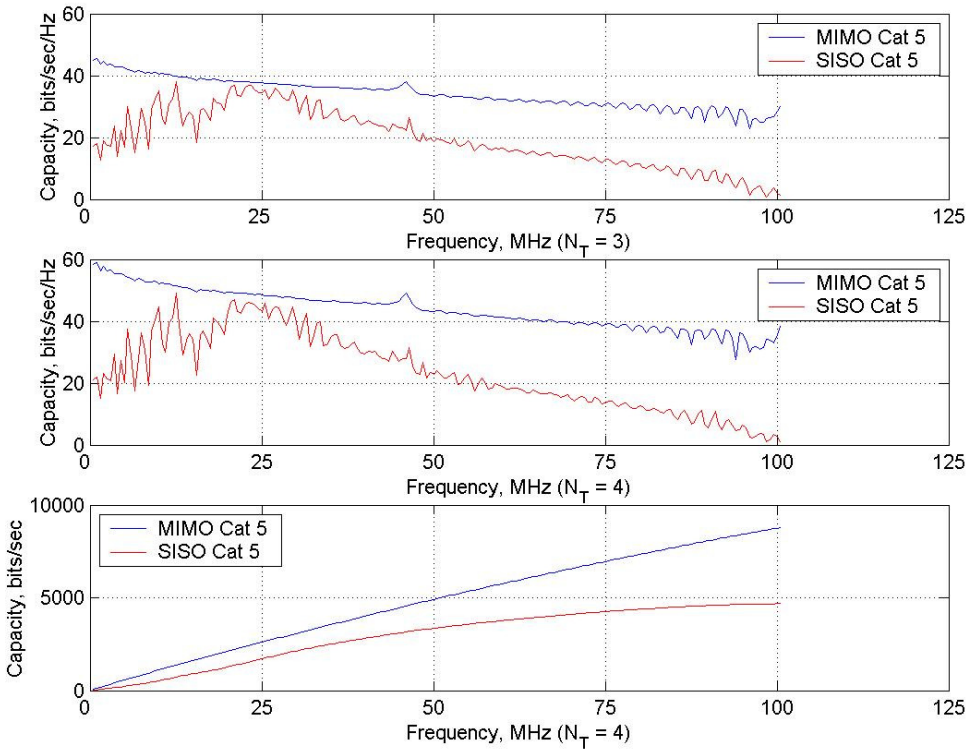

Figures 4.9-4.11: From top to bottom: MIMO and SISO capacity calculations for twisted-pair cat 5 cable with the dimension $N_T = 3$ (top, fig. 4.9). MIMO and SISO capacity calculations for twisted-pair cat 5 cable with the dimension $N_T = 4$ (Middle and bottom, figs. 4.10 and 4.11). Fig. 4.11 depicts cumulative capacity calculations. The transmit power spectral density is $P_0 = -60$ dBm/Hz in all cases.

In figs 4.13 and 4.14, the capacities of the MIMO and SISO communications system in the case of the twisted-pair telephone cable with dimension, $N_T = 5$ are considered with fig. 4.14 depicting cumulative capacity calculations. In fig. 4.12 is the appropriate plot depicting the capacity for $N_T = 3$ reproduced for comparison. Looking at figs. 4.12 and fig. 4.13, and thus comparing the capacity plots where $N_T = 3$ with that where $N_T = 5$, in the case of the SISO communications system, there appears to be marginally greater capacities at frequencies up to 25 MHz. However in the same regard, these capacities are more or less the same at frequencies above 25 MHz. In fig. 4.14, the MIMO capacity plot for the case where $N_T = 5$ may be compared with that where $N_T = 3$ in fig. 4.13. There appears to be an improvement over the frequency range up to 50 MHz. However as the frequency approaches 75 MHz, these two MIMO capacities appear to approach the same value. The cumulative capacity plots in fig. 4.14 reveals that when $N_T = 5$, the MIMO capacity of the twisted-pair telephone cable appears to be increasing reasonably consistently over the entire frequency range whereas in the case of the SISO capacity most of what is gained has occurred at frequencies between 25 MHz and 50 MHz.

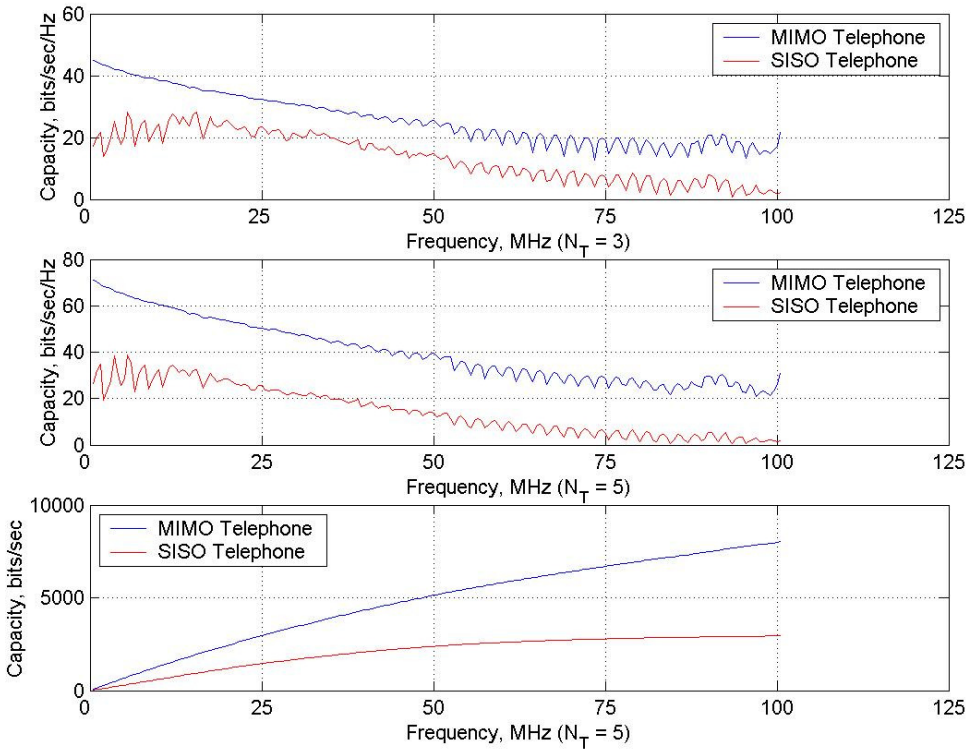

Figures 4.12-4.14: From top to bottom: MIMO and SISO capacity calculations for twisted-pair telephone cable with the dimension $N_T = 3$ (top, fig. 4.12). MIMO and SISO capacity calculations for twisted-pair telephone cable with the dimension $N_T = 5$ (Middle and bottom, figs. 4.13 and 4.14). Fig. 4.14 depicts cumulative capacity calculations. The transmit power spectral density is $P_0 = -60$ dBm/Hz in all cases.

The effect of increasing the dimension N_T has been outlined in the case of the twisted-pair telephone cable and the twisted-pair cat 5 cable. It can however be appreciated that since many of the conclusions drawn in this work are comparative in nature in respect of the three different transmission line channels, it is sufficient that the dimension be $N_T = 3$.

An analysis of MIMO and SISO communications systems based on the three types transmission line channels are now considering for a transmit power spectral density of $P_0 = -80$ dBm/Hz.

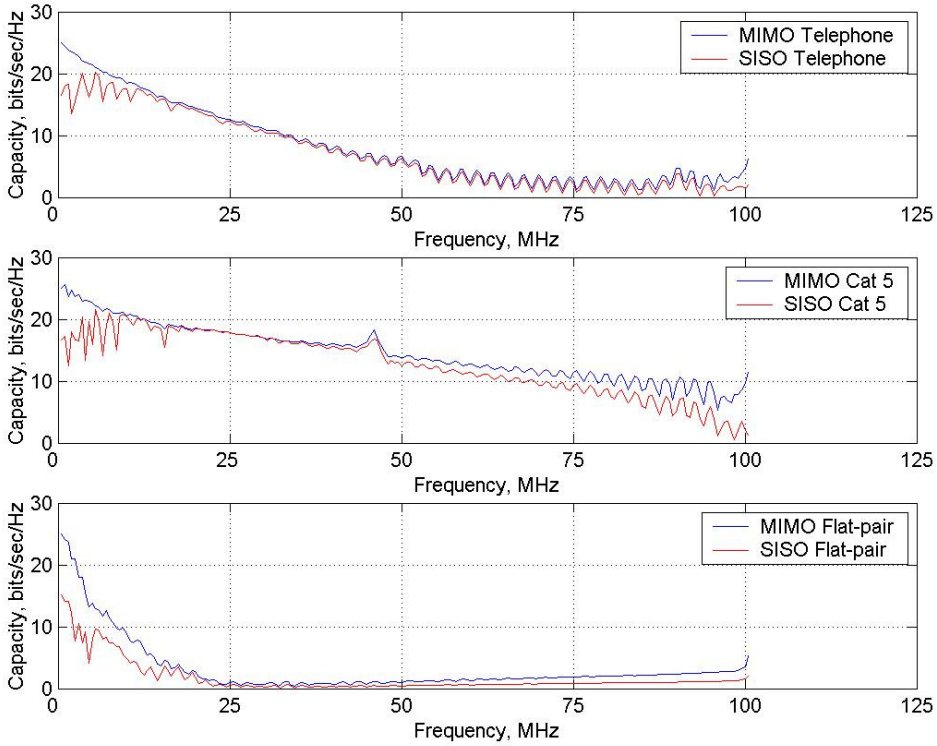

Figures 4.15-4.17: From top to bottom: MIMO and SISO capacity calculations for twisted-pair telephone cable (top, fig. 4.15), cat 5 twisted-pair (middle, fig. 4.16) and flat pair (bottom, fig. 4.17) for the dimension $N_T = 3$. The transmit power spectral density is $P_0 = -80$ dBm/Hz in all cases.

In the case of the MIMO communications system, the lower power spectral density of -80 dBm/Hz, which is used by VDSL systems when operating in known radio frequency bands, offers little improvement. Also, since the results in figs 4.15 – 4.17 assume perfect knowledge of the channel, which in a practical sense may not be

available, it is concluded that the MIMO communications system should not be used when transmitting in radio frequency bands. The cumulative capacity plot is therefore not considered in this case. It is noted finally, in the context of the transmit power spectral density of – 80 dBm/Hz, that similar results were obtained for the case of cat 5 twisted-pair cable when the dimension, $N_T = 4$, and indeed for the case of the twisted-pair telephone cable when $N_T = 5$.

4.5 Capacity calculations on Wireless Channels

The objective of the analysis in this section is to compare the capacities of MIMO and SISO communications systems based on wireless channels. In all of the figures that follow in this section, the term SISO should be understood to refer to the case of one Tx antenna and one Rx antenna with the somewhat ideal situation being considered where effect of multi-path fading is ignored. The SISO capacity is calculated from:

$$C = \sum_{i=1}^{N_T} \log_2 \left[1 + \frac{P}{\varphi} \right] \tag{4.26}$$

In contrast to the case of the SISO communications system, the term MIMO refers to Tx and Rx antenna arrays of various sizes where the effect of multi-path fading is considered. The MIMO capacity is calculated as:

$$C_{\mathbf{D}} = \sum_{i=1}^{N_T} \log_2 \left[1 + \frac{P \left| \bar{\mathbf{D}}_{i,i} \right|^2}{\varphi} \right] \tag{4.27}$$

The units of the continuous channel capacities in equations (4.24) and (4.25) are bits/sec/Hz. These capacities are now considered under following circumstances:

(i) As outlined in chapter 3, all the transfer functions and hence channel matrices pertain to a centre frequency of 5.2 GHz.

(ii) Five channel matrices: $\mathbf{H}_{All}$, $\mathbf{H}_{LOS}$, $\mathbf{H}_{1^{st}\,order(1)}$, $\mathbf{H}_{1^{st}\,order(2)}$ and $\mathbf{H}_{2^{nd}\,order}$ are considered. The four channel matrices: $\mathbf{H}_{LOS}$, $\mathbf{H}_{1^{st}\,order(1)}$, $\mathbf{H}_{1^{st}\,order(2)}$ and $\mathbf{H}_{2^{nd}\,order}$ are compared against $\mathbf{H}_{All}$ in each figure which follows.

(iii) The various channel matrices were normalised in the manner described in section 4.3.

(iv) The receive signal power to noise power ratio denoted: $\frac{P}{\varphi}$ is fixed at a ratio of 18 dB throughout this section. It should be appreciated that the capacities for the MIMO communications systems are examined from the perspective of the channel matrix conditioning or eigenvalue distribution due to various multi-path channel impulse response components.

(v) Since the all of the channel matrices are derived from common sets of experimental data with the obvious exception that various relevant channel impulse response components have been removed, the degree of correlation amongst common channel impulse response components in each channel matrix is exactly the same.

Each of the relevant results will now be presented with some concluding remarks afterwards. The capacity of the MIMO communications system based on the channel matrices denoted: $\mathbf{H}_{All}$ and $\mathbf{H}_{LOS}$ are compared in fig. 4.18. Based on what was described in chapter 3, it has been assumed that the channel matrix $\mathbf{H}_{All}$ is indicative of a Ricean channel and that $\mathbf{H}_{LOS}$ is indicative of a Rayleigh channel.

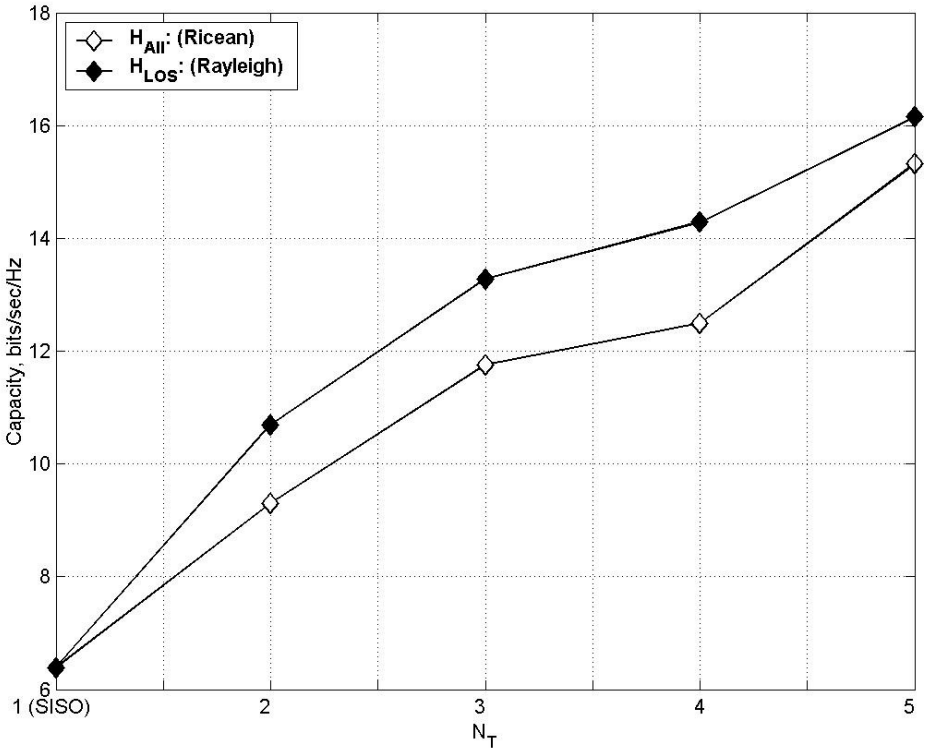

Figure 4.18: MIMO calculations for the channels denoted by the matrices: $\mathbf{H}_{All}$ (Ricean) and $\mathbf{H}_{LOS}$ (Rayleigh) for the dimensions: $N_T = 2,3,4$ and 5. The dimension, $N_T = 1$ refers to the SISO calculation and the ratio: $\frac{P}{\varphi} = 18\,\text{dB}$.

The capacity of the MIMO communications system based on the channel matrices denoted: $\mathbf{H}_{All}$ and $\mathbf{H}_{1^{st}\,order(1)}$ are compared in fig. 4.19.

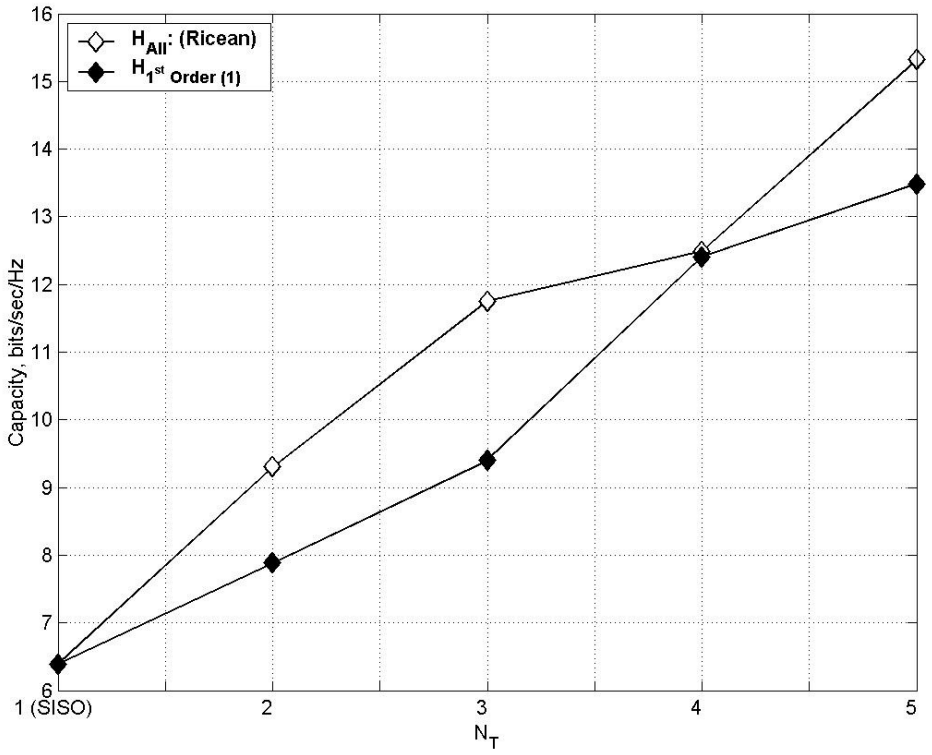

Figure 4.19: MIMO calculations for the channels denoted by the matrices: $\mathbf{H}_{All}$ (Ricean) and $\mathbf{H}_{1^{st}\,order(1)}$ for the dimensions: $N_T = 2,3,4$ and 5. The dimension, $N_T = 1$ refers to the SISO calculation and the ratio: $\frac{P}{\varphi} = 18\,\text{dB}$.

The capacity of the MIMO communications system based on the channel matrices denoted: $\mathbf{H}_{All}$ and $\mathbf{H}_{1^{st}order(2)}$ are compared in fig. 4.20.

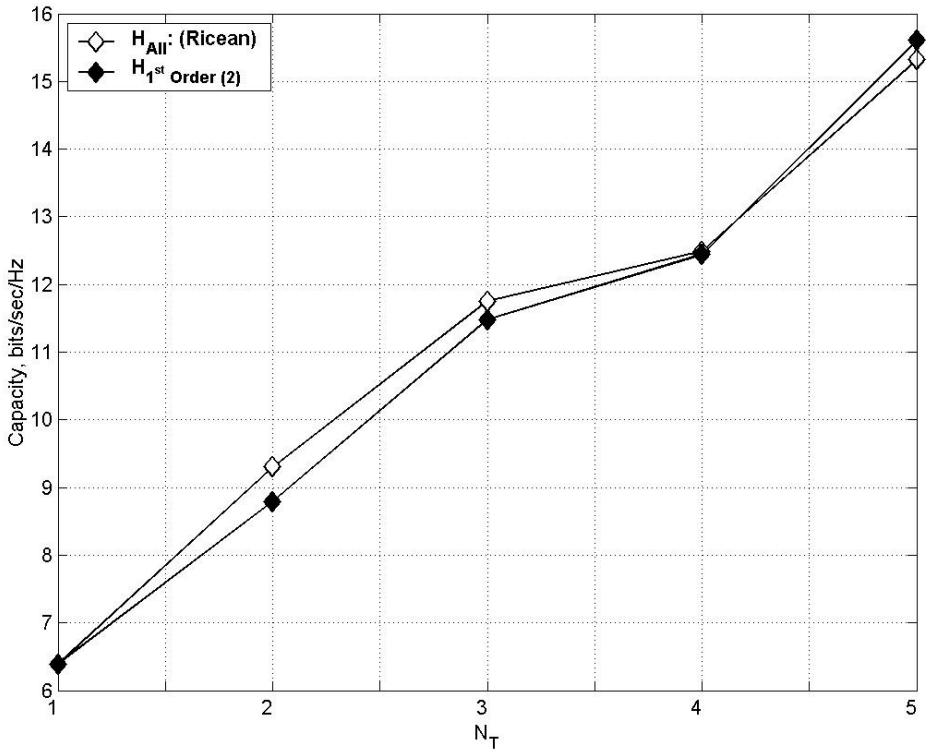

Figure 4.20: MIMO calculations for the channels denoted by the matrices: $\mathbf{H}_{All}$ (Ricean) and $\mathbf{H}_{1^{st}order(2)}$ for the dimensions: $N_T = 2,3,4$ and 5. The dimension, $N_T = 1$ refers to the SISO calculation and the ratio: $\frac{P}{\varphi} = 18$ dB.

Finally, the capacity of the MIMO communications system based on the channel matrices denoted: $\mathbf{H}_{All}$ and $\mathbf{H}_{2^{nd}\,order}$ are compared in fig. 4.21.

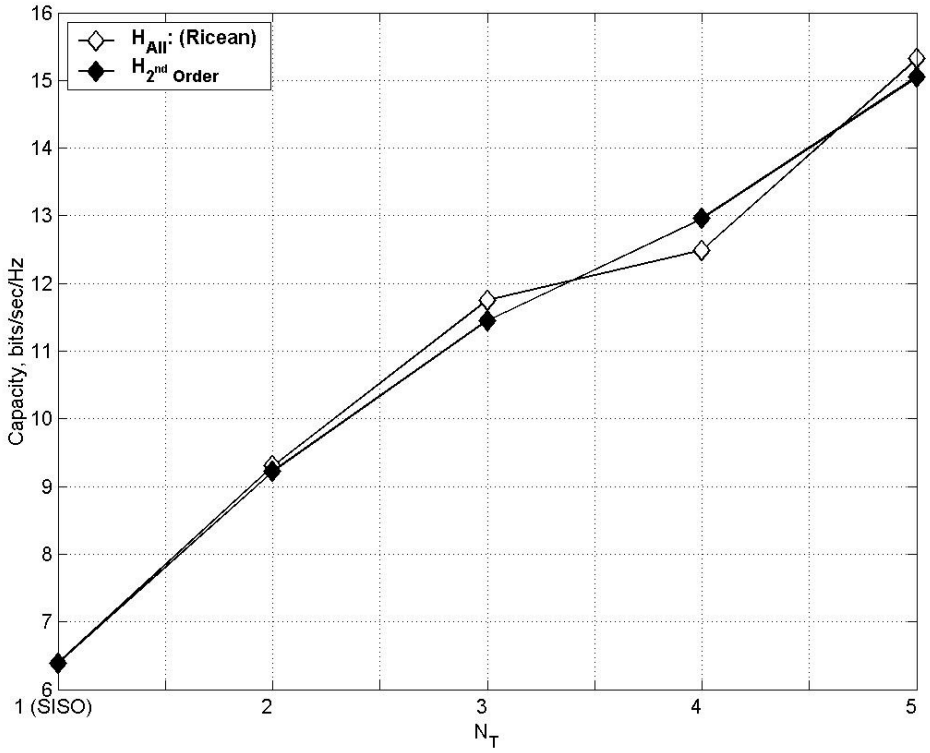

Figure 4.21: MIMO calculations for the channels denoted by the matrices: $\mathbf{H}_{All}$ (Ricean) and $\mathbf{H}_{2^{nd}\,order}$ for the dimensions: $N_T = 2,3,4$ and 5. The dimension, $N_T = 1$ refers to the SISO calculation and the ratio: $\frac{P}{\varphi} = 18\,\text{dB}$.

Examination of fig. 4.18 reveals that removal of the line-of-sight channel impulse component clearly has the effect of increasing the capacity of the MIMO communications system under the conditions stated in (i) to (v). In particular, Gesbert offers the following comment on this result [61]:

"In Ricean channels, increasing the LOS strength at fixed signal to noise ratio reduces capacity".

Durgin extends the argument contained within Gesbert's comment by saying [47]:

"The channel capacity expression (in equation (4.27) in this work) is maximised when the signal power is evenly distributed among the singular values (denoted in this work as: $\sigma_1, \sigma_2, ..., \sigma_{N_T}$). In the absence of multi-path (richness), the singular values become heavily skewed towards a single dominant singular value. Rich multi-path propagation is necessary in order to break the MIMO channel into separate sub-channels."

Durgin's comment clearly extends the argument made by Gesbert's comment since by definition Rayleigh channels exibit a richer multi-path environment than Ricean channels.

Further to this, work by Ozcelik et al. [156] indicates that in general, channel impulse responses that contain dominant channel impulse response components, such as the line-of-sight channel impulse component in the case of Ricean channels, give rise to higher degrees of multi-path correlation and hence lower capacities. However, there exist some literature which argue that Rayleigh channels, which by definition would have no dominant channel impulse response component can sometimes exhibit lower capacities than Ricean channels [154] [155]. Indeed further to this, the work by

Ozcelik et al. [156] has highlighted the fact that Rayleigh fading channels can exist with a high degree of multi-path correlation and can thus lead to low capacities. In relation to this idea, an important aspect of the experimental approach taken in this work should now be highlighted. The degree of correlation of the channel impulse response components, which arise specifically due to the multi-path propagation in the specially built enclosure discussed in chapter 3, is the same in the cases of the experimentally observed wireless channels which are indicative of both the Rayleigh fading statistics and the Ricean statistics. This idea is supported by the fact that the Rayleigh channels were observed experimentally by removing the line-of-sight channel impulse response component using software. Thus, these experimentally observed Rayleigh channels are identical to the experimentally observed Ricean channels but with the obvious exception that in the case of Ricean channels the line-of-sight channel impulse component has not been removed in software. This means that the degree of correlation between the multi-path channel impulse response components must be equivalent in both cases.

Removal of the channel impulse response component, known as first order (1) in fig. 4.19, indicates a drop in capacity when the number of Tx elements and Rx elements is N_T = 2, 3, or 5. However, when N_T = 4, removal of this channel impulse response component seems to have little or no effect on capacity. Fig. 4.20 and fig. 4.21 indicate that removal of the channel impulse response components known as 'first order (2)' and 'second order' have little or no effect on the capacity of the MIMO communications system in the case of wireless channels.

4.5 Summary

In this chapter, calculations of the capacity of MIMO and SISO communications systems were presented which derived from appropriate physical measurements. In the case of the transmission line channels, the novel idea of using the MIMO communications system to enhance transmission lines which were poorly balanced and exhibited a high degree of insertion loss and FEXT was presented. It was thus argued that such a transmission line is indicative of that which would have been deemed out-of-range for high-speed internet connections. MIMO and SISO capacity calculations based on unbalanced flat-pair transmission lines over the frequency range from 300 kHz to 100 MHz were presented and were readily comparable to similar calculations based on balanced twisted-pair cat 5 transmission line measurements and balanced twisted-pair telephone transmission line measurements. It was also seen that when using a low power spectral density of – 80 dBm/Hz, which occurs when VDSL systems are transmitting in known radio band, the capacity gain when using MIMO is minimal. It is therefore clarified that the results presented in terms of the transmission lines are indicative of overall performance given that in reality not all of the frequencies can be used in the context of MIMO because of the aforementioned problem of radio band interference.

In the case of the wireless channels, an experimental methodology for observing wireless channels indicative of fading statistics which were either Rayleigh or Ricean was outlined in chapter 3. Suitable channel matrices were then derived. When the capacity of the MIMO and SISO communications systems based on these channel matrices were calculated in this chapter, the results presented supported the idea that channels whose fading statistics are Rayleigh provide superior performance when the

degree of multi-path correlation and signal to noise ratio were equivalent in either case.

Chapter 5: Multi-Carrier Modulation

5.1 Introduction

The objective of this chapter is to support the conclusions presented in chapter 4 by incorporating various channel impulse responses into an unencoded baseband multi-carrier modulation simulation of a multiple-input/multiple-output (MIMO) communications system. All of these channel impulse responses are contained within vectors which were defined in chapter 3. In the case of the transmission line channels, a novel aspect of the analysis in the chapter is the fact that channel impulse responses of unbalanced flat-pair transmission line channels, will be incorporated into this simulation. A comparative analysis of the same simulation, where instead channel impulse responses of balanced twisted-pair telephone line transmission line channels and balanced twisted-pair cat 5 transmission line channels were incorporated, will be presented. Specifically, this comparative analysis will be seen to support the idea from chapter 4 that the MIMO communications system can enhance transmission lines which would have otherwise been deemed out-of-range for high speed internet connections. In the case of the wireless channels, some justification for referring to the experimentally observed non line-of-sight scenario as Rayleigh channel is provided by comparing the simulation model with mathematically derived matrices whose elements were Rayleigh distributed. Also, results from the simulations confirm the corresponding analysis of chapter 4 where MIMO communications systems based Rayleigh channels exhibited superior performance over MIMO communications based on Ricean channels for fixed receive SNR and common degrees of multi-path correlation.

5.2 MIMO Multi-Carrier Modulation

Section 5.2.1 presents multi-carrier modulation in the context of a single receive (Rx) element and a single transmit (Tx) element. In section 5.2.2, this multi-carrier modulation scheme is used to sound the various channels that can exist between two Tx elements and two Rx elements without making any explicit reference to transmission line or wireless channels per se. In section 5.2.3, the discussion of the previous two sections is combined and extended to describe a simulation of MIMO communications system which uses multi-carrier modulation signals.

5.2.1 Multi-Carrier Modulation Simulation

The multi-carrier modulation scheme which will be used in this simulation is presented in fig. 5.1 [45] [62]:

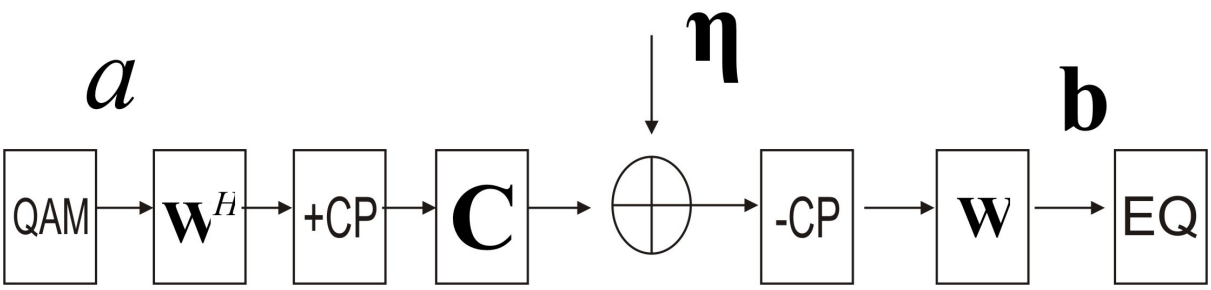

Figure 5.1: Multi-carrier modulation simulation model.

Looking at the left hand side of fig. 5.1, **a** is vector which contains complex scalar elements. In the context of this simulation, **a** is a transmit vector which contains symbols which arise from the modulation scheme of choice which is quadrature

amplitude modulation (QAM). $\mathbf{a}$ is the frequency domain output of a bank of QAM modulators and is defined as:

$$\mathbf{a} = \begin{bmatrix} a_0 \\ a_1 \\ \vdots \\ a_{s-1} \\ 0 \\ a_{s-1}^T \\ a_{s-2}^T \\ \vdots \\ a_1^T \end{bmatrix} \tag{5.1}$$

In a mathematical sense it can now be appreciated that any of the i^{th} scalar elements of the vector, $\mathbf{a}$, is a complex variable, $a_i \in C$, with the exception of one element which is set at zero. In the context of this sub–script notation, transmission occurs over $2s$ sub–bands, so that $2s = 512 = S$. The notation, $(\cdot)^T$, refers to the complex conjugate of a given variable and so the vector $\mathbf{a}$ is composed of a series of elements which are conjugate symmetric about the origin. Consider now the discrete Fourier transform (DFT) written as an $m \times l$ matrix $\mathbf{W}$:

$$\mathbf{W}_{m,l} = \frac{1}{\sqrt{S}} \exp\left\{ - j \frac{2\pi}{S} ml \right\} \tag{5.2}$$

If a vector of dimensions $S \times 1$ is to be transformed, then $0 \le m, l \le S - 1$ and the quantity $j = \sqrt{-1}$. $\frac{1}{\sqrt{S}}$ is a scaling factor [124] which is chosen such that $\mathbf{W}$ be unitary thus:

$$\mathbf{W}\mathbf{W}^H = \mathbf{I} \tag{5.3}$$

Looking at fig. 5.1, and considering equation (5.3), the inverse discrete time Fourier transform (IDFT) matrix operation which is the Hermitian transpose of $\mathbf{W}$, written as $\mathbf{W}^H$. As a result the product $\mathbf{W}^H\mathbf{a} \in R$. This product, $\mathbf{W}^H\mathbf{a}$, is a time domain vector which, when convolved with the channel impulse response, will produce a new time domain vector. However, examination of fig. 5.1 reveals that before this occurs there is a stage marked: '+CP'. This refers to the addition of a cyclical prefix (CP) to the time domain vector, $\mathbf{W}^H\mathbf{a}$. To clarify, normally the term, 'convolution' is understood to refer to a process known as 'linear convolution' where in this instance the time domain vector $\mathbf{W}^H\mathbf{a}$ would ordinarily be multiplied by a Toeplitz matrix which is derived from the channel impulse response. The CP is a repetition of the last L elements of $\mathbf{W}^H\mathbf{a}$. L is chosen so that the CP also acts as a 'guard band' which means that L is of sufficient length to ensure that the channel impulse response does not cause corruption of the elements in the next symbol to be transmitted after the time domain vector $\mathbf{W}^H\mathbf{a}$. This corruption of the next symbol to be transmitted is known as inter symbol interference (ISI). The addition of the CP to $\mathbf{W}^H\mathbf{a}$ means that the operation of linear convolution becomes a process known as circular convolution and proof of this may be found in [42]. As a result of this fact, in fig. 5.1 the matrix, $\mathbf{C}$, is a circulant matrix which is derived from the vector, $\mathbf{h}$. In this chapter, it should be understood that the vector, $\mathbf{h}$, is used to refer to any of the channel impulse response vectors which were defined in chapter 3. In fig. 5.1, the circular convolution appears as a matrix multiplication of an $S \times S$ matrix, $\mathbf{C}$, defined as:

$$\mathbf{C} = \begin{bmatrix} c_0 & c_1 & \cdots & c_{S-1} & 0 \\ 0 & c_0 & c_1 & \cdots & c_{S-1} \\ c_{S-1} & 0 & c_0 & \cdots & c_{S-2} \\ \vdots & \ddots & \ddots & \ddots & \vdots \\ 0 & 0 & c_{S-1} & \ldots & c_0 \end{bmatrix} \tag{5.4}$$

Circulant matrices are diagonalised by the IDFT and DFT matrix operations, thus defining a vector of uncorrelated additive white Guassian noise (AWGN), $\boldsymbol{\eta}$, as:

$$\boldsymbol{\eta} = \begin{bmatrix} \eta_{S-1} \\ \vdots \\ \eta_0 \end{bmatrix} \tag{5.5}$$

The receive vector, $\mathbf{b}$, which is on the extreme right hand side of fig. 5.1, may now be written as:

$$\begin{aligned} \mathbf{b} &= \mathbf{W}\left\{\mathbf{C}\mathbf{W}^H\mathbf{a} + \boldsymbol{\eta}\right\} \\ &= \boldsymbol{\Lambda}\mathbf{a} + \mathbf{W}\boldsymbol{\eta} \end{aligned} \tag{5.6}$$

$\boldsymbol{\Lambda}$ is a diagonal matrix which may be defined by the product, $\mathbf{W}\mathbf{C}\mathbf{W}^H$. The receive vector, $\mathbf{b}$,is therefore equivalent to the transmit vector, $\mathbf{a}$, having a gain profile defined by the diagonal matrix, $\boldsymbol{\Lambda}$, with an additional frequency domain noise vector defined by the matrix-vector product, $\mathbf{W}\boldsymbol{\eta}$. As indicated previously, the CP acts as a 'guard band' which means that it is of sufficient length to ensure that the channel impulse response does not cause corruption of the elements in the next symbol to be transmitted after the time domain vector $\mathbf{W}^H\mathbf{a}$, i.e. it mitigates ISI. However, since the CP also gives rise to circular convolution as described, it mitigates the effect of interference that can occur between sub-bands, known as inter-band interference (IBI), on the basis that the matrix, $\boldsymbol{\Lambda}$, is diagonal.

Finally, it should be noted in this section that this baseband simulation model for multi-carrier modulation is similar to the discrete multi-tone (DMT) modulation, which is a baseband modulation scheme that is often used on digital subscriber lines. It is therefore reasonable to apply this simulation to the case of transmission line channels. In the case of the wireless channels, a passband simulation model for multi-carrier modulation is more pertinent. This distinction serves to highlight the difference between this baseband DMT based simulation and orthogonal frequency division multiplexing (OFDM) which is often used in wireless channels. Both are essentially the same technology with the main difference being that OFDM is in general a passband multi-carrier modulation scheme which incorporates extra circuitry at the transmit and receive ends in order to modulate the complex time domain sun-symbols to a given carrier frequency [96] [74]. However, in this work only the baseband multi-carrier modulation scheme which was outlined will be considered in the case of both the transmission line channels and the wireless channels.

5.2.2 Channel Sounding Sequence Simulation

The objective of this section is to outline how channel transfer functions may obtained using a channel sounding sequence simulation based on the multi-carrier modulation simulation model presented in section 5.2.1. For the sake of clarity in explanation the number of Tx and Rx elements, N_T, is set at 2. The channel sounding sequence is depicted in fig. 5.2

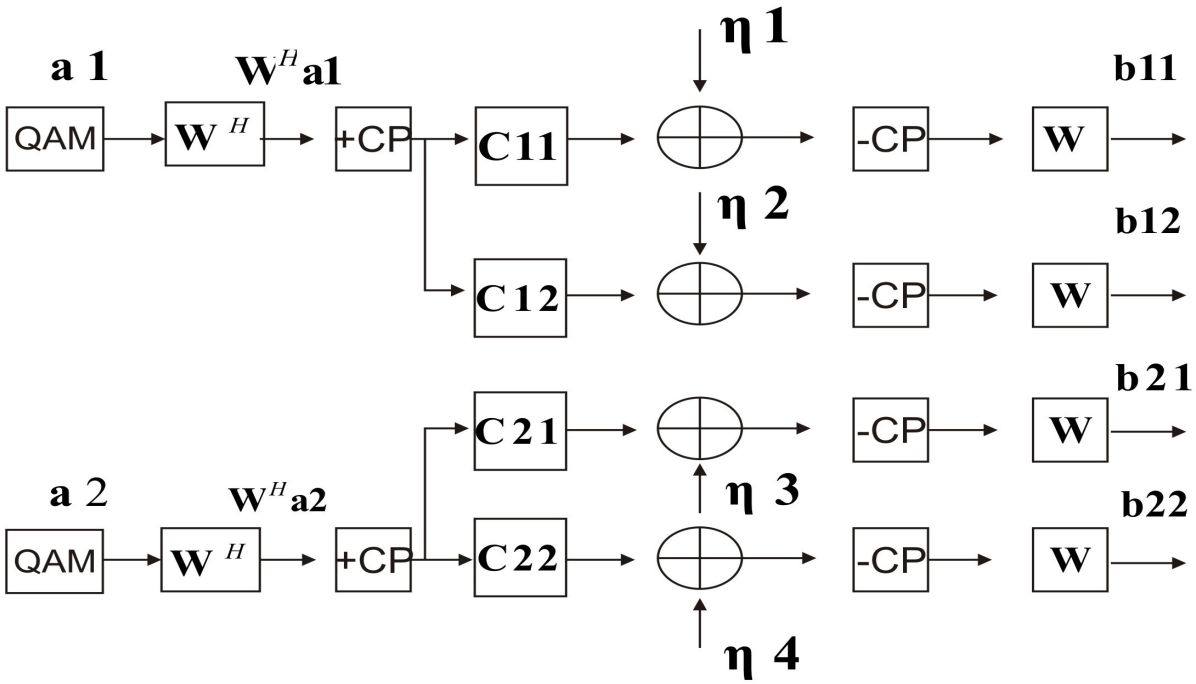

Figure 5.2: Channel sounding sequence which uses a baseband multi-carrier modulation simulation model.

In fig. 5.2, there are two distinct frequency domain transmit vectors denoted, **a1** and **a2**, with: **η1**, **η2**, **η3** and **η4** being vectors of uncorrelated AWGN components similar to the vector **η** previously defined. The circulant matrix, **C11**, represents the channel that exists between the first transmitter and the first receiver. The circulant

matrix, **C12**, represents the channel that exists between the first transmitter and the second receiver. The significance of the other matrices: **C21** and **C22** may now be inferred by example. For this analysis, each of the circulant matrices: **C11**, **C12**, **C21** and **C22** is derived from the appropriate physical measurements in chapter 3. As a result of the matrices: **C11**, **C12**, **C21** and **C22**, there are now four frequency domain receive vectors denoted: **b11**, **b12**, **b21** and **b22**. The absence of blocks marked, 'EQ' should be noted in fig. 5.2. These are not necessary since it is by appropriate comparison of the frequency domain receive vectors, **b11**, **b12**, **b21** and **b22** with the corresponding appropriate frequency domain transmit vectors: **a1** and **a2**, that provides the channel transfer functions for this analysis. The notation, $\overset{3}{(\cdot)}$, appears on the channel matrix, $\overset{3}{\mathbf{H}}_{i,j,\omega}$, to denote that it is a three dimensional matrix. The notation, $(\cdot)_{i,j}$, has its usual significance of referencing the j^{th} transmit element and the i^{th} receive element with respect to matrix elements and the notation, $(\cdot)_{\omega}$, should be thought of referencing the ω^{th} sub-band. $\overset{3}{\mathbf{H}}_{i,j,\omega}$ is now defined as:

$$\overset{3}{\mathbf{H}}_{1,1,\omega} = \left[\frac{\mathbf{b11}_1}{\mathbf{a1}_1}, \frac{\mathbf{b11}_2}{\mathbf{a1}_2}, \frac{\mathbf{b11}_3}{\mathbf{a1}_3}, ..., \frac{\mathbf{b11}_S}{\mathbf{a1}_S} \right] \tag{5.7}$$

$$\overset{3}{\mathbf{H}}_{1,2,\omega} = \left[\frac{\mathbf{b12}_1}{\mathbf{a1}_1}, \frac{\mathbf{b12}_2}{\mathbf{a1}_2}, \frac{\mathbf{b12}_3}{\mathbf{a1}_3}, ..., \frac{\mathbf{b12}_S}{\mathbf{a1}_S} \right] \tag{5.8}$$

$$\overset{3}{\mathbf{H}}_{2,1,\omega} = \left[\frac{\mathbf{b21}_1}{\mathbf{a2}_1}, \frac{\mathbf{b21}_2}{\mathbf{a2}_2}, \frac{\mathbf{b21}_3}{\mathbf{a2}_3}, ..., \frac{\mathbf{b21}_S}{\mathbf{a2}_S} \right] \tag{5.9}$$

$$\overset{3}{\mathbf{H}}_{2,2,\omega} = \left[\frac{\mathbf{b22}_1}{\mathbf{a2}_1}, \frac{\mathbf{b22}_2}{\mathbf{a2}_2}, \frac{\mathbf{b22}_3}{\mathbf{a2}_3}, ..., \frac{\mathbf{b22}_S}{\mathbf{a2}_S} \right] \tag{5.10}$$

From fig. 5.2, it should now be appreciated how channel transfer functions can be obtained from the physical measurements contained within the vectors which were tabulated at the end of chapter 3 in the case of either the transmission line channels or the wireless channels. Furthermore, it can be seen from equations (5.7), (5.8), (5.9) and (5.10) that the three dimensional matrix, $\mathbf{H}^{3}_{i,j,\omega}$, contains channel transfer functions of all the channels that exist between two transmitters and the two receivers at all frequencies indexed from 1 to S.

5.2.3 MIMO Multi-Carrier Modulation Simulation

A multi-carrier modulation simulation model was described in section 5.2.1. This was then extended to a channel sounding sequence in order to derive channel matrices in section 5.2.2. This section outlines an unencoded baseband multi-carrier modulation simulation of a MIMO communications system. By performing a singular value decomposition in an appropriate manner on the three dimensional channel matrix, $\mathbf{H}^{3}_{i,j,\omega}$, the following three dimensional matrices may be derived:

$$\mathbf{U}^{3}_{i,j,\omega} = \begin{bmatrix} \{\mathbf{u11}_1, \mathbf{u11}_2, \mathbf{u11}_3, ..., \mathbf{u11}_S\} & \{\mathbf{u12}_1, \mathbf{u12}_2, \mathbf{u12}_3, ..., \mathbf{u12}_S\} \\ \{\mathbf{u21}_1, \mathbf{u21}_2, \mathbf{u21}_3, ..., \mathbf{u21}_S\} & \{\mathbf{u22}_1, \mathbf{u22}_2, \mathbf{u22}_3, ..., \mathbf{u22}_S\} \end{bmatrix} \tag{5.11}$$

$$\mathbf{U}^{3H}_{i,j,\omega} = \begin{bmatrix} \{\mathbf{u11}_1^T, \mathbf{u11}_2^T, \mathbf{u11}_3^T, ..., \mathbf{u11}_S^T\} & \{\mathbf{u21}_1^T, \mathbf{u21}_2^T, \mathbf{u21}_3^T, ..., \mathbf{u21}_S^T\} \\ \{\mathbf{u12}_1^T, \mathbf{u12}_2^T, \mathbf{u12}_3^T, ..., \mathbf{u12}_S^T\} & \{\mathbf{u22}_1^T, \mathbf{u22}_2^T, \mathbf{u22}_3^T, ..., \mathbf{u22}_S^T\} \end{bmatrix} \tag{5.12}$$

$$\mathbf{V}^{3}_{i,j,\omega} = \begin{bmatrix} \{\mathbf{v11}_1, \mathbf{v11}_2, \mathbf{v11}_3, ..., \mathbf{v11}_S\} & \{\mathbf{v12}_1, \mathbf{v12}_2, \mathbf{v12}_3, ..., \mathbf{v12}_S\} \\ \{\mathbf{v21}_1, \mathbf{v21}_2, \mathbf{v21}_3, ..., \mathbf{v21}_S\} & \{\mathbf{v22}_1, \mathbf{v22}_2, \mathbf{v22}_3, ..., \mathbf{v22}_S\} \end{bmatrix} \tag{5.13}$$

The scalar elements inside each brace, $\{\cdot\}$, comprise $S \times 1$ vectors. Equation 5.11 has been included to highlight the difference between $\mathbf{U}^{3}_{i,j,S}$ and $\mathbf{U}^{3}_{i,j,S}{}^{H}$ where, as described previously, the notation, $(\cdot)^T$ as it is used here refers to the complex conjugate of a given complex number. The vectors contained in equations (5.12) and (5.13) are now used to form the simulation of the MIMO multi-carrier modulation scheme which is depicted in fig. 5.3. The blocks, marked, 'EQ' in fig. 5.3 serve to remove the effect of the channel on the receive vectors in order to produce two vectors denoted $\bar{\mathbf{a1}}$ and $\bar{\mathbf{a2}}$. $\bar{\mathbf{a1}}$ and $\bar{\mathbf{a2}}$ are noisy estimates of the original transmit vectors denoted $\mathbf{a1}$ and $\mathbf{a2}$. As indicated in fig. 5.3, the vectors, $\bar{\mathbf{a1}}$ and $\bar{\mathbf{a2}}$ can be compared with the vectors $\mathbf{a1}$ and $\mathbf{a2}$ respectively, in order to compute bit error rates (BERs).

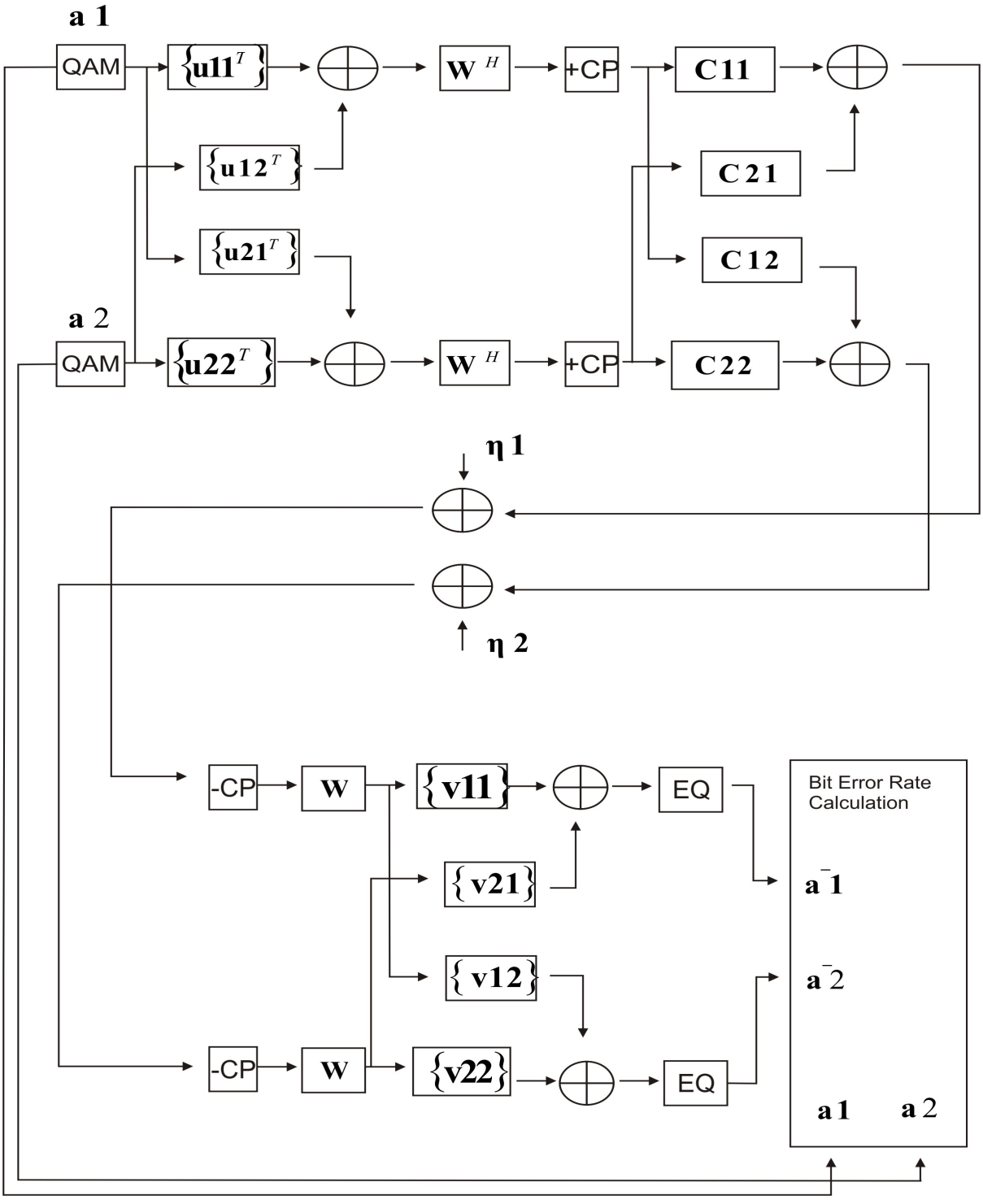

Figure 5.3: Multi-carrier modulation simulation model of a MIMO communications system.

5.3 MIMO Multi-Carrier Modulation Simulations Based on Transmission Line Channels

The MIMO multi-carrier modulation simulation depicted in fig. 5.3 is a SIMULINK [101] simulation. Within each of the QAM blocks is an information source which generates a series of equiprobable binary bits which are then mapped onto QAM symbols. The simulation is considered under a number of conditions:

(i) In common with the capacity calculations in chapter 4, an added white Gaussian noise power spectral density, N_0, of -110 dBm/Hz is assumed. As indicated by Aslanis and Cioffi [171], this level exceeds that set by electronics alone but includes the noise floor set by an echo canceller.

(ii) Again as in chapter 4, a transmit bandwidth of 4.3125 kHz is assumed. This is the bandwidth set by the American National Standards Institute (ANSI) for a discrete multi-tone (DMT) tone in the asymmetric digital subscriber line (ADSL) T1.413 DMT standard [124] [172].

(iii) Various transmit power spectral densities are considered. The lowest one taken is -80 dBm/Hz, which is the transmit power spectral density given in [124] for VDSLs signal that occur in known radio frequency bands. In common with chapter 4, -60 dBm/Hz is also taken since it is the figure given in [124] for nominal transmit power density of high bit-rate digital subscriber line (VDSL) signals. The highest transmit power spectral density considered is -40 dBm/Hz. It is noted that in reality, the noise variance within simulation is adjusted rather than transmit power spectral

density. However, this can readily be done to simulate the various transmit spectral densities outlined given what has been stated in (i) and (ii).

(iv) The simulation considers the balanced twisted-pair telephone cable, the balanced cat 5 twisted-pair and the unbalanced flat-pair are compared for a dimension, $N_T = 3$.

(v) In the case of each transmission line channel type, the relevant time domain channel impulse response vectors from chapter 3, i.e. either $\mathbf{h}_{U(i,j)}$, $\mathbf{h}_{B(i,j)}$ or $\mathbf{h}_{C(i,j)}$ are used to form circulant matrices.

It is argued that since the effect of the various transmission line channels is being compared, it is therefore logical to consider the transmit SNR to facilitate appropriate performance comparison. As in chapter 4, since full channel matrix rank is assumed, the BERs can be computed on each of three orthogonal sub-channels which are pertinent to the dimension being $N_T = 3$. The computed BERs are given in figs 5.4–5.6 for the cases of the balanced twisted-pair telephone cable, the balanced cat 5 twisted-pair and the unbalanced flat-pair respectively.

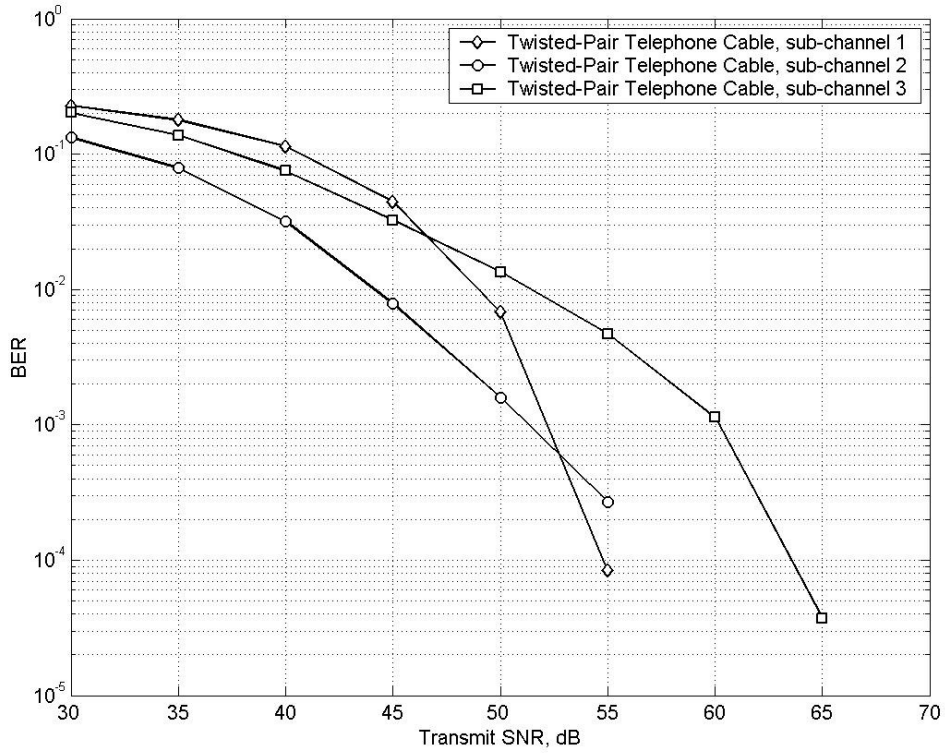

Figure 5.4: Bit error rate (BER) as a function of signal to noise (SNR) for each of the three orthogonal sub-channels for the case of the twisted-pair telephone cables. 30 dB corresponds a transmit power spectral density of – 80 dBm and 50 dB corresponds to a transmit power spectral density of -60 dBm.

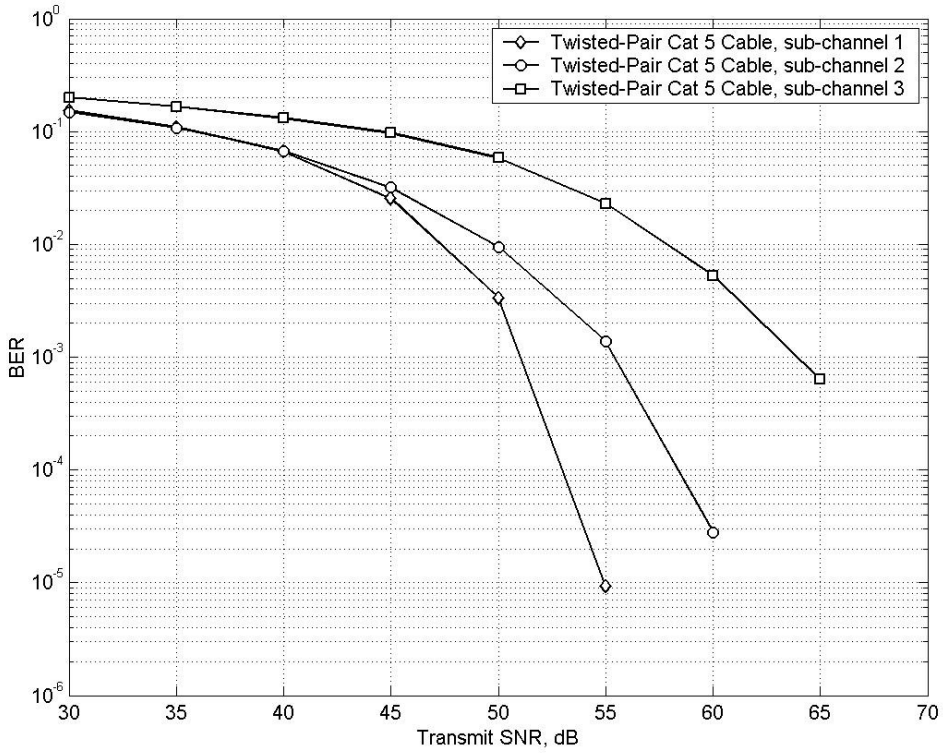

Figure 5.5: Bit error rate (BER) as a function of signal to noise (SNR) for each of the three orthogonal sub-channels for the case of the twisted-pair Cat 5 cables. 30 dB corresponds a transmit power spectral density of –80 dBm and 50 dB corresponds to a transmit power spectral density of -60 dBm.

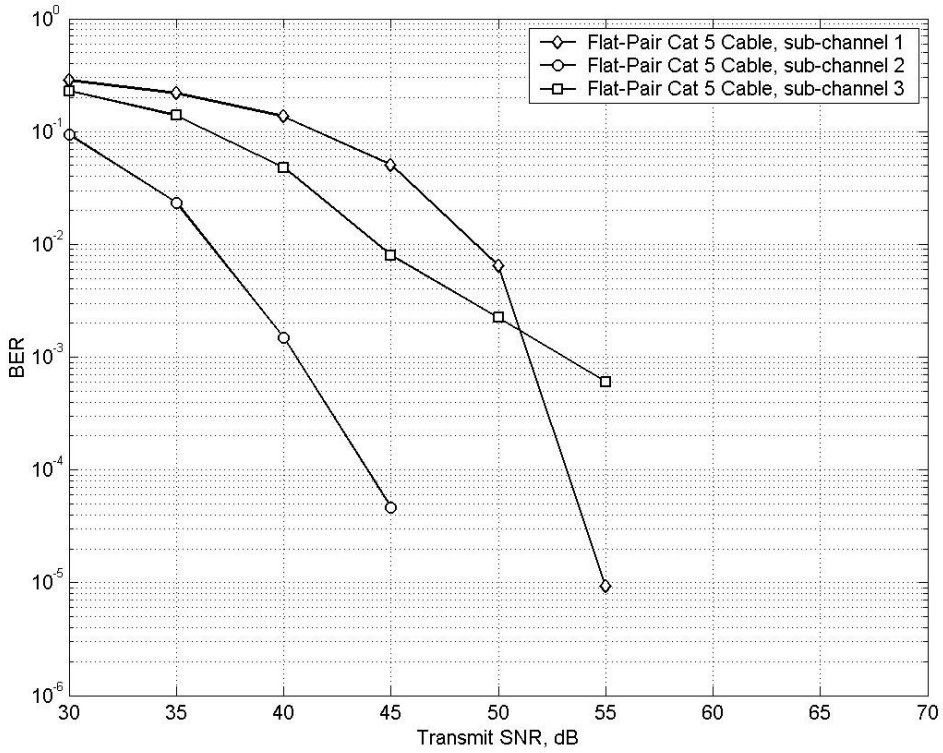

Figure 5.6: Bit error rate (BER) as a function of signal to noise (SNR) for each of the three orthogonal sub-channels for the case of the Flat-pair cables. 30 dB corresponds a transmit power spectral density of –80 dBm and 50 dB corresponds to a transmit power spectral density of -60 dBm.

The multi-carrier modulation scheme is unencoded and although the BERs given in figs 5.4 to 5.6 provide some idea of performance in each case, it is not clear which transmission line channel type performs best. In the context of capacity of MIMO communications systems, Kyritsi and Cox [92] state the following in relation to the orthogonal sub-channel gains:

"the maximum achievable capacity is attainable when all sub-channels have equal gains"

This statement concurs with Durgin's argument which was given in chapter 4 [47], i.e.

"The channel capacity expression is maximised when the signal power is evenly distributed among the singular values"

As a result of this, it would appear that the BER results presented in fig. 5.6, in the context of flat-pair, are indicative of the poorest performance since there appears to be one dominant singular value. However, greater clarity on the performance of the various transmission line channels comes from examination of the singular values which are calculated from the transfer functions which were derived from the channel sounding sequences. Looking at fig. 5.8, it can clearly be seen that the singular values pertaining to the cat 5 twisted-pair remain quite close to each other and do not drop below 0.1 until approximately 50 MHz. The singular values of the twisted-pair telephone cable in fig. 5.7 do not drop below 0.1 until approximately 30 MHz which indicates a slightly poorer performance than the case of the cat 5 twisted-pair. In fig. 5.9, the singular values of the flat-pair start to drop below 0.1 at approximately 10 MHz. Further to this, in light of the previous comments from Durgin, Kyritsi and Cox which pertain to increased performance as a result of numerical similarity of each of the singular values, it is also possible to consider the numerical similarity of each of the singular values given in each of figs 5.7-5.9. Careful examination of figs 5.7-5.9 reveals that the singular values of the Cat5 twisted-pair remain the closest to each other over the entire frequency range than in the case of the other two transmission line types. The results in figs 5.7–5.9 hence indicate that the best performance of the three types of transmission line channels is the twisted-pair Cat 5 transmission line channels followed by the twisted-pair telephone channels with the flat-pair channels

being the worst. However, the BERs presented in fig. 5.6 do indicate that the flat-pair would provide reasonable performance under the conditions specified in (i) – (iv) given sufficient coding effort. These conclusions are consistent with the capacity analysis of MIMO communications systems based on transmission line channels that was presented in chapter 4.

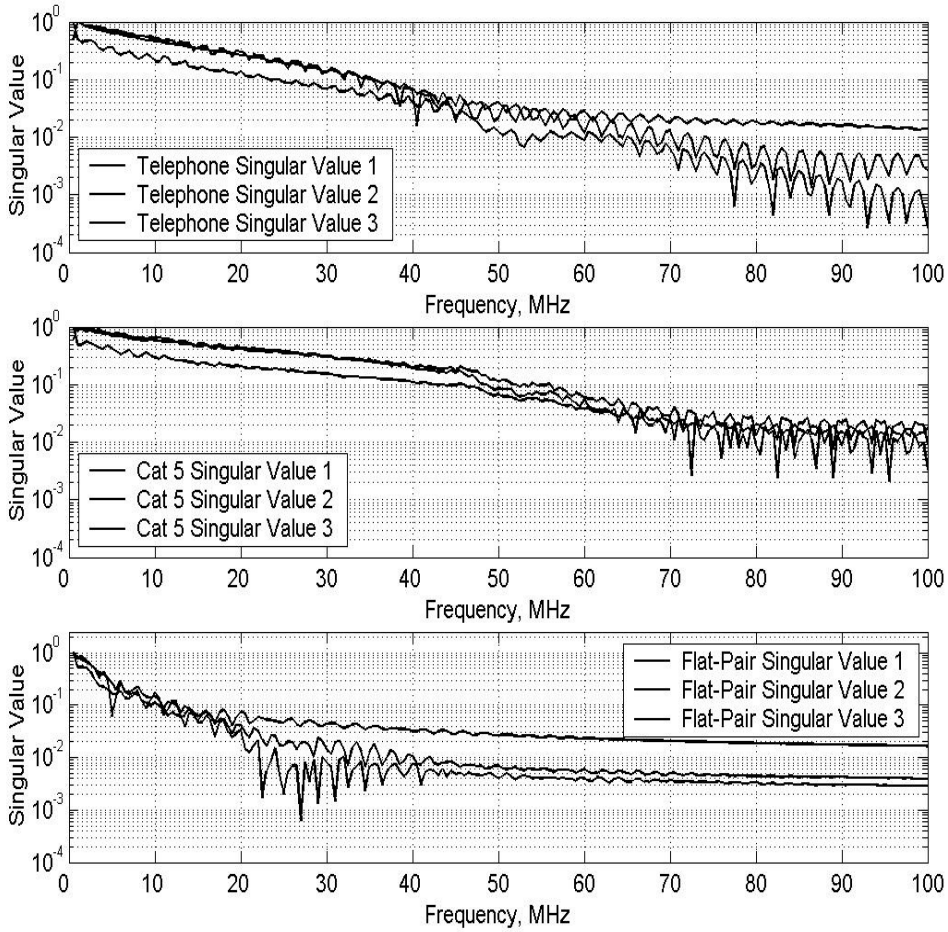

Figures 5.7-5.9: From top to bottom: Singular value calculations derived from channel sounding sequence for twisted-pair telephone cable (top, fig. 5.7), cat 5 twisted-pair (middle, fig. 5.8) and flat pair (bottom, fig. 5.9) for the dimension $N_T = 3$.

5.4 MIMO Multi-Carrier Modulation Simulations Based on Wireless Channels

The MIMO multi-carrier modulation simulation depicted in fig. 5.3 is a SIMULINK [101] simulation. Within each of the QAM blocks is an information source which generates a series of equiprobable binary bits which are then mapped onto QAM symbols. The simulation is considered under a number of conditions:

(i) The families of channel impulse response vectors denoted: $\mathbf{h}_{All}$, $\mathbf{h}_{LOS}$, $\mathbf{h}_{1^{st}\,order(1)}$, $\mathbf{h}_{1^{st}\,order(2)}$ and $\mathbf{h}_{2^{nd}\,order}$ are considered. The four families of channel impulse response vectors: $\mathbf{h}_{LOS}$, $\mathbf{h}_{1^{st}\,order(1)}$, $\mathbf{h}_{1^{st}\,order(2)}$ and $\mathbf{h}_{2^{nd}\,order}$ are compared against $\mathbf{h}_{All}$ in each figure which follows.

(ii) The receive signal power to noise power ratio denoted: $\frac{P}{\varphi}$ is fixed at a ratio of 18 dB at the receiver throughout this section on the basis of the sounding sequence. Thus it can be appreciated that the capacities for the MIMO communications systems are examined from the perspective of the channel matrix conditioning or eigenvalue distribution due to various multi-path channel impulse response components.

(iii) Since the all of the channel matrices are derived from common sets of experimental data with the obvious exception that various relevant channel impulse response components have been removed, the degree of

correlation amongst common channel impulse response components in each channel matrix is equivalent.

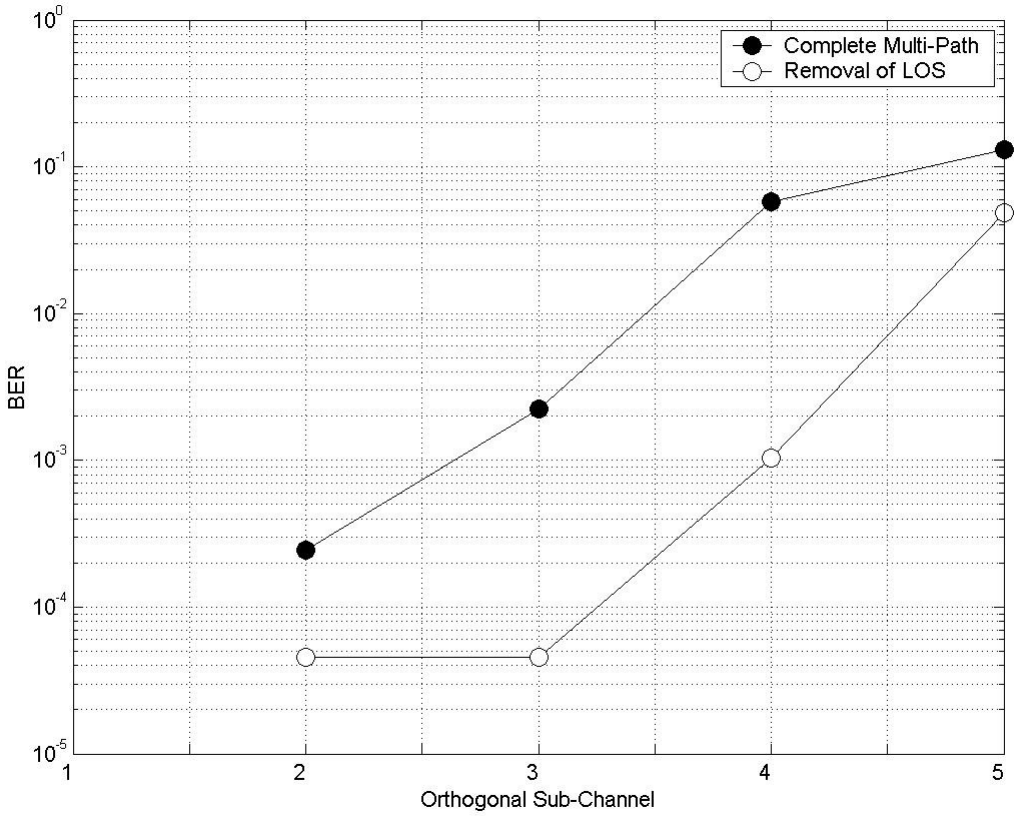

Figure 5.10: Bit error rate (BER) as a function of orthogonal sub-channel for the case of the wireless channels whose channel impulse response vectors were denoted: $\mathbf{h}_{All}$ (Complete Multi-Path) and $\mathbf{h}_{LOS}$ (Removal of LOS). In both cases, the BERs are zero for the first orthogonal sub-channel. The SNR is 18 dB at the receiver.

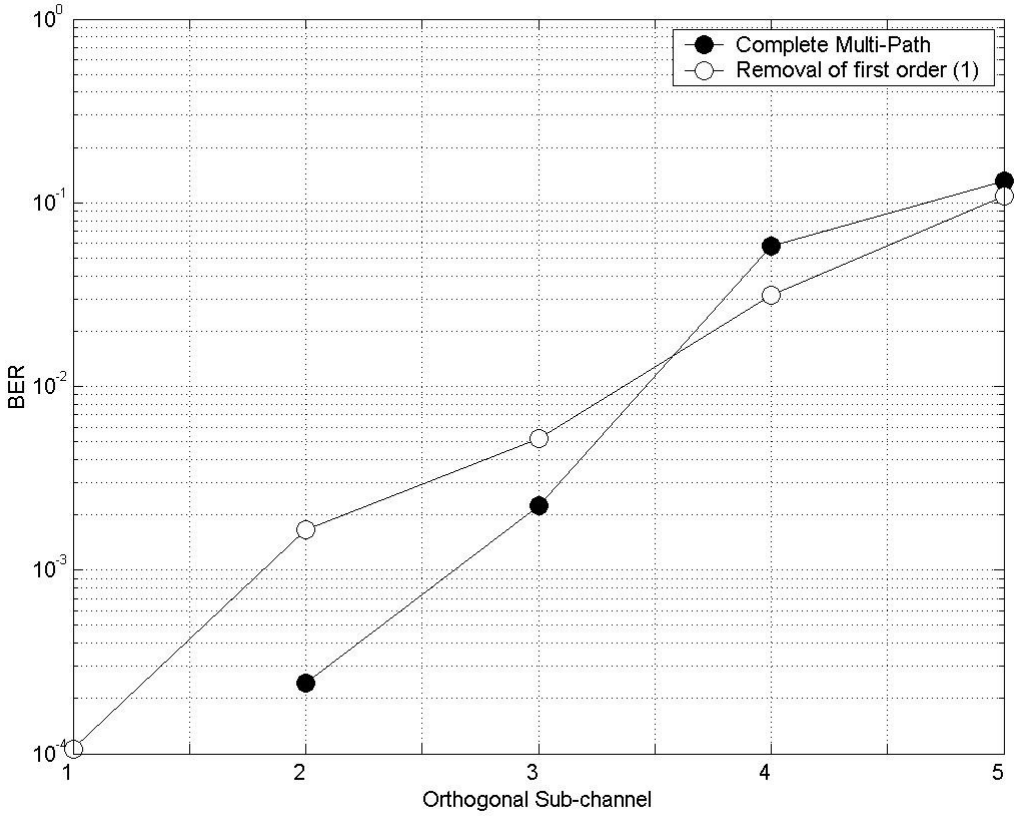

Figure 5.11: Bit error rate (BER) as a function of orthogonal sub-channel for the case of the wireless channels whose channel impulse response vectors were denoted: $\mathbf{h}_{All}$ (Complete Multi-Path) and $\mathbf{h}_{1^{st}\,Order(1)}$ (Removal of first order (1)). In the case of the simulation pertaining to $\mathbf{h}_{All}$, the BER is zero for the first orthogonal sub-channel. The SNR is 18 dB at the receiver.

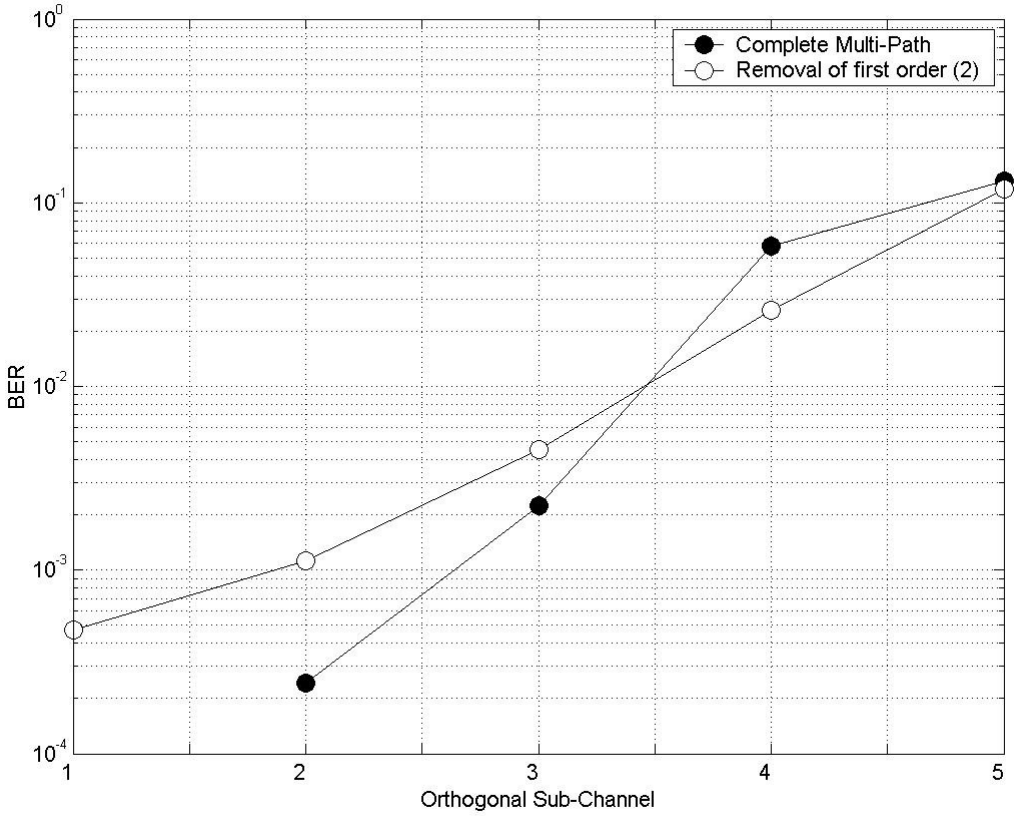

Figure 5.12: Bit error rate (BER) as a function of orthogonal sub-channel for the case of the wireless channels whose channel impulse response vectors were denoted: $\mathbf{h}_{All}$ (Complete Multi-Path) and $\mathbf{h}_{1^{st}\,Order(2)}$ (Removal of first order (2)). In the case of the simulation pertaining to $\mathbf{h}_{All}$, the BER is zero for the first orthogonal sub-channel. The SNR is 18 dB at the receiver.

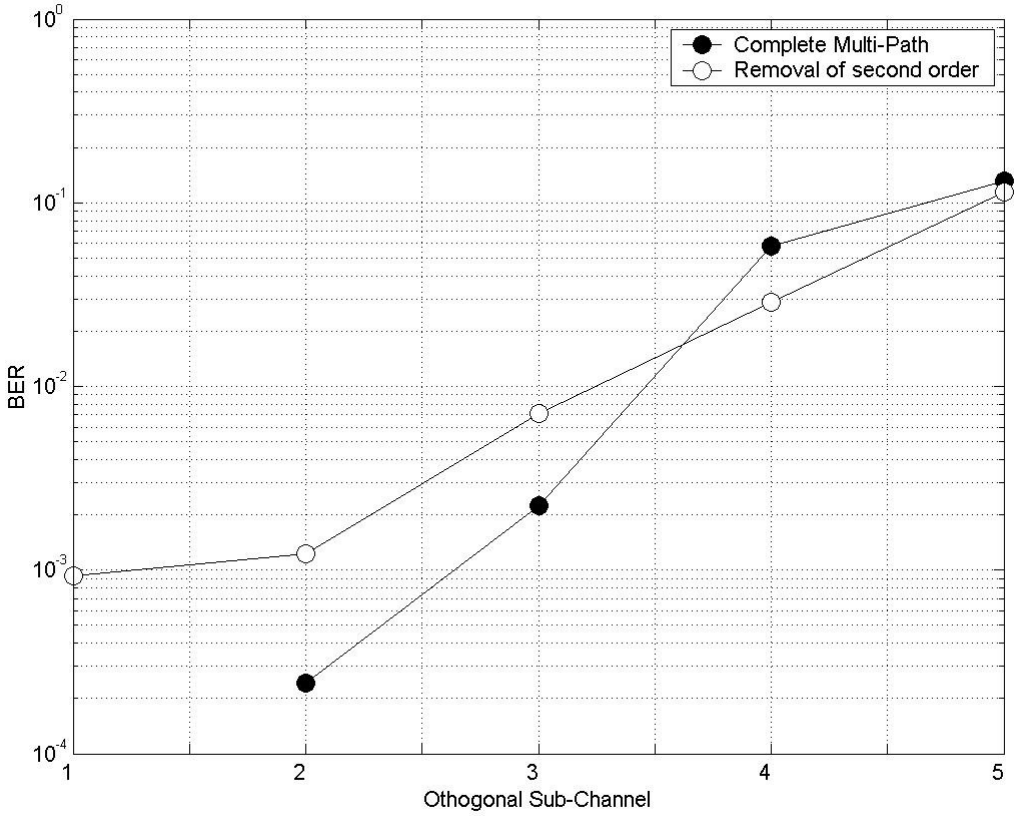

Figure 5.13: Bit error rate (BER) as a function of orthogonal sub-channel for the case of the wireless channels whose channel impulse response vectors were denoted: $\mathbf{h}_{All}$ (Complete Multi-Path) and $\mathbf{h}_{2^{nd}\,Order}$ (Removal of second order). In the case of the simulation pertaining to $\mathbf{h}_{All}$, the BER is zero for the first orthogonal sub-channel. The SNR is 18 dB at the receiver.

In fig. 5.10 it can be seen that removal of the line-of-sight channel impulse response component provides bit error rate performance. The similarity of the bit error rates in the third and fourth orthogonal sub-channels when the line-of-sight component is removed is indicative of a change in channel matrix conditioning. This analysis therefore supports the fact that for a fixed receive SNR, Rayleigh channels exhibit superior performance to Ricean channels. This supports the capacity analysis in chapter 4 where a similar conclusion was reached with respect to the effect of these

fading statistics of the wireless channels in light of the fact that the degree of multi-path correlation was equivalent. Looking at fig.5.11, fig. 5.12 and fig. 5.13, the effect of removing other channel impulse components from the channel impulse response of the wireless channels does give significantly different bit error rates recorded in the MIMO multi-carrier modulation simulation outlined in this chapter.

5.5 Summary

The overall objective of this chapter was to support the capacity based conclusions of chapter 4. MIMO multi-carrier modulation simulations have been described which were based on channels which were experimentally observed in the time domain. Specifically, vectors which contain the channel impulse responses of various transmission line and wireless channels support the analysis. In the case of the transmission line channels, the novel idea from chapter 4 of using the MIMO communications system to enhance transmission lines which would have otherwise been deemed out-of-range for high speed internet connections was supported by considering the flat-pair channels. However, the transmission line analysis in this chapter supported the analysis of chapter 4 where the flat-pair was seen to exhibit the worst overall performance. In the case of the wireless channels, it was seen that there was an improvement in the bit error rates when the line-of-sight channel impulse response component was removed. Again, it is argued that this improvement is indicative of a Rayleigh channel whose multi-path components have equivalent correlation to those of a comparative Ricean channel which has the additional line-of-sight component.

Chapter 6: The Effect of Imperfect Knowledge of the Channel on the Capacity of MIMO Communications Systems

6.1 Introduction

This chapter extends the analysis of chapter 4 by examining the effect of imperfect knowledge of the channel on the capacity of multiple-input/multiple-output (MIMO) communications systems. In the case of the time-invariant transmission line channels, it was discussed in chapter 4 how, in a practical sense, the channel transfer functions are in fact computed from one-port measurements. It will be seen in this chapter that these channel transfer functions may be incorrect and hence there is imperfect knowledge of the transmission line channels. In the case of the time-variant wireless channels, it was assumed in chapter 4 that the channel transfer functions remained constant over an arbitrary period of time known, i.e. the channel was assumed 'quasi-static'. Again, should the wireless channels not be quasi-static, there is imperfect knowledge of the channel. In the case of the transmission line channels, this chapter presents a novel comparative analysis of the capacity of the MIMO communications system based on the unbalanced flat-pair transmission lines, balanced twisted-pair telephone transmission lines and the balanced Cat 5 twisted-pair. In each case, the effect of increasing the extent of the imperfect knowledge of the channel is examined. A similar analysis of the effect of increasing the extent of the imperfect knowledge of the channel on the capacity of MIMO communications systems in the case of the wireless channels is also presented in this chapter. In respect of the wireless channels, this particular analysis parallels the work of Kyritsi [93] and others [103] [138] [137] [14] [20] [113] [64] [143], but with differences to the overall approach which deem

the analysis and its results novel. All the analyses and results within this chapter will also be seen to provide an important foundation for the analyses of chapter 7.

6.2 Imperfect Knowledge of the Channel

Transmission line channels are considered to be time-invariant. In this case, imperfect knowledge of the channel is likely to occur due to incorrect assessment of the channel transfer functions from one-port transmission line measurements. This idea has been outlined in the studies by Bostoen et. al [18], Galli and Waring [57], Wong and Aboulnasr [141] and has been described in a text by Bingham [18]. In contrast to transmission line channels, the wireless channel is considered to be time variant. As a result of this, the channel transfer functions will change with time as a result of multi-path fading in a dynamic environment. Imperfect knowledge of the channel will therefore occur when these channel transfer functions change at a rate incommensurate with the assumption of the quasi-static channel. In other words, the channel transfer functions could change at a rate quicker than the rate at which bursts of information are transmitted. This idea has been outlined in the studies by Médard [103], Weber et al [138] [137], Kyritsi et al. [93], Berriche et al. [14], Cano-Gutierrez et al. [20], and others [113] [64] [143].

Define the extent of the imperfect knowledge of the channel as a matrix $\Delta\mathbf{H}$:

$$\Delta\mathbf{H} \sim CN\left(0, \mathrm{var}\{\Delta\mathbf{H}\}\right) \tag{6.1}$$

$\Delta\mathbf{H}$ is a matrix whose scalar elements are random complex independent and identically distributed. The notation in equation (6.1) indicates that the statistical distribution of these scalar elements is complex normal as identified by the

notation, CN . This notation also indicates that the mean of these scalar elements is set at zero and that their variance is set at an arbitrary variance, $\text{var}\{\Delta\mathbf{H}\}$. Imperfect knowledge of the channel may be defined by the matrix sum of the channel matrix, $\mathbf{H}$, and the extent of the imperfect knowledge of the channel, $\Delta\mathbf{H}$, i.e., $\mathbf{H}+\Delta\mathbf{H}$. A singular value decomposition of the matrix, $\mathbf{H}+\Delta\mathbf{H}$, is given as:

$$\mathbf{H}+\Delta\mathbf{H}=(\mathbf{U}+\Delta\mathbf{U})(\mathbf{D}+\Delta\mathbf{D})(\mathbf{V}+\Delta\mathbf{V})^{H} \tag{6.2}$$

The matrices: $\mathbf{U}+\Delta\mathbf{U}$ and $\mathbf{V}+\Delta\mathbf{V}$ are unitary and the matrix, $\mathbf{D}+\Delta\mathbf{D}$, is a diagonal matrix. Recalling from chapter 4 that in a MIMO communications system where there is perfect knowledge of the channel, the weighted receive vector, $\bar{\mathbf{y}}$, is related mathematically to the weighted transmit vector, $\bar{\mathbf{x}}$, by:

$$\bar{\mathbf{y}}=\mathbf{D}\bar{\mathbf{x}}+\bar{\mathbf{n}} \tag{6.3}$$

Equivalently in the original transmit vector, $\mathbf{x}$, and the receive vector $\mathbf{y}$,are written as:

$$\mathbf{U}\mathbf{y}=\mathbf{U}^{H}\mathbf{H}\mathbf{V}\mathbf{x}+\mathbf{n} \tag{6.4}$$

This is depicted in fig. 6.1. However, when the unitary matrices $\mathbf{U}+\Delta\mathbf{U}$ and $\mathbf{V}+\Delta\mathbf{V}$ are applied to a MIMO communications system, whose channels are defined mathematically by the channel matrix, $\mathbf{H}$, the relationship between the transmit vector, $\mathbf{x}$, and the receive vector, $\mathbf{y}$, may be depicted in fig. 6.2.

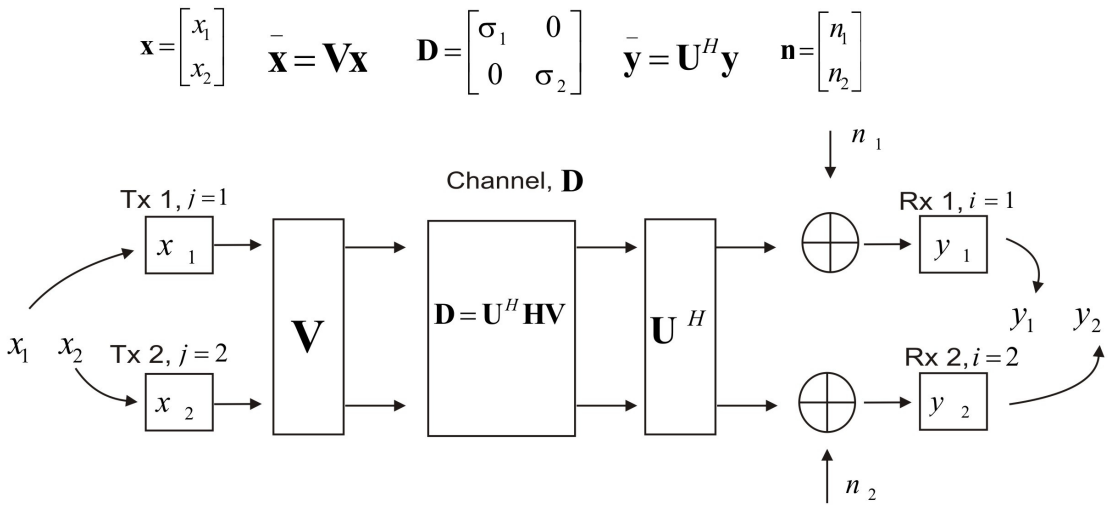

Figure 6.1: The MIMO communications system consisting of two transmit elements and two receivers elements. Equations are written above the various mathematical operations in the MIMO Communications system. N_T is set $N_T = 2$.

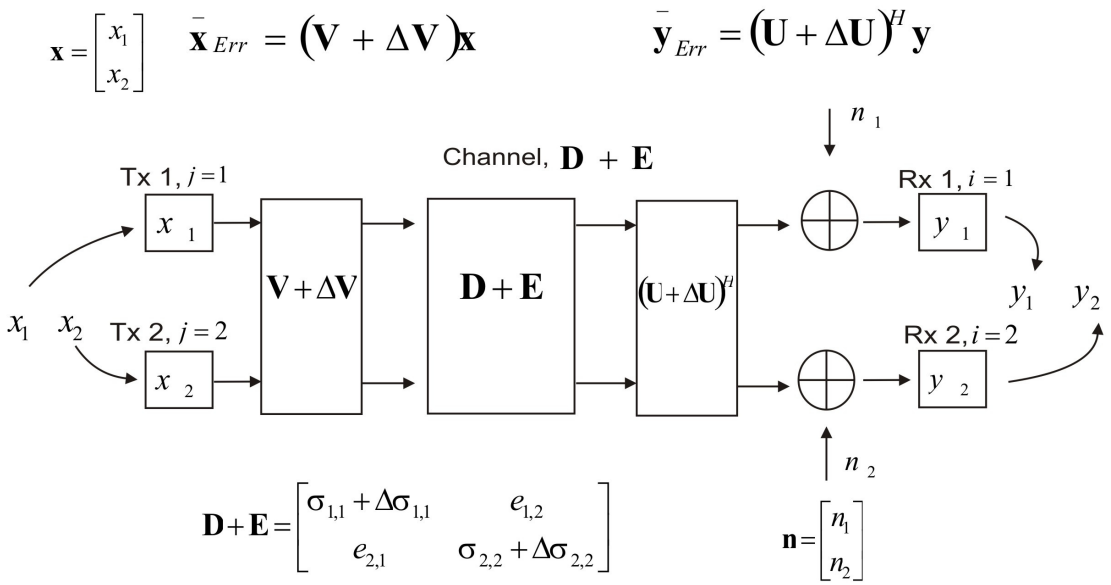

Figure 6.2: The effect of imperfect knowledge of the channel on MIMO communications systems consisting of two transmit elements and two receivers elements. Equations are written above the various mathematical operations in the MIMO Communications system. N_T is set $N_T = 2$.

Looking at fig. 6.2, an erroneously weighted transmit vector, $\bar{\mathbf{x}}_{Err}$, and an erroneously weighted receive vector, $\bar{\mathbf{y}}_{Err}$, have been defined. In this case, the relationship between the transmit vector, $\mathbf{x}$, and the receive vector, $\mathbf{y}$, is written as:

$$(\mathbf{U}+\Delta\mathbf{U})^H\mathbf{y} = (\mathbf{U}+\Delta\mathbf{U})^H\mathbf{H}(\mathbf{V}+\Delta\mathbf{V})\mathbf{x} + (\mathbf{U}+\Delta\mathbf{U})^H\mathbf{n} \tag{6.5}$$

Comparing equation (6.5) with equation (6.4), the matrix vector product of $(\mathbf{U}+\Delta\mathbf{U})^H\mathbf{y}$, in equation (6.5), results in an erroneously weighted receive vector, defined as $\bar{\mathbf{y}}_{Err}$ in fig. 6.2. Similarly, the matrix vector product of $(\mathbf{V}+\Delta\mathbf{V})\mathbf{x}$ results in an erroneously weighted transmit vector, defined as $\bar{\mathbf{x}}_{Err}$ in fig. 6.2. In relation to this, the channel matrix, $\mathbf{D}+\mathbf{E}$, in fig. 6.2 is:

$$\mathbf{D}+\mathbf{E} = (\mathbf{U}+\Delta\mathbf{U})^H\mathbf{H}(\mathbf{V}+\Delta\mathbf{V}) \tag{6.6}$$

Recalling from chapter 4 that the matrix, $\mathbf{D}$, is a diagonal matrix:

$$\begin{aligned}\mathbf{D} &= diag\{\sigma_1,\sigma_2,...,\sigma_{N_T}\} \\ &= \begin{bmatrix} \sigma_1 & 0 & \cdots & 0 \\ 0 & \sigma_2 & \cdots & 0 \\ \vdots & \vdots & \ddots & \vdots \\ 0 & 0 & \cdots & \sigma_{N_T} \end{bmatrix}\end{aligned} \tag{6.7}$$

Thus the matrix, $\mathbf{E}$, is:

$$\mathbf{E} = \begin{bmatrix} \Delta\sigma_1 & e_{1,2} & \cdots & e_{1,N_T} \\ e_{2,1} & \Delta\sigma_2 & \cdots & e_{2,N_T} \\ \vdots & \vdots & \ddots & \vdots \\ e_{N_T,1} & e_{N_T,2} & \cdots & \Delta\sigma_{N_T} \end{bmatrix} \tag{6.8}$$

The diagonal elements of the matrix, $\mathbf{E}$, are perturbations in the singular values which are contained along the main diagonal of the matrix, $\mathbf{D}$. These perturbations, are denoted:

$$\Delta\sigma_1, \Delta\sigma_2, ...\Delta_{N_T}$$

Use of this notation is logical since the diagonal elements of $\mathbf{D}$, i.e. the singular values of $\mathbf{H}$, were denoted $\sigma_1, \sigma_2, ...\sigma_{N_T}$ in equation (6.7). In contrast to the matrix, $\mathbf{D}$, the matrix, $\mathbf{E}$, contains non-zero off-diagonal terms[15]. These non-zero off-diagonal terms indicate a degree of coupling or 'leakage' between the sub-channels which would previously have been viewed as orthogonal by the receiver when the transmit and receive vectors were correctly weighted, i.e. when there was perfect channel knowledge. Combining equations (6.7) and (6.7), the channel matrix, $\mathbf{D}+\mathbf{E}$, may also be written as:

$$\mathbf{D}+\mathbf{E} = \begin{bmatrix} \sigma_1 + \Delta\sigma_1 & e_{1,2} & \cdots & e_{1,N_T} \\ e_{2,1} & \sigma_2 + \Delta\sigma_2 & \cdots & e_{2,N_T} \\ \vdots & \vdots & \ddots & \vdots \\ e_{N_T,1} & e_{N_T,2} & \cdots & \sigma_{N_T} + \Delta\sigma_{N_T} \end{bmatrix} \tag{6.9}$$

This matrix, $\mathbf{D}+\mathbf{E}$, forms the basis for computing the capacity, denoted $C_{\mathbf{D}+\mathbf{E}}$, of MIMO communications systems where there is imperfect knowledge of the channel.

[15]Throughout this work the exponential function has been denoted, $\exp\{\cdot\}$, and the expectation operator has been denoted, $E\{\cdot\}$. As a result, the matrix, $\mathbf{E}$, in equation (6.8) and its scalar elements should not be confused with either the exponential function or the expectation operator.

This capacity, $C_{\mathbf{D+E}}$, is now defined as:

$$C_{\mathbf{D+E}} = E\left\{\sum_{i=1}^{N_T}\log_2\left[1+\frac{P\left|(\mathbf{D}+\mathbf{E})_{i,i}\right|^2}{\varphi_i + P\left[\sum_{j=i}\left\{\left|(\mathbf{D}+\mathbf{E})_{j}\right|^2\right\}-\left|(\mathbf{D}+\mathbf{E})_{i,i}\right|^2\right]}\right]\right\} \tag{6.10}$$

The reader is reminded that equation (6.10) is of the form pertinent to a continuous channel capacity with units of bits/sec/Hz. As before, P is the total receive power, in watts, as detected over all the receivers and φ_i is the noise power, in watts, as detected at the i^{th} receiver. The matrix, $\mathbf{D}+\mathbf{E}$, is ultimately derived from a matrix of random elements, $\Delta\mathbf{H}$, hence the capacity, $C_{\mathbf{D+E}}$, is evaluated with respect to the expectation operator, $E\{\cdot\}$. The use of parenthesis on the matrix, $\mathbf{D}+\mathbf{E}$, emphasises that any relevant qualifying matrix notation makes reference to the entire matrix, $\mathbf{D}+\mathbf{E}$, as it has been defined in equation (6.9). The term:

$$\sum_{i=j}\left\{\left|(\mathbf{D}+\mathbf{E})_{j}\right|^2\right\}-\left|(\mathbf{D}+\mathbf{E})_{i,i}\right|^2$$

quantifies the degree of degree of coupling, or loss in orthogonality, of the sub-channels in the MIMO communications system where there is imperfect knowledge of the channel.

6.3 Capacity Calculations on Transmission Line Channels

In chapter 4, the capacity calculations based on transmission line channels were calculated under a number of conditions. These conditions are now recalled in the context of the analysis to be presented in this section.

(i) An added white Gaussian noise (AWGN) power spectral density, N_0, of -110 dBm/Hz, pertinent to the noise floor set by an echo canceller [171], is assumed.

(ii) The American National Standards Institute (ANSI) discrete multi-tone (DMT) tone transmit bandwidth of 4.3125 kHz is assumed [124] [172]. Capacities are calculated at intervals of approximately 496 kHz, i.e. at 201 intervals between 300 kHz to 100 MHz.

(iii) The lower nominal transmit power density -80 dBm/Hz for high bit-rate digital subscriber line (VDSL) signals yielded little in the way of improvement for MIMO over SISO in chapter 4. Thus only the higher transmit power spectral density of -60 dBm/Hz for high bit-rate digital subscriber line (VDSL) signals [124] is considered here.

(iv) The balanced twisted-pair telephone cable, the balanced cat 5 twisted-pair and the unbalanced flat-pair are compared for a dimension, $N_T = 3$. The cat5 is also examined for a dimension, $N_T = 4$ and the twisted-pair is also examined for a dimension, $N_T = 5$. Cumulative plots of capacity with respect to bandwidth are also presented.

(v) As described in chapter 4, the channel matrix, $\mathbf{H}(f)$, was normalised such that:

$$\bar{\mathbf{H}}(f) = \frac{\mathbf{H}(f)}{\left\|\mathbf{H}(f=1)\right\|_F} \tag{6.11}$$

The capacity calculations in this section are therefore derived from:

$$\bar{\mathbf{H}}(f) + \Delta\mathbf{H}$$

Using:

$$C_{\mathbf{D+E}}(f) = E\left\{\sum_{i=1}^{N_T} \log_2\left[1 + \frac{P\left|\left(\bar{\mathbf{D}}(f) + \mathbf{E}(f)\right)_{i,i}\right|^2}{\varphi_i + P\left[\sum_{j=i}\left\{\left|\bar{\mathbf{D}}(f) + \mathbf{E}(f)\right|_j^2\right\} - \left|\left(\bar{\mathbf{D}}(f) + \mathbf{E}(f)\right)_{i,i}\right|^2\right]}\right]\right\} \tag{6.12}$$

Consider now the effect of increasing the variance, $\mathrm{var}\{\Delta\mathbf{H}\}$, from 0.001 through to 0.01 for the case of the balanced twisted-pair telephone cable with dimension $N_T = 3$ in figs 6.3 and 6.4.

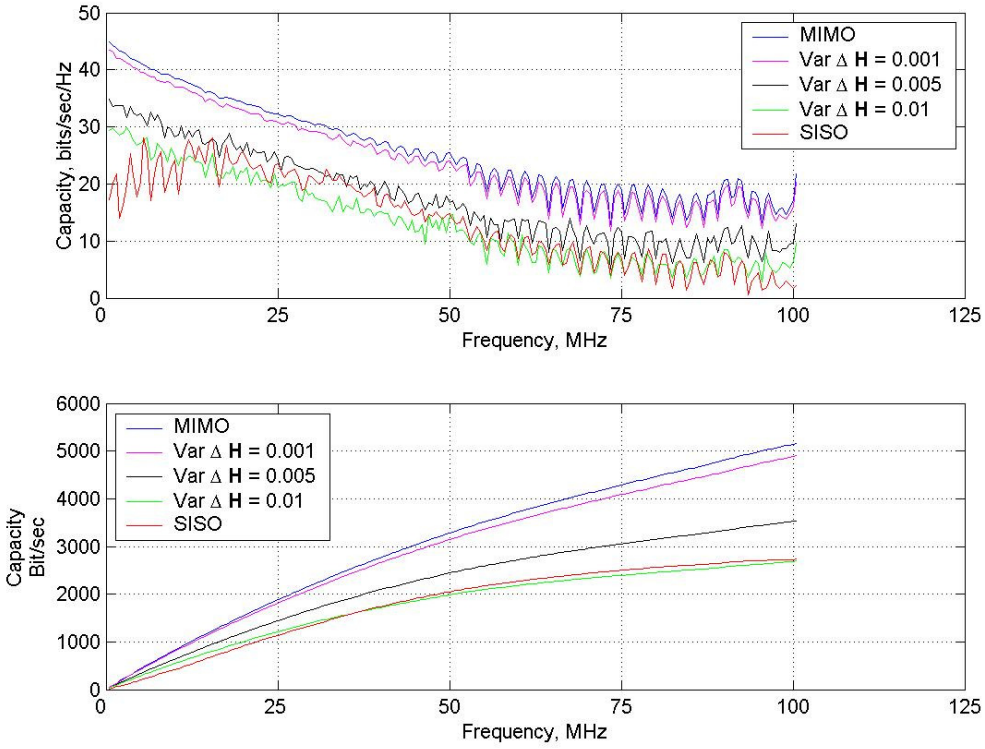

Figure 6.3-6.4: Effect of increasing imperfect knowledge of the channel, $\text{var}\{\Delta\mathbf{H}\}$ = 0.001, 0.005 and 0.01, on MIMO communications system based on balanced twisted-pair telephone cable transmission lines. Upper plot: capacity in bits/sec/Hz. Lower plot: cumulative capacity in bits/sec. In all cases, the dimension $N_T = 3$ and the transmit power spectral density is $P_0 = -60$ dBm/Hz.

It appears from capacity plot in fig. 6.3 that there is a minimal gain in capacity for the case of the MIMO communications system when the extent of the imperfect knowledge of the channel is $\text{var}\{\Delta\mathbf{H}\} = 0.005$. The cumulative capacity plot in fig. 6.4 clarifies that for a MIMO communications system operating over the entire frequency range from 300 kHz to 100 MHz, the extent of the imperfect knowledge of the channel should be between $\text{var}\{\Delta\mathbf{H}\}$ of 0.005 and 0.001. Fig. 6.4 also clarifies that there is no capacity gain for MIMO when $\text{var}\{\Delta\mathbf{H}\}$ is 0.01 in this case.

The effect of increasing the variance, $\text{var}\{\Delta\mathbf{H}\}$, from 0.001 through to 0.01 for the case of the balanced twisted-pair cat 5 cable, with dimension $N_T = 3$, is considered in figs 6.5 and 6.6.

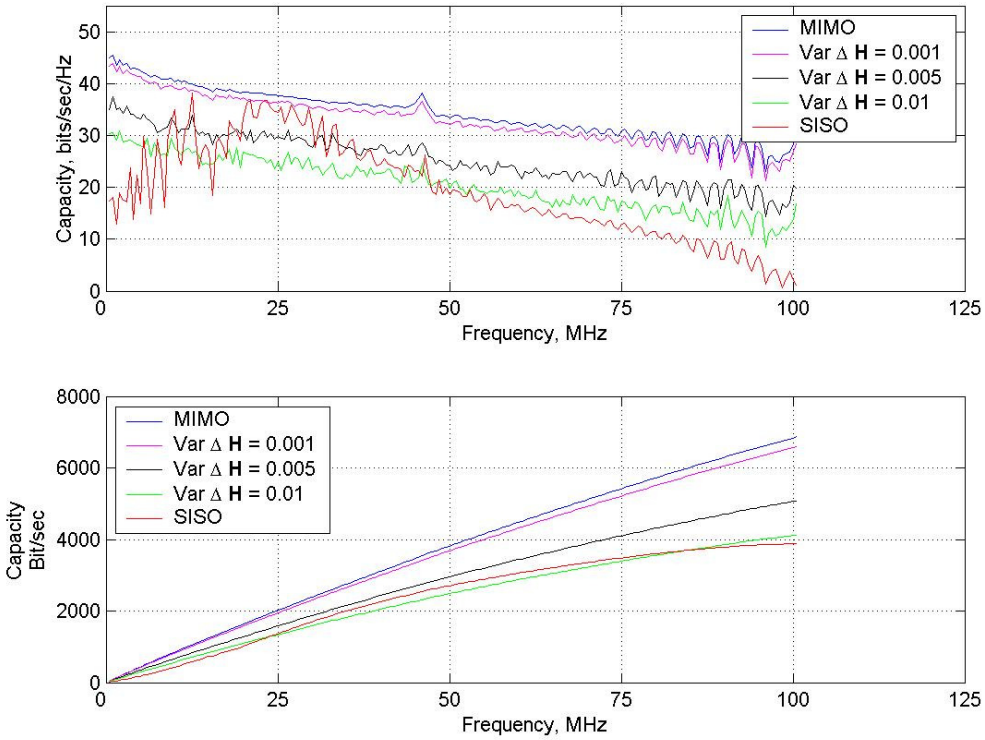

Figures 6.5-6.6: Effect of increasing imperfect knowledge of the channel, $\text{var}\{\Delta\mathbf{H}\}$ = 0.001, 0.005 and 0.01, on MIMO communications system based on balanced twisted-pair cat 5 transmission lines. Upper plot: capacity in bits/sec/Hz. Lower plot: cumulative capacity in bits/sec. In all cases, the dimension $N_T = 3$ and the transmit power spectral density is $P_0 = -60$ dBm/Hz.

Fig. 6.5 indicates that when the imperfect knowledge of the channel is quantified by $\text{var}\{\Delta\mathbf{H}\}$ = 0.01, the MIMO communications system based on the cat 5 twisted-pair transmission line channels appears to perform poorer than the SISO communications system at frequencies up to 50 MHz, but better above 50 MHz. However, the

cumulative capacity plot in fig. 6.6 indicates that there is no capacity gain in the case of MIMO over the entire frequency range from 300 kHz to 100 MHz when $\text{var}\{\Delta\mathbf{H}\}$ = 0.01. Given this extent of imperfect knowledge of the channel, the use of SISO techniques up to 50 MHz is indicated with MIMO techniques being confined to frequencies above 50 MHz. Inspection of fig. 6.5 indicates that a similar argument in respect of a $\text{var}\{\Delta\mathbf{H}\}$ = 0.005 can be made. Comparison of figs 6.3 and 6.4 with figs 6.5 and 6.6, at frequencies above 50 MHz, reveals that performance of the MIMO communications system in the case of cat 5 cable is such that for a given extent of imperfect knowledge of the channel, it does not degrade towards to the performance of the SISO communications to the same extent as the twisted-pair telephone cable.

The effect of increasing the variance, $\text{var}\{\Delta\mathbf{H}\}$, from 0.001 through to 0.01 for the case of the unbalanced flat-pair cable, with dimension $N_T = 3$, is considered in figs 6.7 and 6.8.

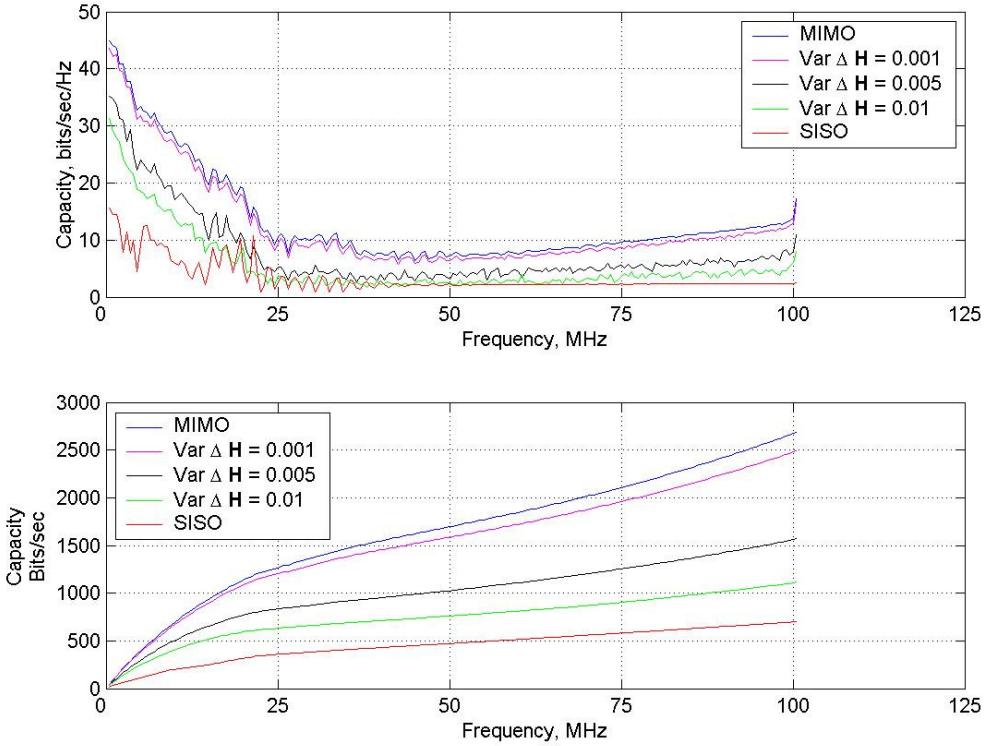

Figures 6.7-6.8: Effect of increasing imperfect knowledge of the channel, $\text{var}\{\Delta\mathbf{H}\}$ = 0.001, 0.005 and 0.01, on MIMO communications system based on unbalanced flat-pair transmission lines. Upper plot: capacity in bits/sec/Hz. Lower plot: cumulative capacity in bits/sec. In all cases, the dimension $N_T = 3$ and the transmit power spectral density is $P_0 = -60$ dBm/Hz.

The results in fig. 6.7 and 6.8 clearly support the idea of low frequency operation for the unbalanced flat pair transmission lines. For the MIMO communications system, at frequencies higher than 25 MHz, the effect of imperfect knowledge of the channel on capacity as quantified by the variances: $\text{var}\{\Delta\mathbf{H}\}$ = 0.001, 0.005 is such that

performance is more or less equivalent to the SISO communications system. As mentioned in chapter 4, some current asymmetric digital subscriber lines (ADSLs) standards operate in the frequencies 2-3 MHz. At frequencies below approximately 10 MHz, the flat-pair exhibits reasonable capacity gain for MIMO with respect to SISO in relation to the variances: $\text{var}\{\Delta\mathbf{H}\} = 0.001, 0.005$. Thus this analysis of imperfect knowledge of the channel further supports the argument for the enhancement of poor quality digital subscriber line using MIMO.

In the case of the balanced twisted-pair cat 5 transmission line, the effect of increasing the dimension, N_T, from 3 to 4 is now considered in figs 6.9-6.11.

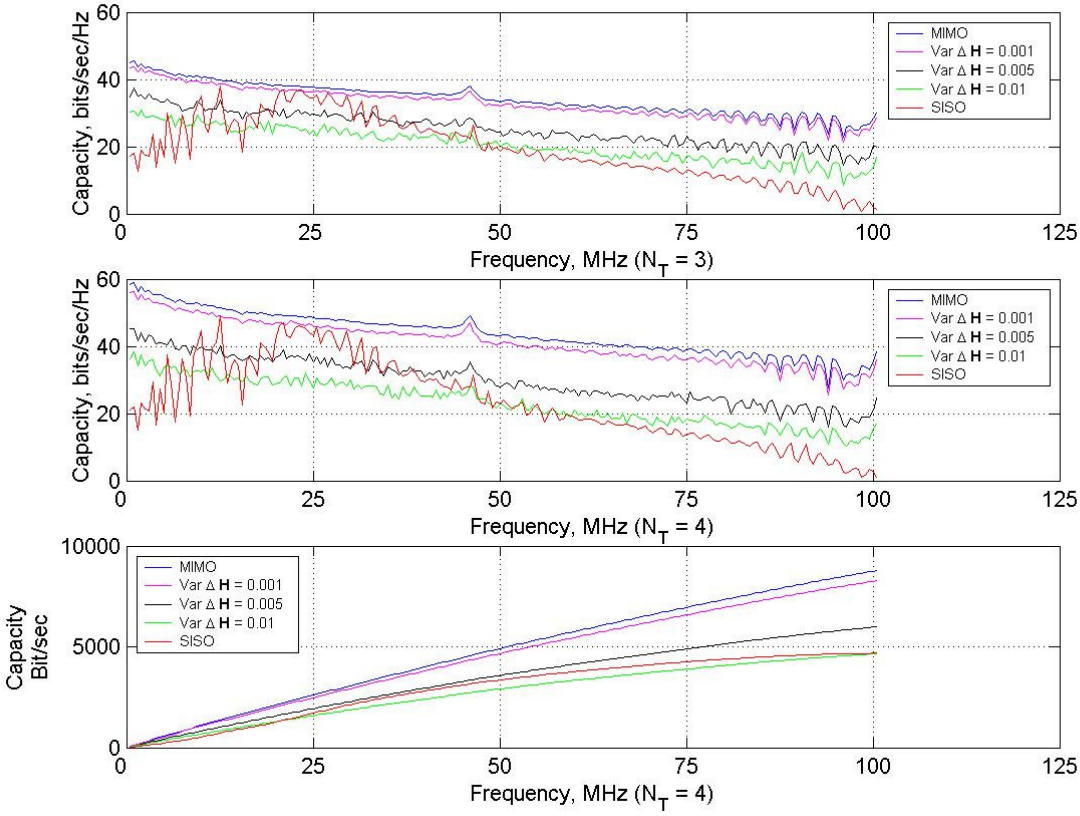

Figures 6.9-6.11: Effect of increasing imperfect knowledge of the channel, var$\{\Delta\mathbf{H}\}$ = 0.001, 0.005 and 0.01, on MIMO communications system based on balanced twisted-pair cat 5 transmission lines. Upper plot: capacity in bits/sec/Hz for $N_T = 3$. Middle plot: capacity in bits/sec/Hz for $N_T = 4$. Lower plot: cumulative capacity in bits/sec for $N_T = 4$. In all cases, the transmit power spectral density is $P_0 = -60$ dBm/Hz.

Similar conclusions can be made regarding the relative performance of MIMO and SISO communications for the case where $N_T = 4$ in figs 6.10 and 6.11 as were made for the case where $N_T = 3$ in figs 6.5 and 6.6. However, comparing fig. 6.9 with 6.10,

where the dimension $N_T = 3$ may be compared directly with the case where $N_T = 4$, for any given variance, $\text{var}\{\Delta\mathbf{H}\}$, there is a greater loss in capacity as N_T increases. This is quite clear from inspection given that the plots in figs 6.9 and 6.10 are to the same scale.

Finally in this section, the effect of increasing the dimension, N_T, from 3 to 5, is now considered for the case of the balanced twisted-pair telephone transmission line in figs 6.13-6.14.

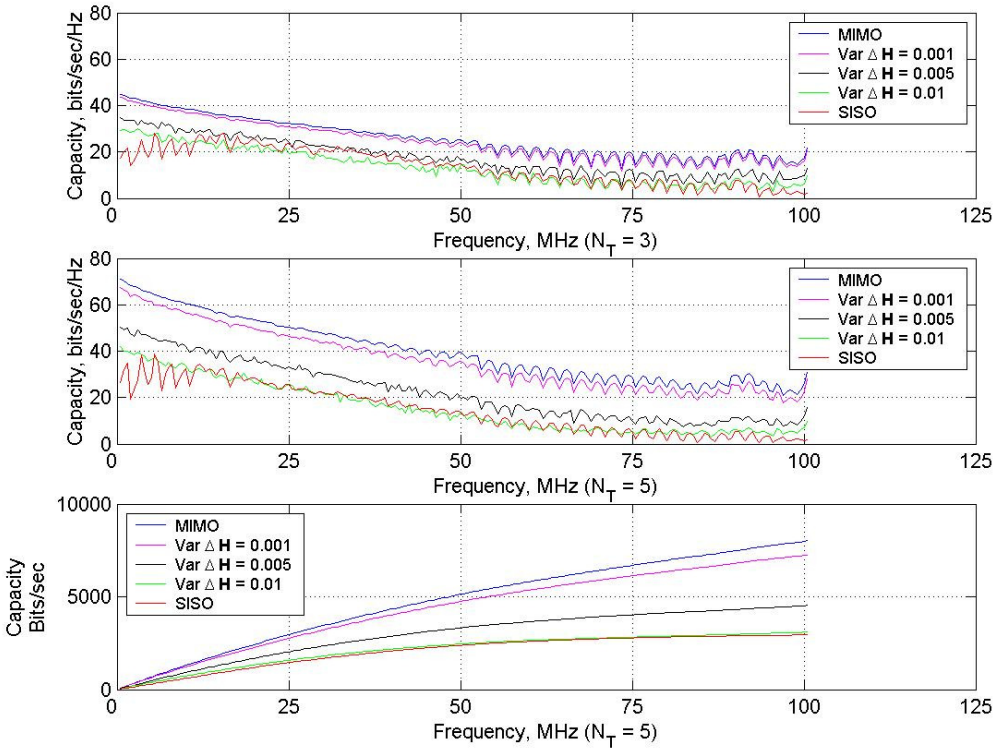

Figures 6.12-6.14: Effect of increasing imperfect knowledge of the channel, $\text{var}\{\Delta\mathbf{H}\}$ = 0.001, 0.005 and 0.01, on MIMO communications system based on balanced twisted-pair telephone transmission lines. Upper plot: capacity in bits/sec/Hz for $N_T = 3$. Middle plot: capacity in bits/sec/Hz for $N_T = 4$. Lower plot: cumulative capacity in bits/sec for $N_T = 4$. In all cases, the transmit power spectral density is $P_0 = -60$ dBm/Hz.

Again, in fig 6.12, there are plots for the case where $N_T = 3$ on the same scale as fig 6.13 for ease of comparison. It is clear again that there is a loss in terms of capacity for any given variance as N_T is increased. This idea of increasing capacity loss for a given variance, $\text{var}\{\Delta\mathbf{H}\}$, as the dimension N_T is increased will be seen to be mirrored in the next section which concerns the wireless channels.

6.4 Capacity Calculations on Wireless Channels

In chapter 4, the capacity calculations based on wireless channels were calculated under a number of conditions. These conditions are now recalled in the context of the analysis to be presented in this section.

(i) As outlined in chapter 3, all the transfer functions and hence channel matrices pertain to a centre frequency of 5.2 GHz.

(ii) The receive signal power to noise power ratio denoted: $\frac{P}{\varphi}$ is fixed at a ratio of 18 dB throughout this section.

(iii) The various channel matrices were normalised in the manner described in section 4.3 of chapter 4. Thus the channel matrix, $\mathbf{H}$, was normalised such that:

$$\bar{\mathbf{H}}(f) = \frac{\mathbf{H}}{\|\mathbf{H}\|_F} \tag{6.13}$$

The capacity calculations in this section are therefore derived from:

$\bar{\mathbf{H}}_{All} + \Delta\mathbf{H}$

Using:

$$C_{\mathbf{D}+\mathbf{E}} = E\left\{\sum_{i=1}^{N_T}\log_2\left[1+\frac{P\left|(\mathbf{D}+\mathbf{E})_{i,i}\right|^2}{\varphi_i + P\left[\sum_{j=i}\left\{\left|(\mathbf{D}+\mathbf{E})_{j}\right|^2\right\} - \left|(\mathbf{D}+\mathbf{E})_{i,i}\right|^2\right]}\right]\right\} \tag{6.14}$$

which is equivalent to equation (6.10). Consider now the effect of increasing the variance, $\text{var}\{\Delta\mathbf{H}\}$, from 0.01 through to 0.01 for the case of the wireless channels as the dimension N_T is also increased from 2 through to 5 in fig. 6.15. As in chapter 4, the SISO communications system is indicated when $N_T = 1$.

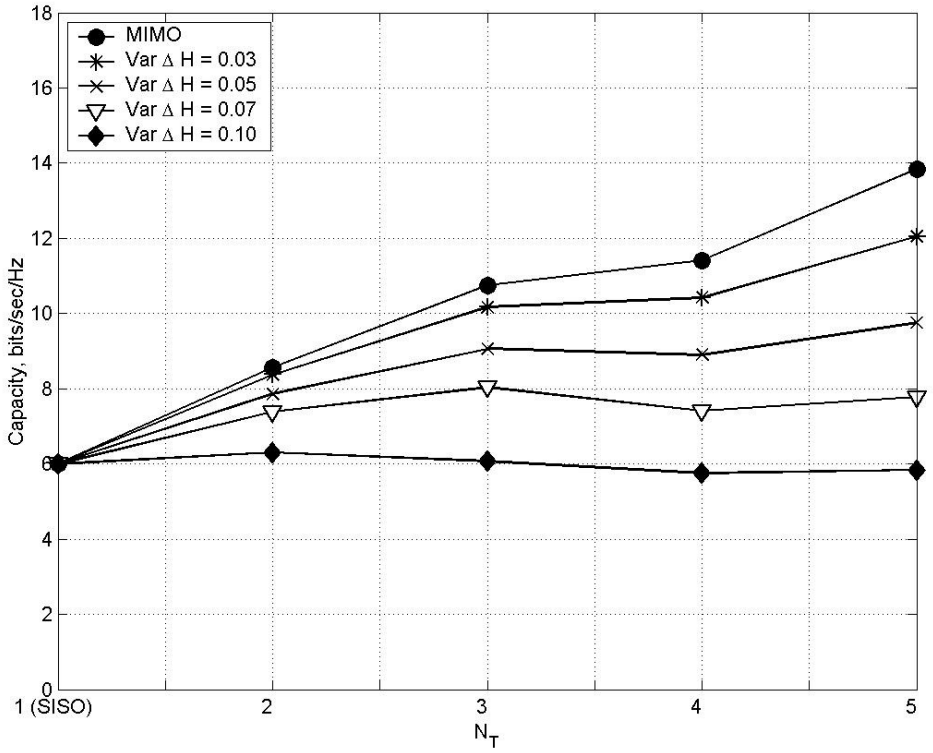

Figure 6.15: Effects of increasing imperfect knowledge of the channel, $\text{var}\{\Delta\mathbf{H}\}$ = 0.03, 0.05, 0.07 and 0.1. and increasing dimension, N_T for a MIMO communications system based on wireless channels. When $N_T = 1$, this refers to a SISO communications system. $\frac{P}{\varphi}$=18 dB.

A number of observations can be made from examination of fig. 6.15:

(i) The variance, $\text{var}\{\Delta\mathbf{H}\}$, should be no greater than 0.03 in order to achieve a linear increase in capacity with respect to the dimension, N_T.

(ii) Although there is a gain in capacity for MIMO with respect to the SISO for a variance, $\text{var}\{\Delta\mathbf{H}\} = 0.05$, the linear increase in capacity ceases for cases where the dimension, $N_T > 3$.

(iii) As the dimension, N_T, is increased along the x-axis, the effect of the imperfect knowledge of the channel, for a given variance, $\text{var}\{\Delta\mathbf{H}\}$, on capacity, becomes more pronounced. This mirrors the transmission line analysis of the previous section.

This analysis indicates that higher dimensions of N_T require a more precise knowledge of the communications channel. Similar observations have been made in the studies of Kyritsi [93] and others [103] [138] [137] [14] [20] [113] [64] [143], however the specific figures quoted in this work which concern the variance, $\text{var}\{\Delta\mathbf{H}\}$, reflect the fact that there are in fact differences in the approach to the analysis taken here.

6.5 Summary

In this chapter, practical reasons for imperfect knowledge of the channel were offered. In light of these, an analysis of the effect on the capacity of MIMO communication systems when there is imperfect knowledge of the channel was considered. The extent of imperfect knowledge of the channel was quantified by the variance, $\text{var}\{\Delta\mathbf{H}\}$, which denoted the variance of complex normally distributed scalar elements of a

matrix: $\Delta\mathbf{H}$. A novel comparative analysis between MIMO communications systems based on various types of transmission line channels was presented. In the case of the balanced twisted-pair telephone lines, a fairly consistent drop in capacity with respect to frequency for a fixed dimension, N_T, and fixed variance, $\text{var}\{\Delta\mathbf{H}\}$ was observed. While increasing the dimension N_T gave an overall greater gain in terms of capacity, the relative drop in capacity for a given variance, $\text{var}\{\Delta\mathbf{H}\}$, increased. This was also seen to be true for the case of the balanced twisted-pair cat 5 channels. Given reasonable capacities for the SISO communications system, at frequencies up to 50 MHz, the idea was therefore offered that MIMO techniques, given imperfect knowledge of the channel, only be used after 50 MHz in the case of cat 5. Finally in relation to the transmission line channels, the idea was further justified that MIMO techniques be used to enhance poorly balanced transmission lines with high insertion losses and FEXT. Given that the unbalanced flat-pair transmission line channels show good capacity gains at relatively low frequencies, even with varying degrees of imperfect knowledge of the channel, current ADSLs standards could therefore be deployed in these circumstances using MIMO. In the case of MIMO communications systems based on wireless channels, it was seen that imperfect knowledge of the channel can prohibit the linear increase in capacity with respect to increasing dimension, N_T. Also, for a given extent of imperfect knowledge of the channel as quantified by the variance, $\text{var}\{\Delta\mathbf{H}\}$, the relative decrease in capacity was seen to become more pronounced. The figures reported in this work are such that a viable MIMO communications system is seen to exist when the extent of the imperfect channel knowledge is quantified by a variance, $\text{var}\{\Delta\mathbf{H}\} = 0.05$. However, given this extent of imperfect knowledge of the channel, the linear increase in capacity with

respect to the dimension, N_T, does not occur when $N_T > 3$. It is therefore concluded that the variance, $\text{var}\{\Delta\mathbf{H}\}$, should be no greater than 0.03 in order to achieve a linear increase in capacity with respect to increasing dimension, N_T.

Chapter 7: Lower Bound on the Capacity of MIMO Communications Systems Based on the Leakage Level

7.1 Introduction

In this chapter, a lower bound on the capacity of MIMO communications systems is derived and results are presented which will be seen to offer a conservative indication of the extent of imperfect knowledge of the channel which still allows for a viable MIMO communications system. It is this lower bound along with calculations of the leakage level, to quantify the extent of the imperfect knowledge of the channel, that entirely define novel contribution of this chapter. In common with chapter 6, a novel comparative analysis of MIMO communications systems based on various transmission line channels is presented. Also, a novel analysis of the MIMO communications systems based on the wireless channels based is presented.

7.2 The Leakage Level

Girand et al. [63] have studied the numerical behaviour of several computational variants of what is known as the 'Gram-Schmidt orthogonalisation process'. The Gram-Schmidt orthogonalisation process, in the context of some arbitrary real valued matrix, $\mathbf{A}$, of full rank whose arbitrary dimension is $N \times M$, produces two matrices $\mathbf{Q}$ and $\mathbf{R}$ which are related mathematically to this matrix, $\mathbf{A}$, in the manner given by:

$$\mathbf{A} = \mathbf{QR} \tag{7.1}$$

The matrix, $\mathbf{R}$, is an upper right triangular matrix and more importantly the matrix $\mathbf{Q}$

is orthogonal. For a more rigorous and detailed account of the Gram-Schmidt orthogonalisation process, the interested reader is referred to [11] [125] [65]. It is important to note however that as a result of the Gram-Schmidt orthogonalisation process, the matrix, $\mathbf{Q}$, has a similar property to the two unitary matrices, $\mathbf{U}$ and $\mathbf{V}$, which were first defined in chapter 4. This property is highlighted by the following expression:

$$\mathbf{Q}\mathbf{Q}^H = \mathbf{Q}^H\mathbf{Q} = \mathbf{I} \tag{7.2}$$

$\mathbf{I}$ is the identitiy matrix of appropriate dimensions. Girand et al. indicate that algorithms which implement this Gram-Schmidt orthogonalisation process can be numerically unstable under certain circumstances. The result of this is the generation of a non-orthogonal matrix, $\bar{\mathbf{Q}}$, where, in contrast to the orthogonal matrix, $\mathbf{Q}$:

$$\bar{\mathbf{Q}}\bar{\mathbf{Q}}^H \neq \mathbf{I}. \tag{7.3}$$

Girand et al. quantify the loss in orthogonality in $\bar{\mathbf{Q}}$ with respect to $\mathbf{Q}$ using the term:

$$\left\| \mathbf{I} - \bar{\mathbf{Q}}\bar{\mathbf{Q}}^H \right\|_F$$

This idea is effectively extended by Nguyen *et al* [110] who, in the context of MIMO communications systems, define a 'leakage level' which is denoted here as: L. L quantifies the loss in orthogonality of the 'eigenmodes' or MIMO sub-channels. Before defining the leakage level in the context of thus work, recall from chapter 6 that the degree of imperfect channel knowledge was quantified by the variance of the scalar elements of a matrix, $\Delta\mathbf{H}$ .The scalar elements of this matrix, $\Delta\mathbf{H}$, were defined

as being identical and independently (i.i.d) complex normally distributed with mean of zero and arbitrary variance, $\text{var}\{\Delta\mathbf{H}\}$ as:

$$\Delta\mathbf{H} \sim CN(0, \text{var}\{\Delta\mathbf{H}\}) \tag{7.4}$$

In the context of MIMO communications systems, this was then seen to give rise to a non-diagonal matrix, $\mathbf{E}$:

$$\mathbf{E} = \begin{bmatrix} \Delta\sigma_1 & e_{1,2} & \cdots & e_{1,N_T} \\ e_{2,1} & \Delta\sigma_2 & \cdots & e_{2,N_T} \\ \vdots & \vdots & \ddots & \vdots \\ e_{N_T,1} & e_{N_T,2} & \cdots & \Delta\sigma_{N_T} \end{bmatrix} \tag{7.5}$$

The diagonal elements of the matrix, $\mathbf{E}$, are perturbations in the singular values which are contained along the main diagonal of the matrix, $\mathbf{D}$, The non-zero off-diagonal terms of the matrix, $\mathbf{E}$, indicate a degree of coupling or 'leakage' between the sub-channels which would previously have been viewed as orthogonal by the receiver when the transmit and receive vectors were correctly weighted. The 'leakage level', L, hence follows from equation (7.5) as:

$$L = E\left\{\|\mathbf{E}\|_F\right\} \tag{7.6}$$

The use of the expectation operator, $E\{\cdot\}$ in equation (7.4) is logical since calculation of the matrix, $\mathbf{E}$, is effectively stochastic in nature. As previously indicated, the notation, $\|\cdot\|_F$, represents the Frobenious norm and may be defined in the context of equation (7.6) as:

$$\|\mathbf{E}\|_F = \sqrt{tr(\mathbf{E}\,\mathbf{E}^H)} \tag{7.7}$$

7.3 Leakage Level Calculations on Transmission Line Channels

In fig. 7.1, the leakage level, L, with respect to both increasing frequency and increasing variance, $\text{var}\{\Delta\mathbf{H}\}$ is plotted in the case of the balanced twisted-pair telephone transmission line channels for the dimension, N_T=3.

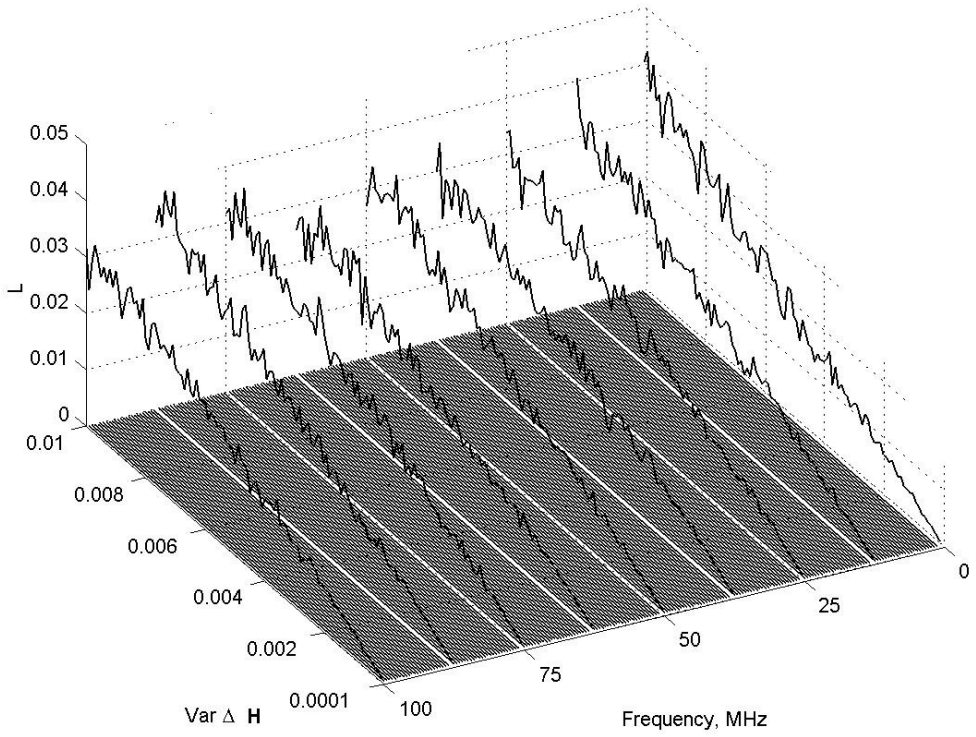

Figure 7.1: A plot of the leakage level, L, as a function of the variance, $\text{var}\{\Delta\mathbf{H}\}$, and frequency in MHz for a MIMO communications system based on balanced telephone transmission line channels. The dimension N_T=3.

Within the frequency range from 300 kHz to 100 MHz, although calculation of the leakage level, L, is clearly stochastic in nature, it can be appreciated by inspection of curves in fig. 7.1 that L is dependent on the $\text{var}\{\Delta\mathbf{H}\}$ but shows little if any dependence on frequency. This supports the conclusion from chapter 6, where it was seen that the relative drop in capacity, $C_{\mathbf{D+E}}$, was equivalent with respect to frequency for a fixed variance, $\text{var}\{\Delta\mathbf{H}\}$ and a fixed dimension, N_T . The same is plotted in fig 7.2 but where the dimension $N_T = 5$.

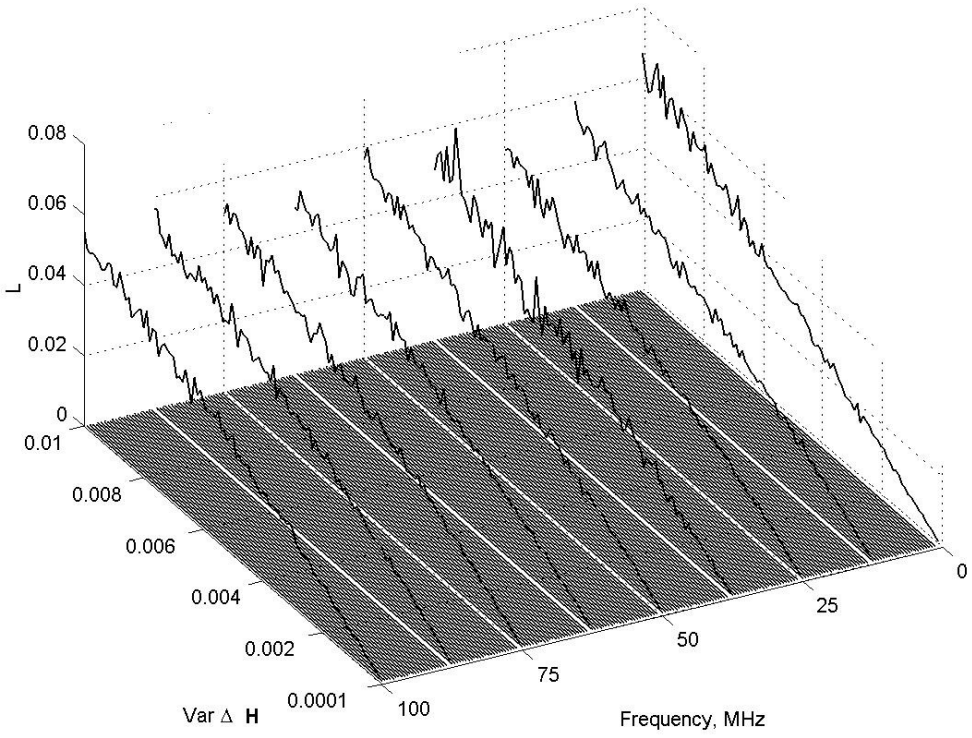

Figure 7.2: A plot of the leakage level, L, as a function of the variance, $\text{var}\{\Delta\mathbf{H}\}$, and frequency in MHz for a MIMO communications system based on balanced telephone transmission line channels. The dimension N_T =5.

Again, fig 7.2 shows L is dependent on the variance, var$\{\Delta\mathbf{H}\}$, but shows little if any dependence on frequency. Clearly as the dimension N_T is increased from 3 to 5, greater values of L are observed. This supports the idea from chapter 6 where greater losses in capacity were observed for a fixed variance as N_T was increased.

In fig. 7.3, the leakage level, L, with respect to both increasing frequency and increasing variance, var$\{\Delta\mathbf{H}\}$ is plotted in the case of the balanced twisted-pair cat 5 transmission line channels for the dimension, N_T=3.

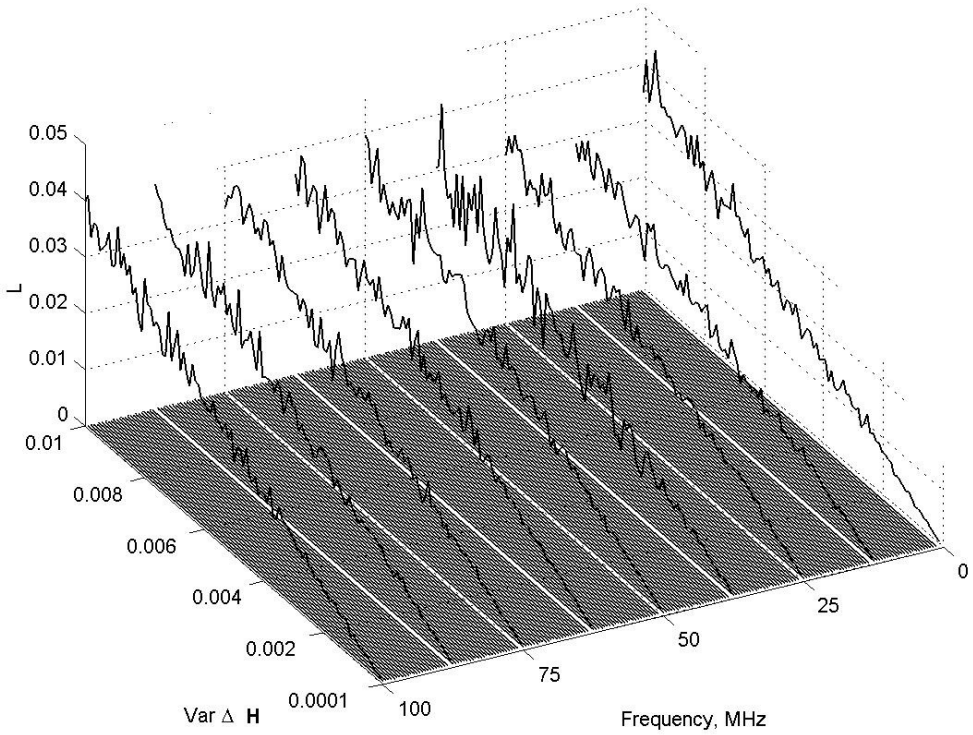

Figure 7.3: A plot of the leakage level, L, as a function of the variance, var$\{\Delta\mathbf{H}\}$, and frequency in MHz for a MIMO communications system based on balanced cat 5 transmission line channels. The dimension N_T=3.

In fig. 7.4, the leakage level, L, with respect to both increasing frequency and increasing variance, $\text{var}\{\Delta\mathbf{H}\}$ is plotted in the case of the balanced twisted-pair cat 5 transmission line channels for the dimension, $N_T = 4$.

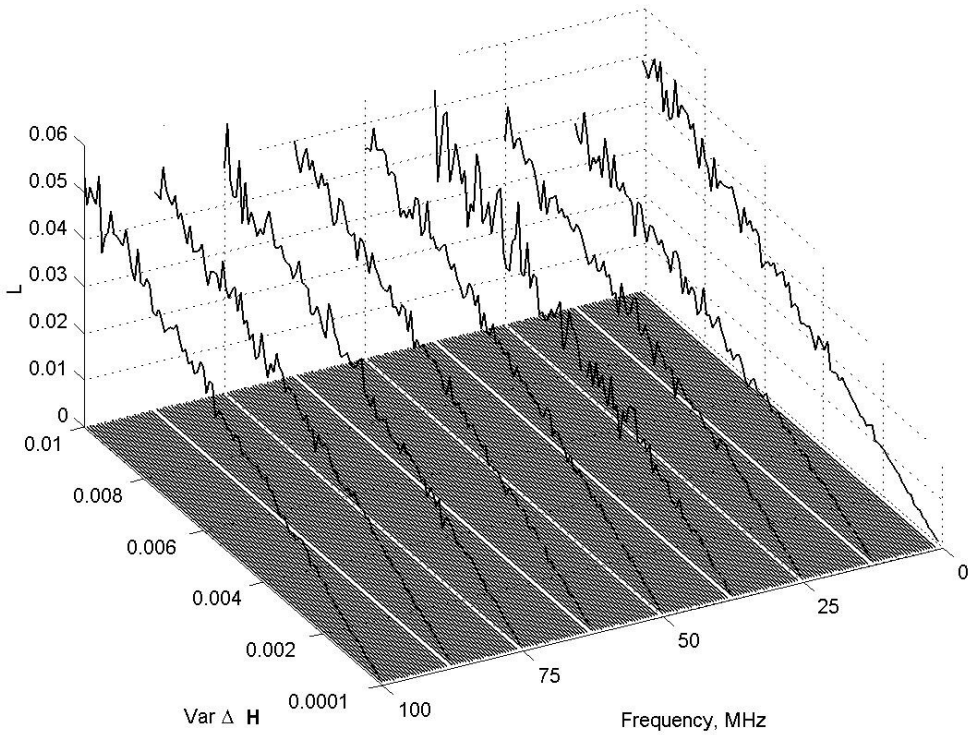

Figure 7.4: A plot of the leakage level, L, as a function of the variance, $\text{var}\{\Delta\mathbf{H}\}$, and frequency in MHz for a MIMO communications system based on balanced cat 5 transmission line channels. The dimension N_T=4.

Figs 7.3 and 7.4 show that L is dependent on the $\text{var}\{\Delta\mathbf{H}\}$ but shows little if any dependence on frequency. When the dimension N_T is increased from 3 to 4, greater values of L are observed. This again supports the idea from chapter 6 where greater losses in capacity were observed for a fixed variance as N_T was increased. Again, this idea will be seen to be mirrored in the analysis of wireless channels. Finally in this section, the leakage level respect to both increasing frequency and increasing variance, $\text{var}\{\Delta\mathbf{H}\}$ is plotted in the case of the unbalanced flat-pair transmission line channels for the dimension, N_T=3.

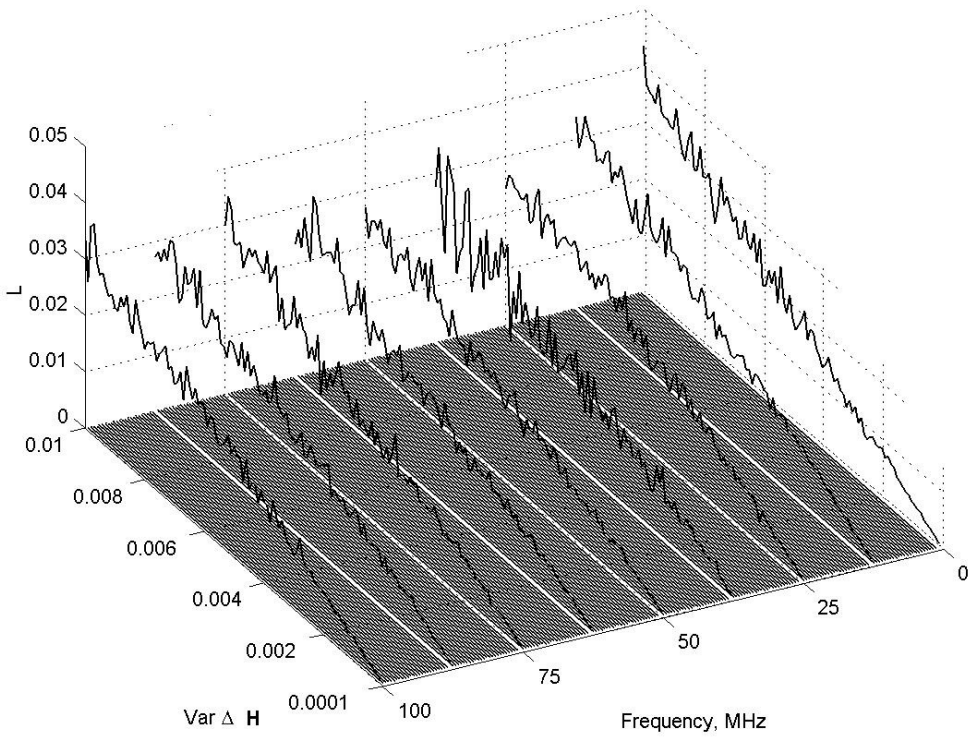

Figure 7.5: A plot of the leakage level, L, as a function of the variance, $\text{var}\{\Delta\mathbf{H}\}$, and frequency in MHz for a MIMO communications system based on unbalanced flat-pair transmission line channels. The dimension N_T=3.

In the case of the flat-pair channels, L is dependent on the $\text{var}\{\Delta\mathbf{H}\}$ and shows a minor dependence on frequency at low frequencies where the leakage level plots are slightly higher. This concurs with the relevant capacity analysis from chapter 6 where it was seen that there were relatively high losses in capacity at lower frequencies.

7.4 Leakage Level Calculations on Wireless Channels

In chapter 6, it was seen that, for MIMO communications systems based on wireless channels, the relative drop in the capacity, $C_{\mathbf{D+E}}$, for a fixed variance, $\text{var}\{\Delta\mathbf{H}\}$, was not consistent with respect to increasing dimension, N_T. In this section, the objective is to support this conclusion by calculation of the leakage level with respect to both increasing dimension, N_T, and increasing variance, $\text{var}\{\Delta\mathbf{H}\}$. In fig. 7.6, the leakage level, L, as a function of increasing variance, $\text{var}\{\Delta\mathbf{H}\}$, when dimension, N_T, = 2,3,4 and 5 is plotted. It can be seen that as the dimension, N_T, increases, the slope of the lines plotted in fig. 7.6 increases. This support the idea that was highlighted in chapter 6, where it was seen that for a given variance, $\text{var}\{\Delta\mathbf{H}\}$, the relative drop in the capacity, $C_{\mathbf{D+E}}$, increases with increasing dimension, N_T. It is clear that higher dimensions of N_T require a more precise knowledge of the communications channel. Again, similar observations have been made in the studies of Kyritsi [93] and others [103] [138] [137] [14] [20] [113] [64] [143], however the specific figures which have been quoted in this work may be attributed to the fact that there are in fact differences in the approach to the analysis taken here. Thus these figures are novel and have not been reported in literature to date.

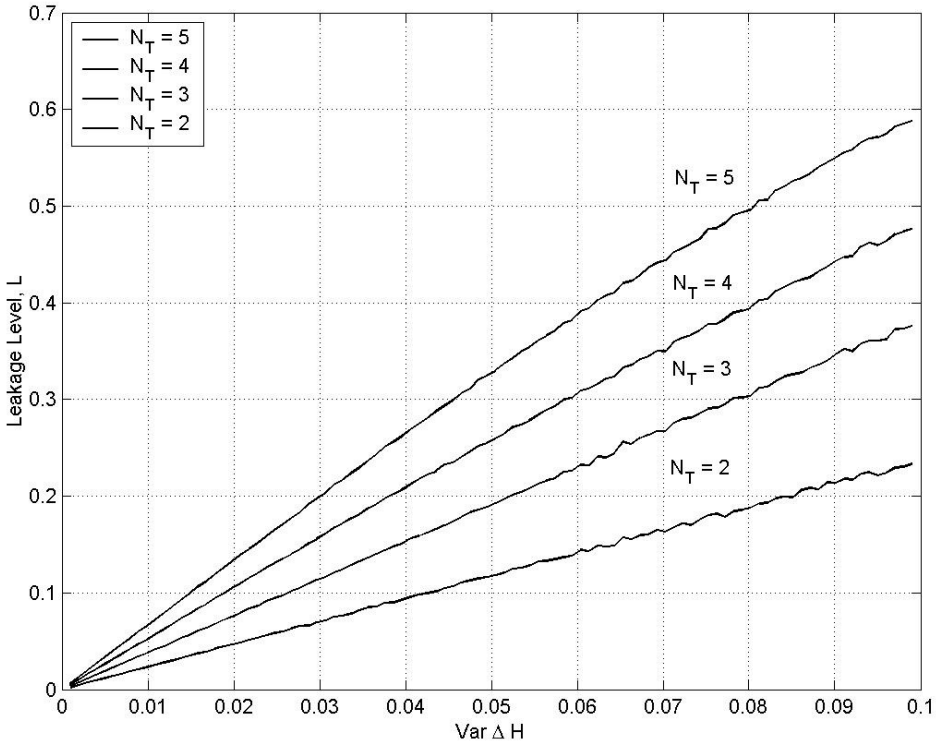

Figure 7.6: A plot of the leakage level, L, as a function of the variance, $\text{var}\{\Delta\mathbf{H}\}$, when the dimension, N_T, = 2,3,4 and 5 for a MIMO communications system based on wireless channels.

7.5 Lower Bound on the Capacity of MIMO Communications Systems

In relation to the effect of imperfect knowledge of the channel on MIMO communications systems, the results which were presented in chapter 6 were stochastic in nature. In relation to this, it is therefore argued that it is a valuable exercise to derive a lower bound on capacity in order to offer a conservative indication of the extent of imperfect knowledge of the channel which would still allow for a viable MIMO communications system to operate. Since the relationship between the variance, $\text{var}\{\Delta\mathbf{H}\}$, and the leakage level, L, has been established, it is thus implicit that there is also a relationship between the capacity and the leakage level, L. With regard to this, it is argued that the results which will be presented in this section add a degree of generality to the discussion since the capacity can now be related to the leakage level, L, as opposed to being merely related to the variance, $\text{var}\{\Delta\mathbf{H}\}$, of the specifically statistically distributed matrix, $\Delta\mathbf{H}$.

Recall from chapter 6, the capacity, $C_{\mathbf{D+E}}$ where there is imperfect knowledge of the channel is given by:

$$C_{\mathbf{D+E}} = E\left\{\sum_{i=1}^{N_T}\log_2\left[1+\frac{P\left|\left(\mathbf{D}+\mathbf{E}\right)_{i,i}\right|^2}{\varphi+P\left[\sum_{j=i}\left\{\left|\left(\mathbf{D}+\mathbf{E}\right)_{j}\right|^2\right\}-\left|\left(\mathbf{D}+\mathbf{E}\right)_{i,i}\right|^2\right]}\right]\right\} \tag{7.8}$$

In this work, a lower bound on this capacity is given by a quantity, $C_{\underset{Lower}{\mathbf{D+E}}}$, defined as:

$$C_{\underset{Lower}{\mathbf{D+E}}} = E\left\{\sum_{i=1}^{N_T}\log_2\left[1+\frac{P\left|\left(\mathbf{D}+\Delta\mathbf{D}+\mathbf{B}\right)_{i,i}\right|^2}{\varphi+P\left[\sum_{j=i}\left\{\left|\underset{j}{\Delta\mathbf{D}}\right|^2\right\}+2\left[\left\|\underset{j}{\Delta\mathbf{D}}\right\|_2\left\|\underset{j}{\mathbf{B}}\right\|_2\right]+\sum_{j=i}\left\{\left|\underset{j}{\Delta\mathbf{B}}\right|^2\right\}-\left|\mathbf{E}_{i,i}\right|^2\right]}\right]\right\} \tag{7.9}$$

Comparing equations (7.8) and (7.9), it is clear that the following identities are required to be proven:

$$\left|\left(\mathbf{D}+\mathbf{E}\right)_{i,i}\right| \geq \left|\left(\mathbf{D}+\Delta\mathbf{D}+\mathbf{B}\right)_{i,i}\right| \tag{7.10}$$

$$\sum\left\{\left|\underset{j}{\left(\mathbf{D}+\mathbf{E}\right)}\right|^2\right\}-\left|\left(\mathbf{D}+\mathbf{E}\right)_{i,i}\right|^2 \leq \sum\left\{\left|\underset{j}{\Delta\mathbf{D}}\right|^2\right\}+2\left[\left\|\underset{j}{\Delta\mathbf{D}}\right\|_2\left\|\underset{j}{\mathbf{B}}\right\|_2\right]+\sum\left\{\left|\underset{j}{\Delta\mathbf{B}}\right|^2\right\}-\left|\mathbf{E}_{i,i}\right|^2 \tag{7.11}$$

Begin the derivation by defining vector norms. In the context of two arbitrary vectors: $\mathbf{f}$ and $\mathbf{g}$, a vector norm on $\in \mathrm{C}^N$ is a function $\|\cdot\|:\in \mathrm{C}^N \rightarrow \in R$ satisfying the following conditions:

$$\|\mathbf{f}\| \geq 0, \text{ equality iff } \forall\,\mathbf{f}=0 \qquad \forall\,\mathbf{f}\in C^N \tag{7.12}$$

$$\|\alpha\mathbf{f}\| = |\alpha|\,\|\mathbf{f}\| \qquad \forall\alpha\in C \text{ and } \forall\mathbf{f}\in C^N \tag{7.13}$$

$$\|\mathbf{f}+\mathbf{g}\| \leq \|\mathbf{f}\|+\|\mathbf{g}\| \qquad \forall\mathbf{f},\mathbf{g}\in C^N \tag{7.14}$$

Now:

Part (i): Prove $\left|(\mathbf{D}+\mathbf{E})_{i,i}\right| \geq \left|(\mathbf{D}+\Delta\mathbf{D}+\mathbf{B})_{i,i}\right|$.

Let a matrix, $\mathbf{D}+\Delta\mathbf{D}$, be defined as follows by performing an appropriate singular value decomposition:

$$\mathbf{D}+\Delta\mathbf{D} = (\mathbf{U}+\Delta\mathbf{U})^{H}(\mathbf{H}+\Delta\mathbf{H})(\mathbf{V}+\Delta\mathbf{V}) \tag{7.15}$$

Recalling from chapter 6 that the matrix, $\mathbf{D}+\mathbf{E}$, is defined as:

$$\mathbf{D}+\mathbf{E} = (\mathbf{U}+\Delta\mathbf{U})^{H}\mathbf{H}(\mathbf{V}+\Delta\mathbf{V}) \tag{7.16}$$

Subtracting equation (7.15) from equation (7.16) then gives:

$$(\mathbf{D}+\mathbf{E})-(\mathbf{D}+\Delta\mathbf{D}) = \left[(\mathbf{U}+\Delta\mathbf{U})^{H}(\mathbf{H})(\mathbf{V}+\Delta\mathbf{V})\right]-\left[(\mathbf{U}+\Delta\mathbf{U})^{H}(\mathbf{H}+\Delta\mathbf{H})(\mathbf{V}+\Delta\mathbf{V})\right] \tag{7.17}$$

Re-arranging equation (7.17) means an expression for the matrix, $\mathbf{E}$, may be given as:

$$\mathbf{E} = \Delta\mathbf{D}-\left[(\mathbf{U}+\Delta\mathbf{U})^{H}(\mathbf{H})(\mathbf{V}+\Delta\mathbf{V})\right] \tag{7.18}$$

For the sake of clarity, let a matrix, $\mathbf{B}$, be defined as:

$$\mathbf{B} = (\mathbf{U}+\Delta\mathbf{U})^{H}(\mathbf{H})(\mathbf{V}+\Delta\mathbf{V}) \tag{7.19}$$

Substituting equation (7.19) into equation (7.18) gives:

$$\mathbf{E} = \Delta\mathbf{D}-\mathbf{B} \tag{7.20}$$

Isolating the diagonal elements of the matrices: $\mathbf{E}$, $\Delta\mathbf{D}$ and $\mathbf{B}$, it is possible to write:

$$diag\{\mathbf{E}\} = diag\{\Delta\mathbf{D}\}-diag\{\mathbf{B}\} \tag{7.21}$$

The notation, $diag\{\cdot\}$ refers to the diagonal elements of a given matrix. Vectors can now be formed from these diagonal matrices whose relationship is given by:

$$\underset{j}{diag}\{\mathbf{E}\} = \underset{j}{diag}\{\mathbf{\Delta D}\} - \underset{j}{diag}\{\mathbf{B}\} \tag{7.22}$$

To clarify, equation (7.22) effectively refers to the relationship between j^{th} vector formed from each of the diagonal matrices implied by an appropriate use of the notation: $\underset{j}{diag}\{\cdot\}$. Define the vector infinity norm, $\|\cdot\|_\infty$, in terms of an arbitrary vector, $\mathbf{f}$, as:

$$\|\mathbf{f}\|_\infty = \max\{|\mathbf{f}|\} \qquad \mathbf{f} \in C^N \tag{7.23}$$

The notation, '$\max\{\cdot\}$', should be read as, 'the maximum scalar element of the vector enclosed in parenthesis'. To simplify the use of notation here, '$|\mathbf{f}|$' should simply be thought of as a vector containing the absolute values of the vector, $\mathbf{f}$. Considering the term, $\underset{j}{diag}\{\mathbf{\Delta D}\} - \underset{j}{diag}\{\mathbf{B}\}$, which appears on the right hand side of equation (7.22), if the vector infinity norm is applied to this expression then the following expression may be written based on the properties of vector norms which were defined in equations (7.12) to (7.14):

$$\left\|\underset{j}{diag}\{\mathbf{\Delta D}\}\right\|_\infty + \left\|\underset{j}{diag}\{\mathbf{B}\}\right\|_\infty \le \left\|\underset{j}{diag}\{\mathbf{\Delta D}\} - \underset{j}{diag}\{\mathbf{B}\}\right\|_\infty \tag{7.24}$$

Substituting equation (7.22) into to equation (7.24) gives as expression:

$$\left\|\underset{j}{diag}\{\mathbf{\Delta D}\}\right\|_\infty + \left\|\underset{j}{diag}\{\mathbf{B}\}\right\|_\infty \le \left\|\underset{j}{diag}\{\mathbf{E}\}\right\|_\infty \tag{7.25}$$

Swapping the left hand side of equation (7.25) with the right hand side of equation (7.25) and thus reversing the inequality sign gives:

$$\left\| \underset{j}{diag}\{\mathbf{E}\} \right\|_\infty \geq \left\| \underset{j}{diag}\{\Delta\mathbf{D}\} \right\|_\infty + \left\| \underset{j}{diag}\{\mathbf{B}\} \right\|_\infty \tag{7.26}$$

In essence, each of the terms in equation (7.26) is representative of a family of N_T scalars since $j = 1,2,...,N_T$. A family of N_T scalars defined by the term, $\left\| \underset{j}{diag}\{\mathbf{D}\} \right\|_\infty$, is added to both sides of equation (7.27) to give:

$$\left\| \underset{j}{diag}\{\mathbf{D}\} \right\|_\infty + \left\| \underset{j}{diag}\{\mathbf{E}\} \right\|_\infty \geq \left\| \underset{j}{diag}\{\mathbf{D}\} \right\|_\infty + \left\| \underset{j}{diag}\{\Delta\mathbf{D}\} \right\|_\infty + \left\| \underset{j}{diag}\{\mathbf{B}\} \right\|_\infty \tag{7.27}$$

Given that the matrices: $diag\{\mathbf{D}\}$, $diag\{\mathbf{E}\}$, $diag\{\Delta\mathbf{D}\}$ and $diag\{\mathbf{B}\}$ are diagonal matrices by definition and given the definition of the vector infinity norm in equation (7.23), then equation (7.27) can be re-written using more convenient notation as:

$$\left|(\mathbf{D}+\mathbf{E})_{i,i,}\right| \geq \left|(\mathbf{D}+\Delta\mathbf{D}+\mathbf{B})_{i,i}\right| \tag{7.28}$$

In respect of part (i): Q.E.D.

Now:

Part (ii) Prove:

$$\sum \left\{ \left| \underset{j}{(\mathbf{D}+\mathbf{E})} \right|^2 \right\} - \left|(\mathbf{D}+\mathbf{E})_{i,i}\right|^2 \leq \sum \left\{ \left| \underset{j}{\Delta\mathbf{D}} \right|^2 \right\} + 2\left[\left\| \underset{j}{\Delta\mathbf{D}} \right\|_2 \left\| \underset{j}{\mathbf{B}} \right\|_2 \right] + \sum \left\{ \left| \underset{j}{\Delta\mathbf{B}} \right|^2 \right\} - \left|\mathbf{E}_{i,i}\right|^2$$

The vector 2-norm may be defined in terms of an arbitrary vector, $\mathbf{f}$:

$$\|\mathbf{f}\|_2 = \sqrt{\sum |\mathbf{f}|^2} = \sqrt{\mathbf{f}^T\mathbf{f}} \qquad \mathbf{f} \in C^N \tag{7.29}$$

Again for the purpose of simplifying the use of notation here, '$|\mathbf{f}|$' should simply be thought of as a vector containing the squares of the absolute values of the vector, $\mathbf{f}$. Also, as has previously been prescribed in this work, the notation, $(\cdot)^T$, refers to the conjugate transpose of a vector. Recalling equation (7.20), which for the sake of clarity is rewritten as:

$$\mathbf{E} = \Delta\mathbf{D} - \mathbf{B} \tag{7.30}$$

Partitioning the terms in equation (7.30) into vectors:

$$\underset{j}{\mathbf{E}} = \underset{j}{\Delta\mathbf{D}} - \underset{j}{\mathbf{B}} \tag{7.31}$$

The relationship between the vector 2-norm which arises from equation (7.31) can be written as:

$$\left\| \underset{j}{\Delta\mathbf{D}} - \underset{j}{\mathbf{B}} \right\|_2 \leq \left\| \underset{j}{\Delta\mathbf{D}} \right\|_2 + \left\| \underset{j}{\mathbf{B}} \right\|_2 \tag{7.32}$$

Equation (7.35) is based on the properties of vector 2-norm outlined in equations (7.12) and (7.14). Substituting equation (7.31) into equation (7.32) gives:

$$\left\| \underset{j}{\mathbf{E}} \right\|_2 \leq \left\| \underset{j}{\Delta\mathbf{D}} \right\|_2 + \left\| \underset{j}{\mathbf{B}} \right\|_2 \tag{7.33}$$

Equation (7.33) is now re-written based on the definition of the vector 2-norm in defined in equation (7.29) previously:

$$\sqrt{\sum\left|\mathbf{E}_j\right|^2} \le \sqrt{\sum\left|\Delta\mathbf{D}_j\right|^2} + \sqrt{\sum\left|\mathbf{B}_j\right|^2} \tag{7.34}$$

Squaring both sides, it is now possible to write:

$$\sum\left|\mathbf{E}_j\right|^2 \le \sum\left|\Delta\mathbf{D}_j\right|^2 + 2\left[\sqrt{\sum\left|\Delta\mathbf{D}_j\right|^2}\sqrt{\sum\left|\mathbf{B}_j\right|^2}\right] + \sum\left|\mathbf{B}_j\right|^2 \tag{7.35}$$

The object here is to set an upper limit on the sums of the squares of the absolute values of the off-diagonal elements of the matrix sum: $\mathbf{D}+\mathbf{E}$. The diagonal elements of the matrix, $\mathbf{D}$, are equal to zero, but the influence of the diagonal elements of $\mathbf{E}$ on equation (7.35) needs to be considered. Each of the diagonal elements of the matrix, $\mathbf{E}$, i.e. $\mathbf{E}_{i,i}$, is subtracted from both sides of equation (7.35) in the following expression:

$$\sum\left|\mathbf{E}_j\right|^2 - \left|\mathbf{E}_{i,i}\right|^2 \le \sum\left|\Delta\mathbf{D}_j\right|^2 + 2\left[\sqrt{\sum\left|\Delta\mathbf{D}_j\right|^2}\sqrt{\sum\left|\mathbf{B}_j\right|^2}\right] + \sum\left|\mathbf{B}_j\right|^2 - \left|\mathbf{E}_{i,i}\right|^2 \tag{7.36}$$

Looking at the definition of the vector 2-norm in equation (7.29), it can be appreciated that the term: $2\left[\sqrt{\sum\left|\Delta\mathbf{D}_j\right|^2}\sqrt{\sum\left|\mathbf{B}_j\right|^2}\right]$ is equivalent to the term: $2\left[\left\|\Delta\mathbf{D}_j\right\|_2\left\|\mathbf{B}_j\right\|_2\right]$. Thus equation (7.36) may be more conveniently as:

$$\sum\left|\mathbf{E}_j\right|^2 - \left|\mathbf{E}_{i,i}\right|^2 \le \sum\left|\Delta\mathbf{D}_j\right|^2 + 2\left[\left\|\Delta\mathbf{D}_j\right\|_2\left\|\mathbf{B}_j\right\|_2\right] + \sum\left|\mathbf{B}_j\right|^2 - \left|\mathbf{E}_{i,i}\right|^2 \tag{7.37}$$

Careful attention to the usage of notation here reveals that the term, $\sum \left| \mathbf{E}_j \right|^2 - \left| \mathbf{E}_{i,i} \right|^2$ is in fact equivalent to: $\sum \left\{ \left| \left(\mathbf{D} + \mathbf{E} \right)_j \right|^2 \right\} - \left| \left(\mathbf{D} + \mathbf{E} \right)_{i,i} \right|^2$ since the matrix, $\mathbf{D}$, is a diagonal matrix, and thus it is possible to write:

$$\sum \left\{ \left| \left(\mathbf{D} + \mathbf{E} \right)_j \right|^2 \right\} - \left| \left(\mathbf{D} + \mathbf{E} \right)_{i,i} \right|^2 = \sum \left| \mathbf{E}_j \right|^2 - \left| \mathbf{E}_{i,i} \right|^2 \tag{7.38}$$

Substitution of equation (7.38) into equation (7.37) gives:

$$\sum \left\{ \left| \left(\mathbf{D} + \mathbf{E} \right)_j \right|^2 \right\} - \left| \left(\mathbf{D} + \mathbf{E} \right)_{i,i} \right|^2 \leq \sum \left| \Delta \mathbf{D}_j \right|^2 + 2 \left[\left\| \Delta \mathbf{D}_j \right\|_2 \left\| \mathbf{B}_j \right\|_2 \right] + \sum \left| \mathbf{B}_j \right|^2 - \left| \mathbf{E}_{i,i} \right|^2 \tag{7.39}$$

In respect of part (ii): Q.E.D.

This expression for the lower bound on the capacity of MIMO communications systems is novel and indeed in common with the work of Médard [103], this lower bound will become infinitely tight as the elements of the matrix, $\Delta \mathbf{H}$, approach zero.

7.6 Lower Bound Calculations on Transmission Line Channels

The lower bound calculations in this section should be thought of as an extension of the calculations from section 6.3 of chapter 6. Recall that the conditions under which the calculations in that section were made were:

(i) An added white Gaussian noise (AWGN) power spectral density, N_0, of -110 dBm/Hz, pertinent to the noise floor set by an echo canceller [171], is assumed.

(ii) The American National Standards Institute (ANSI) discrete multi-tone (DMT) tone transmit bandwidth of 4.3125 kHz is assumed [124] [172]. Capacities are calculated at intervals of approximately 496 kHz, i.e. at 201 intervals between 300 kHz to 100 MHz.

(iii) The lower nominal transmit power density -80 dBm/Hz for high bit-rate digital subscriber line (VDSL) signals yielded little in the way of improvement for MIMO over SISO in chapter 4. Thus only the higher transmit power spectral density of -60 dBm/Hz for high bit-rate digital subscriber line (VDSL) signals [124] is considered here.

(iv) The balanced twisted-pair telephone cable, the balanced cat 5 twisted-pair and the unbalanced flat-pair are compared for a dimension, $N_T = 3$. The cat5 is also examined for a dimension, $N_T = 4$ and the twisted-pair is also examined for a dimension, $N_T = 5$. Cumulative plots of capacity with respect to bandwidth are also presented.

(v) As described in chapter 4, the channel matrix, $\mathbf{H}(f)$, was normalised such that:

$$\bar{\mathbf{H}}(f) = \frac{\mathbf{H}(f)}{\|\mathbf{H}(f=1)\|_F} \tag{7.40}$$

All lower bound capacity calculations in this section are therefore derived from the term:

$$\bar{\mathbf{H}}(f) + \Delta\mathbf{H}$$

using equation (7.9). The lower bound for the various transmission line channels is now calculated and in light of this some sensible leakage levels are suggested in each case. The case of the balanced twisted-pair telephone transmission lines is first considered in figs. 7.7-7.8:

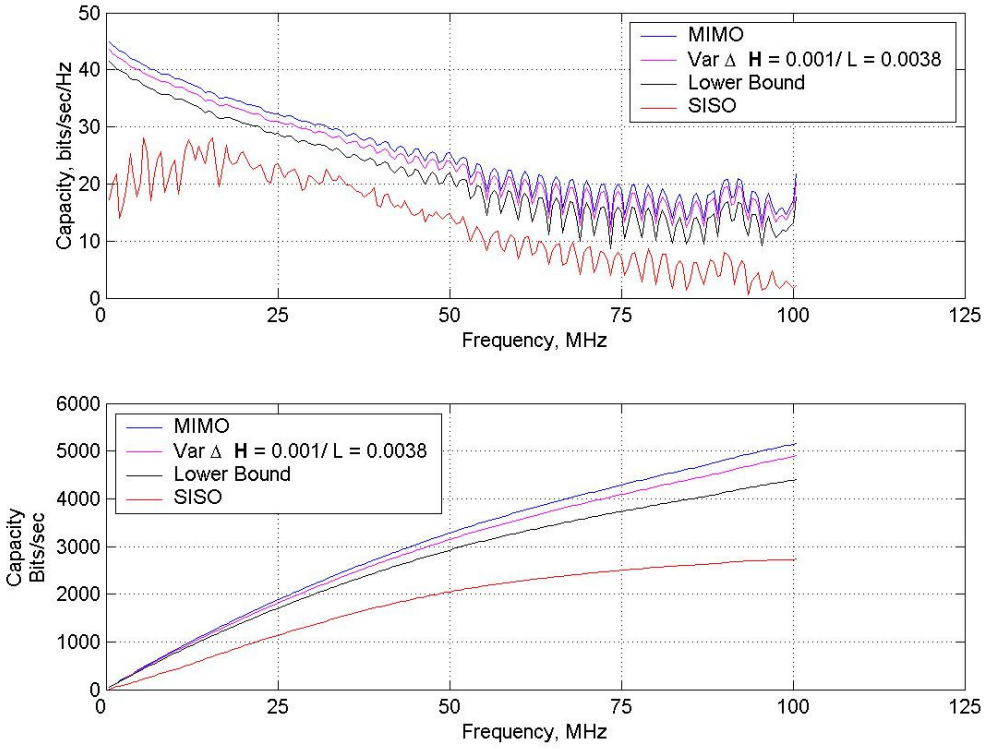

Figures 7.7-7.8: Lower bound on the effect of imperfect knowledge of the channel for a MIMO communications system based on balanced twisted-pair telephone transmission lines with $\text{var}\{\Delta\mathbf{H}\} = 0.001$ and $L = 0.0038$, Upper plot: capacity in bits/sec/Hz. Lower plot: cumulative capacity in bits/sec. In all cases, the dimension $N_T = 3$ and the transmit power spectral density is $P_0 = -60$ dBm/Hz.

While in chapter 6, the extent of imperfect knowledge of the channel could have been greater than $\text{var}\{\Delta\mathbf{H}\} = 0.001$, the results here are more conservative. It is therefore concluded that the extent of imperfect knowledge of the channel be no more than $\text{var}\{\Delta\mathbf{H}\} = 0.001$ for the case of the balanced twisted-pair telephone transmission lines with dimension $N_T = 3$. This is equivalent to a leakage level, $L = 0.0038$. Also, the cumulative capacity plots in fig. 7.8 indicate that the rate of capacity gain with respect to frequency is more or less equivalent for (i) MIMO, (ii) MIMO with

imperfect knowledge of the channel and (iii) the lower bound when $L = 0.0038$ but this is clearly not the case for SISO. In figs. 7.10 and 7.11, this same leakage level is examined for the case where $N_T = 5$. This time a leakage level of 0.0038 corresponds to $\text{var}\{\Delta\mathbf{H}\} = 0.0006$. Fig. 7.7 is reproduced in fig. 7.9 to the same scale for ease of comparison.

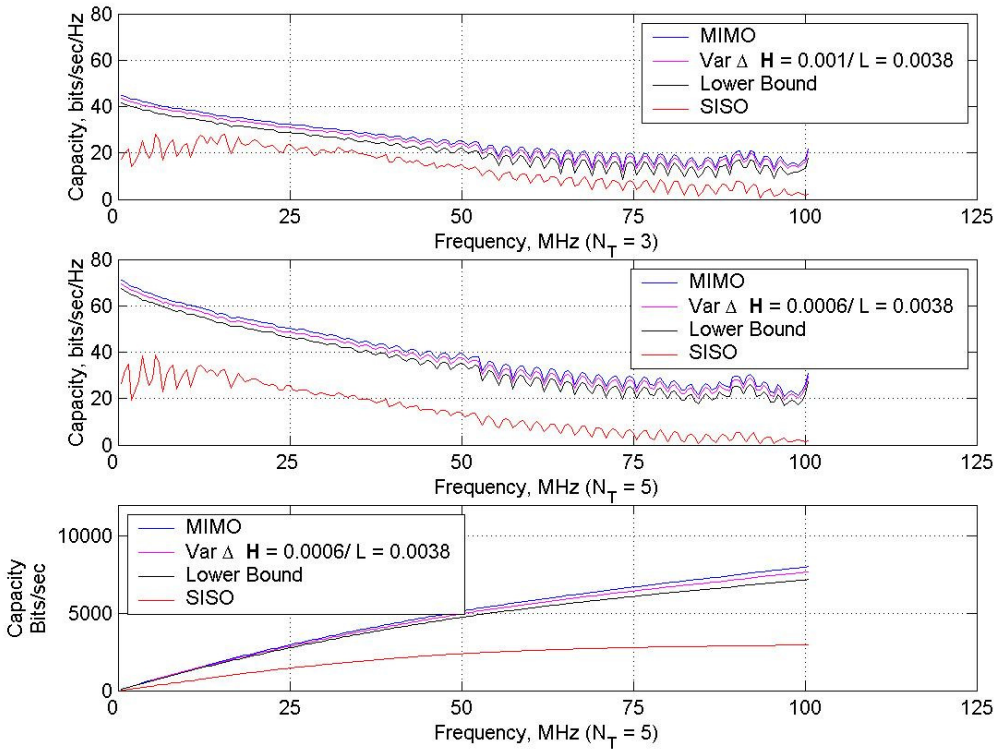

Figures 7.9-7.11: Lower bound on the effect of imperfect knowledge of the channel for a MIMO communications system based on balanced twisted-pair telephone transmission lines. Upper plot: Capacity in bits/sec/Hz for $\text{var}\{\Delta\mathbf{H}\} = 0.001$ and $L = 0.0038$ with $N_T = 3$. Middle plot: Capacity in bits/sec/Hz for $\text{var}\{\Delta\mathbf{H}\} = 0.0006$ and $L = 0.0038$ with $N_T = 5$. Lower plot: Cumulative Capacity in bits/sec for $\text{var}\{\Delta\mathbf{H}\} = 0.0006$ and $L = 0.0038$ with $N_T = 5$. In all cases, the transmit power spectral density is $P_0 = -60$ dBm/Hz.

Comparison of figs. 7.9 and 7.10 reveals that it has clearly become more difficult to maintain a leakage level $L = 0.0038$ as the dimension N_T has increased from 3 to 5. This idea is not surprising since in chapter 6 it was seen that for a given variance, var$\{\Delta\mathbf{H}\}$,the relative drop in capacity was greater with increasing dimension, N_T. It could therefore be argued that there is a 'cost' in increasing the communications system complexity, i.e. increasing the dimension N_T. However there is clearly a benefit obtained for this cost which is that of increased capacity. Further to this, the idea is therefore offered here that given the time invariant nature of the transmission line channel, the increased accuracy of channel knowledge could be gained gradually over time using some kind of feedback technique. Another argument which runs somewhat counter this one is that the benefit gained for the cost of increasing complexity should be that of decreased accuracy of knowledge of the channel. This argument is plausible given comparison of figs. 7.9 and 7.10 where the difference between the relative MIMO and SISO capacities has increased markedly as N_T has increased. On the basis of this argument, in figs 7.13 and 7.14 another leakage level, L, of 0.0127 which corresponds to a variance, var$\{\Delta\mathbf{H}\} = 0.002$, is suggested for the balanced twisted-pair telephone cable transmission lines where the dimension $N_T = 5$. Again fig. 7.7 is reproduced in fig. 7.12 to the same scale for ease of comparison. A possible drawback to this extent of imperfect knowledge of the channel is however highlighted in fig. 7.14 where it is seen that the overall rate of gain in capacity with respect to frequency more closely resembles that of the SISO communications system than it did in fig. 7.11.

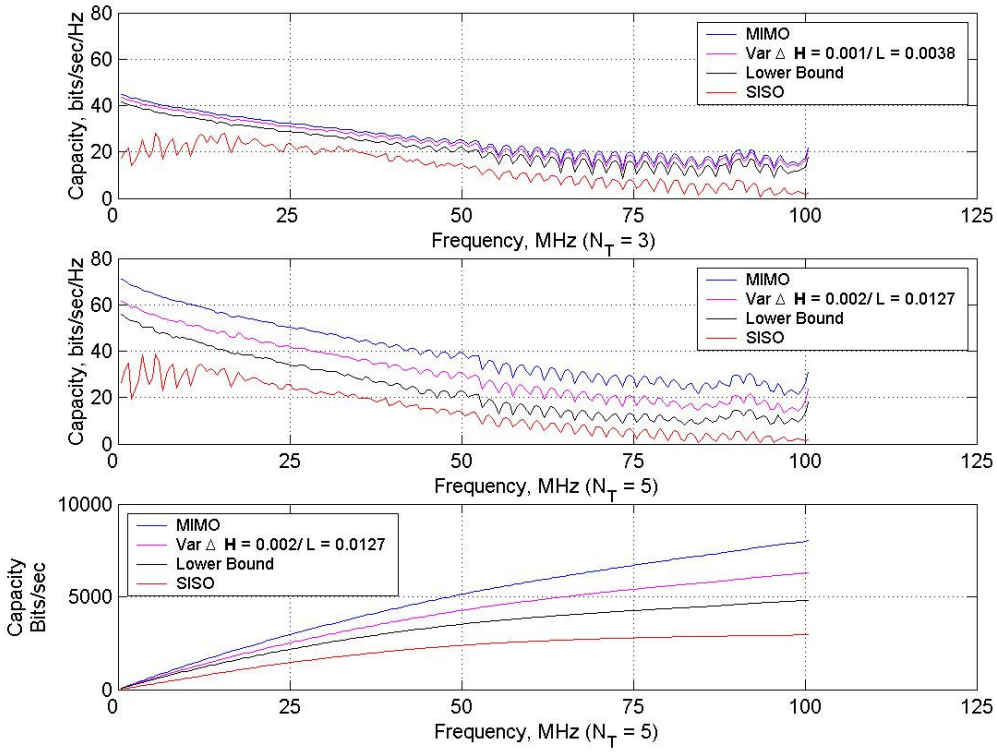

Figures 7.12-7.14: Lower bound on the effect of imperfect knowledge of the channel for a MIMO communications system based on balanced twisted-pair telephone transmission lines. Upper plot: Capacity in bits/sec/Hz for $\text{var}\{\Delta\mathbf{H}\} = 0.001$ and $L = 0.0038$ with $N_T = 3$. Middle plot: Capacity in bits/sec/Hz for $\text{var}\{\Delta\mathbf{H}\} = 0.002$ and $L = 0.0127$ with $N_T = 5$. Lower plot: Cumulative Capacity in bits/sec for $\text{var}\{\Delta\mathbf{H}\} = 0.002$ and $L = 0.0127$ with $N_T = 5$. In all cases, the transmit power spectral density is $P_0 = -60$ dBm/Hz.

The balanced twisted-pair cat 5 transmission line channels are now considered in the context of the lower bound analysis. Recall from chapter 4 that most of what is gained in terms of capacity with respect to frequency for the case of the MIMO communications system occurs at frequencies above 50 MHz. The choice of leakage level will thus reflect this. In figs 7.15 and 7.16, a leakage level of $L = 0.009$, which corresponds to a variance: $\text{var}\{\Delta\mathbf{H}\} = 0.0025$, is considered for a dimension: $N_T = 3$.

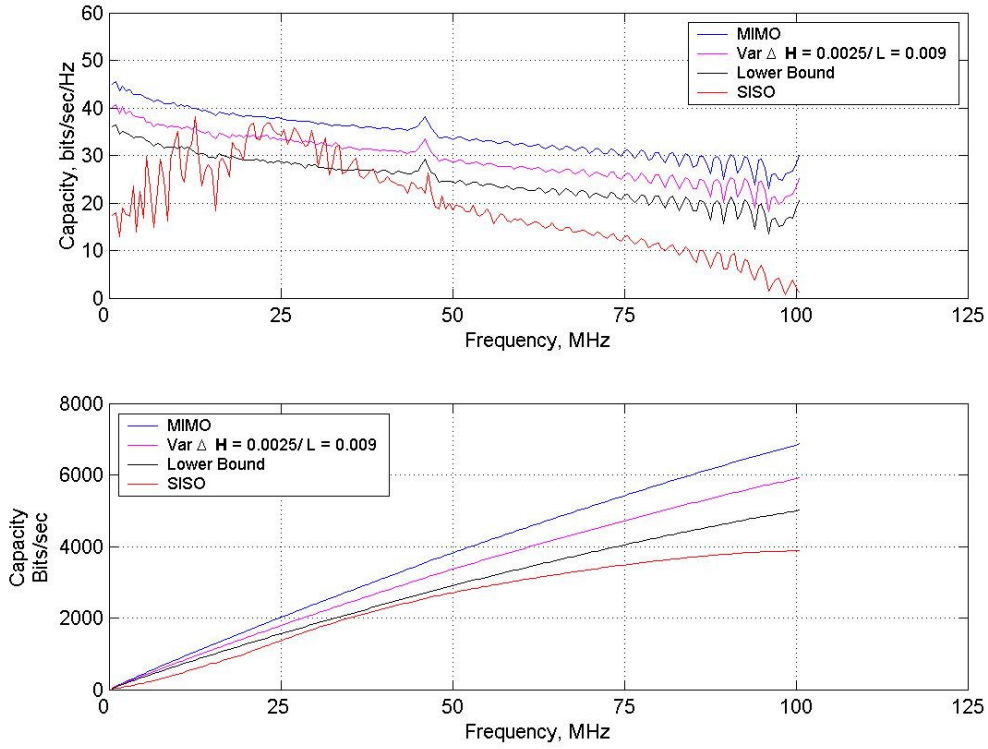

Figures 7.15-7.16: Lower bound on the effect of imperfect knowledge of the channel for a MIMO communications system based on balanced twisted-pair cat 5 transmission lines with $\text{var}\{\Delta\mathbf{H}\} = 0.0025$ and $L = 0.009$, Upper plot: capacity in bits/sec/Hz. Lower plot: cumulative capacity in bits/sec. In all cases, the dimension $N_T = 3$ and the transmit power spectral density is $P_0 = -60$ dBm/Hz.

The lower bound analysis suggests that a leakage level $L = 0.009$ is sensible for the cat 5 cable particularly if, as indicated in chapter 6, the MIMO communications system only be used after a frequency of 50 MHz. The cumulative capacity plot of the lower bound in fig. 7.16 indicates that the relative gain in capacity with respect to frequency is not saturating to the extent that the SISO communications system is after 50 MHz. In figs 7.18 and 7.19, a leakage level of $L = 0.009$, which corresponds this time to a variance: $\text{var}\{\Delta\mathbf{H}\} = 0.0016$, is considered for a dimension: $N_T = 4$ again in

the context of the balanced twisted-pair cat 5 transmission line channels. As was the case in previous analyses, fig. 7.15 is reproduced in fig. 7.17 to the same scale to facilitate ease of comparison for the cases where $N_T = 3$ and $N_T = 4$.

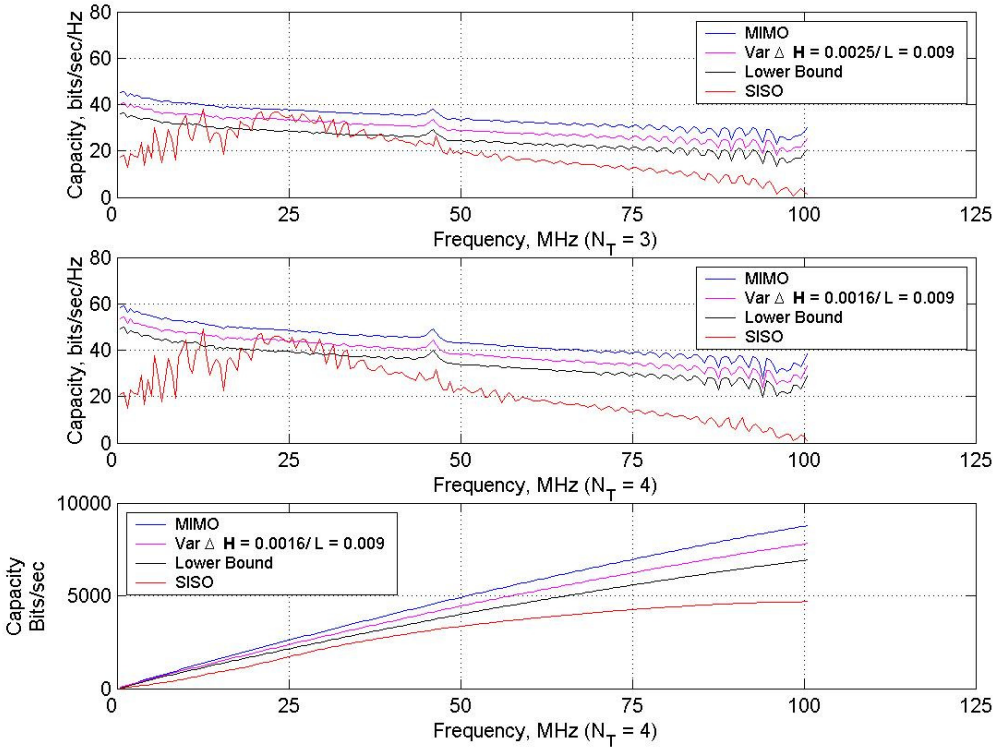

Figures 7.17-7.19: Lower bound on the effect of imperfect knowledge of the channel for a MIMO communications system based on balanced twisted-pair cat 5 transmission lines. Upper plot: Capacity in bits/sec/Hz for $\text{var}\{\Delta\mathbf{H}\} = 0.0025$ and $L = 0.009$ with $N_T = 3$. Middle plot: Capacity in bits/sec/Hz for $\text{var}\{\Delta\mathbf{H}\} = 0.0016$ and $L = 0.009$ with $N_T = 4$. Lower plot: Cumulative Capacity in bits/sec for $\text{var}\{\Delta\mathbf{H}\} = 0.0016$ and $L = 0.009$ with $N_T = 4$. In all cases, the transmit power spectral density is $P_0 = -60$ dBm/Hz.

As was the case in figs. 7.9 and 7.10 for the case of the balanced twisted-pair telephone transmission lines, the relative drop in capacity, when the leakage level is held constant, is equivalent as the dimension N_T is increased. Comparing figs. 7.17 and 7.18, it can be seen that the discrepancy in capacity between the lower bound and the SISO system is more or less equivalent for the case where is $N_T = 3$ and $N_T = 4$. Also, the cumulative capacity in fig. 7.19 exemplifies reasonable capacity gain after 50 MHz for this leakage level. It is therefore concluded that a leakage level, $L = 0.009$ indicates a good conservative indication of the extent of imperfect knowledge of the channel that can be tolerated for balanced cat 5 twisted-pair transmission line channels for either $N_T = 3$ and $N_T = 4$. Interestingly, the decrease in variance $\text{var}\{\Delta\mathbf{H}\}$ required to maintain this leakage level as N_T is increased from 3 to 4 is quite small.

Finally in this section, the unbalanced flat-pair transmission line channels are considered. Recall from previous chapters that these transmission line channels are indicative of transmission line channels that exhibit poor balance, high degrees of far end crosstalk (FEXT) and high insertion losses. Specifically from chapter 6, it was concluded that for the MIMO communications system, at frequencies higher than 25 MHz, the effect of imperfect knowledge of the channel on capacity as quantified by the variances: $\text{var}\{\Delta\mathbf{H}\} = 0.01$ and 0.005 is such that the performance is more or less equivalent to the SISO communications system. Thus the emphasis in this case is on the performance of the unbalanced flat-pair transmission line channels at frequencies below 20 MHz. This approach was seen to be justified since as mentioned in chapter 4, some current asymmetric digital subscriber lines (ADSLs) standards operate in the frequencies 2-3 MHz. It was seen in chapter 6 that at frequencies below

approximately 10 MHz, the flat-pair exhibits reasonable capacity gain for MIMO with respect to SISO in relation to the variances: $\text{var}\{\Delta\mathbf{H}\}$ = 0.001, 0.005. Thus the analysis in this chapter focuses on refining this observation by using the lower bound and hence suggesting a sensible leakage level.

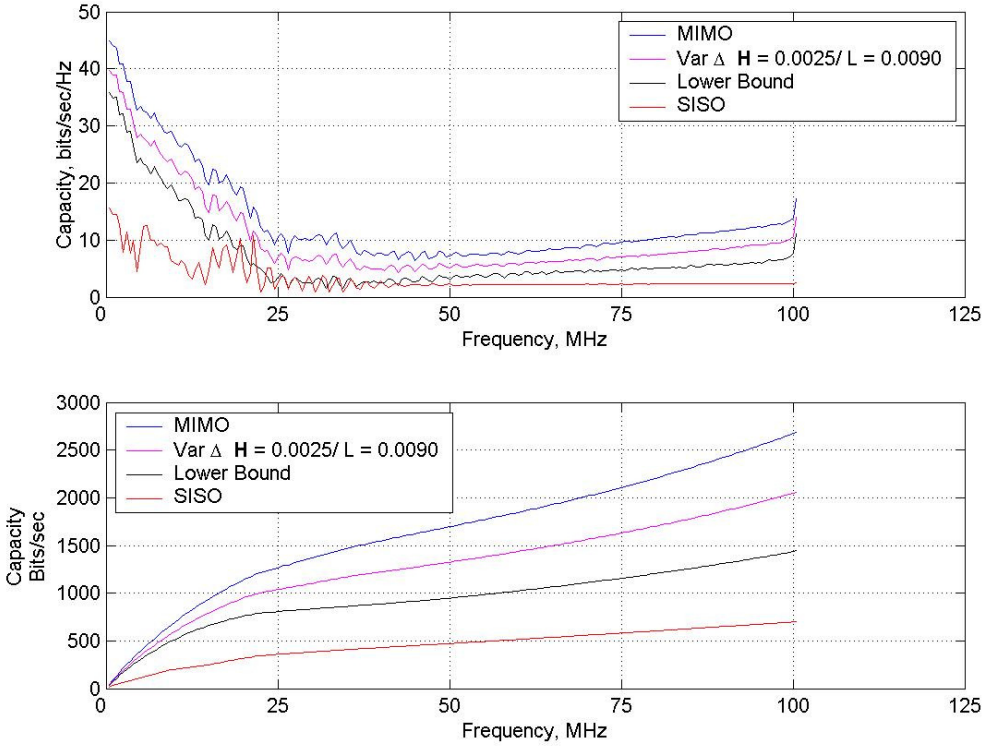

Figures 7.20-7.21: Lower bound on the effect of imperfect knowledge of the channel for a MIMO communications system based on unbalanced flat-pair transmission lines with $\text{var}\{\Delta\mathbf{H}\}$ = 0.0025 and L = 0.0090, Upper plot: capacity in bits/sec/Hz. Lower plot: cumulative capacity in bits/sec. In all cases, the dimension $N_T = 3$ and the transmit power spectral density is $P_0 = -60$ dBm/Hz.

The results in fig. 7.20 indicate that the extent of the imperfect knowledge of the channel be quantified by: $\text{var}\{\Delta\mathbf{H}\}$ = 0.0025. Reasonable capacity gains for MIMO over SISO are indicated at low frequencies. The cumulative capacity plots in fig. 7.21 indicate a reasonable rate of gain in capacity with respect to frequency for frequencies up to 25 MHz. Comparing the lower bound curve with the SISO curve in respect of this observation, relatively little is gained in terms of capacity for the case of the SISO system. A leakage level, L, of 0.0090 is hence indicated.

7.7 Lower Bound Calculations on Wireless Channels

The lower bound calculations in this section should be thought of as an extension of the calculations from section 6.4 of chapter 6. Recall that the conditions under which the calculations in that section were made were:

(i) As outlined in chapter 3, all the transfer functions and hence channel matrices pertain to a centre frequency of 5.2 GHz.

(ii) The receive signal power to noise power ratio denoted: $\frac{P}{\varphi}$ is fixed at a ratio of 18 dB throughout this section.

(iii) The various channel matrices were normalised in the manner described in section 4.3 of chapter 4. Thus the channel matrix, $\mathbf{H}$, was normalised such that:

$$\bar{\mathbf{H}}(f) = \frac{\mathbf{H}}{\|\mathbf{H}\|_F} \tag{7.41}$$

The capacity calculations in this section are therefore derived from the term:

$$\bar{\mathbf{H}}_{All} + \Delta\mathbf{H}$$

using equation (7.9). The leakage level calculations in fig. 7.6 of section 7.4 showed that when the dimension, N_T, was increased, the effect of the imperfect knowledge of the channel as quantified by a given variance, $\text{var}\{\Delta\mathbf{H}\}$, gave rise to comparatively greater leakage levels. As a result of this, table 7.1 and table 7.2 present the variance, $\text{var}\{\Delta\mathbf{H}\}$, which arises at the various values of the dimension, N_T, for a fixed leakage level, L. In table 7.1, the values of the variance, $\text{var}\{\Delta\mathbf{H}\}$ which pertain to a leakage level, L, of 0.1 are given.

N_T	$\text{var}\{\Delta\mathbf{H}\}$
2	0.0436
3	0.0267
4	0.0198
5	0.0158

Table 7.1: Table showing the dimension, N_T, from 2–5 and the corresponding variance, $\text{var}\{\Delta\mathbf{H}\}$, pertaining to a leakage level, $L = 0.1$.

The leakage level of 0.1 is considered in fig. 7.22 by calculating the expected capacities using the variances in table 7.1 and then the corresponding lower bounds.

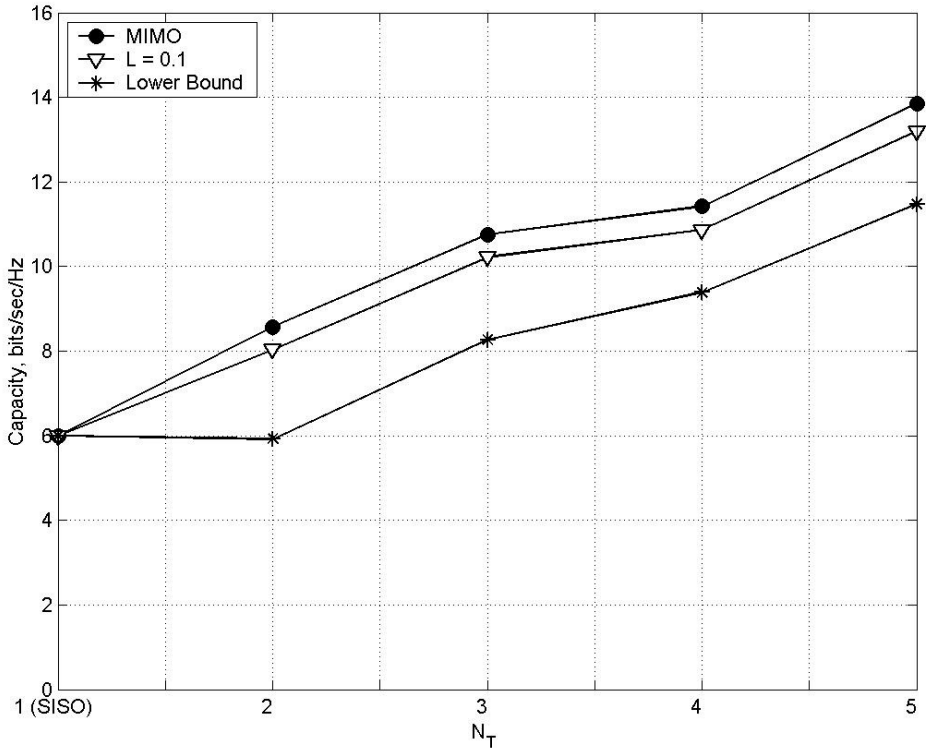

Figure 7.22: Effect of imperfect knowledge of the channel for a leakage level, $L = 0.1$ with and increasing dimension, N_T for a MIMO communications system based on wireless channels. When $N_T = 1$, this refers to a SISO communications system. $\frac{P}{\varphi}$=18 dB.

The expected capacities indicate reasonable capacity gains for all dimensions N_T from 2 to 5 in respect of the SISO case. However the lower bound provides more conservative results given that it indicates no gain in capacity for the MIMO system over the SISO system when N_T is 2. As a result of this, a leakage level of 0.05 is now considered. The appropriate variances are given in table 7.2.

N_T	$\text{var}\{\Delta\mathbf{H}\}$
2	0.0217
3	0.0136
4	0.0098
5	0.0076

Table 7.2: Table showing the dimension, N_T, from 2 – 5 and the corresponding variance, $\text{var}\{\Delta\mathbf{H}\}$, pertaining to a leakage level, $L = 0.05$.

The leakage level of 0.05 is considered in fig. 7.23 by calculating the expected capacities using the variances in table 7.2 and then the corresponding lower bound capacities. The expected capacities indicate almost equivalent capacities to the case where there is perfect knowledge of the channel. The capacities indicated by the lower bound are however a little more conservative. It is thus indicated that the leakage level be between 0.1 and 0.005 for the case of the wireless channels. It may be concluded that the benefit of increasing communications system complexity can be a trade-off between capacity and extent of knowledge of channel. This is exemplified in fig. 7.22 where the effect of increasing the dimension N_T allows for relatively low, but still reasonable, capacity gains (but none in the case where N_T =2). However the effect increasing the dimension N_T in fig 7.23 provides higher capacity gains at the expense of increased accuracy of knowledge of the channel.

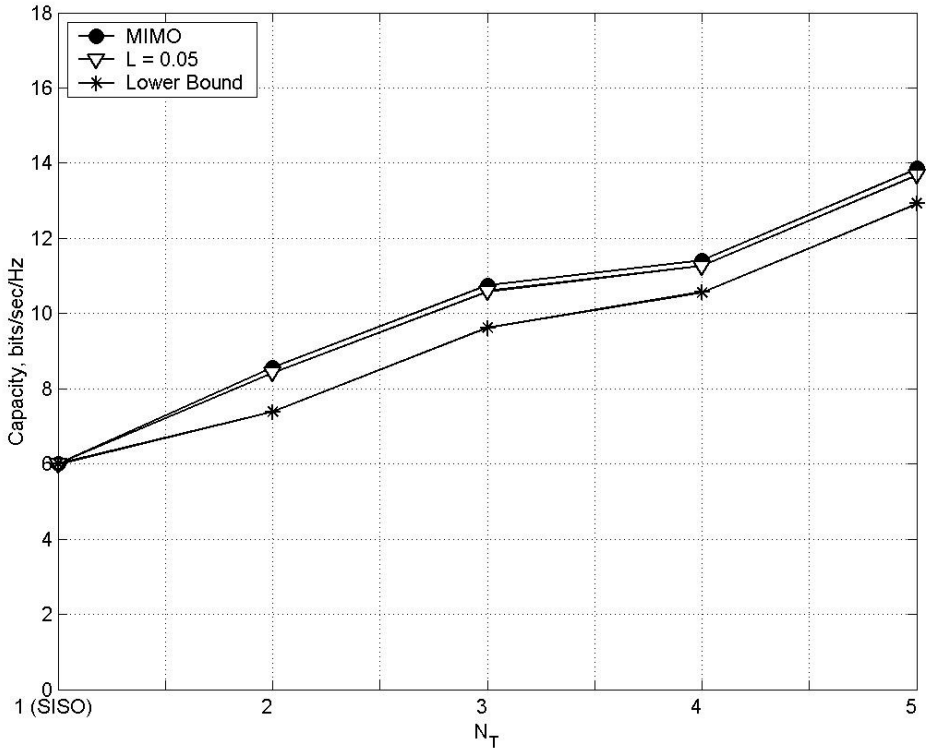

Figure 7.23: Effect of imperfect knowledge of the channel for a leakage level, $L = 0.05$ with and increasing dimension, N_T for a MIMO communications system based on wireless channels. When $N_T = 1$, this refers to a SISO communications system. $\frac{P}{\varphi}$=18 dB.

7.8 Summary

In this chapter, the leakage level, L, was defined in order to quantify the extent of the imperfect knowledge of the channel. Although, the leakage level was seen to be related to the variance, $\text{var}\{\Delta\mathbf{H}\}$, it can be appreciated that the leakage level introduces a degree of generality into the discussion in that the matrix, $\Delta\mathbf{H}$, may be defined in an alternative manner with reproducibility of the results contained within this chapter. Also, for any given dimension, N_T, the drop in capacity remains

consistent when the extent of the imperfect knowledge of the channel is quantified by the leakage level. A novel lower bound on the capacity of MIMO communications systems where there is imperfect knowledge of the channel was also derived in this chapter. As a result of this lower bound, conservative indications of the extent of the imperfect knowledge of the channel which could be tolerated in providing a viable MIMO communications systems were then offered.

In the case of balanced telephone transmission line channels, a leakage level $L = 0.0038$ was initially proposed for the case where the dimension $N_T = 3$ and $N_T = 5$. The idea was then offered that there can be one of two possible benefits to increasing the dimension N_T from 3 to 5. This benefit can come in the form of either a high capacity gain or a lower capacity gain but with less of a necessity on the accuracy of the knowledge of the channel. In respect of the latter benefit, a higher leakage level, L, of 0.0127 was thus proposed for the dimension $N_T = 5$.

For the case of the balanced cat 5 twisted-pair transmission line channels, the emphasis was on the operation of the MIMO communications system at frequencies above 50 MHz since the SISO system performed almost as well at lower frequencies. It was concluded that a leakage level, $L = 0.009$ indicated a good conservative indication of the extent of imperfect knowledge of the channel that can be tolerated for either $N_T = 3$ or $N_T = 4$ for good MIMO system operation at frequencies above 50 MHz. Interestingly, the decrease in variance $\text{var}\{\Delta\mathbf{H}\}$ required to maintain this leakage level, as N_T was increased from 3 to 4, was quite small.

In the case of the flat-pair transmission line channels, relatively low frequency operation at frequencies below 25 MHz was considered with appropriate justification. On the basis of this, a leakage level, L, of 0.0090 was indicated.

In the context of the wireless channels, two leakage levels were considered, these were: 0.1 and 0.05. Expected capacities and lower bound capacities were calculated in either case. Considering the leakage level of 0.1, the expected capacities indicated reasonable capacity gains for all dimensions from N_T from 2 to 5. However the lower bound provided more conservative results and given that it indicated no gain in capacity for the MIMO system over the SISO system when $N_T = 2$, the lower leakage level of 0.05 was considered. In light of this, capacity gains were seen at all dimensions N_T from 2 to 5 for the lower bound. It was therefore concluded that the leakage level be between 0.1 and 0.05 for the case of the wireless channels. The trade-off between increased capacity gain and decreased accuracy of knowledge of the channel as the dimension N_T was increased has thus been highlighted.

Chapter 8: Summary and Future Work

8.1 Summary

Various analyses and simulations of MIMO communications systems based on physical measurements have been presented. In respect of this, a comparison of MIMO communications systems based on various experimentally observed transmission line channels and wireless channels has been considered.

In chapter 2, the concepts of single-input/single-output (SISO) and multiple-input/multiple-output (MIMO) communications systems were clarified in the context of transmission line and wireless communications systems. The problem of far end crosstalk (FEXT) in transmission line communications systems was highlighted. Also, the problem of multi-path propagation in high bandwidth wireless links was highlighted. While much of the literature and this thesis use the capacity of the continuous channel as a metric for communications system performance, the channel capacity for discrete channels was introduced and compared. The discrepancy between the discrete channel capacity and the continuous channel capacity has been highlighted and it is argued that since the much of the analysis in the thesis seeks to examine MIMO systems in a comparative manner with respect to appropriate SISO communications systems, the results presented herein along with conclusions drawn are indicative.

Having established appropriate background theory and mathematical notation in chapter 2, chapter 3 then discussed the physical measurements which would be used to support the analyses and simulations which would be developed in subsequent chapters. In particular, the different methodologies with regard to making

measurements of unbalanced transmission lines and balanced transmission lines were outlined as well as the virtual array approach to making the physical measurements in respect of the wireless channels. Three types of transmission line channels were considered: unbalanced flat-pair, balanced twisted-pair cat 5 and balanced twisted-pair telephone transmission lines. It was established in chapter 3 that the unbalanced flat-pair transmission lines exhibited measurements which were indicative of poorer performance in terms of data transmission than in the cases of the balanced cat 5 and telephone transmission lines. Specifically, both the insertion loss and the degree of FEXT on the unbalanced flat-pair transmission lines increased more rapidly with frequency than in the cases of the balanced transmission lines. The idea was therefore offered that the measurements on the flat-pair were indicative of digital subscriber lines (DSLs) which would be deemed out-of-range for high speed internet connections due to one or any combination of: (i) poor balance, (ii) high degrees of FEXT and (iii) high insertion losses. The physical measurements of the wireless channels allowed for the identification of the various multi-path components within the channel impulse response which were clearly indicative of the spatial dimensions of the specially built reflective enclosure where these measurements were made. Further to this idea, there was experimental observation indicative of wireless channels whose fading statistics were Rayleigh and Ricean. The experimental approach was such that the degree of correlation of the multi-path components was seen to be equivalent in the case of the Rayleigh and Ricean channels using this methodology. This fact was then seen to be important in interpreting some of analytical results which were based on experimental observation of these wireless channel fading statistics.

Although chapter 2 introduced the idea of a MIMO communications system, chapter 4 gave a more mathematically detailed description of this. It was seen how a MIMO

communications system was able to transmit data over a communications channel defined by a matrix of channel transfer functions, $\mathbf{H}$. This was shown to be achieved by creating a series of orthogonal sub-channels or 'eigenmodes' which were related mathematically to this matrix of channel transfer functions, $\mathbf{H}$. Having described this, an appropriate expression for the capacity, in bits/sec/Hz, of MIMO communications systems was then derived. In the case of the transmission line channels, two transmit power spectral densities were considered: -80 dBm/Hz and -60 dBm/Hz. The lower transmit power spectral density (PSD) of -80 dBm/Hz occurs when digital subscriber lines (DSLs) operate in known radio bands whereas the higher power spectral density of -60 dBm/Hz occurs when DSLs are not operating in known radio bands. It was seen that the capacity gain for MIMO systems over SISO systems was minimal when the transmit PSD was -80 dBm/Hz, thus only -60 dBm/Hz was considered. When the MIMO communications system was applied to the unbalanced flat-pair transmission line channels, it was seen that that the MIMO communications systems provided a significant increase in performance at frequencies below approximately 15 MHz. Given that some asymmetric DSL standards operate in the 2-3 MHz frequency range, this thus indicated that the MIMO communications system could greatly enhance the performance of the aforementioned out-of-range DSLs. The capacity analysis of cat 5 transmission lines indicated only using MIMO at frequencies above 50 MHz since most of what was gained in terms of capacity occurred at these frequencies. Since cat 5 cabling is generally restricted to 100 metres, it is proposed that MIMO may be used to extend the length of this cabling. In contrast, in the case of balanced telephone transmission lines the MIMO capacity gain was reasonably consistent with respect to entire frequency range of 300 kHz to 100 MHz. It is clarified that the results presented in terms of the transmission lines are indicative of overall performance given that in

reality not all of the frequencies can be used in the context of MIMO because of the aforementioned problem of radio band interference. When the MIMO communications system was applied to the wireless channels, it was seen that when the line-of-sight channel impulse response component was removed from the measurements, the capacity was greater than for the case where all of the channel impulse components were present. This observation is indicative of the fact that Rayleigh channels permit better performance than Ricean channels in the context of MIMO communications systems. However, this result holds on the basis that the degree of correlation of the multi-path channel impulse response components remains the same in the case of the Rayleigh and Ricean fading statistics. This was seen to be an important aspect of the experimental observation of the aforementioned wireless channels.

The objective of chapter 5 was to support the conclusions of chapter 4 by developing a multi-carrier modulation based simulation. It was seen that the bit error rates recorded were indeed indicative of eigenmode gain distributions that could then be correlated with corresponding calculations of capacity. In the case of the transmission line channels, the unbalanced flat-pair exhibited the worst performance since it had one dominant eigenmode gain. On the other hand, it could be concluded that the cat 5 transmission line scheme had more evenly distributed eigenmode gains indicating superior performance. Similar conclusions could be drawn when the Ricean and Rayleigh channels were compared. When the line-of-sight channel impulse response component was removed, the bit error rates, as recorded on each of the eigenmodes, became more similar to one another. This indicated a more even distribution of eigenmode gains and hence higher capacities.

The objective of chapter 6 was thus to investigate the effect of imperfect knowledge of the channel on the capacity of MIMO communications systems. Reasons for imperfect knowledge of the channel were stated in the relevant context, i.e. non-quasi static wireless channel and incorrect assessment of channel transfer functions from one-port transmission line measurements. The extent of imperfect knowledge of the channel was quantified by the variance, $\text{var}\{\Delta\mathbf{H}\}$, of a matrix, $\Delta\mathbf{H}$, defined as: $\Delta\mathbf{H} \sim CN(0, \text{var}\{\Delta\mathbf{H}\})$. In the case of both the balanced twisted-pair telephone lines and the balanced twisted-pair cat 5 transmission lines, a fairly consistent drop in capacity with respect to frequency for a fixed number of transit and receive elements, N_T, and fixed variance, $\text{var}\{\Delta\mathbf{H}\}$ was observed. However, the relative drop in capacity increased as N_T was increased for a given fixed variance, $\text{var}\{\Delta\mathbf{H}\}$. Thus a given extent of imperfect knowledge of the channel as characterised by the variance, $\text{var}\{\Delta\mathbf{H}\}$, becomes more detrimental to performance as the dimension, N_T, increases. The unbalanced flat-pair transmission line channels showed good capacity gains at relatively low frequencies, even with varying degrees of imperfect knowledge of the channel. Thus the idea was further reinforced the idea that current 2-3 MHz ADSLs standards could therefore be deployed in the circumstances of poor balance, high insertion losses and high degrees of crosstalk using MIMO techniques. A similar analysis was performed on the capacity of MIMO communications systems based on wireless channels. It was concluded that as the amount of antennas used in the transmitter and receiver array was increased, the performance of the MIMO communications systems became more sensitive to the effect of a given variance of the random matrix. These particular results in the context of the MIMO communications system based on wireless channels paralleled the work of Kyritsi [93] and others [103] [138] [137] [14] [20] [113] [64] [143]. However since, in this

work, the extent of the imperfect knowledge of the channel is quantified by the variance of the complex normally distributed scalar elements of a matrix, the results themselves will be seen to be novel.

The focus of chapter 7 was to extend the analysis of chapter 6 by seeking to address the stochastic nature of the calculations therein by applying a lower bound on the capacity of MIMO communications systems when there is imperfect knowledge of the channel. In doing this, chapter 7 provides some insight into the required accuracy of the knowledge of the channel in order to provide a viable MIMO communications system. Furthermore, the analysis of chapter 7 makes reference to a quantity known as the leakage level. The purpose of incorporating the leakage level into the analysis is to introduce a degree of generality into the discussion with regard to quantifying the extent of the imperfect knowledge of the channel. Specifically, the use of the leakage level as a metric for imperfect knowledge of the channel means that the matrix, $\Delta\mathbf{H}$, may be defined in an alternative manner, e.g. a different statistical distribution, with reproducibility of the results contained within this chapter. Also, for any given dimension, N_T, the drop in capacity remains consistent when the extent of the imperfect knowledge of the channel is quantified by the leakage level. Further to this, the novelty of the approach to the analysis of this chapter 7 can best be summarised by the fact that the derivation of lower bound on the capacity is entirely novel. Combining this lower bound with concept of the leakage level further extends the novelty of the results that are given. The results in this chapter propose a leakage level $L = 0.0038$ for the case of the balanced telephone transmission line channels. Further to this, the idea is then offered that there can be one of two possible benefits to increasing the dimension N_T from 3 to 5. This benefit can come in the form of either a high capacity gain or a lower capacity gain but with less of a necessity on the

accuracy of the knowledge of the channel. In respect of the latter benefit, a higher leakage level, L, of 0.0127 was thus proposed for the dimension $N_T = 5$. For the case of the balanced cat 5 twisted-pair transmission line channels, it was concluded that a leakage level, $L = 0.009$ indicated a good conservative indication of the extent of imperfect knowledge of the channel that can be tolerated for either $N_T = 3$ or $N_T = 4$ for good MIMO system operation at frequencies above 50 MHz. In the case of the flat-pair transmission line channels, MIMO system operation at frequencies below 25 MHz was considered with appropriate justification. On the basis of this, a leakage level, L, of 0.0090 was indicated. In the case of the wireless channels, a trade-off between increased capacity gain and decreased accuracy of knowledge of the channel as the dimension N_T was increased was highlighted. This trade-off was clarified when two leakage levels were considered, these were: 0.1 and 0.05. A leakage level of 0.05 ensured that there was a linear increase in capacity as the dimension N_T was increased from 2 through to five but a leakage level of 0.1 only ensured increases in capacity when N_T was greater than 2.

8.2 Future Work

In respect of MIMO communications systems based on the of transmission line channels, personal correspondence with Michail Tsatsanis of Aktino technology [133] has revealed that their modem designs are based on the QR decomposition. It is therefore reasonable that future work would, in this regard, encompass simulation models of MIMO communications systems which would be based on the QR decomposition. Incorporating physical measurements of the various transmission line channels encountered in this work would therefore allow for the appropriate

comparative analysis of these MIMO communications systems based on the QR decomposition.

In the context of the MIMO communications system based wireless channels, future work could focus on space-time block coding that was first described in chapter 2. Since, space-time block codes essentially function on the basis of the quasi-static wireless channel, much of the analysis in chapters 6 and 7 should be applicable to an examination of the performance of space-time block codes when the assumption of the quasi-static channel no longer holds. Clearly, a multi-carrier modulation simulation model of space-time block codes, similar to the multi-carrier modulation simulation model discussed in chapter 5, could also be developed.

The multi-carrier modulation model presented in chapter 5 could be extended to incorporate appropriate channel coding, such as turbo codes, to improve BER performance. Also the multi-carrier modulation simulation model presented in chapter 5 could be extended to incorporate orthogonal pre-coding techniques such as Walsh-Hadamard (WH) pre-coding [44] [45] [112] [56] which, in the context of MIMO systems, could be applied either spatially or temporally. Specifically some recent work has considered peak to average power (PAPR) reduction in the context of OFDM signals in quasi-orthogonal space-time block codes [177]. Since a feature of WH pre-coding is PAPR reduction [176], it is thought that the WH technique could be applied spatially, temporally or in a combination of spatial and temporal manners as a low complexity alterative to selective mapping technique outlined in [177].

In other recent work [178], the authors have discussed the effect of interference at cellular boundaries when MIMO is applied to mobile technology. In a similar manner to chapters 6 and 7 of this work, they quantify losses in the orthogonality due to the

fact that eigenvectors have been applied as a result of singular value decompositions made on neighbouring (different) channels. While some capacities have been calculated in [178], it is argued that the lower bound analysis discussed in this thesis could extend the novelty of the analysis in [178].

While the analysis of chapter 4 sought to examine different propagation scenarios for MIMO, it is clarified that the design of the antenna is also important in this regard. In [179] [180], the recent work therein addresses a novel antenna design proposal specifically for MIMO referred to as an, 'Intelligent Quadrifilar Helix Antenna' (IQHA). The IQHAs are defined in [179] [180] under different specifications and are then compared, in terms of their performance in the context of a MIMO system, with half wavelength spaced dipole antennas using an appropriate measurement campaign. It is argued that incorporating the IQHAs into an analysis similar to that described in chapter 4 of this thesis would strengthen the analysis of [179] [180] given that different types of channel, i.e. Rayleigh and Ricean, under specific experimental conditions have been considered.

The literature on discrete channel capacity calculations in the context of MIMO communications systems does not appear to be extensive. Notwithstanding this, the capacities of some discrete channels have been calculated in [173] [174] [175] in relation to MIMO. It is argued that the results presented in this thesis could be presented comparatively in respect of various discrete channel capacities with appropriate re-usage of the analytical framework used herein with novelty.

Appendix A: Operating Point Calculations for FSK and PSK Modulation

For the case of FSK, the operating points can be calculated from [157]:

$$\frac{E_b}{N_0} = \frac{2\left[erf^{-1}\left(1 - \frac{P_e}{\frac{1}{2}[M-1]} \right) \right]^2}{\log_2 M} \tag{A.1}$$

$$\frac{R_b}{B} = \frac{2\log_2 M}{M} \tag{A.2}$$

For the case of PSK, the operating points can be calculated from [157]:

$$\frac{E_b}{N_0} = \frac{2\left[\frac{erf^{-1}(1-P_e)}{\sin\left[\frac{\pi}{M}\right]} \right]^2}{\log_2 M} \tag{A.3}$$

$$\frac{R_b}{B} = \frac{\log_2 M}{2} \tag{A.4}$$

Where the error function, $erf(x)$, is defined as:

$$erf(x) = \frac{2}{\sqrt{\pi}} \int_0^x \exp(-z^2) dz \tag{A.5}$$

Its relationship with the inverse error function $erf^{-1}(x)$ is expressed simply as:

$$y = erf(x), \qquad x = erf^{-1}(y) \tag{A.6}$$

References

[1] Agilent, “Agilent AN 154 S-parameter Design: Application Note” Agilent Technologies, http://www.sss-mag.com/pdf/AN154.pdf, accessed 22/03/2007.

[2] Alamouti, S.M., “A Simple Transmit Diversity Technique for Wireless Communications”, *IEEE Journal on Selected Areas in Communications*, Vol. 16, Issue 8, Oct. 1998, pp 1451 – 1458

[3] Ammann, M.J., John, M., “Optimum Design of Printed Strip Monopole”, *IEEE Antennas and Propagation Magazine*, Vol 47, No.6, pp 59-61, Dec 2005.

[4] Andersen. J.B., “Antenna Arrays in Mobile Communications - Gain, Diversity and Channel Capacity”, *Radio Science Bulletin,* No. 290, pp 4-7, September 1999.

[5] Andersen. J.B., “Array Gain and Capacity for Known Random Channels with Multiple Element Arrays at Both Ends”, *IEEE Journal on Selected Areas in Communications,* Volume 18, no.11 pp 2172-2178, November 2000.

[6] Anreddy, V.R., Ingram, M.A., “Capacity of Measured Ricean and Rayleigh Indoor MIMO channels at 2.4 GHz with Polarization and Spatial Diversity”*, Proc. IEEE Wireless Communications and Networking Conference, 2006. WCNC 2006,* Vol. 2, 3-6 April 2006, pp 946 – 951.

[7] Ariyavisitakul, S. L., “Turbo Space-Time Processing To Improve Wireless Channel Capacity”, *Proc. IEEE International Conference on Communications (ICC)*, 2000. Vol. 3, pp 1238 – 1242, June 2000.

[8] Ariyavisitakul, S. L., “Turbo Space-Time Processing to Improve Wireless Channel Capacity”, *IEEE Transactions on Communications*, Vol. 48, Issue 8, pp 1347 – 1359, August 2000.

[9] Arnold, B., "An Investigation into Using Singular Value Decomposition as a Method of Image Compression", *University of Canterbury, Department of Mathematics and Statistics* September 2000.

[10] Arogyasami, J. P., "An Overview of MIMO Communications-A Key to Gigabit Wirless" Invited Paper, *Proc. IEEE* , Vol 92, No. 2, February 2004.

[11] Ayres, F., *Theory and Problems of Matrices*, McGraw-Hill Publishing, 4th Edition 1987.

[12] Baher, H., *Analog and Digital Signal Processing*, Wiley 2nd Edition, 2001.

[13] Bello, P.A., "Characterisation of Randomly Time-Variant Linear Channels", *Proc. IEEE Transactions*, CS-11 (4), pp 360-393, 1963.

[14] Berriche, L., Abed-Meriam, K., Belfiore, J.C., "Investigation of the Channel Estimation Error on MIMO Systems Performance", *Proc. 13th Signal Processing Conference*, Antalya, Turkey, Sep 4-8, 2005

[15] Bingham, J.A.C., *ADSL, VDSL and Multicarrier Modulation*, Wiley Series in Telecommunications and Signal Processing, 2000.

[16] Blum, R.S., Winters, J.H., "On Optimum MIMO with Antenna Selection", *IEEE Communications Letters,* Vol. 6, Issue 8, Aug. 2002 pp 322 – 324

[17] Blum, R.S. Winters, J.H., Sollenberger, N.R., "On the Capacity of Cellular Systems with MIMO", *Communications Letters, IEEE*, Volume 6, Issue 6, June 2002 Page(s):242 – 244

[18] Bostoen, T., Boets, P., Zekri, M., Van Biesen, V., Pollet, T., Rabijns, D., "Estimation of the Transfer Function of a Subscriber Loop by Means of a One-Port Scattering Parameter Measurement at the Central Office", *IEEE Journal on Selected Areas in Communications*, Vol. 20, No.5, June 2002.

[19] Brown, T.W.C., *Antenna Diversity for Mobile Terminals,* PhD Thesis, Centre for Communications Systems Research, School of Electronics and Physical Sciences, University of Surrey, Guildford, Surrey, England, 2002.

[20] Cano-Gutierrez, A., Stojanovic, M., Vidal, J., "Effect of Channel Estimation Error on the Performance of SVD-Based MIMO Communication Systems", *Proc. 15th IEEE International Symposium on Personal, Indoor and Mobile Radio Communications, 2004.* 5-8 Sept. 2004 pp. 508 - 512 Vol.1

[21] Cendrillon, R., Rousseaux, O., Moonen, M., "Power Allocation and Optimal Tx/Rx Structures for MIMO Systems", *Proc.* 24th *Symposium on Information Theory in the Benelux de Koningshof, Veldoven, The Netherlands, May 22 and 23,* eprint.uq.edu.au/archive/00001788/01/power_pertxconst.pdf

[22] Chambers, P., Downing, C., "Experimental Study of the Capacity of a Multiple-Input / Multiple-Output (MIMO) Twisted-Pair Cable.", *Proc. Irish Signals and Systems Conference,* University of Limerick, June 2003.

[23] Chambers, P., Downing, C., "Bandwidth, Spectral Efficiency and Capacity Variation in Twisted-Pair Cable", *Proc. Irish Signals and Systems Conference,* Queen's University, Belfast, June 2004.

[24] Chambers, P., Downing, C. and Baher, H., "SIMULINK Simulation of a Stationary Indoor MIMO Wireless System.", *Proc. Irish Signals and Systems Conference* (ISSC), Dublin City University (DCU), September 2005.

[25] Chambers, P., Downing, C. and Baher, H., "Effect of a Measurement Based Error on the Capacity of a 5 x 5 Twisted – Pair MIMO Communications System." *Proc. 10th High Frequency Postgraduate Student Colloquium*, University of Leeds, September 2005.

[26] Chambers, P., Downing, C. and Baher, H., "Effect of Measurement Error on the Capacity of a MIMO Wireless System.", *Proc. IEEE Symposium on Signal Processing and Information Technology*, Titania Hotel, Athens, Greece, December 2005.

[27] Chambers, P., Downing, C. and Baher, H., "Analysis of UWB Measurements for MIMO Communications Systems", *Proc. Union Radio-Scientifique Internationale (U.R.S.I) Physical Layer Wireless Communications Colloquium*, Royal Irish Academy, 27th April 2006.

[28] Chambers, P., Downing. C. and Baher, H., "Capacity Variation in a MIMO Picocell Wireless Link Based on UWB Measurements." *Proc. Irish Signals and Systems Conference* (ISSC), Dublin Institute of Technology, June 2006.

[29] Chambers, P., Downing. C. and Baher, H., "DMT Modulation on an Economical Cabling Scheme." *Proc. Irish Signals and Systems Conference* (ISSC), Dublin Institute of Technology, June 2006.

[30] Chambers, P., Downing. C. and Baher, H., "Effect of a Measurement Error on the BER of an UWB MIMO OFDM Wireless Link." *Proc. Irish Signals and Systems Conference* (ISSC), Dublin Institute of Technology, June 2006.

[31] Chambers, P., Downing. C. and Baher, H., "BER Variation in an UWB OFDM MIMO Communications System Based on Measurements Made in a Picocell Wireless Environment.", *Proc. European Conference on Antennas and Propagation*, Acropolis, Nice, France, November 2006.

[32] Chambers, P., Downing. C. and Baher, H., "Lower Bound on the Shannon Capacity of MIMO Space-Time Wireless Communications Systems Based on the Leakage Level", *Proc. 2007 Loughborough Antennas and Propagation Conference (LAPC 2007)*, Loughborugh, England.

[33] Chambers, P., Downing. C. and Baher, H., "Capacity and Eigenvalue Analysis of a MIMO OFDM Communications System Based on Picocell UWB Measurments", *Proc. Irish Signals and Systems Conference* (ISSC), Derry 2007. (pending notification of acceptance).

[34] Chang, K., *RF and Microwave Wireless Systems*, Wiley 2000

[35] Chiurtu, N., Rimoldi, B., "Varying the Antenna Locations to Optimize the Capacity of Multi-Antenna Guassian Channels", *Proc. 2000 IEEE International Conference on Acoustics, Speech and Signal Processing* Vol. 5, 5-9 June 2000 pp 3121-3123.

[36] Chiurtu, N., Rimoldi, B., Telatar, E., "Dense Multi Antenna Systems", *Information Theory Workshop, 2001. Proceedings. 2001 IEEE* 2-7 Sept. 2001 pp 108-109.

[37] Chiurtu, N., Rimoldi, B., Telatar, E., "On the Capacity of multi-antenna Guassian Channels", *Information Theory Workshop, 2001. Proc. 2001 IEEE,* 24-29 June 2001 pp 53-59

[38] Chuah, C.-N., Foschini, G.J., Valenzuela, R.A., Chizhik, D., Ling, J., Kahn, J.M., "Capacity Growth of Multi-Element Arrays in Indoor and Outdoor Wireless Channels", *Proc. Wireless Communications and Networking Conference, 2000. WCNC. 2000 IEEE*, Vol 3, 23-28 Sept. 2000 pp: 1340 – 1344.

[39] Chiurtu, N., Rimoldi, B., Telatar, E., Puali, V., "Impact of Correlation and Coupling on the Capacity of MIMO Systems", *Proc.3rd IEEE International Symposium on Signal Processing and Information Technology, 2003. ISSPIT 2003.* , 14-17 Dec. 2003 pp 154 – 157.

[40] Choi, Y.S., Molisch, A.F., Win, M.Z., Winters, J.H., "Fast Algorithms for Antenna Selection in MIMO Systems." *Proc. IEEE 58th Vehicular Technology Conference, 2003. VTC 2003-Fall. 2003* Vol. 3, 6-9 Oct. 2003 pp 1733 - 1737

[41] Couch II, L.W., *Digital and Analog Communications Systems*, Prentice-Hall 1997.

[42] Daly, D., *Efficient Multi-Carrier Communication on the Digital Subscriber Loop*, PhD Thesis, Department of Electrical and Electronic Engineering, Faculty of Engineering and Architecture University College Dublin National University of Ireland, May 2003.

[43] Dannen, G., "The Einstein-Szilard Refrigerators." *Scientific American,* , Vol. 276 Issue 1, pp 90-96, January 1997 Scientific American Archive Online.

[44] de Frein, C., Fagan, A.,D., "Precoded OFDM-An Idea Whose Time Has Come" *Proc. Irish Signals and Systems Conference* (ISSC) 2004, Queen's University, Belfast, pp 363-368

[45] de Frein, C., Fagan, A.,D., "Maximum Likelihood Frequency Detection for Precoded OFDM" *Proc. Irish Signals and Systems Conference* (ISSC) 2006, Dublin Institute of Technology, Dublin, 2006 pp 277-282

[46] Driessen, P.F., Foschini, G.J.; "On the Capacity Formula for Multiple-Input/Multiple-Output Communications Systems: A Geometric Interpretation", *IEEE Transactions* , Vol. 47, Issue 2, Feb. 1999 pp173–176.

[47] Durgin, G.D., *Space-Time Wireless Channels*, Prentice Hall Communications and Emerging Technologies Series, 2003.

[48] Eshel, G., "The Singular Value Decomposition", *http://geosci.uchicago.edu/~gidon/geos31415/genLin/svd.pdf,* Accessed March 2007

[49] Fang, J.L., Cioffi, J.M., "A Temporary Model for EFM/MIMO Cable Characterisation", www-isl.stanford.edu/~cioffi/dsm/t1e1pap/mimo.pdf

[50] Farrokhi, F.R., Lozano, A., Foschini, G.J., Valenzuela, R.A., "Spectral Efficiency of Wireless Systems with Multiple Transmit and Receive Antennas", . *Proc. The 11th IEEE International Symposium on Personal*, *Indoor and Mobile Radio Communications 2000,* Vol. 1, 18-21 Sept. 2000 pp 373 - 377

[51] Farrokhi, F.R., Lozano, A., Foschini, G.J., Valenzuela, R.A., "Spectral Efficiency of FDMA/TDMA Wireless Systems with Transmit and Receive Antenna Arrays", *IEEE Transactions on Wireless Communications,*1, Issue 4, Oct. 2002 pp 591 – 599.

[52] Federal Communications Commission, "FCC notice of proposed rule making, revision of part 15 of the commission's rules regarding ultra wideband transmission systems", Federal Communications Commission, Washington, DC, E – T Docket 98 – 153.

[53] Flanagan, M., Fagan, A., D., "A General Formulation for Least-Squares Problems", *Proc. Irish Signals and Systems Conference (ISSC) 2004*, pp 21-26.

[54] Foley, J.B., *On the Design of Noise Cancelling Adaptive Filters*, PhD Thesis, Department of Microelectronics and Electrical Engineering, Trinity College, Dublin Ireland, 1988.

[55] Foschini, G.J., "Layered Space-Time Architecture for Wireless Communications in a Fading Environment When Using Multi-Element Antennas", *Bell labs Technical Journal*, pp 41-59, Autumn 1996.

[56] Gaffney, B., Fagan, A.,D., ”MB-OFDM UWB Interference Rejection To and From Coexisting Narrowband Systems” *Proc. Irish Signals and Systems Conference* (ISSC) 2005, Dublin City University, Dublin, 2005 pp 188-193.

[57] Galli, S., Waring, D.L., “Loop Makeup Identification Via Single Ended Testing: Beyond Mere Loop Qualification”, *IEEE Journal on Selected Areas in Communications,* Vol. 20, Issue 5, June 2002 pp. 923 – 935

[58] Gershman, A., Sidiropoulos, N., *Space-Time Processing for MIMO Communications*,Wiley,2005.

[59] Gesbert, D., Akhtar, J., “Breaking the Barriers of Shannon’s Capacity: An Overview of MIMO Wireless Systems.” *Telenor’s Journal: Teletronik* 2002, pp 1-9

[60] Gesbert, D., Bolcski, H., Dhananjay, A.G., Pualraj, J., “Outdoor MIMO Wireless Channels: Models and Performance Prediction.” *IEEE Journal on Selected Areas in Communications,* Vol 50, No. 12, December 2002

[61] Gesbert, D., Shafi, M., Da-shan Shiu, Smith, P.J., Naguib, A., “From theory to practice: an overview of MIMO space-time coded wireless systems.” *IEEE Journal on Selected Areas in Communications,* Vol. 21, Issue 3, April 2003 pp 281– 302

[62] Ginis, G., Cioffi, J.M., “Vectored Transmission for Digital Subscriber Line Systems”, *IEEE Journal on Selected Areas in Communications*, Vol. 20, No. 5, June 2002, pp 1085-1104..

[63] Girand, L., Langou, J., Rozloznik, M., “On the Loss of Orthogonality in Gram-Schmidt Orthogonalization Process”, *CERFACs* Technical Report No. TR/PA/03/25

[64] Goldsmith, A. and Yoo, T., “Capacity of Fading MIMO Channels with Estimation Error”. *Proc*. *IEEE ICC* 2004*,* Paris, France June 2004.

[65] Golub, G., Van Loan, C., F., *Matrix Computations*, Society of Industrial and Applied Mathematics SIAM, 3rd Edition 1996.

[66] Gowers, E., *The Complete Plain Words*, Pelican Books, 1976.

[67] Grennan, T., Downing, C., Foley, B., "Capacity Variation of Indoor Radio MIMO Systems Using a Deterministic Model" *Proc. Irish Signal and Systems Conference,* University of Limerick, July 2003. pp 548-553

[68] Grennan, T., Downing, C., Foley, B., "MIMO Capacity Enhancement by Adjusting Element Positions Using Metropolis Algorithm in a Deterministic Model" *Proc. Irish Signal and Systems Conference,* Dublin Institute of Technology, July 2006. pp 265-270

[69] Hanlen, L., "Water-Filling with Channel correlation", *Proc. Australian communication theory workshop* pp 1-5.

[70] Hartley, R.V.L., "Transmission of Information," *Bell System Technical Journal*, July 1928.

[71] Haykin, S., Moher, M., *Modern Wireless Communications*, Prentice Hall 2005.

[72] Haykin, S., Moher, M., *Introduction to Analog and Digital Communications*, Wiley, 2007.

[73] Haynes, T., "A Primer on Beamforming", March 26 1998, www.spectrumsignal.com/publications/beamform_primer.pdf, Accesssed 21/06/2007.

[74] Heath, R.W., "Wireless Systems", *http://wireless.ece.utexas.edu/,* Wireless Systems Engineering Lab (WSEL), The University of Texas at Austin. Accesssed 21/06/2007.

[75] Helenius, J., Yaohui, L., Renfors, M., Laakso, T., "Analysis of VDSL Capacity Based on Channel Measurements", *Finnish Signal Processing Symposium (FINSIG'99, Oulu, Finland)*, pp. 262-266, May 1999.

[76] Hochwald, B.M., Marzetta, T.L., "Unitary Space-Time Modulation for Multiple-Antenna Communications in Rayleigh Flat Fading", *IEEE Transactions on Information Theory*, Vol. 46, no.2, pp 543-564, Mar. 2000

[77] Hughes, B.L., "Differential Space-Time Modulation", *IEEE Transactions on Information Theory*, Vol. 46, no. 7, pp 2567-2578, November 2000.

[78] IEEE, "IEEE Working Group 11. IEEE Std 802.11-1999 Part 11: Wireless LAN Medium Access Control (MAC) and Physical Layer (PHY) Specifications: High Speed Physical Layer in the 5 GHz Band", IEEE 1999.

[79] Jafarkhami, H., and Tarokh, "Multiple Transmit Antenna Differential Detection from Generalised Orthogonal Designs", *IEEE Transactions on Information Theory*, Vol 47, no. 6, pp 2626-2631, September 2001

[80] Jakes, W.C. Jr., *Microwave Mobile Communications*, John Wiley and Sons, New York, 1974.

[81] Jenson, M.A., Wallace, J.W., "A Review of Antennas and Propagation for MIMO Wireless Communications", *IEEE Transactions on Antennas and Propagation*, Vol. 52, Issue 11, Nov. 2004 pp 2810 – 2824.

[82] Jiang, S. J., Ingram, M. A., "Distributed Source Model for Short-Range MIMO", *Proc. IEEE 58th Vehicular Technology Conference (VTC), Fall 2003* 6-9 Oct. 2003, Vol: 1, pp 357-362

[83] Jiang, S. J., Ingram, M. A., "Path Models and MIMO Capacity for Measured Indoor Channels at 5.8 GHz", *Proc. 9th IEEE International Symposium on Antenna Technology and Applied Electromagnetics*, pp. 601-607, Aug. 2002.

[84] Jiang, S. J., Demirkol, M. F., Ingram, M. A., "Measured Capacities at 5.8 GHz of Indoor MIMO Systems with MIMO Interference", *Proc. IEEE 58th Vehicular Technology Conference (VTC), Fall 2003* 6-9 Oct. 2003 Vol: 1, pp: 388- 393.

[85] Kaliath, T., "Sampling Models for Linear Time-Variant Filters", *MIT Research Lab. of Electronics*, Cambridge, Mass., Rept. No. 352, May 25, 1959.

[86] Kai Y., Bengtsson, M., Ottersten, B., McNamara, D., Karlsson, P., Beach, M., "Second Order Statistics of NLOS Indoor MIMO Channels Based on 5.2GHz Measurements", *Proc. Global Telecommunications Conference*, 2001. (GLOBECOM '01), Vol 1, pp 156-160.

[87] Kelleher, A., *Onset and Ornament Detection and Music Transcription for Monophonic Traditional Irish Music*, MPhil Thesis, Faculty of Applied Arts, Dublin Institute of Technology, Ireland, 2005

[88] Kennedy, G., *Electronic Communications Systems*. McGraw–Hill International Editions 1984.

[89] Klema, V.C., Laub, A.J., "The Singular Value Decomposition: Its Computation and Some Applications", *IEEE Transactions on Automatic Control*, Vol. AC-225, No.2, April 1980, pp164-176.

[90] Knapp, J., Julius, J, "New Public Safety Applications and Broadband Internet Access among Uses Envisioned by FCC Authorization of Ultra-Wideband Technology," Federal Communications Commission News Release, February 14, 2002, http://ftp.fcc.gov/Bureaus/Engineering_Technology/News_Releases/2002/

[91] Kuo, F.F., *Network Analysis and Synthesis*, Wiley 1966.

[92] Kyritsi, P., Cox, D., C., "Modal Analysis of MIMO Capacity in a Hallway", *Proc. IEEE Global Telecommunications Conference, 2001*. (GLOBECOM '01). Vol. 1, 25-29 Nov. 2001 pp: 567 – 571.

[93] Kyritsi, P., Valenzuela, R.A., Cox, D.C., "Channel and Capacity Estimation Errors" *IEEE Communications Letters*, Vol. 6, No.12, December 2002, pp 517-519.

[94] Leach, S., "Singular Value Decomposition-A Primer", Draft Manuscript, Department of Computer Science, Brown University, Providence, RI 02912, *www.cs.brown.edu/research/ai/dynamics/tutorial/Postscript/SingularValueDecomposition.ps - Accessed March 2007*

[95] Loyka, S., Kouki, A., "On the Use of Jensen's for MIMO Channel Capacity Estimation", *Proc. Canadian Conference on Electrical and Computer Engineering,* Vol. 1, 13-16 May 2001, pp475 - 480

[96] Magesacher, T, "OFDM and DMT in a Nutshell: Track #2: xDSL Physical Layer", *MUSE Autumn School 2006,* October 19-20, 2006, Bilbao

[97] Maharaj, B.T., Linde, L.P., Wallace, J.W., Jensen, M., "A Cost-Effective Wideband MIMO Channel Sounder and Initial Co-Located 2.4 GHz and 5.2 GHz Measurements", *Proc. IEEE International Conference on Acoustics, Speech, and Signal Processing (ICASSP '05)*, 18-23 March 2005 Vol. 3, pp iii/981- iii/984.

[98] Martone, M., "Multiantenna Digital Radio Transmission", *Artech House Publishers, 2002.*

[99] Moloney, A., *A CMOS Monolithically Integrated Photoreceiver Incorporating an Avalanche Photodiode*, PhD Thesis, Department of Electrical and Electronic Engineering, University College Cork, Ireland, 2003

[100] Maurer, J., Waldschmidt, C., Kayser, T., Wiesbeck, W., "Characterisation of the Time-Dependent Urban MIMO Channel in FDD Communication Systems", *Proc. The 57th IEEE Semiannual Vehicular Technology Conference, 2003.* VTC 2003-Spring. Vol. 1, 22-25 April 2003 pp 544 - 548

[101] MATLAB/SIMULINK, *www.themathwoks.com*, accessed: 21/06/2007

[102] McWilliams, B., "Weather Eye, The Laws of Science Have Heat and Energy", *The Irish Times*, p 28, The Bulletin Page, Friday 16 July 2004.

[103] Médard, M., "The Effect Upon Channel Capacity in Wireless Communications of Perfect and Imperfect Knowledge of the Channel", *IEEE Transactions on Information Theory*, Vol. 46, No.3 May 2003, pp 933-946.

[104] Melzer, T., "SVD and Its Application to Eigenvalue Problems", *http://www.prip.tuwien.ac.at/~melzer/lehre/statpr/apponly.pdf*, Accessed March 2007.

[105] Moler, C., *Numerical Computing with MATLAB*, Society of Industrial and Applied Mathematics SIAM 2004.

[106] Molisch, A.F., Win, M.Z., Choi, Y.S., Winters, J.H., "Capacity of MIMO Systems with Antenna Selection", *IEEE Transactions on Wireless Communications,* Volume 4, Issue 4, July 2005, pp1759 – 1772

[107] Musser, G., "Taming Maxwell's Demon" *Scientific American,* Feb. 1999, Vol. 280 Issue 2, p24.

[108] Mujtaba, S.A., "MIMO Signal Processing-The Next Frontier for Capacity Enhancement", *Proc. IEEE 2003 Custom Integrated Circuits Conference*, pp 263-270.

[109] Naguib, N., Seshadri, N., Calderbank, R., "Increasing Data Rate Over Wireless Channels", *IEEE Signal Processing Magazine*, Vol. 17, pp 76-92, May 2000.

[110] Nguyen, H., T., Leus, G., Khaled, N., "Prediction of Eigenvectors for Spatial Multiplexing MIMO Systems in Time-Varying Channels", *Proc. The IEEE International Symposium on Signal Processing and Information Technology (ISSPIT)*, Athens, Greece, December 2005.

[111] Ozcelik, H., Herdin, M., Hofstetter, H., Bonek, E., "Capacity of Different MIMO Systems Based on Indoor Measurements at 5.2 GHz", *Proc. 5th European Personal Mobile Communications Conference 2003*, April 2003, pp 463-466.

[112] Park, M., Jun, J., Cho, N., Hong, D., Kang, C., "PAPR Reduction in OFDM Transmission Using the Hadamard Transform", *Proc. IEEE International Conference on Communications*, pp 430-433, vol.1, June 2000.

[113] Primolevo, G., Simeone, O., Spagnolini, "Effects of Imperfect Channel State Information on the Capacity of Broadcast OSDMA-MIMO Systems", *Proc. 5th IEEE Workshop on Signal Processing Advances in Wireless Communications*, Portugal, July 11-14, 2004

[114] Rappaport, T.S., *Wireless Communications*, Prentice Hall, 1996.

[115] Ratnarajah, T., "Non-Central Quadratic Forms on Complex Random Matrices and Applications", *Proc. IEEE Workshop on Statistical Signal Processing,* Bordeaux, France, Jul. 17-20, 2005.

[116] Rogers, G., and Mayhew, Y., *Engineering Thermodynamics Work and Heat Transfer*, Longman Scientific/John Wiley and Sons, Copyright 1992,

[117] Sabath, F., Mokole, E.L., "Definitions and Classification of Ultra-Wideband Signals and Devices". *The Radio Science Bulleti*n, No. 310, pp 12-26, June 2005.

[118] Salvekar, A.A., Louveaux, J., Aldana, C., Fang, J.L., de Carvalho, E., Cioffi, J.M., "Profile Detection In Multiuser Digital Subscriber Line Systems", *Proc. IEEE Journal on Selected Areas in Communications*, Vol. 20, Issue 5, June 2002 pp 1116 – 1125

[119] Sandhu, S., Heath, R., Pualraj, A., "Space-Time Block Codes Versus Space-Time Trellis Codes", *Proc. IEEE International Conference on Communications, 2001 ICC 2001*, Volume 4, 11-14 June 2001 pp 1132 - 1136 vol.4

[120] Saunders, S.R., *Antennas and Propagation for Wireless Communications Systems*, John Wiley & Sons, 1999.

[121] Schmücking, D., Schenk, M., Wörner, A., "Crosstalk Cancellation for Hybrid Fiber Twisted-Pair Systems", *Proc. Global Telecommunications Conference, 1996. GLOBECOM '96. Communications: The Key to Global Prosperity*, Vol. 2, 18-22 Nov. 1996 pp 783 – 787.

[122] Shannon, C.E., "A Mathematical Theory of Communication", *The Bell System Technical Journal,* Vol. 27, pp. 379–423, 623–656, July, October 1948.

[123] Song, L.Y., Burr, A.G., "Successive Interference Cancellation for Space-Time Block Codes over Time-Selective Channels", *IEEE Communications Letters* Vol. 10, Issue 12, pp 837–839, December 2006.

[124] Starr, T., Cioffi, J.M., Silverman, P.J., *Understanding Digital Subscriber Line Technology*, Prentice Hall 1999.

[125] Stewart, G.W., *Matrix Algorithms Volume 1: Basic Decompositions*, Society of Industrial and Applied Mathematics SIAM, 1998.

[126] Stewart, G.W., "On the Early History of the Singular Value Decomposition", *Society of Industrial and Applied Mathematics SIAM Review* Volume 35, Issue 4, December 1993, pp 551-566

[127] Sumit, R, Foerster, J., Somayzulu, R., L., Srinivasa, Dave, G, " Ultrawideband Radio Design: The Promise of High–Speed, Short–Range Wireless Connectivity", *Proc. the IEEE,* Vol . 92, No. 2, February 2004

[128] Tarohk, V., Jafarkhami, H., Calderbank, A.R., "Space-Time Block Codes for Orthogonal Designs", *IEEE Transactions on Information Theory*, Vol. 45, No. 5, July 1999.

[129] Tarokh, V., Naguib, N., Seshadri, N., Calderbank, A.R., "A Differential Detection Scheme for Transmit Diversity", *IEEE Journal on Selected Areas on Communications*, Vol. 18, pp 1169-1174, July 2000

[130] Tarokh, N., Seshadri, N., Calderbank, A.R., "Space-Time Codes for High Data Rate Wireless Communications", *IEEE Transactions on Information Theory*, Vol. 44, pp 744-765, March 1998.

[131] Tirkkonen, O., Boariu, A., Hottinen, A., "Minimal Non-Orthogonality Rate 1 Space-Time Block Code for 3+ Tx Antennas", *Proc. IEEE International Symposium on Spread Spectrum Technology*, 2000, pp 429-432.

[132] Tranter, W.H., Shanmungen, K.S., Rappaport, T.S., Kosbar, K.L., *Principles of Communications Systems Simulations with Wireless Applications*, Prentice Hall, 2004.

[133] Tsatsanis, M., Aktino Technology, Private Correspondence.

[134] Vetterling, W.T., Press, W.H., Teukolski, S.A., Flannery, B.P., *Numerical Recipes in C: The Art of Scientific Computing*, *Cambridge University Press* 1988-1992.

[135] Vucetic, V., Yuan, J., *Space-Time Coding*, John Wiley & Sons, 2003.

[136] Wang, Y.H., Tan, T.N., Zhu, Y., "Face Verification Based on Singular Value Decomposition and Radial Basis Function Neural Network", *Proc.The 4th. Asian Conference on Computer Vision (ACCV'2000)*, Taipei, Taiwan, 2000.

[137] Weber, T., Meurer, M., "Imperfect Channel State Information in MIMO-Transmission", *Proc. IEEE Vehicular Technology Conference*, Vol. 2. pp 693-697, March 2004.

[138] Weber, T., Sklavos, K., Meurer, M., "Imperfect Channel State Information in MIMO-Transmission", *IEEE Transactions on Communications*, Vol 34, Issue 3, March 2006, pp 543-552.

[139] Wennstrom, M., *On MIMO Systems and Adaptive Arrays for Wireless Communications*, PhD Thesis, Uppsala University Signals and Systems, 2002.

[140] Winters, J.H., "On the Capacity of Radio Communication Systems with Diversity in a Rayleigh Fading Environment", *IEEE Journal on Selected Areas on in Communications.*, Vol. SAC-5, pp. 871-878, June 1987.

[141] Wong, K., Aboulnasr, T., "Single-Ended Loop Characterization", *Proc. 37th Midwest Symposium on Circuits and Systems*, 3-5 Aug 1994 Vol. 2, pp 1323-1326

[142] Yan, W., Sumei, S., Lei, Z.,"A Low complexity VBLAST OFDM detection algorithm for wireless LAN systems", *IEEE Communications Letters*, Vol., Issue 6, June2004, pp. 374-376

[143] Xu, Z.,"Perturbation Analysis for Subspace Decomposition with Applications in Subspace-Based Algorithms", *IEEE Transactions on Signal Processing*, Vol. 50, No. 11 November 2002, pp 2820-2830.

[144] Young, E.C., *The Penguin Dictionary of Electronics,* Penguin, 1988.

[145] Zheng, F.C., Burr, A.G., "Signal Detection for Orthogonal Space-Time Block Coding over Time-Selective Fading Channels: A PIC Approach for the G_i Systems", *IEEE Transactions on Communications*, Vol. 53, Issue 6, pp 969 – 972, June 2005.

[146] Zheng, F.C., Burr, A.G., "Signal Detection for Orthogonal Space-Time Block Coding over Time-Selective Fading Channels: The H_i Systems" *IEEE Transactions on Wireless Communications*, Vol. 5, Issue 1, pp 40 – 46, January 2006.

References Added in Proof

[147] Berrou. C., Glavieux, A., Thitimajshima, P., "Near Shannon Limit Error-Correcting Coding and Decoding: Turbo Codes (1), *Proc. IEEE International Communications Conference (ICC 93)*, Geneva. Technical Program, Conference Record, Communications, Vol. 2, pp 1064 – 1070, May 1993

[148] Brigham, E.,O., *The Fast Fourier Transform and its Applications*, Prentice-Hall, 1988

[149] Downing, C.P., *Locally Convergent Adaptive IIR Filtering*, PhD Thesis, Department of Microelectronics and Electrical Engineering, Trinity College, Dublin Ireland, 1990.

[150] Foschini, G.F. and Gans, M.J., "On Limits of Wireless Communication in a Fading Environment When Using Multiple Antennas". *Wireless Personal Communications,* Volume 6, no.3 pp 311-335, March 1995.

[151] Galli, S., Waring, D.L., "Loop Makeup Identification Via Single Ended Testing: Beyond Mere Loop Qualification", *IEEE Journal on Selected Areas in Communications,* Vol. 20, Issue 5, June 2002 pp. 923 – 935

[152] Teletar, E, "Capacity of Multi-Antenna Guassian Channels", *AT&T Bell Labs.* Internal Tech MEMO, June 1995.

[153] McKay, M.R., Collings, I.B., "General Capacity Bounds for Correlated Rician MIMO Channels", *IEEE Transactions on Information Theory*, Vol. 51, Issue 9, Sept. 2005, pp 3121-3145.

[154] Del Galdo, G., Hennhofer, M., Haardt, M., "Analysis of MIMO Channel Measurements", *Proc. 13th IFAC Symposium on System Identification (SYSID 2003)*, Rotterdam, The Netherlands, pp. 85-89, Aug. 2003.

[155] Bohagen, F., Orten, P., Geir, E.,O., "Construction and Capacity Analysis of High-Rank Line-of-Sight MIMO Channels", *Proc. 2005 IEEE Wireless Communications and Networking Conference,* Vol. 1, March 2005, pp 432– 437.

[156] Ozcelik, H., Herdin, M., Hofstetter, H., Bonek, E., "How MIMO capacity is Linked to Single Element Fading Statistics.", *Proc. International Conference on Electromagnetics in Advanced Applications.* Torino, September 2003.

[157] Haykin, S., *Communications Systems, 3rd Edition,* John Wiley and Sons, 1994

[158] Haykin, S., *Communications Systems, 4rd Edition,* John Wiley and Sons, 2003

[159] Ungerboeck, G., "Channel Coding with Multi-Level/Phase Signals", *IEEE Transactions on Information Theory,* Vol IT-28, No.1, Jan 1982

[160] Agazzi, O., Messerschmitt, D.G., Hodges, D.A., "Non-Linear Echo Cancellation of Data Signals" *IEEE Trans. Communications* COM-30 pp. 2421-2433, Nov. 1982

[161] Varnica, N., Ma, X., Kavcic, A., "Capacity of Power Constrained Memoryless AWGN Channels with Fixed Input Constellations", IEEE Proc. Globecom 2002, pp 1339-1343, Nov 2002.

[162] Dai, H., Poor, V.H., "Crosstalk Mitigation in DMT VDSL with Impulse Noise", *IEEE Trans. Circuits and Systems-1; Fundamental Theory and Applications*, pp 1205-1213, Vol. 48, No. 10, Oct. 2001.

[163] Kalet, I., Shamai, S., "On the Capacity of a Twisted-Wire Pair: Gaussian Model", *IEEE Trans. Communuications*, pp 379-383, Vol. 38, No. 3, March 1990

[164] Shamai, S., "On the Capacity of a Twisted-Wire Pair: Peak Power Constraint", pp368-378*, IEEE Trans. Communications*, Vol.38, No.3, March 1990

[165] Cioffi, J.M., *A Multi-Carrier Primer*, Amati Communications Corporation and Stanford University.

[166] Forney, D.G. Jr., Ungerboeck, G., "Modulation and Coding for Linear Gaussian Channels", pp 2384-2415, *IEEE Trans. Information Theory,* Vol. 44, No.6, October 1998

[167] Aldis, J.P., Burr, A.G., "The Channel Capacity of Discrete Time Phase Modulation in AWGN", *IEEE Trans. Information Theory,* Vol. 39, No. 1, January 1993.

[168] Ungerboeck, G., "Trellis-Coded Modulation with Redundant Signal Sets: Parts I-II, *IEEE Communications Mag.* vol. 25, February 1987

[169] Agilent/Hewlett Packard, *8753B Network Analyser and Operating Programme Reference: System Operating and Programming Manual,* November 1988.

[170] Radionics Catalogue, www.radionics.ie, accessed 1/04/2008

[171] Aslanis, J.T., Cioffi, J.M., "Achievable Information Rates on Digital Subscriber Loops: Limiting Information Rates with Crosstalk Noise", *IEEE Trans. Communications*, pp 361-372, Vol.40, No.2, February 1992

[172] ANSI *Asymmetric digital subscriber line (ADSL) Metallic Interface*, ANSI Standard T.413-1995, ANSI, New York.

[173] Ng., S.X., Hanzo, L., "On the MIMO Channel Capacity of Multidimensional Signal Sets", *IEEE Trans. Vehicular Technology*, pp 1594–1598, Vol. 3, Sept. 2004.

[174] Ng., S.X., Hanzo, L., "On the MIMO Channel Capacity of Multidimensional Signal Sets", *IEEE Trans. Vehicular Technology*, pp 528-536, Vol. 55, Mar. 2006.

[175] Zhu, H., Shi, Z., Farhang-Boroujeny, B., Schlegel, C., "An Efficient Statistical Approach for Calculation of Discrete Capacity of MIMO Channels" submitted to *IEEE Trans. Communications*., May 2003.

[176] Park, M., Jun, H., Cho, J., Hong, D., Kang, C., "PAPR Reduction in OFDM Transmission Using Hadamard Transforms," *IEEE International Conference on Communications 200*0, pp. 430-433, June 2000.

[177] Alharbi, F.S., Chambers, J.A., "Peak to Average Power Ratio Mitigation in Quasi-Orthogonal Space-Time Block Coded MIMO OFDM Systems Using Selective Mapping", *Loughborough Antenna and Propagation Conference 2008 (LAPC 08)*, pp 157-160, March 2008

[178] Brown, T.W.C., Eggers, P. C. F., Olesen, K., "Simultaneous 5GHz Co-channel MIMO Links at Microcellular Boundaries: Interference or Cooperation?", *IET Microwaves, Antennas and Propagation*, vol. 1, issue 6, pp1152-1159, December 2007.

[179] Brown, T.W.C., Saunders, S.R., "The Intelligent Quadrifilar Helix: A Compact Antenna for IEEE 802.11n", *European Conference of Antennas and Propagation (EuCAP)*, November 2007.

[180] Brown, T.W.C., Saunders, S.R., "Measured Performance Comparison of Spaced Monopoles and a Compact Intelligent Quadrifilar Helix for IEEE 802.11n Applications", *IET Smart Antennas and Cooperative Communications Seminar*, October 2007.

List of Publications

The following publications have been produced:

- Chambers, P. and Downing. C., "Experimental Study of the Capacity of a Multiple-Input / Multiple-Output (MIMO) Twisted-Pair Cable", Proc. *Irish Signals and Systems Conference* (ISSC), University of Limerick, July 2003.

- Chambers, P., Downing. C. and Baher, H., "Bandwidth, Spectral Efficiency and Capacity Variation in Twisted-Pair Cable", Proc. *Irish Signals and Systems Conference* (ISSC), Belfast, July 2004.

- Chambers, P., Downing, C. and Baher, H., "SIMULINK Simulation of a Stationary Indoor MIMO Wireless System.", Proc. *Irish Signals and Systems Conference (ISSC)*, Dublin City University (DCU), September 2005.

- Chambers, P., Downing, C. and Baher, H., "Effect of a Measurement Based Error on the Capacity of a 5 x 5 Twisted – Pair MIMO Communications System." Proc. *10^{th} High Frequency Postgraduate Student Colloquium*, University of Leeds, September 2005.

- Chambers, P., Downing, C. and Baher, H., "Effect of Measurement Error on the Capacity of a MIMO Wireless System.", Proc. *IEEE Symposium on Signal Processing and Information Technology*, Titania Hotel, Athens, Greece, December 2005.

- Chambers, P., Downing, C. and Baher, H., "Analysis of UWB Measurements for MIMO Communications Systems", *Union Radio-Scientifique Internationale* (U.R.S.I) Physical Layer Wireless Communications Colloquium, Royal Irish Academy, 27th April 2006.

- Chambers, P., Downing. C. and Baher, H., "Capacity Variation in a MIMO Picocell Wireless Link Based on UWB Measurements." Proc. *Irish Signals and Systems Conference* (ISSC), Dublin Institute of Technology, June 2006.

- Chambers, P., Downing. C. and Baher, H., "DMT Modulation on an Economical Cabling Scheme." Proc. *Irish Signals and Systems Conference* (ISSC), Dublin Institute of Technology, June 2006.

- Chambers, P., Downing. C. and Baher, H., "Effect of a Measurement Error on the BER of an UWB MIMO OFDM Wireless Link." Proc. *Irish Signals and Systems Conference* (ISSC), Dublin Institute of Technology, June 2006.

- Chambers, P., Downing. C. and Baher, H., "BER Variation in an UWB OFDM MIMO Communications System Based on Measurements Made in a Picocell Wireless Environment.", Proc. *European Conference on Antennas and Propagation*, Acropolis, Nice, France, November 2006.

- Chambers, P., Downing. C. and Baher, H., "Lower Bound on the Shannon Capacity of MIMO Space-Time Wireless Communications Systems Based on the Leakage Level", Proc. *2007 Loughborough Antennas and Propagation Conference* (LAPC 2007), Loughborough, England.

- Chambers, P., Downing. C. and Baher, H., "Capacity and Eigenvalue Analysis of a MIMO OFDM Communications System Based on Picocell UWB Measurements", Proc. *Irish Signals and Systems Conference* (ISSC), Derry 2007.

- Chambers, P., Downing. C. and Baher, H., "Comparison of MIMO Communications Systems Based on Unbalanced and Balanced Transmission Line Channels", Proc. *2008 Loughborough Antennas and Propagation Conference* (LAPC 2008), Loughborough, England.

- Chambers, P., Downing, C., “Lower Bound on the Capacity of SVD MIMO Communications Systems Based on Experimentally Observed Wireless and Transmission Line Channels”, *Union Radio-Scientifique Internationale* (U.R.S.I) Physical Layer Wireless Communications Colloquium, Royal Irish Academy, 2008.